The Dissertation Committee for Juan Clemente Bermúdez Santana certifies that this is the approved version of the following dissertation:

SEQUENCE STRATIGRAPHY AND DEPOSITIONAL HISTORY OF THE UPPER CAÑON DEL TULE, LAS IMAGENES, AND LOWER CERRO GRANDE FORMATIONS, CENTRAL PARRAS BASIN, NORTHEASTERN MEXICO.

Committee:

Richard T. Buffler, Supervisor

William L. Fisher

Earle F. McBride

Francisco J. Vega

Timothy F. Lawton

SEQUENCE STRATIGRAPHY AND DEPOSITIONAL HISTORY OF THE UPPER CAÑON DEL TULE, LAS IMAGENES, AND LOWER CERRO GRANDE FORMATIONS, CENTRAL PARRAS BASIN, NORTHEASTERN MEXICO.

by

Juan Clemente Bermúdez Santana, B.S., M.Sc.

DISSERTATION

Presented to the Faculty of the Graduate School of

The University of Texas at Austin

in Partial Fulfillment

of the Requirements

for the Degree of

DOCTOR OF PHILOSOPHY

The University of Texas at Austin

December, 2003

Dedication

With all my heart and love to the sweet memory of my sister Juve.

Acknowledgements

I will be forever grateful with my advisor Dr. Richard T. Buffler for his endless support and guidance since the first day I became involved in this important stage of my life. I express to him my sincerest and endless gratitude for the deep and positive impact he made on my professional and human formation, for his encouragement, and friendship.

I also appreciate the advising of Dr. William L. Fisher, who always had a friendly hand and the smile that all international students miss when not at home. Dr. Earle F. McBride was always "after me". I always kept into my mind and heart his way of thinking, which was a challenge for me to improve and to do my best during the development of my project. His comments greatly improve my dissertation. I also received the benefit of the wide and deep knowledge of Dr. Kristian Soegaard on the spectacular stratigraphy of the Parras Basin. Kris, I always wanted to share with you the last stories that those rocks told me about that particular area of the big Parras. Life denied to me the great opportunity to discuss with you the final results. I dedicate the modest stratigraphic value of this work into your memory. I began to familiarize with the biostratigraphy of the Parras and La Popa basins thanks to some articles and friendly support kindly provided by Dr. Francisco J. Vega, who also studied part of the fossil material collected during the development of my work. Also appreciated are the constructive comments and critical revision of my interpretations exposed by Dr. Timothy Lawton, which greatly improved the results herein included.

In 1996, I received the benefit of a scholarship for doctoral studies from the Instituto Mexicano del Petróleo (IMP). The scholarship was the result of a program for the formation of human resources for the petroleum industry started by Dr. Francisco Barnes de Castro. The program continued later under the leadership of Dr. Gustavo Chapela Catañares, current IMP Director General. I

appreciate the distinction that my sponsor institution made on my benefit and feel committed to retribute that distinction with my effort and dedicated work for the benefit of the oil industry of my country. I thank to M. Sc. Baldomero Carrasco, Dr. Alfredo Arriola, Dr. Pedro Salmerón, Dr. Esteban Cedillo, Mr. Alfredo Molina; and Lics. Gerardo de Alba, Alma Corona, Gustavo Flores, and Felipe de Jesús López for the support I received from all of them at the different stages of my studies.

The conclusion of my doctoral program and even this dissertation would not had been a reality without the confidence and supportive friendship of Dr. Mario Guzmán. I will also be forever grateful to my dear friends at the IMP: Carmen Rosales, Manuel Grajales, Ricardo Torres, Marcelo Aguilar, Marce Ugarte, Julio César González, Jose Antonio Gómez, Gustavo Murillo, Ma. Antonieta Sánchez, Paty Padilla, and Jorge Alvarado. I would not omit to mention by reasons of space or less thankfulness, the solidarity and supportive frienship of my colleagues Jorge Jacobo, Monica Ayala, Liz Lara, Ricardo Casar, René Téllez, Humberto Alzaga, Arturo Ortíz, Juan Jose Valencia, Ismael Gallo, Sonia Franco, Mónica Granados, Carlos Cantú, and all the nice people of “Los Amigos de Juan”.

I benefited with the support for fieldwork kindly provided by M. en C. Aarón del Valle, geologist Lenin Loredo, Sr. Adrián Quintana, and Sr. César Melo. M. en C. Ricardo Martínez and Dr. Manuel Grajales also provided support to use the equipment at IMP petrography and diagenesis lab. Technician Guillermo Aguilar Palma (IMP) made all of the thin sections involved in this study. The SEM images of charophytes included here were obtained with the technical support of Marcela Ugarte (IMP). Pictures of ammonites and some *Exogyra* were taken at the IMP photography lab by technician Hector Amézcua and geologist Daniel Olvera. I appreciate the support of all of these persons and recognize as well their technical abilities directly or indirectly imprinted into some pages of this dissertation.

Dr. Keith Young at the Department of Geological Sciences of the University of Texas at Austin, M. en C. María E. Gomez (IMP), and Dra. Ana Bertha Villaseñor at the Instituto de Geología at UNAM (IG-UNAM) studied the ammonites collected in this study. Gastropods and bivalves were identified and photographed by Dr. Francisco Vega Vera and Biol. Roberto Cozátl (IG-UNAM). Processing of samples for calcareous nanofossil studies were performed by Dra. Ma. Antonieta Sánchez and M. en C. Patricia Padilla (IMP). Dr. Marcelo Aguilar (IMP) and paleontologist Victoria González at the Escuela de Ciencias de la Tierra at Instituto Politécnico Nacional (ECT-IPN) made the general identification of some benthonic forams. Dr. Robert L. Folk (UT-DoGS) provided support for the initial identification of charophytes of Las Imágenes Formation. Later, the author initiated a review of basic literature on this fossil group encouraged by paleontologist Carmen Rosales (IMP). Dra. Lucia Capra at Instituto de Geofísica (UNAM) and Dr. Jacinto Robles at Universidad Michoacana at Morelia City conducted the studies of some clay samples. I sincerely express my endless gratitude to all these persons and institutions.

I always received the unconditional support from my dear friend Jose Luis Macias (Instituto de Geofísica, UNAM) with whom not only shared common and professional interests but also sad moments. No matter what life reserves for us, we will be forever friends. I appreciate the support and friendship of Amy Daniels, Nanang Halik, and Hongzhuan Ye at UT Dallas. I thank also to Patty Ganey-Curry of the UTIG, who always gave me a hand until I finished my dissertation.

I appreciate the financial assistance for my fieldwork provided by the IMP, the Department of Geological Sciences' Geology Foundation, the Geological Society of America (Grant No 6324-98), and the Gulf Coast Association of Geological Societies (Financial Aid-To-Students Grant, 1998). The International Office also provided financial assistance highly appreciated at not easy times. I express to its staff my gratitude for the warm and kind treatment from everyone I

dealed with in that office. I thank in particular to Mrs. Becky Conn, Michael Smith, and my English teacher Robert Johansen. I keep in mind too, a grateful memory of my classmates and friends Gundogan Coskun, Jennifer Beall, Ozgur Sipaougli, Cengiz Tolga Vur, Fachi Liu, Félix Díaz, Orlando Ortega, Mulugeta Fehesa, Janize and José Guzman, Wade Hutchings, Steve Royer, Laura Faulkenberry, Rogeiro Schiffer and Senira Katah; and of Dennis Trombatore, Bill Woods, Amadeo Gonzáles, and Philip Guerrero; staff members always willing to help.

A special and deep acknowledgement is for my dear wife María Teresa Quintana, who was always beside and even in front of me; always reminding me the goal, pointing out and lighting the way with her empowered character, lovely patience, and comprehension. I am proud of my children Alan and Carlos, who did not give up, remained strong, and overcome successfully the cultural and language barriers I never could. When living in Austin, my family and I began to be blessed with the love and friendship of Laura and Daniel Gomez; Sezin and Cem Okan Kilic; Rocío and Baltazar Lucero; and my PEMEX colleagues Faustino Monroy and July; Pedro Gómez and Doris; Jorge Barrios and Norma; Javier Hernández and Paty.

Finally but not less important was the support, in the widest meaning of the word, that my family and I received from my dear mother Cira Santana and my sisters Arbelia, Ale, Juve, Chabe and my brother Robe; our endless gratitude and love for all of them. We also appreciate the support of my cousins Temo, Cecilia, Israel, Adher, Arsemis and La Tia Mago.

SEQUENCE STRATIGRAPHY AND DEPOSITIONAL HISTORY OF THE UPPER CAÑON DEL TULE, LAS IMAGENES, AND LOWER CERRO GRANDE FORMATIONS, CENTRAL PARRAS BASIN, NORTHEASTERN MEXICO.

Publication No. _____

Juan Clemente Bermúdez Santana, Ph. D.
The University of Texas at Austin, 2003

Supervisor: Richard T. Buffler

This dissertation describes the results of a field-oriented sequence stratigraphic study of a 900-m-thick Maastrichtian interval in the middle portion of the Upper Cretaceous Difunta Group. Basic analysis of rock features and their stratigraphic arrangement were used to subdivide the interval into transgressive (TST), highstand (HST), and falling stage (FSST) systems tracts and to recognize their bounding surfaces.

The progradational offshore to lower shoreface highstand (HST) deposits of the upper Cañón del Tule Formation and the underlying transgressive (TST) deposits, contain gastropods and bivalves common in shallow marine Lower Maastrichtian strata. However, the occurrence of the ammonite *Coahuilites sheltoni* restricts these rocks to the lower Upper Maastrichtian.

In the Late Maastrichtian, the final stage of shallow marine sedimentation of the upper Cañón del Tule Formation was characterized by an abrupt change. Accommodation space was reduced in proximal settings, and the shoreline and

coarse-grained facies belts migrated basinward in response to a relative sea level fall (forced regression). Wave scouring of the seafloor, and rip and longshore currents produced a regionally extended forced regression surface and sequence boundary characterized by meter-scale gutter casts.

The FSST upper shoreface to foreshore deposits of the uppermost Cañón del Tule Formation include a ridge-forming sandstone of variable thickness. Its internal stratigraphic architecture suggests that high-frequency pulses of sea level risings punctuated the forced regression. During this process, thick, aggradational red deposits of the lower Las Imágenes Formation (FSST) accumulated over the adjacent coastal plain until an intermittent marine transgression began. The initial transgressive pulses occurred across a rapidly subsiding coastal plain, which favored the development of charophytes in fresh and brackish water environments, associated with benthonic foraminifers, ostracods, oysters, *Ophiomorpha* and *Thalassinoides*. Mixed-load probably meandering rivers drained the coastal plain bounded by lagoons and extensive shoreface and offshore environments for this part of the Late Maastrichtian Gulf Coast of México. After this stage of intermittent marine transgression, shallow seas and transgressive (TST) deposits of the lower Cerro Grande Formation covered the region.

Table of Contents

List of Figures

Note: Figure 3.2 can be printed in a plotter or in a color printer using 11x17" paper size.

List of Plates

List of Attached Oversize Figures

Note: all the attached oversize figures require a plotter to print them.

CHAPTER 1

INTRODUCTION

This dissertation describes the results of a sequence stratigraphic study of a Maastrichtian sedimentary succession confined to the middle part of the Late Cretaceous-Early Tertiary Difunta Group. The studied strata include shallow-marine and coastal plain siliciclastic deposits extensively exposed in the central Parras Basin, northeastern (Figs. 1.1 and 1.2). In this area, the sedimentary rocks of the Difunta Group record three major regressive-transgressive (RT) cycles included within seven lithostratigraphic units overlying the Parras Shale (Fig. 1.2). The seven units include a sedimentary section more than 3700 m thick (McBride *et al*., 1974; Soegaard *et al*., *in press*), whose deposition occurred during alternating regressive and transgressive cycles along the ancient margin of the Gulf of México (Baker, 1970; Crawley, 1975; Warning, 1977).

The study interval is bounded at its bottom and top by maximum flooding surfaces and is roughly equivalent to the entire intermediate RT cycle (Fig. 1.2). At the bottom, the studied sequence mostly includes mudstone and sandstone of the upper Cañón del Tule Formation. Its middle part is a prominent ridge-forming unit composed by stacked upper shoreface to foreshore sandstone of the uppermost Cañón del Tule Formation, overlain by coastal plain red beds of Las Imágenes Formation (McBride *et al*., 1974). On top, the sequence includes shallow marine sandstone, siltstone, and mudstone of the lower Cerro Grande Formation (Fig. 1.2). The study interval in the middle part of the Difunta Group (Fig. 1.2) includes almost 900 m of strata well exposed over an area covering 1700 km^2 (Fig. 1.3). The extensive outcrops in this area provides a valuable opportunity to understand not only the sedimentary evolution of the middle Difunta

Figure 1.1 Regional location map of the Parras, La Popa and south Sabinas basins, northeastern México. The Sierra Madre Oriental (SMO) structural front, the basins outline, and the areas in green mapped as Lower Cretaceous carbonates are taken from Halik (1998).

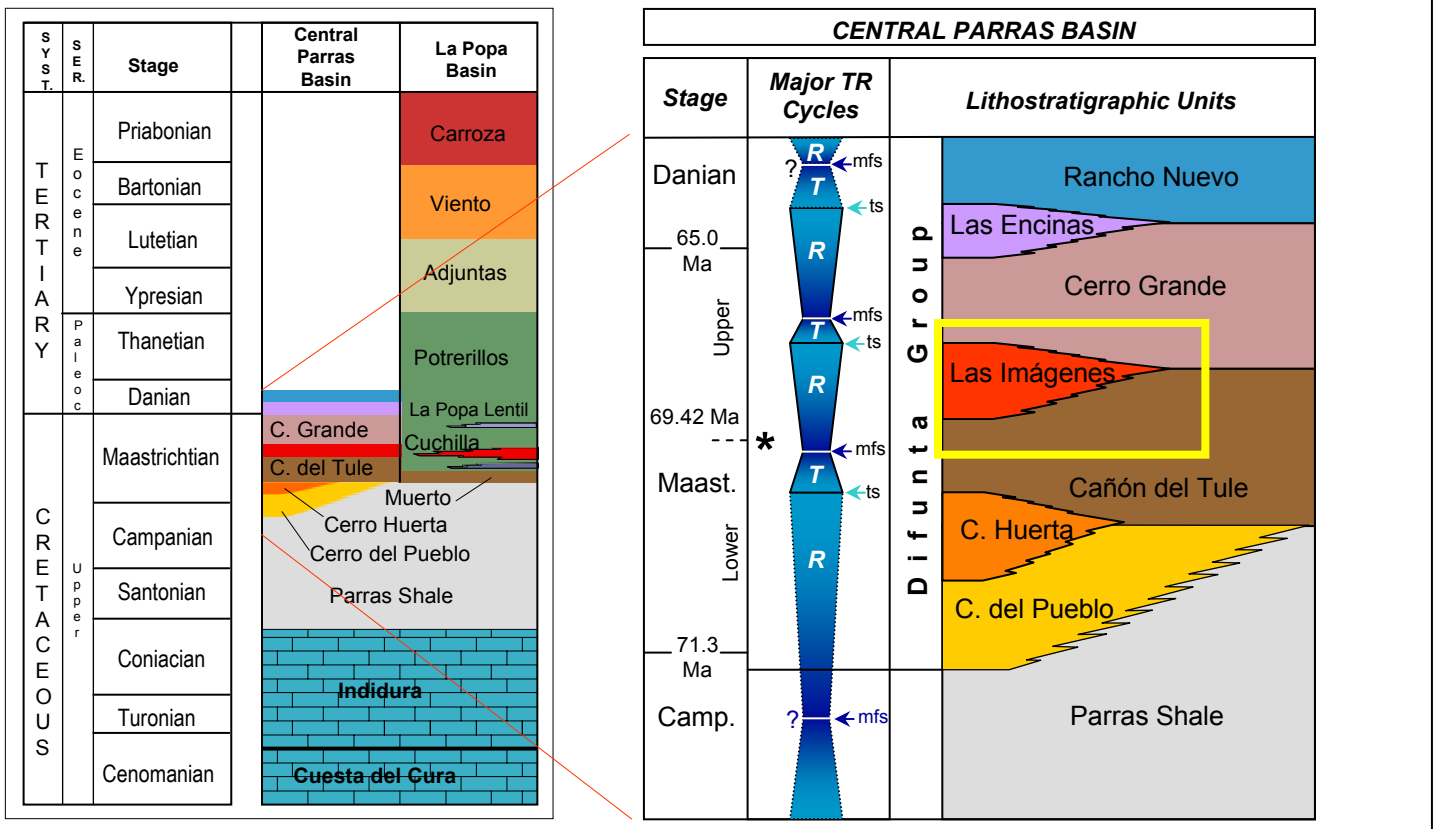

Figure 1.2 Stratigraphic nomenclature of the Difunta Group for the central Parras and La Popa basins, northeastern México. In the central Parras basin (right) the clastic sediments of the Difunta Group record three major regressive-transgressive (RT) cycles. The Cerro Huerta, Las Imágenes and Las Encinas prograding wedges consist mainly of coastal plain red beds deposits. The Cerro del Pueblo, Cañón del Tule, Cerro Grande and Rancho Nuevo formations are composed mainly of shallow marine mudstone and sandstone. The study interval is shown within the rectangle. The asterisk (*) indicates the lowermost stratigraphic ocurrence of *Coahuilites sheltoni* Böse, an index ammonite of the lower part of the Upper Maastrichtian collected from beds of the upper Cañón del Tule. The absolute values for the chronostratigraphic boundaries and informal sub-stages for the Maastrichtian are taken from Hardenbol *et al*., 1998. (ts) transgressive surface; (mfs) maximum flooding surface. Charts construction based on the previous work by McBride *et al*., 1974; Vega-Vera *et al*., 1989 and 1999; Soegaard *et al*., 1997; Soegaard *et al., in press*; and the paleontological information obtained in this study.

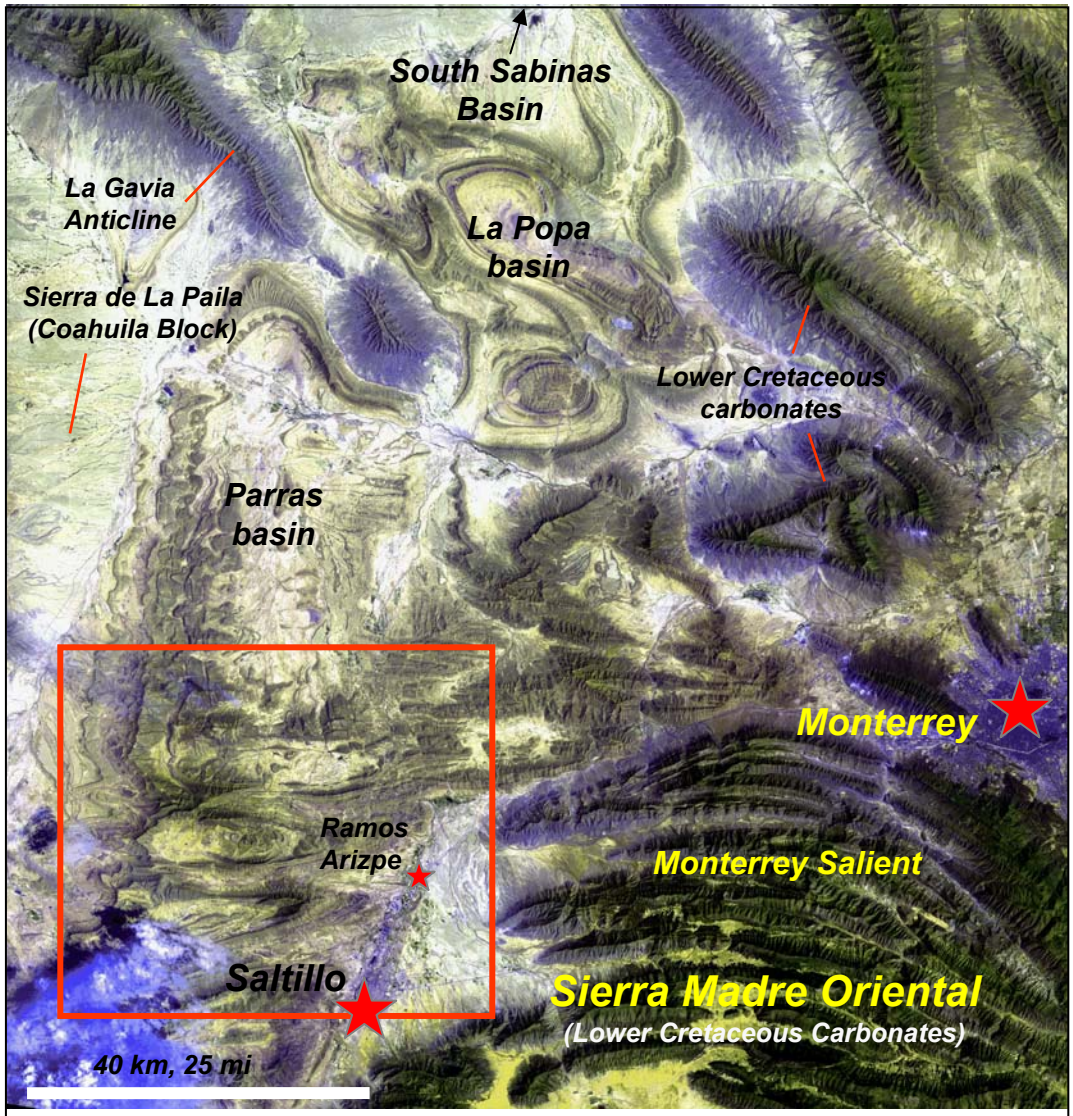

Figure 1.3 Landsat TM scene of the Parras and La Popa basins, northeastern México. The study area within the square covers 1700 km^2 and is located west of the Sierra Madre Oriental (SMO) flexure referred as the Monterrey Salient. Scene obtained by processing the bands 7 (red), 5 (green) and 1 (black). Scene acquisition date: 04/22/86.

Group, but also the depositional history of the Parras Basin and the sedimentary evolution of northeastern México.

Crawley (1975) proposes that the Cerro Grande and other Difunta Group deposits are part of the Cretaceous clastic wedges that accumulated on the east side of the uplifting Cordilleran region of North America. More recent studies in the Parras and La Popa basins propose that the rocks of the Difunta Group were deposited in an extensive foreland basin, filled during the Late Cretaceous-Early Tertiary (Dillman and Casey, 1985; Freydier *et al*., 1996; Ye, 1997; Soegaard *et al*., *in press*). Halik (1998) suggests that the clastic sedimentation in the immediate foreland of the Sierra Madre Oriental extends to the south Sabinas Basin (Fig. 1.3). According to his interpretations, the fluvial-deltaic sediments of the Difunta Group were deposited in a foreland setting similar to those of the Rocky Mountains in the western United States.

However, some special features suggest that the orogenic front now occupied by the Sierra Madre Oriental to the south, was not a source of sediments for the infilling of the adjacent Parras Basin (Fig. 1.3). Even though the Sierra Madre Oriental is basically composed of Lower Cretaceous carbonates, there is a remarkable absence of carbonate fragments within the Difunta Group sandstones (McBride *et al*., 1974; Arney, 1998; Garrick, 1999). Crawley (1975), who studied the composition of pebbles collected from strata of the Cerro Grande Formation, concluded that these coarse well-rounded particles are dominantly composed of Lower Cretaceous chert and have shapes characteristic of river abrasion. He states that their high morphological and compositional maturity suggest transportation of at least 200 km and establishes as the source area the chert-bearing Cretaceous sedimentary rocks in the foothills of the Sierra Madre Occidental in western México.

Moreover, it has been proposed that the sediments that constitute the rocks of the Difunta Group were transported axially into the basin by large rivers flowing from west to east. Crawley (1975), who developed petrographic studies of the Cerro Grande Formation (Fig. 2.1), concluded that the majority of the rocks of this unit are calcite-cemented sandstones and siltstones rich in volcanic rock fragments and plagioclase. According to him, the source areas that supplied detritus for the rocks of the Cerro Grande Formation were largely composed of andesites and rhyolites. He proposes that the source of sediments was located 300 to 600 km west of the depositional site, in the area occupied at the present time by the Sierra Madre Occidental in western México (McBride *et al*., 1974; McBride *et al*., 1975). Based also on petrographic studies of sandstones, Arney (1998) and Garrick (1999) later confirmed that a volcanic arc active during the latest Cretaceous in western México was one of the main sources of sediments for the Difunta Group. They concluded that the Sierra Madre Oriental never supplied detritus to the Parras or La Popa basins, which suggests that the Parras is a unique depositional setting, somewhat different from a typical foreland basin where the main source of sediments is the uplifted fold-thrust belt.

Although the previous works established the basic stratigraphic foundation for the Parras Basin, most of them have a regional character (Imlay, 1936; Weidie, 1961; Murray *et al*., 1962; McBride *et al.*, 1974). Only the most recent studies use sequence stratigraphy approaches (Ye, 1997; Soegaard *et al*., 1997; Halik, 1998; Soegaard *et al*., *in press*). It is noteworthy that in many of the previous studies the fossil content, of particular value for paleoenvironmental interpretations and chronostratigraphic control of the units, has been underestimated. Poor paleontological control has allowed in some cases, the units to be placed within an inaccurate time-stratigraphic framework, which makes difficult interbasinal correlations and the interpretation of the depositional history and tectonic evolution of the Parras and surrounding basins. Detailed sequence stratigraphic studies intended to refine the stratigraphy in this area, must be

supported by a strong paleontological control of the units. This control would facilitate the interpretation of depositional environments, would enable the reliable interbasinal correlation of units, and extend the most significant sequence stratigraphic surfaces across the area.

This field-oriented sequence stratigraphic study focused less on stratigraphic regional issues and more on detailed aspects of an interval limited to the middle portion of the Difunta Group. Its main objective was to place the units and significant stratigraphic surfaces within a sequence stratigraphic frame of reference. The framework was developed through the measurement of sixteen stratigraphic sections with a special attention to their fossil content, stacking patterns, and lithology. As a result, a simplified sequence stratigraphic model supported by new paleontological data with worldwide correlation potential was developed and used to interpret the depositional history of the study interval. Both the model and the interpretation of the sedimentary evolution of the studied strata constitute the most significant contributions of this work.

Additional objectives of this study were to contribute to the understanding of the sources and pathways of sediment supply, evaluate controls of sedimentation, and obtain additional information on the sedimentary petrography of the studied rocks. All of these are topics addressed in this dissertation. A geologic map of the central Parras Basin compiled during the development of this field-oriented project is also included herein as a contribution to support future research within the area.

CHAPTER 2

BACKGROUND

2.1. Location of the Study Area

The Parras Basin is located in the northeastern Mexican State of Coahuila, southwest of Laredo, Texas (Fig. 1.1). Monterrey and Saltillo, the capital cities of Nuevo León and Coahuila, respectively, are the most important urban, industrial, and commercial concentrations in the region. The Parras Basin extends from just east of Torreón in the west, to Monterrey in the east and is bounded to the south by the Sierra Madre Oriental (SMO) fold-thrust belt. The SMO is one of the four main and large mountain chains in Mexico, which constitutes a prominent physiographic and structural feature that extends from central to northwestern Mexico following a southeast to northwest general trend (Figs. 1.1 and 2.1). West of Monterrey, the SMO deformation belt has a particular structural flexure referred as the Monterrey Salient (Fig. 1.3). To the north, the Parras Basin is bounded by the Sierra de la Paila, which is also referred to as the Coahuila Block. This mountain range is composed of Lower Cretaceous carbonates. The northwest-southwest anticline structure named La Gavia defines a structural boundary that separates the Parras from the clastic and carbonate sediments of La Popa Basin to the northeast (Fig. 1.3).

The area studied in this work, located in the central Parras Basin, covers a surface of 1700 km^2. Saltillo (578,046 inhabitants*) and Ramoz Arizpe (39,853 inhabitants*) are the largest cities in the area (Figs. 2.1 and 2.2). Other important

* Source: XII Censo General de Población y Vivienda (2000). Inst. Nacional de Estadística Geografía e Informática (INEGI): http://www.inegi.gob.mx

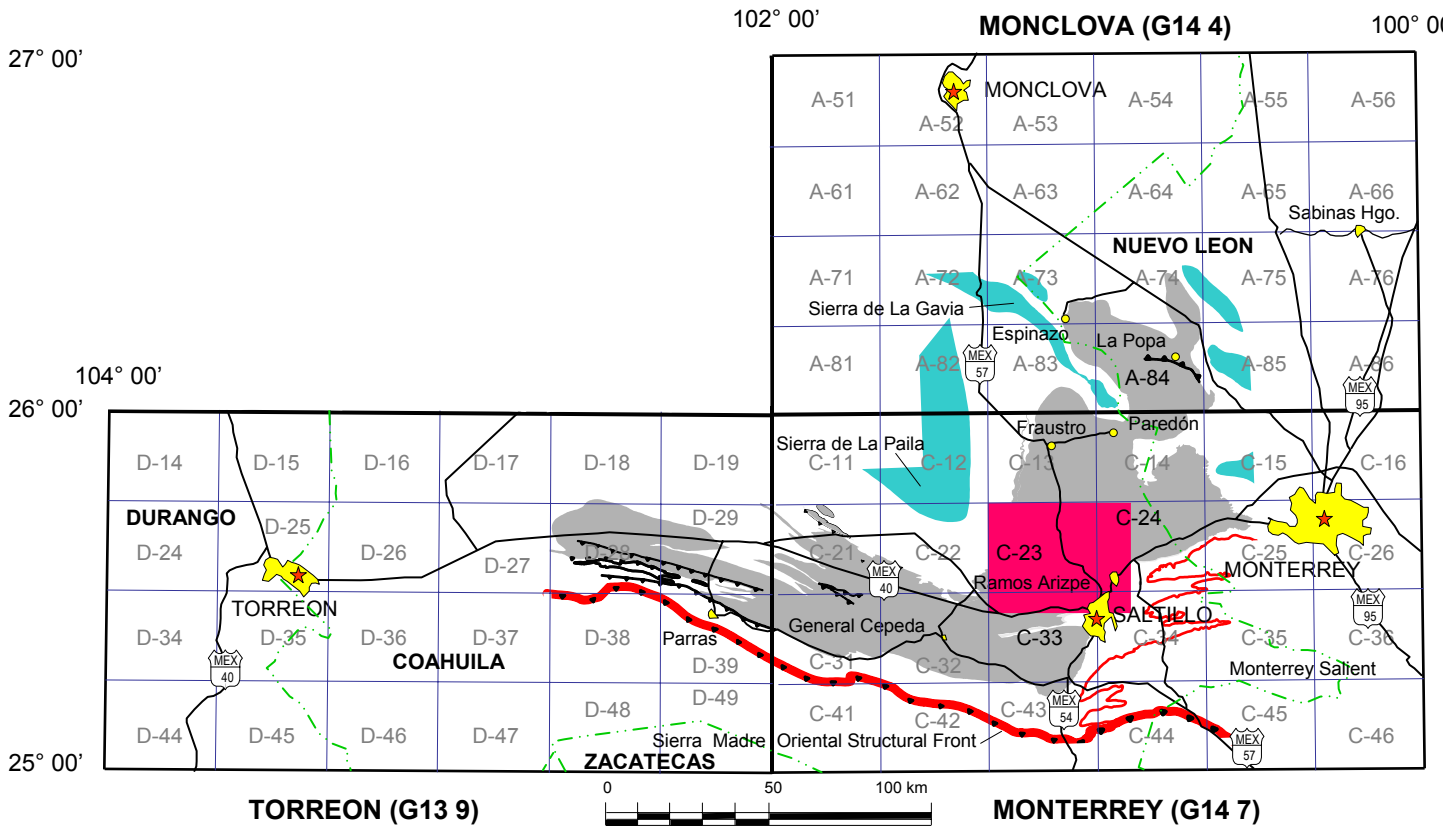

Figure 2.1 Study area location and index map of topographic sheets of the Parras and La Popa basins. Sheets Torreón, Monclova and Monterrey at scale 1:250,000. Small rectangles equivalent to sheets at scale 1:50,000. The study area within the central Parras basin includes the map San Miguel (G14 C23) and partial areas of the Ramos Arizpe (G14 C24), Saltillo (G14 C33) and Arteaga (G14 C34). Basin outline taken from Soegaard *et al*. (1997). Sheets nomenclature by the Instituto Nacional de Estadística Geografía e Informática (INEGI: http://www.inegi.gob.mx)

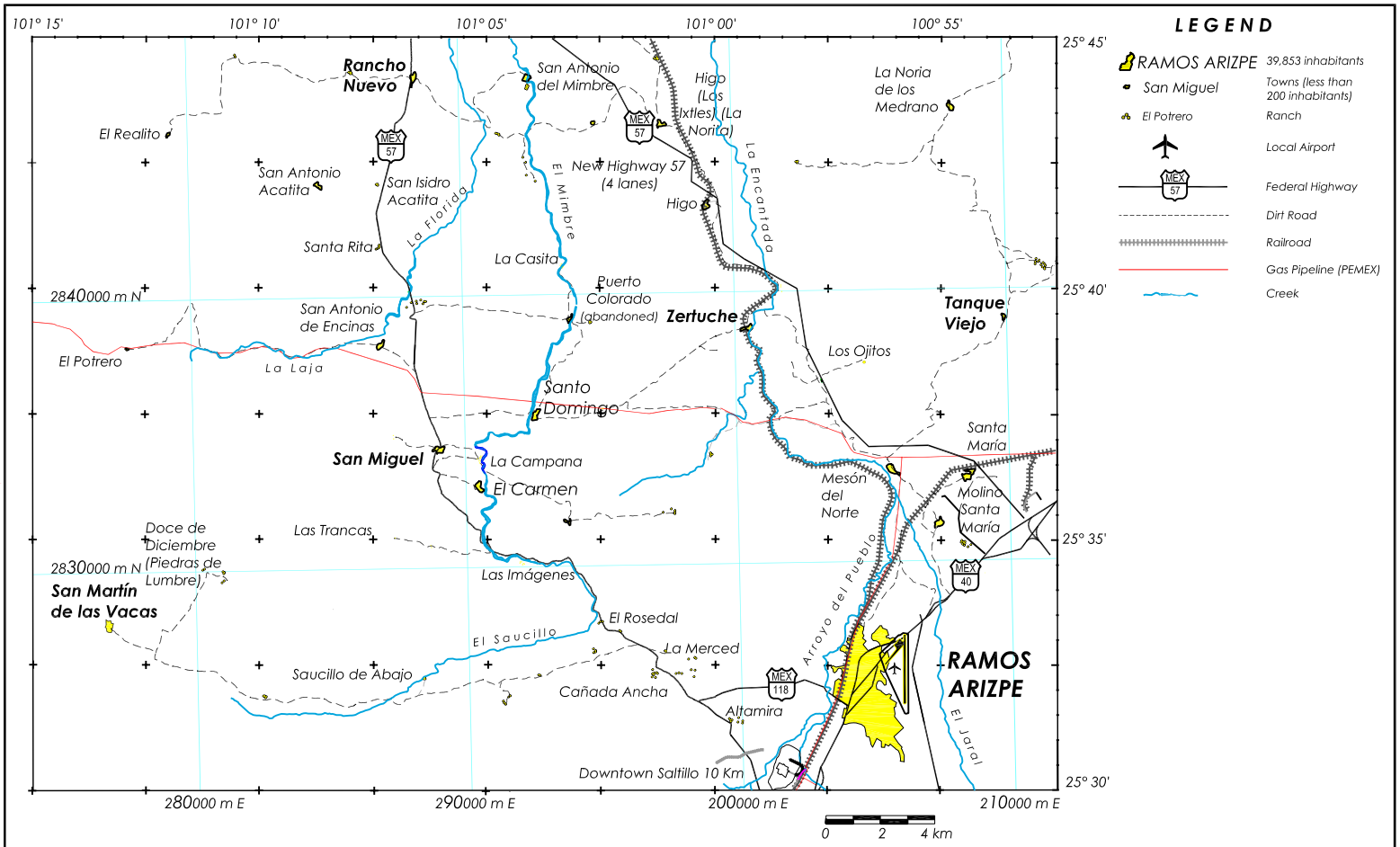

Figure 2.2 Main populations and communications network of the northern study area. Map construction based on the topographic maps scale 1:50,000, San Miguel (G14C23) and Ramos Arizpe (G14C24) edited by the INEGI. The grid in blue = UTM coordinates; the grid in black (crosses) = geographic coordinates. A geologic map of the central Parras Basin covering the whole study area (1700 square Km) is included in the Appendix A.

localities are Rancho Nuevo to the north; Tanque Viejo and Zertuche to the east; San Antonio de Encinas, Santo Domingo and San Miguel in the central portion; and El Saucillo de Abajo and San Martín de las Vacas to the south and southwest (Fig. 2.2).

The network of roadways includes the old Federal Highway 57, the new four-lane Highway 57, and Highways 54 and 40 (Fig. 2.2). Railroads connect Torreón, Saltillo, and Monterrey with the rest of the country; and a network of dirt roads and trails access the main towns, villages, and ranches. A gas pipeline property of Petróleos Mexicanos (PEMEX) crosses the entire study area from west to east. The main perennial creeks within the area are La Laja-La Florida on the west, El Saucillo-El Mimbre in the middle part, El Jaral-Arroyo del Pueblo and La Encantada to the east (Fig. 2.2).

2.2. Tectonic Setting

The initial studies by Imlay (1937) of the clastic sediments of the "*Difunta Formation*" suggest that sedimentation during the Campanian occurred in a slowly sinking Parras geosynclinal basin, surrounded by elevated land masses of Lower Cretaceous limestone. Weidie *et al.* (1966) and Weidie and Murray (1967 conclude that the Upper Cretaceous and lower Tertiary clastic sediments of the Difunta Group were deposited in deltaic environments. According to them, deltas were located within the subsiding Parras Basin and adjacent areas between the present-day Sierra Madre Oriental and the carbonate Coahuila Platform (Fig. 1.3). They point out that although the Parras Basin had been previously considered to be a "foredeep", there was little or no evidence to apply this term to the basin. Weidie and Murray (1967) disagreed with the use of the term "foredeep" because they also conclude that the Parras Basin was not formed adjacent to any active orogenic belt and that the basin never was deep. McBride *et al.* (1971) describe similar conclusions when they suggest that the clastic sediments of the Difunta

Group in the Parras Basin were deposited in deltaic environments within a shallow embayment off the ancestral Gulf of Mexico. Later, McBride *et al.* (1974) also recognize that particular definitions of a “foredeep” basin were applicable to the Parras and La Popa basins, but decided avoid the use of this term because of its ambiguity.

Based on fieldwork and satellite imagery interpretation, Dillman and Casey (1985) made a structural and tectonic interpretation of the Parras Basin, which they consider an erosional remnant of a Maastrichtian-Paleocene foreland basin. According to them, early thrusting of the thick Mesozoic carbonates of the SMO and flexure of the foreland produced an asymmetrical depression and thick accumulations of detritus along the SMO structural front (Fig. 2.1).

As pointed out by Ye (1997), diverse interpretations have been proposed to explain the origin of the Parras Basin. For instance, the Parras has been considered as a cratonic, transpressive-controlled, strike-slip or normal fault-controlled basin. A different interpretation based on regional tectonics and stratigraphic studies have led Freydier *et al*. (1996), Ye (1997), and Soegaard *et al* (*in press*) to propose that the sediments of the Difunta Group in the Parras-La Popa basins are remnants of an extensive foreland basin filled during the Latest Cretaceous-Early Tertiary. The studies by Ye (1997), Halik (1998), and Soegaard *et al*. (1997) emphasize the geometry of the basin. They define a thickening of lithostratigraphic units on the south and southwest Parras Basin and interpret considerably higher rates of subsidence in the areas adjacent to the SMO structural front (>1 m/1000 yr according to Soegaard *et al*., *in press*). However, they recognize that the Sierra Madre Oriental fold-thrust belt was not a positive element during the Difunta Group deposition and concluded that the effect of topographic load created by the modest relief of the SMO is not sufficient to explain the high rates of subsidence and great cumulative thickness in the Parras Basin.

Ye (1997) proposes that the differential high subsidence and exaggerated thickness of the Difunta Group of more than 6000 m (Soegaard *et al*., *in press*) can be explained as a consequence of subcrustal load produced by a subduction process. Subduction involved collision and the final suture between eastern Mexico and the Guerrero terrane (Freydier *et al*., 1996). This event involved westward subduction, the consumption of an oceanic crust beneath the Guerrero terrrane, and the final closure of the Arperos Basin leading to a suture between the two crustal blocks below the SMO fold-thrust belt (Freydier *et al.* 1996; Ye, 1997; Soegaard *et al*., *in press*). Halik (1998) also proposes that the clastic sedimentation in the immediate foreland of the Sierra Madre Oriental extends to the south Sabinas Basin (Fig. 1.3). He states that the fluvial-deltaic sedimentary rocks of the Difunta Group were deposited in a foreland setting similar to those of the Rocky Mountains in the western United States. Soegaard *et al*. (*in press*) consider the Powder River and San Juan basins of the western U.S. as analogous of the Difunta foreland basin (Freydier *et al*., 1996; Halik, 1998), which includes the Parras, La Popa and south Sabinas basins.

Although the Parras resembles a foreland basin, the features described in the previous paragraphs suggest that this basin is a unique depositional setting, somewhat different from a typical foreland basin where the main source of sediments is an uplifted fold-thrust belt. For purposes of comparison the tectonic and structural elements, geometries of units and sources of sediment supply in a foreland basin are described in Figure 2.3. DeCelles and Giles (1996) recognize four discrete depozones and define a foreland basin system as elongated regions of sediment accumulation that form between a contractional orogenic belt and an adjacent craton. According to them, this contractional process is the result of geodynamics related to the orogenic belt and its associated subduction complex. They also point out that it is generally accepted that the foreland basin sediments are derived mainly from an active contractional orogenic fold-thrust belt with less sediment input derived from the cratonward side of the basin. The orogenic

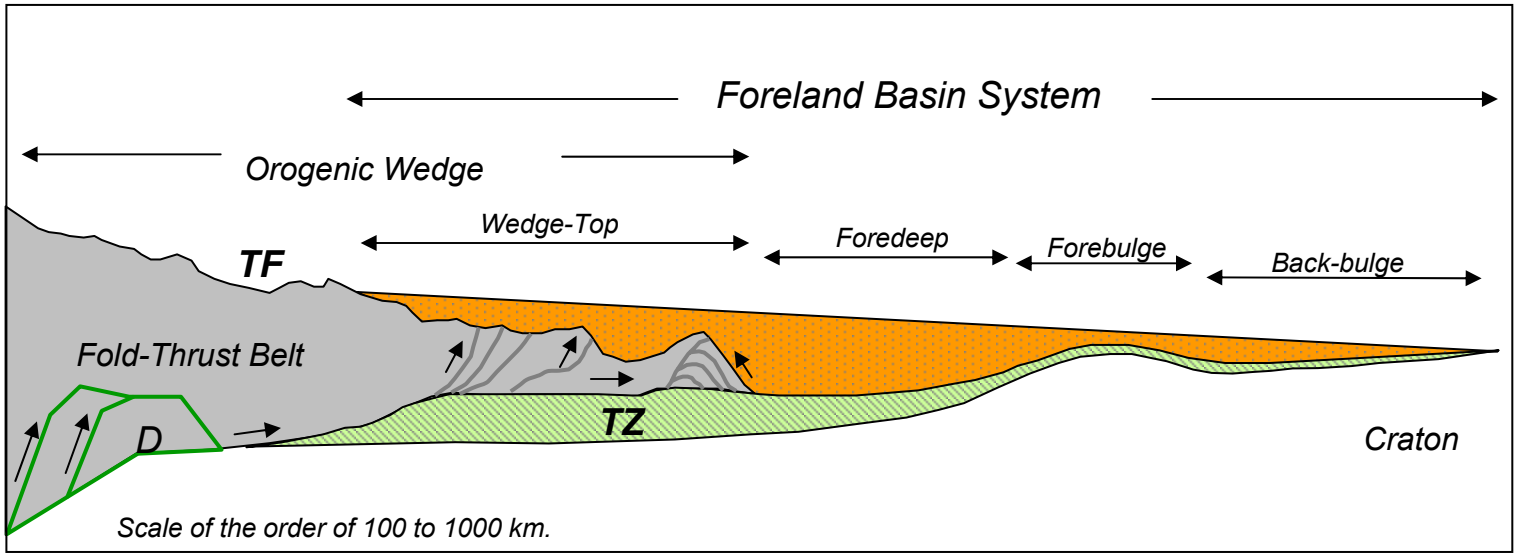

Redrawn from an original figure by Decelles and Giles (1996).

TF: Topographic Front of the Thrust Belt.
D: Schematic Duplex.
TZ: Frontal Triangle Zone.

Figure 2.3 Schematic cross section of a *Foreland Basin System.* Structural elements and four depozones are shown at approximately proportional scale. In a foreland basin the main source of sediment supply for the infilling of the depozones is the fold-thrust belt. Higher rates of subsidence in the inmediate foredeep produced major accomodation space and thicker units toward the orogenic front and thinner toward the craton.

wedge-top (Fig. 2.3) is the proximal depozone adjacent to the orogenic belt characterized by sediments accumulated on top of the inverse faulted frontal sector of the orogenic wedge, including “piggy back” and thrust top basins. Extreme coarseness, common tectonic unconformities, and progressive deformation characterize the deposits of this depozone. The foredeep is the space of major sediment accumulation between the front of the orogenic wedge and the forebulge. The sedimentary units deposited in the foredeep thicken considerably and interfingers with the distal sediments of the wedge-top depozone. The foredeep sediments are mainly derived from the fold-thrust belt with minor contributions of the forebulge and craton. The backbulge is the depozone adjacent to the craton, which receives sediments both from the forebulge and from the cratonic area in the distal part of the foreland basin system.

Several studies describe how the Difunta lithostratigraphic units thicken toward the Saltillo area (McBride *et al*., 1974; Crawley, 1975; Ye, 1997; Halik, 1998). High rates of subsidence and stratal geometries resembling a foredeep depozone have also been interpreted and described by Ye (1997), Halik (1998), and Soegaard *et al.* (1997). However, there are some special features that differentiate the Parras from a foreland basin system previously described in the scheme of DeCelles and Giles (1996; Fig. 2.3). For instance, the SMO orogenic belt was not the source of sediments, as would be expected in foreland basins. Even though the Sierra Madre Oriental is basically composed of Lower Cretaceous carbonates, there is a remarkable absence of carbonate fragments within the Difunta Group sandstones (McBride *et al*., 1974; Crawley, 1975; Arney, 1998; Garrick, 1999). Furthermore, it has been proposed that the sediments were transported axially to the basin by large rivers flowing from west to east. Apparently the sediments were eroded from hinterlands located somewhere in the area occupied at the present time by the Sierra Madre Occidental, in western Mexico (McBride *et al*., 1974; McBride *et al*., 1975). Crawley (1975), concluded

that an alluvial plain laid between the source area and the shoreline of the Cerro Grande Formation, in the middle Difunta Group (Fig. 2.4).

Petrographic studies of sandstones of the Difunta Group developed by Arney (1998) and Garrick (1999) conclude that the main source of sediments for the infilling of the Parras and La Popa basins was an ancient volcanic arc active during the latest Cretaceous in western Mexico. A paleogeographic reconstruction map of northern Mexico for the Maastrichtian illustrates the uplifted and deposition areas. The map shows the Alisitos Magmatic Arc as the main provider of sediments for the Parras, La Popa, Sabinas basins and all of eastern Mexico (Goldhammer and Johnson, 2001, Fig. 2.4)

All of the previously mentioned stratigraphic, sedimentologic, and tectonic features make the Parras Basin remarkably interesting, especially when considering that its Difunta Group sedimentary fill records the tectonic and sedimentary evolution from the Campanian to Early Tertiary. In particular, the study of the central sector of the Parras Basin where the Difunta Group is well exposed, is important for the interpretation of its depositional history and for better understanding of the tectonic evolution of northeastern Mexico (Fig. 1.3).

2.3 Stratigraphy

The initial geologic studies that describe the rocks now included within the Difunta Group began with some general reports of Cretaceous rocks in the Parras Basin area (Hill, 1891; Burckhardt, 1930). Some other studies were published to describe Cretaceous and Tertiary fossils in northern Mexico and southern Texas (Böse, 1906; 1928). The interested reader may consult Murray *et al.* (1962), who

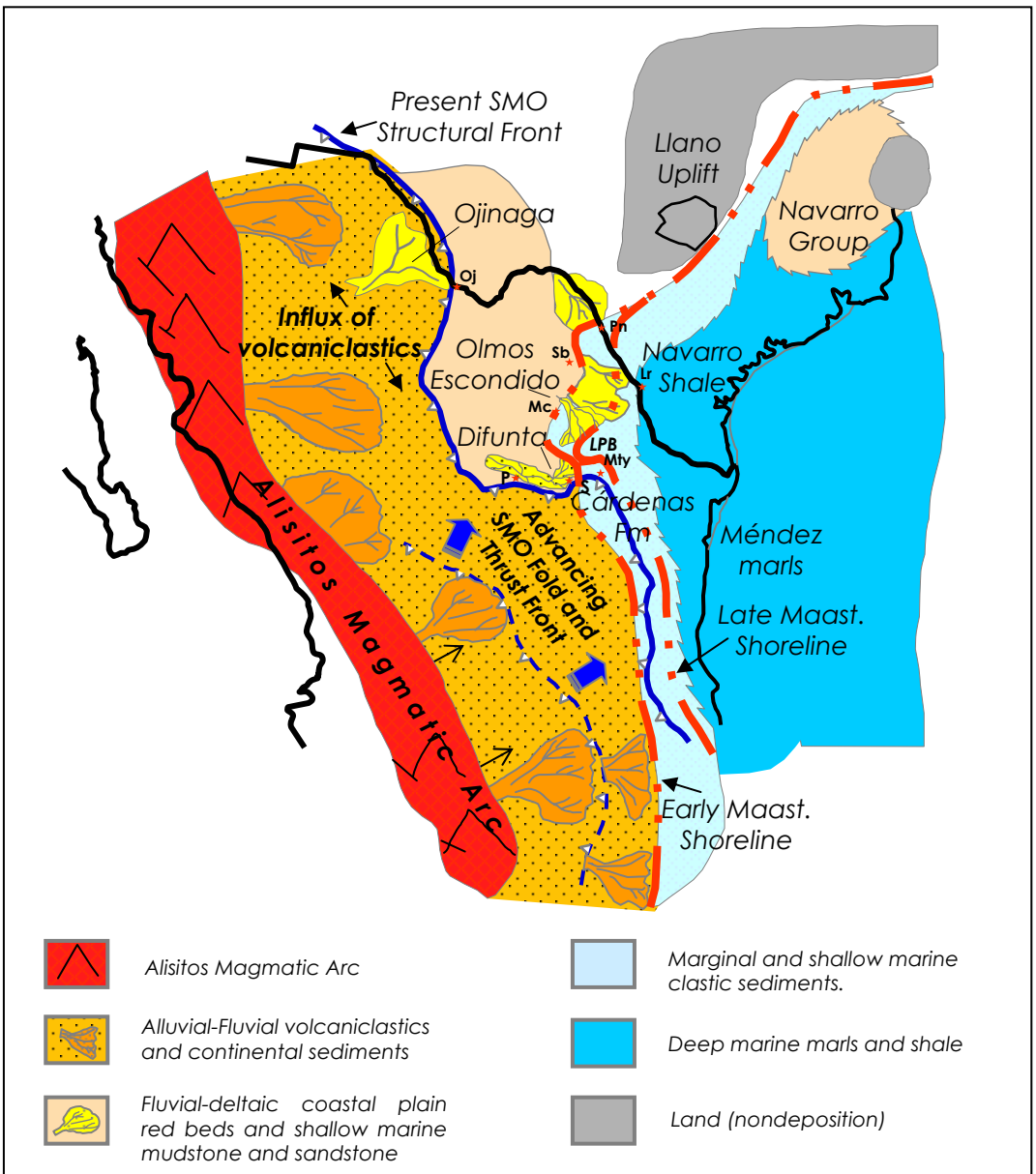

Figure 2.4 Northern México paleogeographic map for the Maastrichtian. Large amounts of coarse volcaniclastic sediments were eroded from an inland-migrating magmatic arc and deposited in alluvial-fluvial systems. Extensive fluvial-deltaic and shallow marine sedimentation occurred eastward of the advancing Sierra Madre Oriental deformation belt during a regional eastward migration of the shorelines. Fluvial-deltaic sedimentation has been reported in the Parras, Sabinas and Ojinaga basins. Modified from Goldhammer and Johnson (2001) and complemented with the paleogeographic sketches by Ye (1997); and Araujo and Estavillo (1985). Mty: Monterrey; S: Saltillo; P: Parras; Mo: Monclova; Oj: Ojinaga; Pn: Piedras Negras; Lr: Laredo; LPB: La Popa Basin. Refer to the text for additional explanation.

provide a longer list of previous works that deal with different topics related to the Parras Basin. The term *Parras Basin* was initially used by Imlay (1936, 1937), who mapped and described a series of latest Cretaceous clastic rocks extensively exposed on the eastern side of the Laguna de Mayran, northwest of the City of Parras (Fig. 2.1). The word *Parras* is used in Spanish language to name the grape-producing plant also known as vid. Imlay (1936, 1937) named the Parras Basin after the City of Parras de la Fuente (Fig. 2.1), founded in 1598 and named as the *Villa de Santa María de las Parras* by the Spaniard explorer Captain Antón Martín Zapata and the jesuit priest Juan Agustín de Espinosa (web page http://www.parrascoahuila.turincon.com, maintained by Samuel Ulloa, Parras City chronist; 2003). Imlay (1937) also coined the terms *Parras Shale* and *Difunta Formation*. The first term has remained in the current stratigraphic nomenclature (Fig. 1.2); the second one was redefined by Weidie (1961), who elevated the *Difunta Formation* to the rank of group. Weidie also proposed the first scheme of subdivision of the Difunta Group into seven formations and provided the first geologic map of the Parras Basin. Later, Murray *et al*. (1962) formalized the formational subdivision by describing type localities for the seven units of the group in the Parras Basin (Fig. 1.2). The word *Difunta* is used in Spanish to refer to a dead woman; apparently, Imlay (1936) took the name from the *Cerro* (mountain) or *Arroyo* (creek) Difunta located in his study area.

The coastal plain and shallow marine sedimentary rocks of the Difunta Group in the Parras and La Popa basins were deposited during alternating progradational and retrogradational episodes that produced a complicated intertonguing of rock units and vertical superposition of facies (Fig. 2.5). Based on alternating clastic wedges and sandstone marker-beds, McBride *et al.* (1974) synthesized the stratigraphy and structure of the Difunta, subdividing the group into seven formations in the western and central Parras Basin. The Cerro Huerta, Las Imágenes, and Las Encinas formations consist mainly of delta-plain and flanking coastal-plain red bed prograding wedges (McBride *et al.,* 1974), which

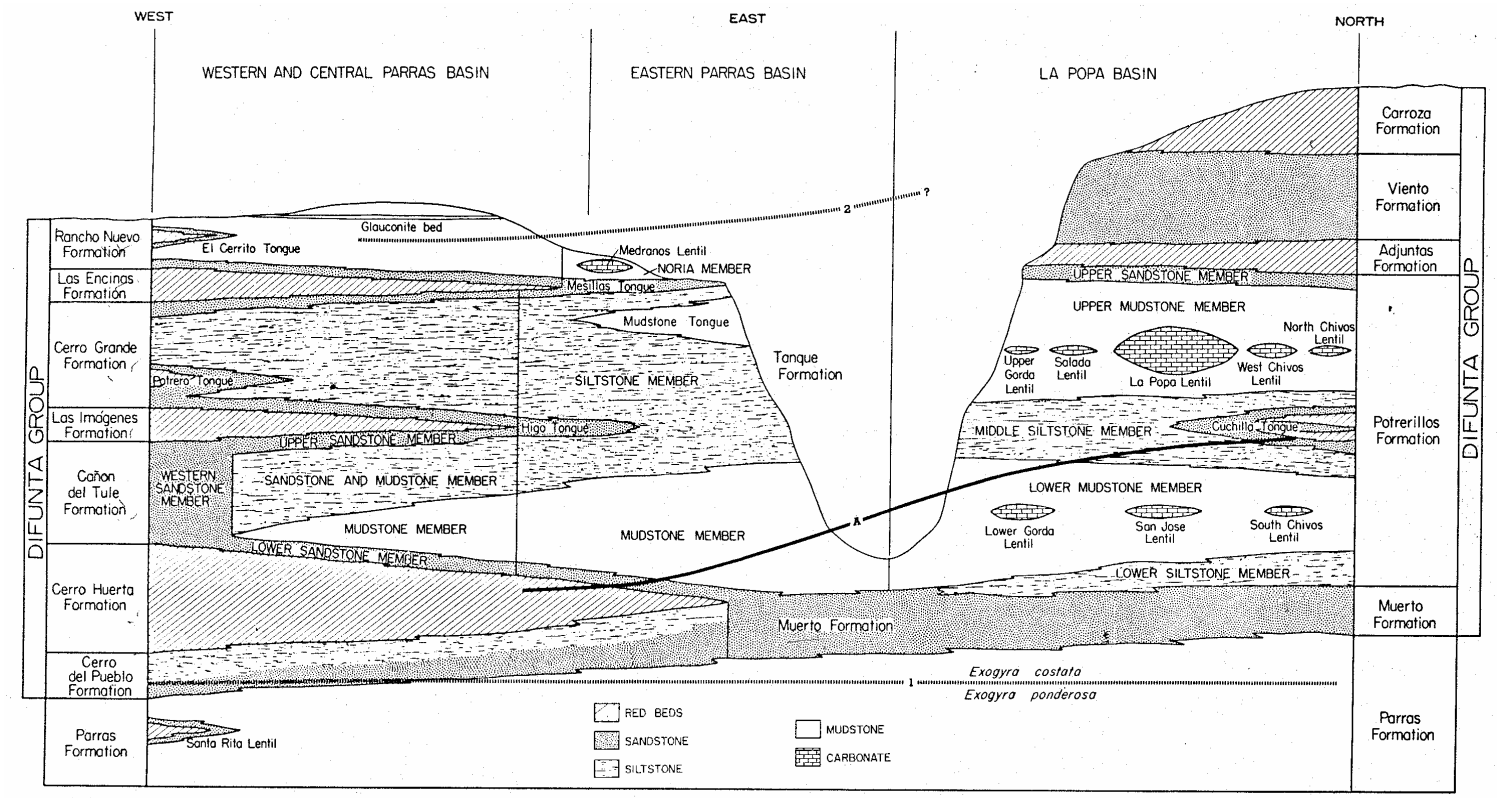

Figure 2.5 Stratigraphy and correlation between the Parras and La Popa basins. Based on alternating clastic wedges the Difunta Group was subdivided into seven formations in the central Parras Basin. A stratigraphic complexity and a poor paleontological control produced the units have been placed within an unaccurate time-stratigraphic framework. Two possible options are proposed in this correlation where only the Muerto formation can be mapped between the Parras and La Popa basin. Line A correlates the Cerro Huerta, Las Imagenes and Las Encinas formations with the Cuchilla Tongue, Adjuntas and Carroza formations, respectively (see also Fig. 2.7, Scheme A) . Option B (see Fig. 2.6, Scheme B) assumes that lines of correlation are parallel with the event 1 throughout the section. (Adapted from McBride *et al*., 1974).

extend laterally along the basin and pinch out into marine units within the eastern Parras and La Popa Basin. The Cerro del Pueblo, Cañón del Tule, Cerro Grande and Rancho Nuevo formations are mostly composed of shallow marine mudstone and sandstone.

The initial correlations between the Parras and La Popa Basin were uncertain because only the Muerto Formation could be mapped across both basins (McBride *et al.,* 1974; Fig. 2.5). In addition, the absence of diagnostic fossils and a complex stratigraphy compelled McBride *et al.* (1974) to propose two options of correlation for the rocks of the Difunta Group. In Scheme A (Figs. 2.5 and 2.6), the Cerro Huerta, Las Imágenes and Las Encinas formations in the Parras Basin correlate respectively with the Cuchilla Tongue, Adjuntas, and Carroza formations in La Popa Basin. This scheme assumes that the Rancho Nuevo Formation is exclusive of the Parras Basin (Fig. 2.6, Scheme A). The second option, Scheme B, assumes that the lines of correlation are parallel with the Event 1 defined by the last occurrence of *Exogyra ponderosa* and the first appearance of *Exogyra costata*, a Late Cretaceous bivalve. According to this second option, the Cerro Huerta, Las Imágenes, and Las Encinas formations are equivalent to the Muerto, Cuchilla, and Adjuntas formations (Fig. 2.6, Scheme B). Paleontologic data also allowed McBride *et al.* (1974) to assign the Difunta Group a range from the latest Campanian to earliest Paleocene, tentatively placing the Cretaceous-Tertiary boundary within the Rancho Nuevo and the Carroza formations (Fig. 2.6, Scheme B).

After the studies developed in the 1970's (Baker, 1970; McBride *et al*., 1974; Laudon, 1975; Crawley, 1975; Warning, 1977), the chronostratigraphic framework of the Parras Basin was modified with the incorporation of new paleontological data. Vega-Vera and Perrilliat (1989) dated the Adjuntas Formation as early Eocene based on the presence of the mollusks *Venericardia planicostata* and *Turitella mortoni postmortoni*. In the same year, Vega-Vera *et al*.,

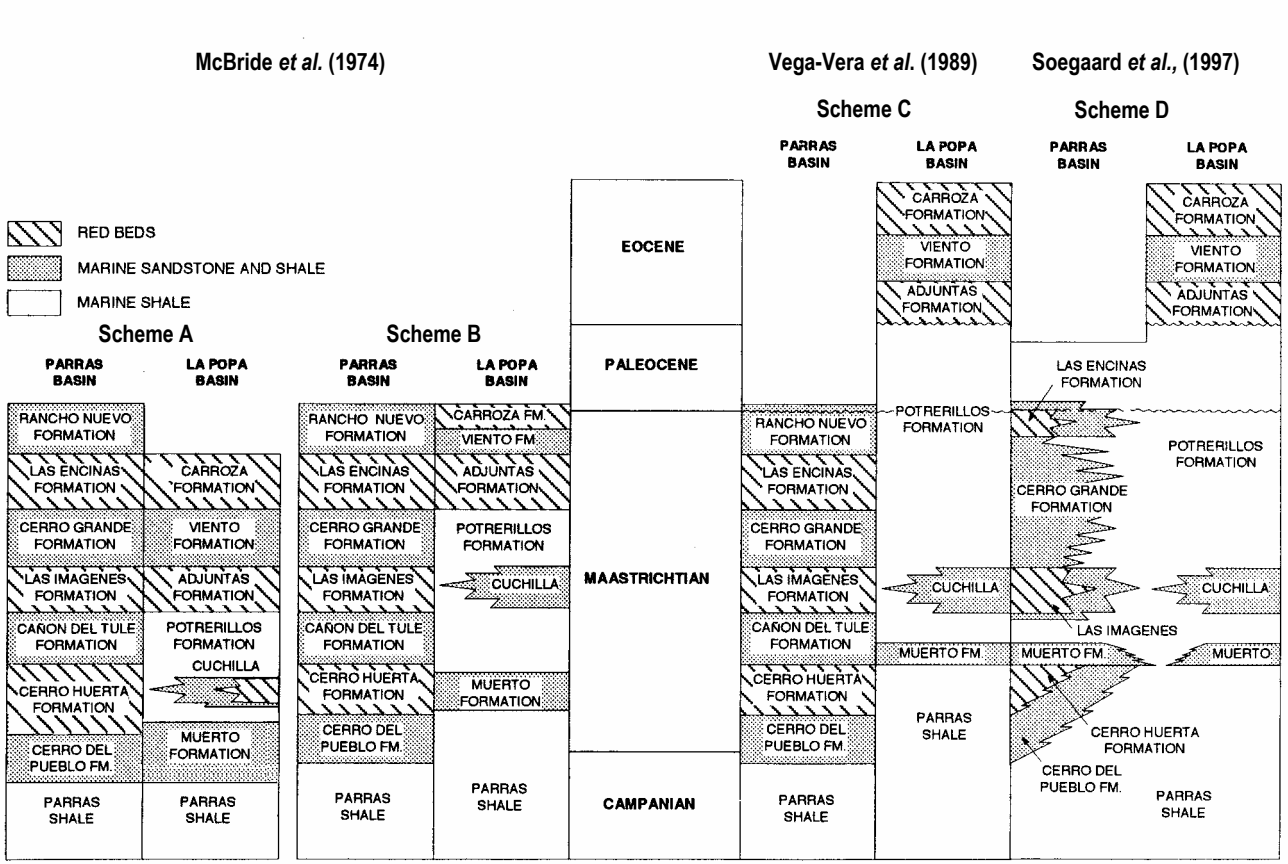

Figure 2.6 Correlation schemes for the lithostratigraphic units of the Difunta Group, Parras and La Popa basins. Schemes A and B were modified according to the original cross section by McBride *et al.* (1974, Fig. 2). Note that Scheme D represents a tentative revision of the stratigraphic subdivision outlined by McBride *et al.* (1974, Schemes A and B) and Vega Vera *et al*. (1989, Scheme C). Modified from Soegaard *et al*. (1997).

(1989) reported several specimens of *Cimomi haltomi*, a nautiloid found both in the Potrerillos and the Rancho Nuevo formations. The occurrence of *C. haltomi* allowed them to document the presence of Paleocene strata and to conclude that the Cretaceous-Tertiary boundary was included within these two formations (Fig. 2.6, Scheme C). Later, based on new discoveries of ostreids by C. Perrilliat (preliminary unpublished report), Soegaard *et al*. (1997) proposed moving the position of the Cretaceous-Tertiary boundary downward, from the upper Rancho Nuevo into Las Encinas Formation (Fig. 2.6, Scheme D). Soegaard *et al*. (1997) also proposed a tentative revision of the stratigraphic subdivision for the Difunta Group. In this latest scheme, they abandon the term Rancho Nuevo Formation in order to avoid stratigraphic truncations and favor extending the Potrerillos Formation into the northeastern Parras Basin (Fig. 2.7).

All the contributions mentioned above made possible a better understanding of the stratigraphy of the Parras Basin and provided a valuable starting point for the development of this research project. However, although the previous works established the stratigraphic foundation for the Parras Basin, most of them have a regional character and only the most recent studies use sequence stratigraphy approaches (Ye, 1997; Halik, 1998; Soegaard *et al*., *in press*). Ye (1997) in particular, provides the first sequence stratigraphic framework for the synorogenic Difunta Group deposits. His work made important conceptual changes concerning the basin geometry and its stratal architecture, providing an explanation on differential rates of subsidence based on the regional tectonics of the Parras, surrounding foreland basins, and the tectonic evolution of the Sierra Madre Oriental.

The study by Halik (1998) focuses less on regional tectonic issues and addresses detailed aspects of a limited interval in the middle part of the Difunta Group including the Cañón del Tule and the Muerto formations. Undoubtedly, his most important contribution is the detailed description of his studied interval and

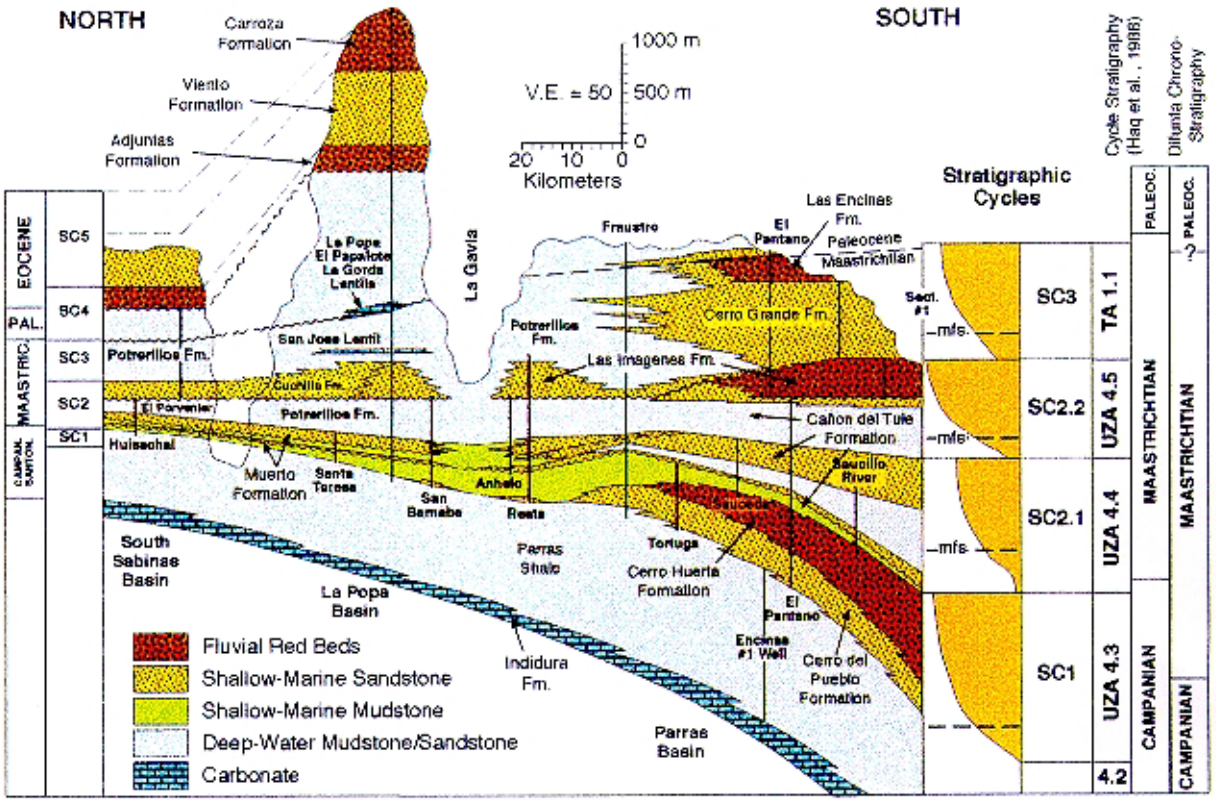

Figure 2.7 Revised stratigraphy of the Parras, La Popa, and south Sabinas basins. The Difunta Group is sudivided into five stratigraphic cycles, overall progradational units, whose boundaries coincide with the top of fluvial red beds overlain by fossil-bearing marine rocks. Note that in order to avoid truncations, Soegaard *et al*. (1997) proposed to abandon the term Rancho Nuevo Formation (uppermost Difunta Group in the Parras basin) and to extend the Potrerillos Formation into the notheastern Parras Basin. Original figure from Soegaard *et al*. (1997); stratigraphic cycles added by Halik (1998). Reproduced under the kind permission of Dr. Kristian Soegaard.

the identification of significant sequence stratigraphic surfaces (i.e., regressive surfaces of submarine erosion) that were extended beyond lateral facies transitions and correlated across the entire Parras, La Popa, and south Sabinas Basin. Halik (1998) also proposes an informal subdivision of the Difunta Group recognizing five stratigraphic cycles. Each cycle is bounded by a transgressive surface that separates fluvial red beds below from fossil-bearing marine transgressive sediments above (Fig. 2.7). The major sequence stratigraphic surfaces bounding systems tracts interpreted in this study are labeled following the stratigraphic nomenclature proposed by Halik (see Halik's Fig. 2.7; 1998).

The recent studies within the Parras Basin (Ye, 1997; and Halik, 1998) included an extensive mapping program of the Difunta Group using remote sensing techniques, airborne panoramas, and aerial photographs. These studies established the basis for a more refined stratigraphy and a better understanding of the lateral equivalence of the units (Fig. 2.7). More recently, Soegaard *et al*. (*in press*) compiled most of the previous work including stratigraphic, sequence stratigraphic, paleontological, and petrographic data from Arney (1998) and Garrick (1999). This compilation provides an integrated interpretation of the Difunta foreland basin within a regional tectonic context. According to Soegaard *et al.* (*in press*), the Difunta basin evolution can be subdivided into two depositional stages. An initial stage controlled by subsidence that mostly affected the early evolution of the Parras Basin, and a late stage in which the emplacement of salt strongly influenced the final depositional history of La Popa Basin (see also Lawton *et al*., 2001).

2.4 The Study Interval

The stratigraphic interval subject to study and described in this dissertation is confined to the middle portion of the Difunta Group (Fig 1.2). It includes from the bottom to the top, the shallow marine rocks and the coastal plain red beds

deposited during an overall regressive episode (upper Cañón del Tule and Las Imágenes formations) and the overlying marine strata deposited during a subsequent transgressive event (lower Cerro Grande Formation). This regressive-transgressive (RT) major cycle is one of at least three major cycles recorded by the Difunta Group in the central Parras Basin. Every regressive cycle is bounded at the bottom by a maximum flooding surface (mfs); and a transgressive surface (ts) on top of the red sediments of every prograding wedge. The study interval includes a maximum thickness of almost 900 m of siliciclastic rocks well exposed over an area of 1700 km^2 (Fig. 1.3), described and studied at sixteen stratigraphic sections (Fig. 2.8).

2.5 Objectives and Significance of Research

In some of the previous studies of the Parras Basin the fossil content, of particular value for paleonvironmental interpretation and an accurate chronostratigraphic control of the units, has been underestimated. Several factors including a poor paleontological control, the remarkable thickness of the Difunta Group consisting of more than 6000 m of sediments, a complex stratigraphy accentuated by lateral changes of facies, similar lithologies, studies of regional character, etc., have produced units that have been placed within an inaccurate time-stratigraphic framework. Uncertainties on the age of the units produced wrong schemes of correlation that affected the interpretation of the sedimentary evolution and basin geometry. The stratigraphic understanding and the initial schemes of correlation in the Parras Basin have evolved and been gradually improved once new biostratigraphic surveys have been incorporated (McBride *et al*., 1974; Vega-Vera *et al.,* 1989; Soegaard *et al*., 1997; Halik, 1998; Soegaard *et al*., *in press*; Figs. 2.5 to 2.7).

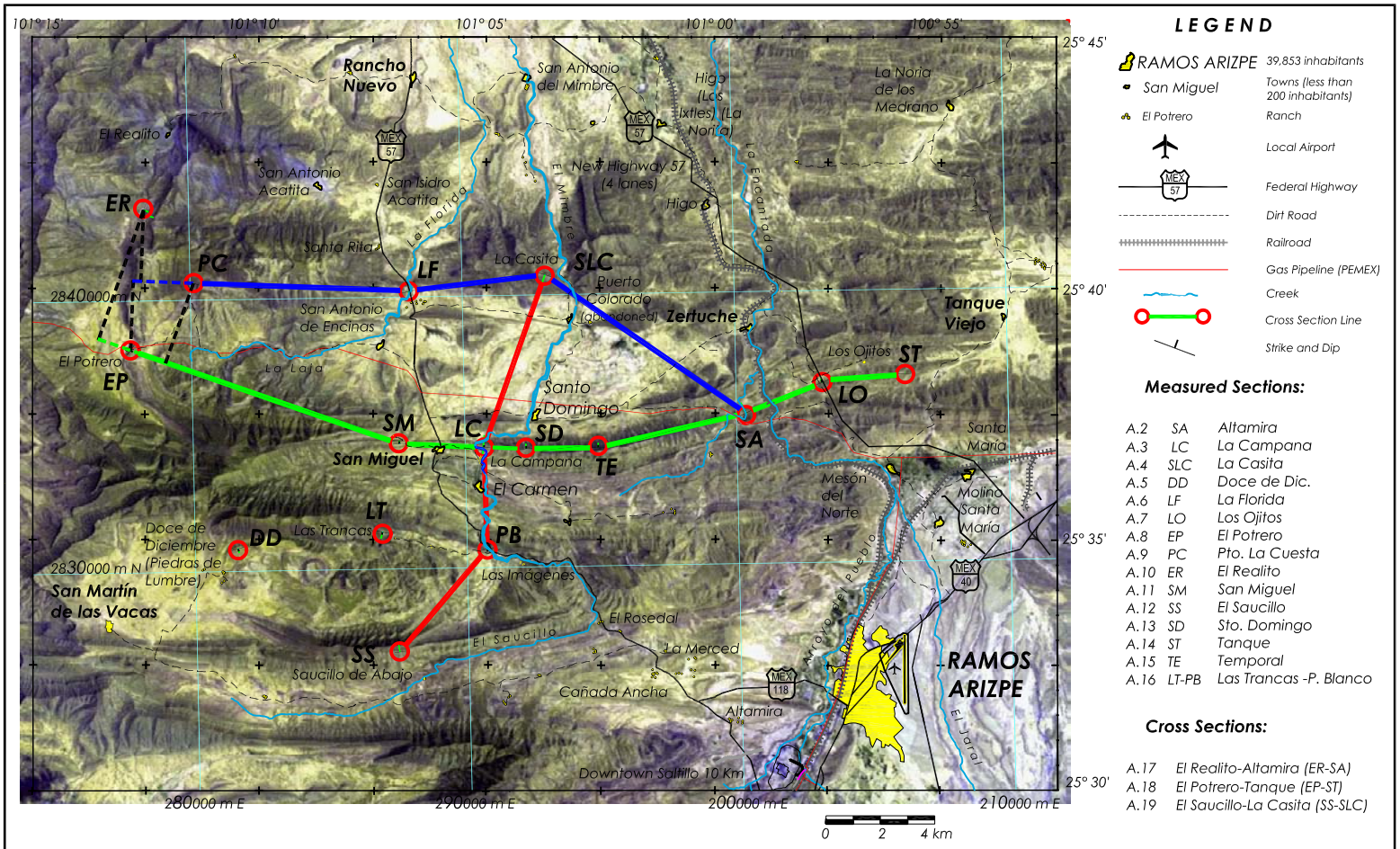

LEGEND

RAMOS ARIZPE — 39,853 inhabitants
San Miguel — Towns (less than 200 inhabitants)
El Potrero — Ranch
Local Airport
Federal Highway
Dirt Road
Railroad
Gas Pipeline (PEMEX)
Creek
Cross Section Line
Strike and Dip

Measured Sections:

A.2	SA	Altamira
A.3	LC	La Campana
A.4	SLC	La Casita
A.5	DD	Doce de Dic.
A.6	LF	La Florida
A.7	LO	Los Ojitos
A.8	EP	El Potrero
A.9	PC	Pto. La Cuesta
A.10	ER	El Realito
A.11	SM	San Miguel
A.12	SS	El Saucillo
A.13	SD	Sto. Domingo
A.14	ST	Tanque
A.15	TE	Temporal
A.16	LT-PB	Las Trancas -P. Blanco

Cross Sections:

A.17 El Realito-Altamira (ER-SA)
A.18 El Potrero-Tanque (EP-ST)
A.19 El Saucillo-La Casita (SS-SLC)

Figure 2.8 Location of the studied sections and cross sections lines of correlation. The dashed lines in black, perpendicular to the lines in colors, indicate the projection of one section to the main line of correlation. The cross sections and stratigraphic columns are included in Appendix A (Figs. A.2 to A.19).

This study utilized a sequence stratigraphic approach to describe a particular interval in the central Parras Basin. It is considered that detailed studies intended to refine the stratigraphy in the Parras and surrounding basins must be supported by a systematic paleontological control of the units instead of isolated paleontological surveys. Therefore, the establishment of a sequence stratigraphic framework based on the detailed measurement of continuously exposed stratigraphic successions, with special attention to their fossil content, was the main objective of the project. It was also considered that placing the units within a frame of time is of particular importance to interpret the depositional history of the studied interval and is the initial step to place the most significant sequence stratigraphic surfaces within an interbasinal scheme of correlation and regional context.

The current knowledge about sources and dispersal pathways suggest that sediments were carried from west to east into the Parras Basin, supplied from volcanic-plutonic sources located in western Mexico (McBride *et al*., 1974; Crawley, 1975; Arney, 1998; Garrick, 1999. Fig. 2.4). A related goal of the project was to provide additional data about depositional environment of sandstones based on petrographic studies. Additional objectives were to evaluate the role that an axial input of sediments and differential subsidence played as controls of sedimentation, as well as to understand the influence that these controls exerted over the facies distribution and units geometries. In general, this sequence stratigraphic study was intended to interpret the depositional history of the study strata.

The regional evolution of northern Mexico for the Late Cretaceous-Early Tertiary is related to the Laramide orogeny. This tectonic event produced uplift and a progressive eastward advance of the front of deformation of the SMO fold-thrust belt and an associated general eastward migration of the shorelines (Goldhammer and Johnson, 2001; Fig. 2.4). Once the Difunta Group was

exposed in the Early Tertiary, the eroded siliciclastic rocks became the source of sediments for the infilling of the Burgos, Tampico-Tuxpan, and oil-producing basins in the Gulf of Mexico. Therefore, contributing to the refinement of the stratigraphy and understanding of the depositional history of the Parras Basin is crucial to understanding the evolution of the surrounding basins in northeastern Mexico.

2.6 Field and Laboratory Procedures

This study was a field- and laboratory-oriented project. The primary data of research were outcrop information obtained from sixteen measured sections (Fig. 2.8), whose added thicknesses are almost 4000 m (about 2.5 mi) of stratigraphic section.

Measurement of Stratigraphic Sections

Measured sections are scattered within the study area (Fig. 2.8). They were measured using a 2-m-long graduated stick, range finder, tape, and compass and described at meter-scale. Most of them represent continuous exposures of sedimentary successions (see the attached oversize Figs. A.2 to A.16). During the measuring process, paint marks spaced every 1 m apart were made on the outcrops for use as description and sampling references. The marks remained on the outcrops to facilitate the identification of specific horizons for subsequent additional sampling after the initial paleontologic or petrographic studies, and for additional stratigraphic observations.

For most of the measured sections, two horizons were useful as valuable horizons of reference. The first one, also used as a “zero mark”, was a distinctive sharp erosional surface of regional extent located at the bottom of a thick sandstone unit at the uppermost Cañón del Tule Formation. A second one was the contact of the previously mentioned sandstone unit with the red sediments of

Las Imágenes Formation (see La Campana or El Saucillo sections for reference, Figs. A. 3 or A.12). The thickness of this sandstone body ranges from 2 m to 65 m from one to another location. The distinctive surface at its base is well-exposed and its easy to identify throughout the area. Geographic coordinates of all of the measured sections were obtained with a GPS instrument, either for the zero marks of reference or for any other particular horizon.

The geologic contacts and surfaces mentioned in the previous paragraph were used as lines of reference for the construction of three sequence stratigraphic cross sections of correlation. A charophyte-bearing interval was also an important stratigraphic level of reference, especially for the western part of the study area. The location of the measured sections and the orientation of the cross section lines of correlation are shown in Figure 2.8. The sequence stratigraphic cross sections are attached at the end of document (Figs. A.17 to A.19).

Description and Recording of Outcrop Data

The measurement of the stratigraphic sections included outcrop description and direct recording of stratal thicknesses, lithology, grain size and grain size trends, sedimentary structures, and relative degree of bioturbation. Outcrop descriptions allowed a precise recording of vertical trends of stacking patterns, lithology, and grain size variations. These data in combination with fossil content were the main criteria to propose the position of significant stratigraphic surfaces (i.e., maximum flooding and transgressive surfaces) and for paleoenvironmental interpretations.

Fossil Recovering, Sampling, and Biostratigraphic Studies

Special attention was paid to the fossil content of the studied sections. Only selected horizons considered favorable for each particular purpose or fossil

group were sampled. The macrofossils collected include ammonites, gastropods, and bivalves. Thin sections of some samples were made in order to study their microfossil content, especially from the shallow marine rocks of the upper Cañón del Tule and the lower Cerro Grande formations. Microfossils observed in thin section include benthonic foraminifers, ostracods, and diverse biogenic and shell fragments. Aditionally, 19 samples were processed to study their calcareous nanofossil content. Fossil content, except charophytes, was studied by paleontologist of different institutions (see acknowledgements).

A well-preserved and abundant assemblage of charophyte gyrogonites and small thin-shelled ostracods were recovered and completely isolated from the containing sediment. Samples were collected at several locations from outcrops of Las Imágenes Formation. The charophyte gyrogonites are calcified, coarse to fine-grained sand-size, spherical to ovoidal fossilized particles. They are described in the literature as remains of aquatic plant-like organisms with genetic affinity to green algae. These fossils are commonly found in non-marine sedimentary rocks since the Silurian, with a few species living today in fresh to brackish water environments (Tappan, 1980). In two locations, the gyrogonites of Las Imágenes Formation are confined in cemented horizons associated with benthonic foraminifers and ostracods. Due to their excellent preservation and morphological diversity, Chapter 4 describes and illustrates some specimens of the charophyte assemblage found in Las Imágenes Formation. The author of this dissertation partially described and identified some of the specimens.

Treatment of Charophytes-bearing Samples and SEM Analysis

Sample treatment for biostratigraphical studies were performed by conventional techniques used by every fossil group specialist. Because charophyte gyrogonites were mostly confined in soft clay, lab treatment for these samples consisted of a simple washing technique using sieves and fresh water.

The recovered specimens were immersed in a solution of acetone and placed within a sonic vibrator during 5 to 10 minutes to remove clay remains. In order to obtain SEM photographs, some selected gyrogonites were mounted on a small platform and introduced within a BAL-TEC carbon vaporizer model CED030, where the microfossils were covered by a vaporized carbon layer at vacuum conditions. The Scanning Electron Microscope used in this study, was a Carl Zeiss equipment model DSM 960A, installed at the laboratory of petrography and diagenesis of the Instituto Mexicano del Petróleo (IMP) at Mexico City, operated by a technician of the same institution (see acknowledgements).

X-rays and Chemical Analysis of the Charophyte-bearing Clays

The charophyte gyrogonites of Las Imágenes Formation were recovered from horizons of white greenish clay interbedded with red mudstone and siltstone. Semi-quantitative chemical and x-ray analyses of three samples of the charophyte-bearing clays were performed to obtain their elemental and clay composition. Analyses were performed at the labs of the Instituto de Geofísica (UNAM) and Universidad Mihoacana at Morelia City (see acknowledgements).

Petrographic Studies

Several thin sections of sandstones were qualitatively studied focusing on the observation of framework components and the interpretation on provenance; no grain counting was done. Studied thin sections were selected from major sandstone units of the upper Cañón del Tule and Las Imágenes Formation. All photomicrographs included in this dissertation were taken using conventional petrographic microscope equipped with a digital image analyzer.

2.7 Geologic Map of the Central Parras Basin

During the fieldwork conducted in this study, multiple observations were made about the distribution of lithostratigraphic units. New outcrop locations never previously identified were mapped and new field observations were made. All these observations were used to compile a preliminary geologic map of the study area (Fig. A.1). The geologic map was constructed with the aid of a base map that includes the main cities, towns, highways, dirt roads, railroads, pipelines, as well as the most important creeks in the area. All of these features were digitized from topographic maps at scale 1:50,000 edited by INEGI (http://www.inegi.gob.mx), a Mexican government institution. The topographic sheets and their nomenclature used for the compiling process of the base map are indicated in Figure 2.1.

The mapped lithostratigraphic units in the geologic map (Fig. A.1) include the Parras Shale and the seven formations that comprise the Difunta Group in the central Parras Basin (Fig. 1.2). The units are labeled following the stratigraphic nomenclature defined by McBride *et al.* (1974). The mapping process was performed using a complete set of INEGI´s air photographs that include the lines 145 to 151, scale 1:75,000, taken in 1994 and 1991, in a north-south flight direction. The most important geologic contacts and mapped units were checked in the field and geographic coordinates of some outcrops were obtained with a conventional GPS instrument. The geologic map was also compiled with the support of previous geologic maps of McBride *et al*. (1974) and Soegaard *et al.* (1997). A Landsat TM image of northeastern Mexico was also valuable for the mapping process. The details of the Landsat image are indicated in Figure 1.3.

The compiled base map was reduced to the appropriate scale to fit the air photographs scale and the photo interpreted geologic units. The produced geologic map proved to be useful for the fieldwork, since it contains the most important roadways, infrastructure and populations centers useful as references. The geologic map of the central Parras Basin compiled during the course of this

study (Fig. A.1) is herein presented as a contribution that can be used as a starting point for future research in the area. The geologic map is still preliminary and incomplete, especially in the eastern part of the study area, where additional fieldwork observations are needed. The work developed during the construction of the new four-lane Highway 57 in the eastern study area exposed new outcrops and the new roadway connects localities of previous difficult access.

CHAPTER 3

SEQUENCE STRATIGRAPHY: SYSTEMS TRACTS AND BOUNDING SURFACES; FACIES ASSOCIATIONS

3.1 Generalized Stratigraphy and Sequence Stratigraphic Model

Sequence stratigraphy and interpreted facies association of the middle Difunta Group are summarized in a general stratigraphic column based on La Campana Section (Figs. 3.1 and A.2). For description and identification purposes, the major surfaces bounding systems tracts are conventionally labeled following the stratigraphic cycles' nomenclature proposed by Halik (see Halik's Fig. 2.7; 1998). The study interval is 358 m thick at La Campana Section and is confined within the stratigraphic cycles SC 2.2 and SC 3 (Fig. 2.7). More precisely, the study interval lies between the maximum flooding surfaces MFS 2.2 and MFS 3, which occur within the shallow marine clastic sediments of the upper Cañón del Tule and the Cerro Grande formations (Fig. 3.1). The intervals below and above the bounding flooding surfaces were also studied in the measured sections for stratigraphic and stacking pattern control. These intervals are also described in this chapter to place the description within a general sequence stratigraphic context.

An idealized sequence stratigraphic model based generally on the longest east-west El Potrero-Tanque cross section (Fig. A.18) and other measured sections, provides a general overview of the study interval. The model illustrates also the interpreted system tracts, their bounding surfaces, facies associations, and main lines of correlation (Fig. 3.2). When possible, the bounding surfaces and units are described in this chapter in stratigraphic order, from the bottom to the top. In this descriptive process, both the generalized stratigraphic column (Fig. 3.1) and the sequence stratigraphic model (Fig. 3.2) are frequently cited for a quick identification of the units and surfaces described. The reader, however, is

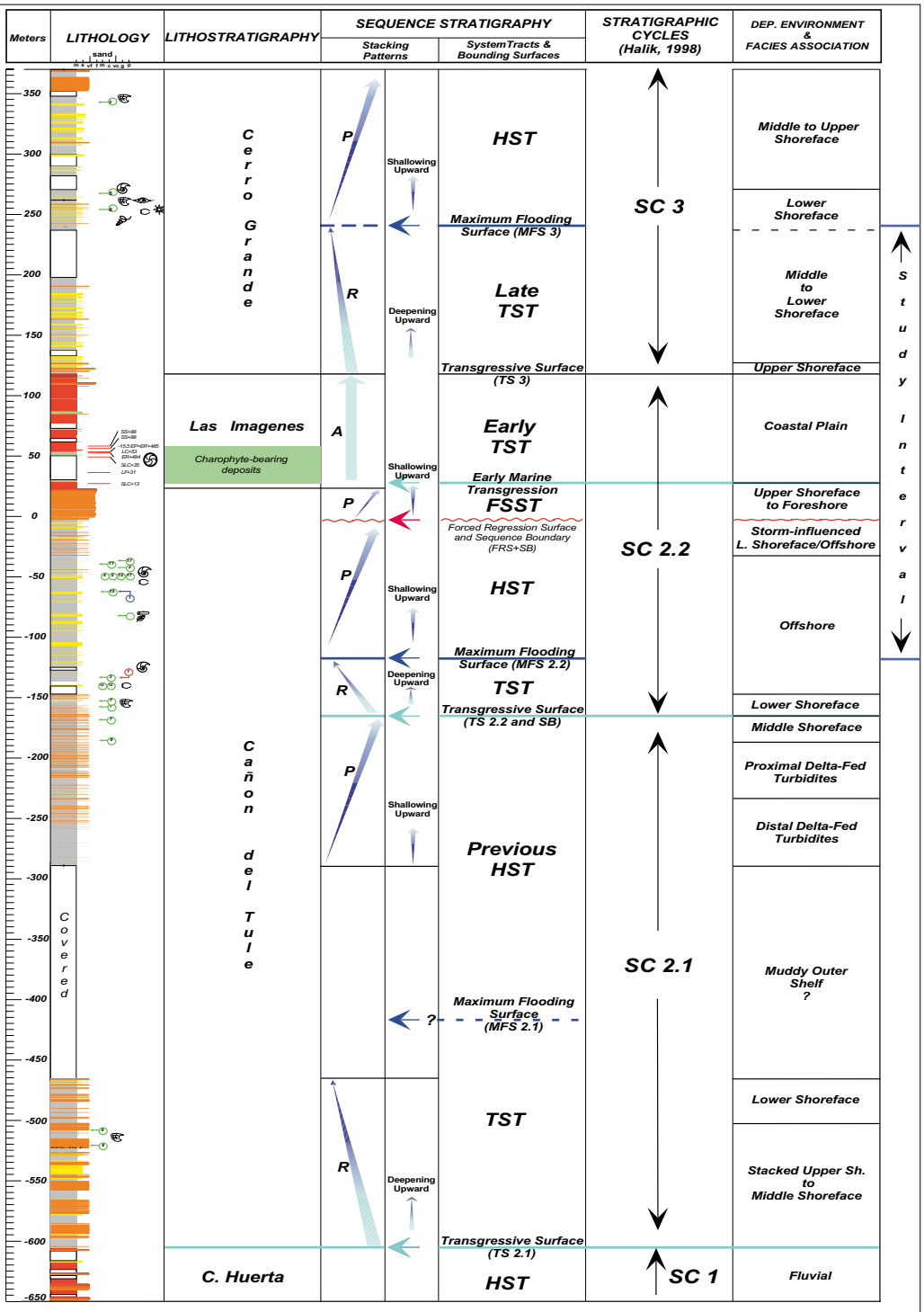

Figure 3.1 Generalized stratigraphic column of the middle Difunta Group at La Campana Section. The study interval is included between the MFS 2.2 and the MFS 3. Stratigraphic cycles proposed by Halik (1998). (P) Progradational, (A) aggradational and (R) retrogradational stacking patterns. Note that fossils occur adjacent to flooding surfaces. See the text and Fig. A.3 for symbols explanation.

Figure 3.2 The Previous HST, the TST, and the HST deposits of the upper Cañón del Tule Formation include a succession of shallow marine rocks deposited in offshore to lower shoreface environments within a ramp-type foreland basin, where the highest subsidence was localized in the western proximal settings. These deposits change laterally eastward to their deeper equivalents in distal areas subjected to sediment starvation and condensed sedimentation. The MFS 2.2 lies within a thick muddy interval underlain by fining- and deepening-upward deposits characterized by a retrogradational stacking pattern (TST). Thickening and shallowing-upward strata (HST) overlie the same surface. The MFS 2.2 defines the lower boundary of the study interval. Both the TST and HST deposits contain an assemblage of gastropods and bivalves typical of the Early Maastrichtian. However, the occurrence of the index ammonites *Coauhuilites sheltoni* and *C. cavinsi* within the same beds, indicates a lower Upper Maastrichtian age for these deposits.

The erosional vacuity below the FSST sandstone unit in orange shown in (b) represents a diachronously developed unconformity and sequence boundary (FRS-SB). The forced regression surface and sequence boundary (FRS+SB) originated during a sea level fall that exceeded the subsidence rate, reduced accommodation space in nearshore proximal settings, and forced the shoreline and facies belts to migrate basinward. The erosional vacuity was produced by multiple surfaces of submarine erosion that partially removed the deep HST deposits and cannibalized much of the laterally equivalent FSST deposits (yellow-green FSST unit). Consequently, relatively deeper-water highstand (HST) deposits (muddy offshore to lower shoreface) are overlain directly by coarser and shallower upper shoreface to foreshore sandstone (orange FSST). Over the adjacent coastal plain, thick, mostly aggradational red deposits of the lower Las Imágenes Formation (FSST) accumulated. In the central Parras Basin, the forced regression process produced submarine erosion along 24 km in a west to east direction and for at least 170 km in a north to south direction. The contact between the coastal plain FSST red deposits and the underlying shallow marine FSST sandstone is gradational and suggests a smooth shoreline regression, which did not involve fluvial incision, erosion, or sequence boundary development. Eventually the FSST red beds of the coastal plain extended to the east and northeast, reaching their maximum areal distribution.

Following the maximum east and northeast progradation of the FSST red deposits, a relative sea level rise began and the shoreline started to migrate landward. In the eastern study area, a subtle change from progradational to retrogradational stacking patterns and deepening-upward conditions suggest the development of the transgressive surface TS 3 and deposition of the overlying Early TST sediments. In this area, the transgressive surface (TS 3) was inferred to be located at the top of the thinnest and more distal expression of the FSST deposits (orange FSST sandstone) within a completely marine section, where the FSST red beds of the lower Las Imágenes Formation are absent (Altamira Section). In the coastal plain, some horizons of the Early TST red deposits contain rare benthonic foraminifers, ostracods, oyster shell deposits, and highly bioturbated red beds. Additionally, an abundant, diverse, and well-preserved assemblage of fossil charophytes within a regionally extended interval of Las Imágenes Formation suggests that the initial transgressive pulses favored the development of charophytes within marginal marine settings (marshes, small lakes or ponds, and lagoons). Above the charophyte interval, widespread sandstone sheets with benthonic foraminifers and echinoderm plates also suggest intermittent signals of transgression across a rapidly subsiding coastal plain.

Finally, the shoreline definitively migrated landward, shallow seas gradually covered the coastal plain, and fine-grained marine transgressive deposits (Early and Late TST) of the lower Cerro Grande Formation were diachronosusly deposited over the red Early TST deposits of Las Imágenes Formation. In the central study area, transgressive upper shoreface sandstones were deposited over the red Early TST mudstones of Las Imágenes Formation (La Campana Section, Fig. 3.20). In some locations, the transgressive surface TS 3 is characterized by a lag of chert pebbles and *Glossifungites* (commonly observed at firmgrounds of transgressive surfaces); and the overlying deposits contain a diverse assemblage of marine fossils. In the western part of the study area, the Late TST fine-grained marine deposits overlie non-red fluvial conglomerates. The Late TST deposits of the lower Cerro Grande Formation are a fining- and deepening-upward succession that becomes muddier upward, to the MFS 3, the upper boundary of the study interval. This surface lies within a fossiliferous gray mudstone with rotalid-type benthonic foraminifers and echinoderm fragments. Above the MFS 3, a progradational succession of mudstone, siltstone, and upward-thickening sandstones were deposited in lower to upper shoreface environments. See the text and figures for additional explanations.

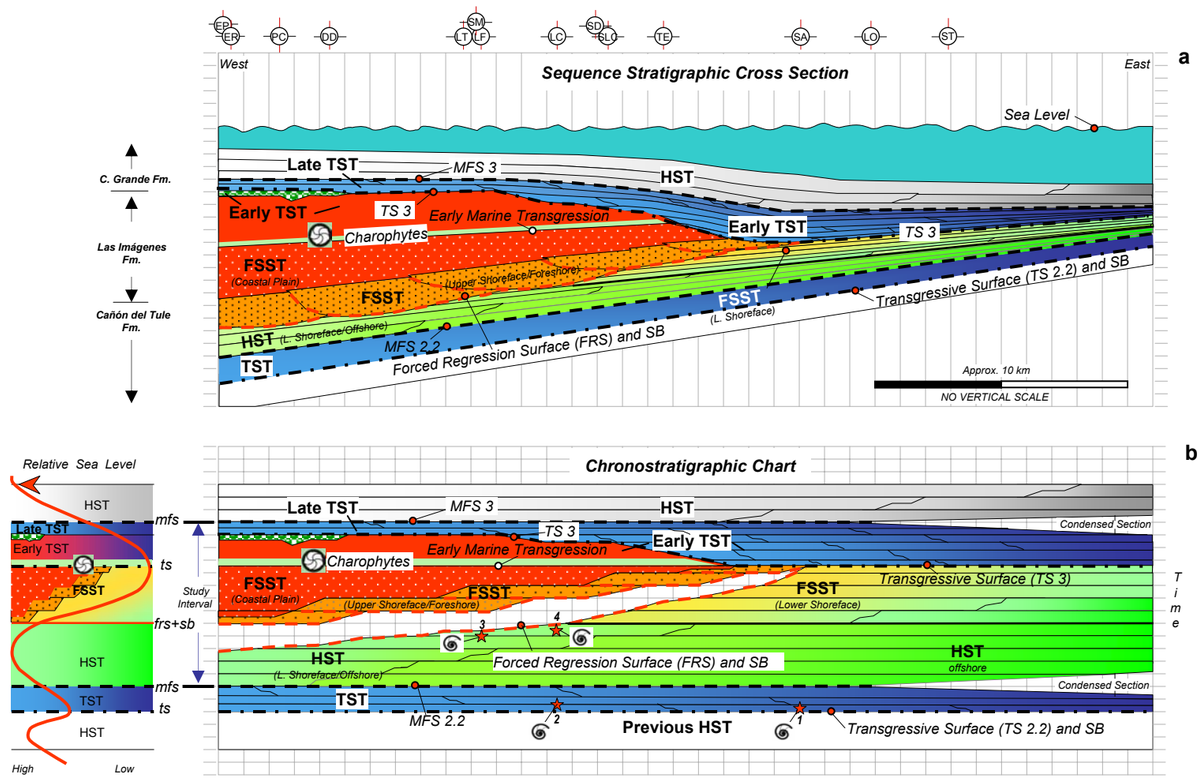

S y s t e m s T r a c t s a n d F a c i e s A s s o c i a t i o n s

- HST. Lower shoreface mudstone and siltstone; upward-thickening upper shoreface sandstone (upper La Campana and Altamira sections).
- Early-Late TST. Upper shoreface sandstone; middle to lower shoreface black shale, siltstone and sandstone. Mostly offshore gray mudstone and thin bedded siltstone (Los Ojitos Section).
- Early TST. Coastal plain red mudstone, siltstone, and channel-fill sandstone. Strand plain(?) sheet sandstone. Fluvial conglomerates (western study area).
- Early TST. Lacustrine and lagoonal charophyte-bearing deposits.
- FSST. Coastal plain red mudstone, siltstone ad sandstone. Channel-fill and floodplain red deposits.
- FSST. Sharp-based, stacked, upper shoreface to foreshore sandstone. Gutter cast at the bottom.
- FSST. Lower shoreface gray mudstone, siltstone and thin-bedded sandstone. Mostly offshore outer shelf (?) gray mudstone and thin-bedded sandstone (Los Ojitos and Tanque sections).
- HST. Offshore to storm-influenced lower shoreface gray mudstone, siltstone, and thin-bedded sandstone.
- TST. Lower shoreface to offshore gray mudstone and siltstone.
- Previous HST. Mostly delta-fed turbidites; middle and upper shoreface.

S y m b o l s

- Progradational stacking pattern.
- Retrogradational stacking pattern.
- Forced Regression Surface and Seq. Boundary (FRS-SB)
- Maximum Flooding Surface (MFS)
- Transgressive Surface (TS)
- Stratigraphic section location (projection to a west to east line. See Fig. A.18 for names and location).
- (1,3,4) *Coahuilites sheltoni* Böse occurs at 12.8 m above the TS 2.2 at the Altamira (SA) Section; 20 m below the FRS at La Florida (LF) and at 40 m below the same surface at La Campana (LC) Section. (2) *Coahuilites cavinsi* Böse and *Euthrepoceras planoventer* Stephenson occur at 32.5 m above the TS2.2 at La Campana (LC) Section.

Figure 3.2 Schematic sequence stratigraphic model of the central Parras Basin for the Late Maastrichtian. The west to east dip-oriented stratigraphic cross section (a) is an idealized interpretation across the central Parras Basin based generally on El Potrero-Tanque (EP-ST) cross section (Fig. A.18) and other masured sections in the study area. The cross section (a) shows the interpreted systems tracts, bounding surfaces, and facies associations for the shallow marine to coastal plain rocks of the upper Cañón del Tule, Las Imágenes, and lower Cerro Grande formations. The circles on top of the diagram represents the location of the measured sections projected into the west to east cross section line. The chronostratigraphic chart (b), projected directly from the cross section (a) above, represents the same stratigraphic units and surfaces developed through time, and the small chart on the left shows an interpretation of the relative sea level variation during the sedimentary evolution of the basin. The bounding surface nomenclature is based on Halik (1998); HST, TST, and FSST are abbreviations of Highstand, Transgressive, and Falling Stage Systems Tracts (see an additional explanation of the figure in the facing page).

referred to the original stratigraphic sections and cross sections of correlation (attached at the end of document) for additional descriptions and a better scale of observation.

Basic analysis of vertical grain-size trends and bed thickness, lithology, and sedimentary structures, allowed the studied strata to be subdivided into highstand (HST), transgressive (TST), and falling stage systems tracts (FSST) based on their progradational, aggradational, and retrogradational depositional architectures (Van Wagoner *et al*., 1988). The selection of sequence stratigraphic surfaces was based on the changes from a particular depositional architecture to another. Maximum flooding surfaces (MFS), for instance, are proposed at the stratigraphic horizons where a change from a retrogradational to a progradational stacking pattern occurs and an increase in fossil content is evident. In contrast, the change from progradational to retrogradational stacking patterns defined transgressive surfaces (TS). Progradational parasequence sets characterized by coarsening and thickening-upward successions were assigned to HST. These units are interpreted to be deposited in shallowing-upward conditions when sediment supply exceeded the rate of accommodation space being created by rising relative sea level. Retrogradational parasequence sets characterized by thinning-upward beds and fining-upward grain size trends were assigned to TST. These deepening-upward successions are interpreted to be deposited during relative sea level rises and when accommodation space exceeded the low rates of sediment input (Emery and Myers, 1996).

In this study, the interpretation of shoreface environments was based on sand to mud ratio, sandstone bed thickness, degree of bioturbation, and primary sedimentary structures. Although there is not a common agreement on shoreface zone subdivisions, the profile subdivision of beach and shoreface environments simplified from Elliot (1986) and Boggs (2001) was here adopted (Fig. 3.3). According to this simplified profile, shoreface extends seaward of the swash zone

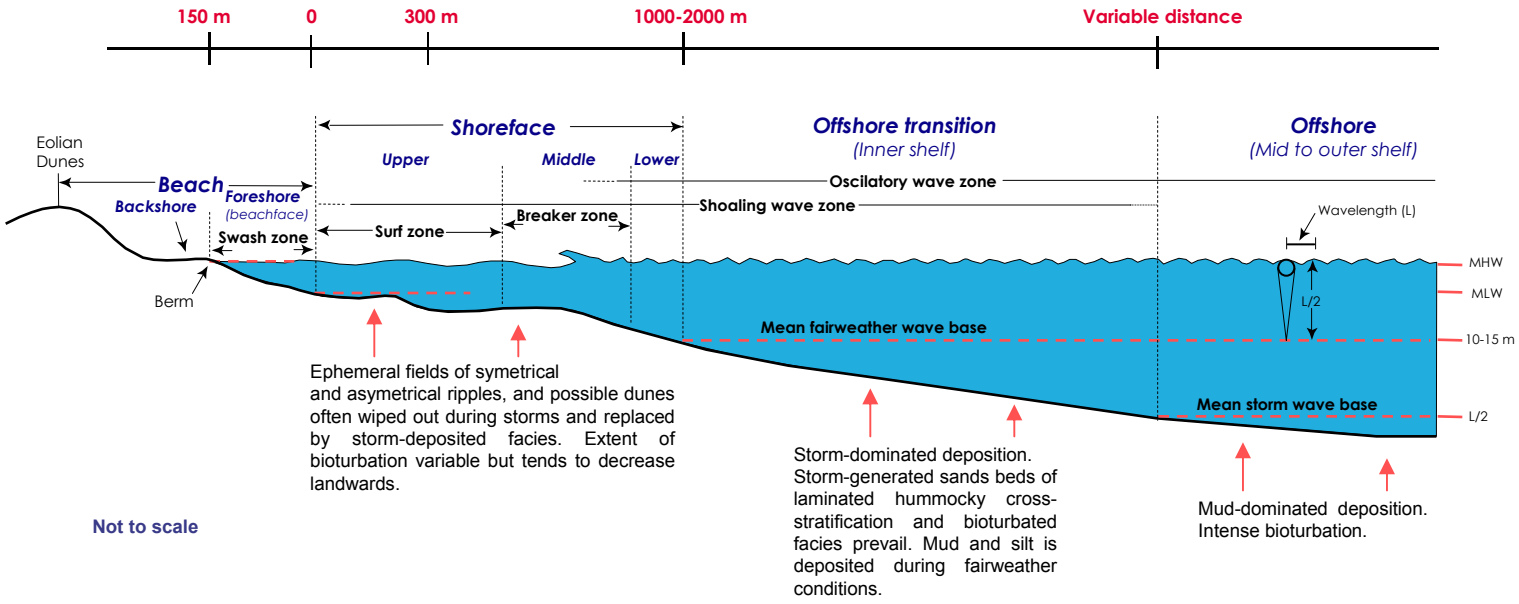

Figure 3.3 Generalized profile of the beach and shoreface subenvironments, processes and facies. Deposition of the upper Cañon del Tule Formation occurred in shallow marine environments under the influence of waves, storms, longshore and rip currents. Deeper muddy offshore deposits adjacent to the maximum flooding surface (MFS 2.2) were probably not subjected or were less affected by storm processes. The depth of the fairweather wave base is commonly on the order of 10-15 m, but this depth can be significantly lowered during storms. Hampson and Storms (2003) consider the offshore transition and offshore zones equivalents of the inner and mid to outer shelf, respectively. (MLW) Mean Low Water Level; (MHW) Mean High Water Level; (L) Wavelength. Schematic profile simplified from Elliot (1986) and Boggs (2001); complemented with horizontal distances from Howard *et al*. (1972) and Hampson and Storms (2003). See the text for additional explanations.

to the area in which a relatively steep ramp merges with the inner shelf (Fig. 3.3). This scheme suggests an offshore transition zone and the subdivision into upper, middle, and lower shoreface environments, which correspond roughly to the surf, breaker, and outer shoaling zones (Boggs, 2001). The foreshore, upper, middle, and lower shoreface subenvironments are distinguished by a particular suite of textures and sedimentary structures. Their boundaries are variable and their lateral distribution depends on the physical energy, which is a limiting factor of biological manifestations (Galloway and Hobday, 1996).

The *Skolitos* ichnofacies characterized by vertical, cylindrical, branched, or u-shaped burrows (*Skolitos*, *Ophiomorpha*, *Thalassinoides* and *Diplocaterion*) is typical of sandy shoreline environments, but it may grade seaward into shallow shelf environments. The *Glossifungites* ichnofacies includes u-shaped borings and is characteristic of marine to non-marine semi-consolidated substrates (Pemberton *et al*., 2001). *Glossifungites* is commonly associated to marine transgressive firm grounds (Posamentier and Allen, 1999).

The foreshore, beach face, or fore beach deposits develop within the wave swash and intertidal zone that extends between the mean high- and low-tide levels (Fig. 3.3). Sediments of the foreshore predominantly include fine- to medium-grained sand with parallel lamination dipping gently (2-3°) seaward or landward. Heavy-mineral thin laminae commonly alternate with layers of quartoze sand. Some foreshore sands may display high-angle, landward-dipping cross-lamination caused by foreshore ridge migration. A slope break in the beach profile (berm) separates the foreshore from the backshore. The backshore is intermittently inundated only during storm conditions. It is a depositional environment characterized by landward-dipping horizontally laminated sand commonly overlain by small- to medium-scale eolian trough cross-bedded beds disturbed by roots, crustacean burrows, and land-dwelling organisms (Boggs, 2001).

Upper shoreface deposits develop within the inner surf zone, below the mean high water level (MHW) and above the mean fairweather wave base, where deposition is dominated by powerful onshore, offshore, and longshore currents (Fig. 3.3). It is the zone dominated by coarse sedimentation characterized by thick accumulations of multidirectional trough cross-bedded sets and a low proportion of mud (Elliot, 1986; Boggs, 2001). Bidirectional cross-lamination oriented parallel to the shoreline is also common. Trace fossils such as *Skolitos* are common but not abundant.

Middle shoreface deposits form within the breaker zone, under high-energy conditions produced by powerful waves and associated longshore and rip currents. Deposits include approximately equal proportions of fine- to medium-grained sand and mud. Individual units up to 1 m thick include trough cross-bedded sandstone, parallel laminated and ripple-cross laminated mudstone, siltstone, and sandstone. Vertical burrows such as *Skolitos* and *Ophiomorpha* are common (Boggs, 2001), and the storm deposits are thicker and more lenticular than their lower shoreface equivalents (Galloway and Hobday, 1996).

Lower shoreface deposits accumulate in the outer shoaling zone, above the mean fairweather wave base, under relatively low-energy conditions in areas where the shoreface grades into the shelf (Fig. 3.3). Mud and silt with less proportions of thin-bedded sandstone dominate deposition in this environment. In high wave-energy regimes, lower shoreface is characterized by parallel-laminated sand that may contain low-amplitude undulations or hummocky cross-stratification. The effects of storms, particularly important in the middle and lower shoreface, may strongly modify the deposits formed under normal wave-energy conditions, causing erosion and redeposition of sediments. Graded Bouma-like beds are common in sandstones interbedded with shelf mud. Low-energy lower shoreface environments typically contain higher proportions of burrowed mud and silt than the middle and upper shoreface environments, and sand commonly

preserves ripples produced by wave oscillation. Lower shoreface deposits are commonly obliterated by bioturbation, which tends to decrease landward. Trace fossils such as *Thalassinoides* may be common (Boggs, 2001).

Rodríguez *et al.* (2001) analyzed the variations in progradational mid-Holocene to present shoreface architecture along an extensive area of the Texas coast in the Gulf of México. Their study was based on the analysis of echo-sounding profiles, 120 sediment cores obtained between 3 to 16 m water depth, distributed along 30 shoreface transects that extend from the coastline to distances of 16 km offshore. They recognized three broad sedimentological shoreface associations of facies. The upper shoreface, composed almost entirely of sand; the proximal lower shoreface, composed of sand with thick- to medium-bedded (50-10 cm) mud; and the distal lower shoreface, dominated by mud with medium- to thinly-bedded (20-30 cm) sand. Similar sand to mud proportions and thickness of sandstone beds observed by Rodríguez *et al.* (2001) were used in this study to interpret the upper, middle (proximal), and lower (distal) shoreface subenvironments. The intervals interpreted as offshore (shelf deposits) are dominated by mudstone and destruction of primary sedimentary structures by bioturbation.

3.2 UPPER CAÑON DEL TULE FORMATION

3.2.1 Previous Highstand Systems Tract (Previous HST)

Delta-Fed Turbidites/ Middle and Upper Shoreface

The lowermost studied unit comprises the upper portion of an overall progradational and shallowing-upward succession conventionally named in this study as the Previous Highstand Systems Tract (Previous HST; Figs. 3.1 and 3.2). This unit is characterized by a turbiditic cyclic succession of stacked upward-thickening muddy parasequences capped by sheet-like massive or planar-laminated thin- to medium thick-bedded sandstones. This cyclic succession

grades upward into medium- to thick-bedded fossiliferous sandstone and mudstone. The best exposures were studied at the lowermost La Campana (Fig. 3.4), Altamira, and El Saucillo sections (Figs. A.3, A.2, A.12; cross sections A.18 and A.19).

At La Campana Section, the exposed upper part of the Previous HST is 124 m thick and can be subdivided into three sedimentary packages based on lithology, sandstone/mudstone content, and cyclicity (Figs. 3.1 and A.3). These packages consist of a thickening- and coarsening-upward vertical facies succession that from base to top includes (**1**) distal delta-fed turbidites, (**2**) proximal delta-fed turbidites, and (**3**) middle to upper shoreface sediments; overall deposited in shallowing-upward conditions. The succession reaches its maximum sandstone content and shallowest conditions on top, where a marine transgressive surface (TS 2.2) defines its upper boundary (Figs. 3.1, 3.2 and A.3). The transgressive surface (TS 2.2) is described at the end of this subchapter.

(**1**) The distal delta-fed turbidites are mostly composed of thick intervals of gray mudstone capped by sheet-like, very thin-bedded, and upward-thickening planar-laminated sandstone (Fig. 3.4 and A.3). At their bases some sandstone beds display east-west oriented groove casts and flute casts that on average indicate paleocurrent flow orientation of south 82° east (Fig. 3.4c, d). The proximal delta-fed turbidites (**2**) are basically similar but consist of thinner cycles of bioturbated gray mudstone capped by thin- to medium-bedded, upward-thickening, massive or planar-laminated sandstone (Fig 3.4a, b). Abundant groove casts are oriented on average in an east-west direction. The overlying interval (**3**) contains mudstone and thick shallow-marine sandstones. They are less cyclic in character, and are interpreted as middle (La Campana Section, Fig. A.3) to upper shoreface deposits (El Saucillo Section, Fig. A.12).

Figure 3.4 Delta-fed turbidites at the lower La Campana Section. Previous HST deposits are characterized by a progradational turbiditic cyclic succession of upward-thickening muddy cycles capped by sheet-like massive or planar-laminated thin- to thick-bedded sandstone. Thinner beds capping each muddy cycle in (a) grade upward into thicker sandstone strata in (b). Sandstone beds contain at their bottoms abundant and well developed east-west oriented groove casts (c), and flute casts (d) that indicate paleocurrent flow orientation of south 82° east. Turbiditic deposits grade upward into middle to upper shoreface sandstone, and downward into deeper outer shelf mudstone.

Stratigraphycally, the Previous HST deposits grade downward into deeper and more distal muddy outer shelf deposits (Fig. 3.1). The maximum depth is reached at the maximum flooding surface (MFS 2.1) within the lower Cañón del Tule Formation (mudstone member of McBride *et al.,* 1974). At La Campana Section, this muddy interval including the maximum flooding surface (MFS 2.1) is covered (Fig. 3.1). However, the interval was described by Halik (1998) at his Saucillo River and El Pantano sections (Halik´s Fig. 3.10 and Appendix C, 1998). Halik interpreted a maximum flooding surface (MFS 2.1) on top of a transgressive systems tract (shoreface deposits), that directly overlie the red fluvial deposits of the Cerro Huerta Formation (Fig. 3.1).

The sheet-like character of mostly planar-laminated sandstone beds with well-developed groove and flute casts suggest deposition under high flow regime conditions. The stacking of beds into an upward-thickening progradational succession of parasequences suggest that sediments were probably transported into shallow-marine settings by submerged distributary channels that discharged fine-grained sediments creating turbiditic conditions. Excellent outcrops of laterally equivalent delta-fed cyclic deposits also occur along Highway 57 at El Saucillo River, nearby El Rosedal (Fig. 2.8). These outcrops were described by Soegaard *et al*. (1997; AAPG field trip 10, stop 7) and Halik (1998) at his Saucillo River Section. They mention that paleocurrent data from 25 flute casts indicate a mean paleocurrent flow orientation of north 75° east. Halik (1998) points out that individual sandstone beds, laterally exposed for hundreds of meters, consist of upward-fining Ta-d Bouma sequences. He also suggests that the absence of wave-generated structures and intervals devoid of bioturbation might indicate deposition in relatively deep-water conditions below the wave base.

In general, the sediments included into the Previous HST contain badly preserved fossils that do not indicate specific paleoenvironmental conditions. However, their occurrence and degree of preservation is consistent with a

shallow-marine environment. Gastropods, bivalves, and badly preserved ammonite fragments are common in this interval at La Campana Section and whole specimens of *Exogyra* sp. and *E. costata* were observed sporadically distributed at the Altamira and El Saucillo sections (Figs. A.2, A.12; cross sections A.18 and A.19). The samples -211.2 LC and -190.5 LC from La Campana Section (proximal delta-fed turbidites) contain an assemblage of badly preserved but diverse association of *Micula.* These calcareous nannofossils have a wide stratigraphic distribution that spans from the Turonian to the Maastrichtian (E. Lara-Corona, personal comm., 1999). Isolated chambers of small, hematitized, benthonic foraminifers were observed in thin section (samples -215LC and -228LC; Fig. A.3).

The occurrence of *Exogyra costata* at La Campana Section (interval -150 to -170 m; Fig. A.3) suggests that the age by stratigraphic position of the Previous HST is Early Maastrichtian considering that previous studies established the Campanian-Maastrichtian boundary at the lower Cerro del Pueblo Formation (McBride *et al*., 1974; see also Figs. 1.2, 2.6 and 2.7). On the other hand, the age of the transgressive unit (TST) overlying the Previous HST, is Late Maastrichtian based on the occurrence of *Coahuilites sheltoni* Böse (Fig. 3.2). A discussion of the age of the fossil assemblage contained within the TST and HST is included in the subchapters 3.2.3 and 3.2.5.

At La Casita Section (Fig. A.4), the delta-fed turbidite succession was poorly developed. The cyclic turbiditic succession at this locality has high mudstone content and displays a less defined progradational character. At El Saucillo Section (Fig. A.12), located in the southwestern study area, the delta-fed turbidites contain thicker sandstone beds on top of each individual cycle. All the progradational units finish with stacked upper shoreface sandstone on top (Fig. A.12). An explanation to this lateral variability from one to another section is probably related to their position within the basin. Muddy sections eastward and

northward are located at more distal areas, where fine sediments were deposited (i.e., La Casita Section, Fig. A.4).

3.2.2 Transgressive Surface (TS 2.2) and Sequence Boundary (SB)

The Previous HST is bounded on top by the transgressive surface (TS 2.2) identified in outcrop as an erosive discontinuity and interpreted as a marine ravinement surface (Figs. 3.1 and 3.2). The surface has a few centimeters of relief and lies within a 1.2-m-thick sandstone bed at La Campana Section (Fig. A.3). The same surface was placed on top of the uppermost thickest sandstone bed that caps the progradational succession at the Altamira, La Casita, and El Saucillo sections (Figs. A.2, A.4, and A.12) where it defines a boundary between a progradational upward-shallowing stacking pattern below (Previous HST) from an upward-deepening retrogradational stacking pattern (TST) above (Fig. 3.1).

The transgressive surface TS 2.2 is also interpreted as a sequence boundary (Fig. 3.2). On shelf environments, sequence boundaries are characterized by subaerial exposure and unconformity development. In these environments, coastal or offshore marine deposits of the transgressive systems tract commonly overlie lowstand or highstand offshore marine deposits of the previous sequence. In the vertical facies configuration observed below and above the TS 2.2, there is no evidence of subaerial exposure on top of the HST deposits. In this case, the lowstand systems tract is inferred to be locally or totally absent, leading to a superposition of transgressive over highstand deposits. In other words, the sequence boundary and the transgressive surface TS 2.2 are amalgamated into a single surface. In such instance, the surface can be referred as *merged sequence boundary/transgressive surface* (Posamentier and Allen, 1999).

The transgression that produced the surface TS 2.2 seems to have not produced significant submarine erosion of sediments on top of the HST deposits, since the facies below and above the surface are not considerably different. In other words, the interval below and above the transgressive surface TS 2.2 looks like a conformable succession in which the surface is defined by a change from progradational to retrogradational stacking pattern. This apparent conformity that separates older HST deposits below from younger TST deposits above is not in contradiction with the sequence boundary definition, since sequences are bounded by unconformities and their correlative conformities. It is thus interpreted that the sequence boundary at the top of the HST represents the laterally equivalent conformity of an unconformity that theoretically may occur somewhere up dip in proximal environments located landward or that such unconformity was nowhere developed.

The development of unconformities in proximal settings of foreland basins is apparently controlled by subsidence rates. Posamentier and Allen (1999) suggest that an increment of accommodation on the thrust belt side of a foreland caused by tectonic tilting and high subsidence are the most common factors causing a lowering of fluvial equilibrium profile. A lowering of the equilibrium profile in the coastal plain prevents the fluvial systems to incise over the underlying marine rocks, and therefore, the development of sequence boundary unconformities. The transgressive surface TS 2.2 is interpreted as a surface developed when the rate of relative sea level rise accelerated to a point where the rate of new accommodation created exceeded the rate of sediment input. Thus, the transgressive surface represents the first significant marine-flooding surface that overlies the highstand regressive section below.

3.2.3 Transgressive Systems Tract (TST)
Lower Shoreface to Offshore

The unit in blue that lies above the transgressive surface TS 2.2 (Fig. 3.2) is characterized by a clear decreasing grain-size trend upward, intervals progressively devoid of sand, higher mud content, and an increment in the number and diversity of fossils. These strata, stacked in a fining- and deepening-upward retrogradational succession are interpreted as transgressive systems tract (TST) deposits (La Campana Section, Figs. A.3 and 3.1). The TST deposits are well-exposed at the Altamira, La Campana, La Casita, and El Saucillo sections (Figs. A.2 to A.4 and A.12; cross sections A.18 and A.19) where the succession includes lower shoreface sediments at the bottom to offshore muddy sediments on top. Lower shoreface deposits consist of massive bioturbated fossiliferous mudstone and thin-bedded planar-laminated sandstone that transitionally grade upward into fossiliferous offshore sediments characterized by muddy-silty cycles devoid of sand. The beds stack in a non well-defined upward-thinning pattern, but a fining-upward grain size trend suggests deepening-upward conditions. The maximum depth in the succession is interpreted to be reached at the maximum flooding surface (MFS 2.2) tentatively placed within a thick mudstone interval (Figs. A.2 to A.4 and A.12; cross sections A.18 and A.19).

At La Campana Section (Fig. A.3), the TST is characterized by muddy intervals that contain abundant *Exogyra costata* Say and a diverse assemblage of other bivalves, gastropods, and ammonites (Plates 2, 3, 5, and 6). Unidentified benthonic foraminifers and diverse fragments of biogenic origin were also observed in thin sections of several samples. The fossil content of the transgressive (TST) unit, but especially the ammonites, were the most precise and useful fossils for chronostratigraphic control. For instance, the lowermost occurrence of *Coahuilites sheltoni* Böse (1928) was recorded within beds of the

lower part of the TST (Fig. 3.2) at the Altamira Section (Fig. A.12, sample -202.2 SA. See also the cross section A.19).

Coahuilites sheltoni and several ammonite species collected in this study were identified by Dr. K. Young of the University of Texas at Austin. According to K. Young (personal communication, 1997), *C. sheltoni* (Plates 1 and 3) is an index ammonite of the upper part of the Lower Maastrichtian. However, Cobban and Kennedy (1995) and Kennedy *et al*. (1996) concluded that *C. sheltoni* is restricted to the *Hoploscaphites birkelundi* Zone, the lowermost zone of the Upper Maastrichtian (Fig. 3.5). They arrived at this conclusion after studying numerous specimens from the Escondido Formation of Trans-Pecos Texas and Coahuila in northern México.

It is considered that it is not significant the slight difference between the age of *C. sheltoni* suggested by K. Young and the stratigraphic distribution observed by Cobban and Kennedy (1995) and Kennedy *et al*. (1996) for the same species. In fact, the assignment of *C. sheltoni* either to the top of the Lower or to the base of the Upper Maastrichtian is relative, since it depends on the position that the ammonite specialists of the Subcommission on Cretaceous Stratigraphy select for the Upper/Lower Maastrichtian boundary (Kennedy *et al*., 1998).

Although the subdivision into Lower and Upper Maastrichtian is still informal, the most accepted ammonite zonations of the U.S. Western Interior place the Lower/Upper Maastrichtian boundary at the base of the *Hoploscaphites birkelundi* Zone (Jagt and Kennedy, 1994; Kennedy *et al*., 1998; Hardenbol *et al*., 1998; Fig. 3.5). Consequently, based on the stratigraphic distribution of *Coahulites sheltoni* observed by Cobban and Kennedy (1995) and Kennedy *et al*. (1996), and the most commonly accepted ammonite zonations for the Maastrichtian of North America, the strata that yielded several specimens of *C.*

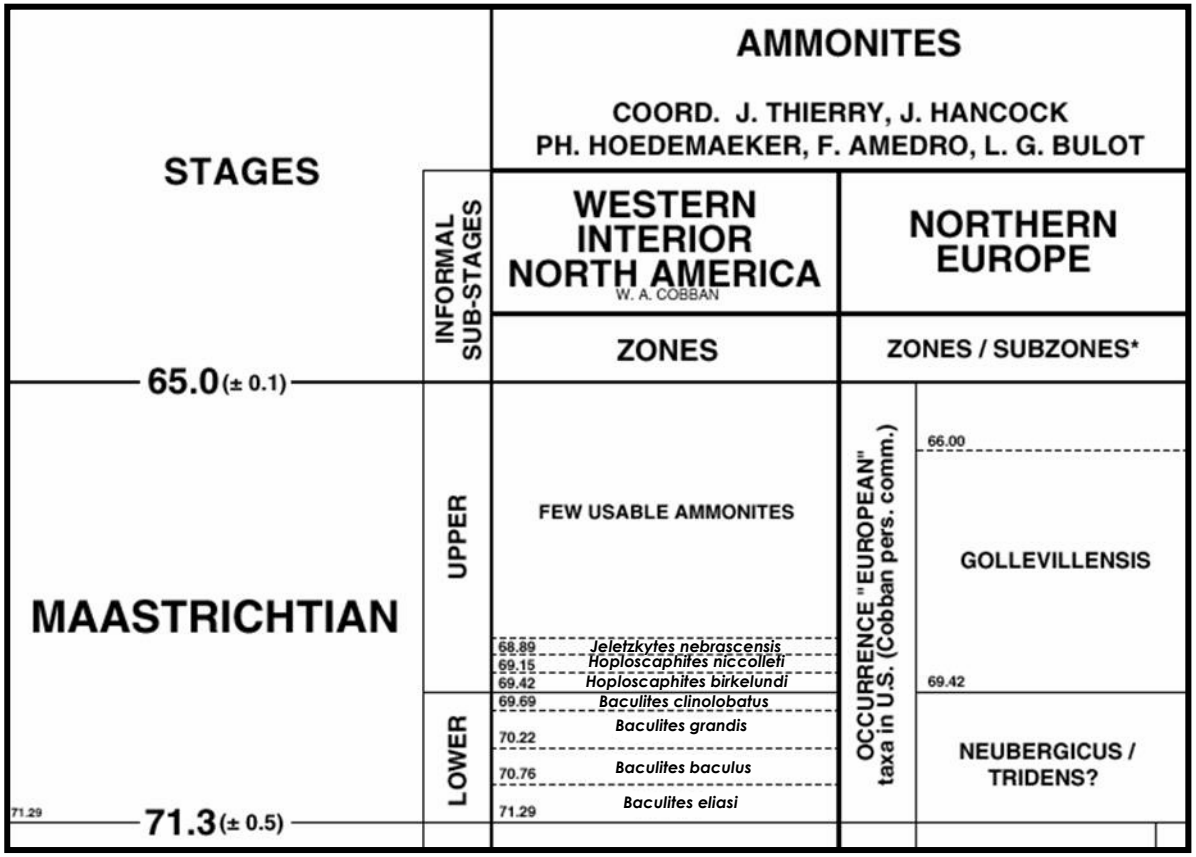

Figure 3.5 Ammonite zonation for the Maastrichtian recognized in the US Western Interior and its correlation with northern Europe. According to Cobban and Kennedy (1995) and Kennnedy *et al*. (1996), *Coahuilites sheltoni* Böse (1928) is restricted to the *Hoploscaphites birkelundi* Zone, the lowermost zone of the Upper Maastrichtian. The most accepted ammonite zonations of the US Western Interior place the Lower/Upper Maastrichtian boundary at the base of the *Hoploscaphites birkelundi* Zone. Modified from Hardenbol *et al*. (1998) and complemented with the zonations of Jagt and Kennedy (1994) and Kennedy *et al*. (1998).

sheltoni in the study area are from the lower part of the Upper Maastrichtian. Those strata include the transgressive (TST) and the overlying highstand (HST) systems tracts of the upper Cañón del Tule Formation (Fig. 3.2).

Some other ammonites collected from the transgressive unit (TST) were identified as *Eutrephoceras planoventer, Sphenodiscus intermedius,* and *Coahuilites cavinsi* (La Campana Section, Fig. A.3; Plates 2 and 3) associated with left and right valves of the bivalves *Trachycardium* sp*., T. eufalense*, and *Periplomya sulcatina* (Plates 5 and 6). Cobban and Kennedy (1995), who examined numerous specimens of *Coahuilites sheltoni* from the Escondido Formation, concluded that the three *Coahuilites* species initially described by Böse in 1928 (*C. sheltoni*, *C. orynskii*, and *C. cavinsi*) are conspecific (synonymous of the same individual) and selected the unique name *sheltoni* for the species. Based on the conclusion of Cobban and Kennedy (1995), the beds that besides *C. sheltoni* also contain *C. cavinsi* are from the base of the Upper Maastrichtian. *Coahuilites cavinsi* and *C. aff. cavinsi* were collected from beds of the transgressive (TST) and highstand (HST) systems tracts of the upper Cañón del Tule Formation (La Campana Section, Fig. A.3; Plate 3).

3.2.4 Lower Maximum Flooding Surface (MFS 2.2)

The transgressive systems tract (TST) is bounded on top by the maximum flooding surface MFS 2.2 (Figs. 3.1 and 3.2). The surface was tentatively placed within a thick muddy interval at the stratigraphic level that suggests a change from a retrogradational to a progradational stacking pattern. The best exposures of the muddy interval where this surface was interpreted occur at La Campana, Altamira, and El Saucillo sections (Figs. A.3, A.2 and A.12). In these sections, above the maximum flooding surface, there is a clear increment in the siltstone and sandstone content and the stacked beds thicken upward. Shallowing-upward conditions can also be interpreted by the occurrence of hummocky cross-stratified

sandstone beds and storm deposits that indicate deposition above the storm wave base (i.e., El Saucillo Section, Fig. A.12). The position of the maximum flooding surface (MFS 2.2) and the underlying transgressive and the overlying retrogradational succession is illustrated in the Altamira, La Campana, and La Casita sections (Figs A.2 to A.4 and A.12; cross sections A.18 and A.19). The MFS 2.2 constitutes the lower boundary of the study interval (Fig. 3.1 and 3.2).

3.2.5 Highstand Systems Tract (HST)

Offshore to Storm-influenced Lower Shoreface

The highstand systems tract (HST, lower green unit in Fig. 3.2) is the lowermost unit of the study interval (see also Fig. 3.1). The HST is an overall progradational upward-coarsening sedimentary succession composed of offshore deep deposits below and storm-influenced lower shoreface deposits above (Figs. A.2 to A.4 and A.12; cross sections A.17 and A.19). Offshore sediments almost devoid of sand are characterized by thick and highly bioturbated fossiliferous mudstone that stack in parasequences capped by thick siltstone or very thin-bedded sandstones. Individual siltstone beds commonly contain fossiliferous horizons composed of whole specimens of mollusks or shell fragment lags. Offshore deposits grade upward into lower shoreface sediments mostly composed of massive highly bioturbated or microlaminated mudstone capped by thin planar-laminated or hummocky cross-stratified sandstone.

Swaley and hummocky cross-stratification suggests that deposition of the HST occurred above the storm wave base and therefore, under the influence of storm processes. Additional observations that also support this interpretation are the occurrence of meter-scale sandstone units interpreted as storm deposits, which commonly contain lags at their bottoms (Fig. 3.6). Lags are composed of shell fragments and diverse biogenic debris, which suggests that high-energy

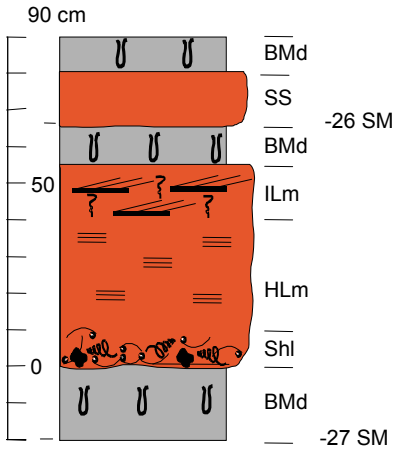

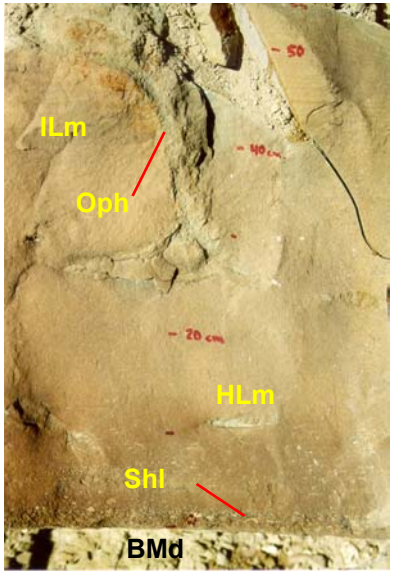

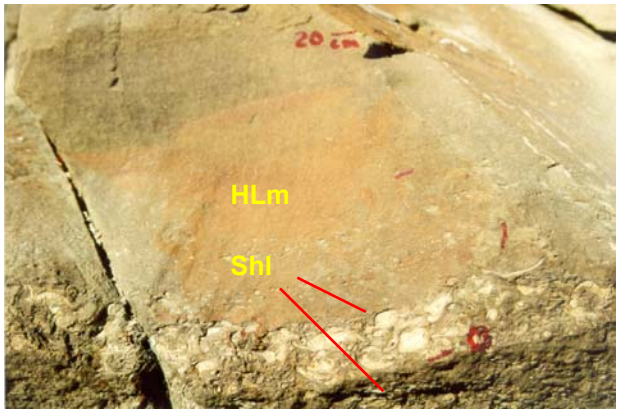

L E G E N D

- Undifferentiated shell fragments
- Gastropods
- Bivalves
- *Ophiomorpha* (Oph)
- Bioturbation (undifferentiated)
- -27 SM Sample
- Bioturbated Mudstone (BMd)
- Fine-grained Sandstone (SS)
- Inclined Cross Lamination (ILm)
- Horizontal Lamination (HLm)
- Mud clasts

Figure 3.6 Lower shoreface storm deposits at the San Miguel Section. Photographs show details of a storm bed characterized by a lag (Shl) composed of diverse shell fragments and mollusks. Sandstone bed is encased within highly bioturbated mudstone, bounded on top and bottom by sharp surfaces. The column on the left illustrates the sedimentary structures. *Ophiomorpha* (Oph) appears on top of the fine-grained sandstone. Stick is 50 cm long.

conditions periodically predominated. Wave energy during storms appears to have produced reworking of nearshore sediments and breakage of mollusk shells that were later mixed and concentrated in layers 5 to 10 cm thick. Highly bioturbated mudstone on top of sandstone indicates deposition in quiet conditions, after the storm process waned and fairweather conditions returned (Fig. 3.6). Other horizons are characterized by well-cemented mudstone beds that contain abundant mollusk fragments, ammonites, and hematitized benthonic foraminifers (i.e., La Florida Section; Fig. A.6, Plates 1 and 12).

The best exposures of the storm-influenced lower shoreface deposits occur at La Campana (Fig. 3.7), La Florida, and San Miguel sections (Figs. 3.6, A.3, A.6, and A.11). The HST is bounded at its bottom by the maximum flooding surface (MFS 2.2) previously described. Its upper boundary is a complex erosional surface located at the bottom of a thick sharp-based ridge-forming sandstone of the uppermost Cañón del Tule Formation (Figs. 3.1, 3.2, and 3.7; see also cross sections A.17 to A.19). This surface is described at the end of this subchapter.

Well-preserved specimens of *Coahuilites sheltoni* and other ammonites were recovered from different stratigraphic levels of the highstand (HST) offshore to storm-influenced deposits (Fig. 3.7). The best preserved specimen was collected from a well-cemented mudstone horizon located just 19 m below the erosional surface located at the bottom of the sharp-based ridge-forming sandstone of the uppermost Cañón del Tule Formation (La Florida Section, Fig. A.6; Plate 1). It was previously mentioned that *C. sheltoni* also occurs at the lowermost part of the underlying TST deposits at the Altamira Section (Fig. A.19). Thus, according to the stratigraphic distribution of *Coahulites sheltoni* observed by Cobban and Kennedy (1995) and Kennedy *et al*. (1996) in the US Western Interior, the interval between its lowermost and uppermost occurrence can be

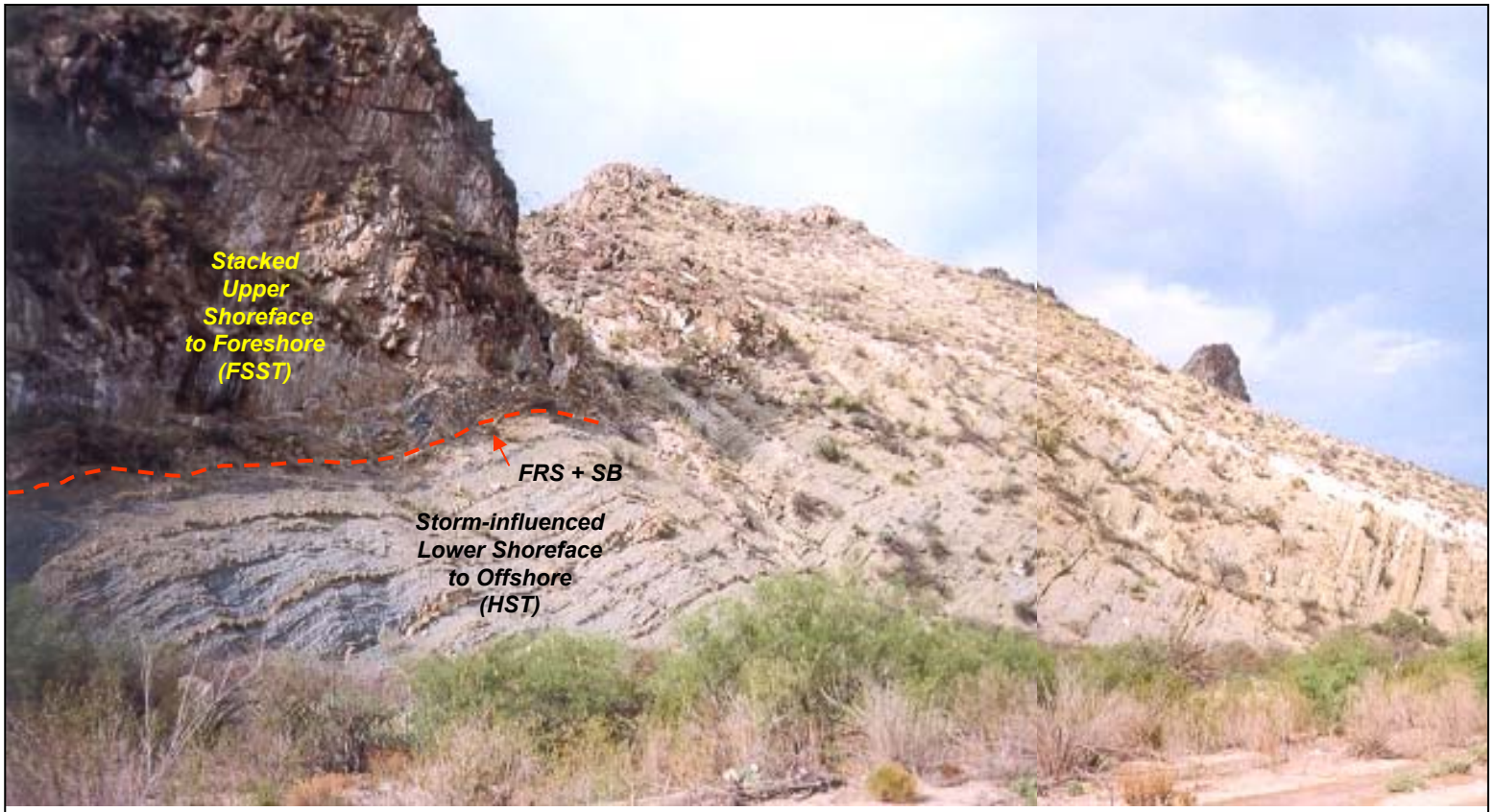

Figure 3.7 The forced regression surface and associated deposits at El Saucillo River, nearby La Campana, Coahuila. The erosional surface (FRS+SB) at the bottom of the thick sharp-based upper shoreface sandstone of the uppermost Cañón del Tule Formation (FSST) is interpreted to have been produced by a basinward migration of the shoreline associated with a process of forced regression during a lowering of relative sea level. The surface represents a truncation of facies, since it separates shallower upper shoreface sandstone above (FSST) from deeper lower shoreface muddy sediments below (HST). The intermediate middle shoreface facies association is missing. The muddy HST deposits contain storm deposits and the interbedded mudstone commonly contains ammonites, gastropods, and bivalves. The outcrop is locally affected by lateral faulting.

accurately assigned to the lower part of the Upper Maastrichtian (Figs. 3.2 and 3.5).

A rich association of gastropods and bivalves collected from beds of the HST (Fig. 3.2) and the underlying transgressive unit (TST) was studied by F. Vega and R. Cozátl (Instituto de Geología, UNAM; 1998). The association includes *Exogyra costata* Say*, Periplomya sulcatina* (Shumard), *Trachycardium eufalense* (Conrad), *Scaphites sp., Stantonella* sp., *Pholadomya occidentalis* Morton*, Trachycardium* sp., and *Periplomya sp.* (F. Vega, written comm., 1998; Plates 5-6). F. Vega states that these organisms lived in shallow-marine infralitoral zones and that the interpreted climate for the region was warm and semiarid. F. Vega also points out that according to previous studies this association of gastropods and bivalves is typical of Early Maastrichtian strata. However, it is concluded here that the stratigraphic range of that assemblage of gastropods and bivalves may slightly extends upward into the lower part of the Upper Maastrichtian since the previously mentioned fossils were collected from the same beds that contain *Coahuilites sheltoni* and *C. cavinsi*. It was discussed before, that the assignment of *C. sheltoni* either to the top of the Lower or to the base of the Upper Maastrichtian depends on the position chosen for the Upper/Lower Maastrichtian boundary (Fig. 3.5).

Lithology, sedimentary structures, intensity of bioturbation and fossil content suggest that the deposition of the shoreface deposits of the upper Cañón del Tule Formation, including the transgressive and highstand systems tracts (Fig. 3.2), occurred under the action of waves, storms, rip currents, and longshore currents (Fig. 3.3). Deposition of deeper muddy offshore deposits both above and below the maximum flooding surface (MFS 2.2) occurred below the mean storm wave base. Therefore, these deposits were not subjected or were less affected by storm processes. The lateral distribution of facies with minor variabilities in east to west dipping direction suggests a wide and low gradient ramp-type depositional

setting (Fig. 3.3). Ye (1997) suggests a southeastward-dipping ramp whose geometry was related to lithospheric flexural deflection where sediments were supplied axially into the Parras Basin from western and southern highs.

3.2.6. Forced Regression Surface and Sequence Boundary (FRS+SB)

The upper boundary of the HST is an erosional surface located at the bottom of a thick, sharp-based sandstone unit (labeled FSST) within strata of the uppermost Cañón del Tule Formation (Fig. 3.2, 3.7 and 3.8a, b). This erosional surface of regional extent was observed in most of the studied sections, and it represents a well-defined stratigraphic horizon of correlation (cross sections A.17 to A.19). The surface on top of the HST defines a facies dislocation that separates relatively deeper muddy sediments below (storm-influenced lower shoreface to offshore) from shallower and coarser sediments above (sharp-based upper shoreface to foreshore sandstone). The intermediate middle shoreface facies association is missing (Figs. 3.7 and 3.8a). Its regional expression, erosional character, and the overlapping of relatively shallower over deeper facies associations are interpreted to be the result of a seaward shoreline migration and basinward shift in facies produced by a lowering in relative sea level. This process of seaward shoreline migration induced by a relative sea level fall is termed forced regression (Posamentier, 1992).

In the central Parras Basin, a variable meter-scale undulatory relief (Figs. 3.8a, b and 3.9b, d) characterizes the forced regression surface (FRS). At Las Trancas-Palo Blanco Section (Fig. A.16), channel-like meter-scale gutter casts scour the underlying lower shoreface to offshore (HST) mudstone deposits (Fig. 3.8b). These erosional structures, filled with undulatory laminated fine-grained sandstone, characterize the lowermost 2 m of the FSST upper shoreface deposits that overlie the forced regression surface. The thickest sandstone above the gutter casts (Fig. 3.8b) commonly contains tool marks at its lower stratification

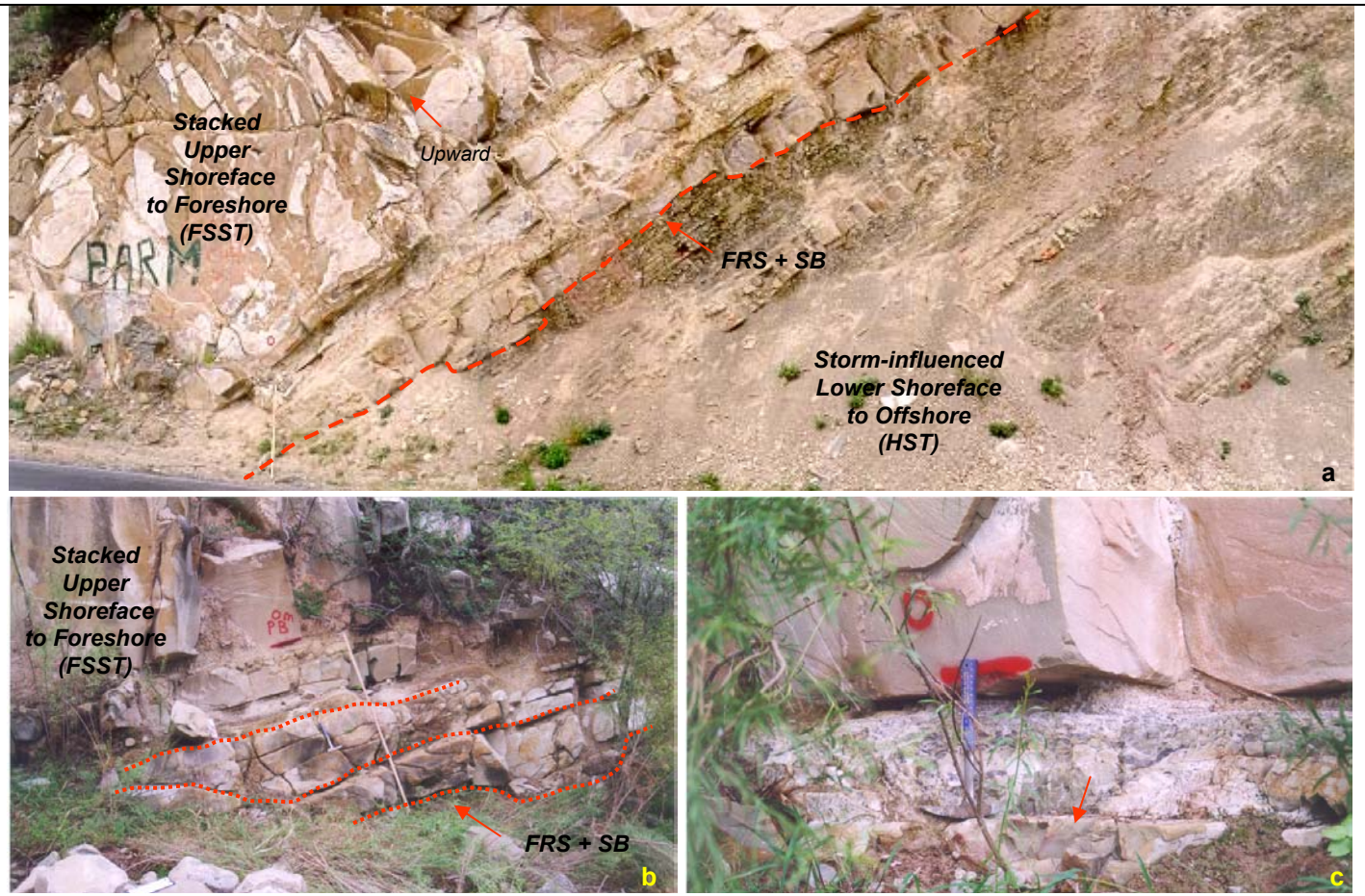

Figure 3.8 The forced regression surface and associated deposits at La Florida and Las Trancas-Palo Blanco sections. Note in (a) the undulatory erosional relief of the forced regression surface (FRS+SB). *Coahuilites sheltoni*, an index ammonite of the lower Upper Maastrichtian was collected at 19 m below the surface (see Fig. A.6 and Plate 1). (b) shows meter-scale channel-like gutter casts that characterized the bottom of the FSST deposits at Las Trancas-Palo Blanco Section. The arrow in (c) points out a small gutter cast located above the big gutter casts shown in (b). Wood stick is 2 m long.

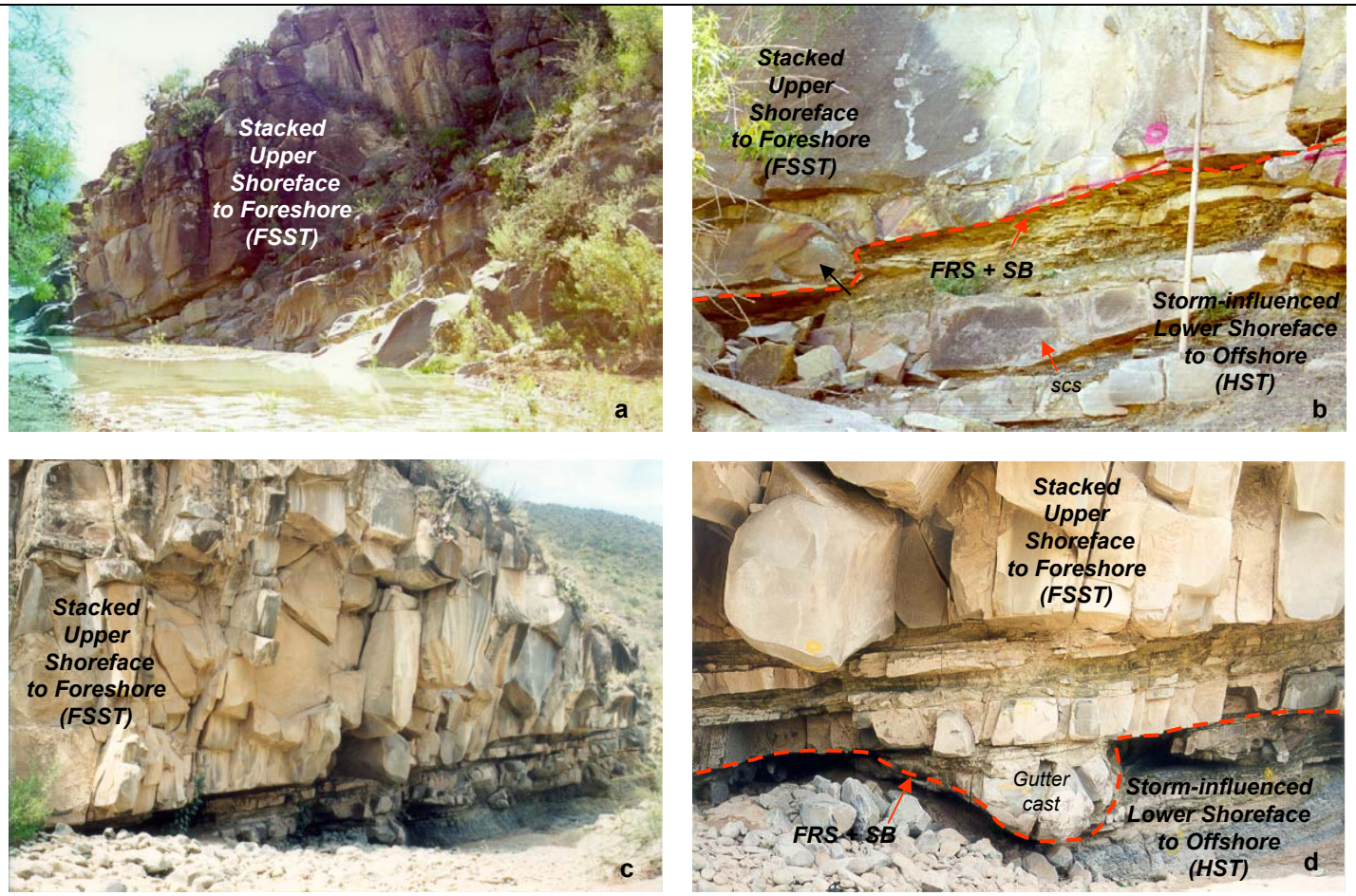

Figure 3.9 The forced regression surface and overlying FSST deposits at El Realito Section. The sharp-based FSSTsandstone in (a) is 33 m thick. Note in (b) the undulatory erosional relief of the forced regression surface (FRS+SB), the amalgamated gutter cast (black arrow), and the sandstone wedge resembling swaley cross-stratification (scs). The FSST sandstone deposits in (c) contains meter-scale gutter casts (d) at its bottom, scouring into deeper HST gray mudstone. Lower photographs are from El Arpa Canyon nearby El Realito. Stick is 2 m long.

surface and the individual sandstone beds are separated by thin-bedded gray mudstone that also contain centimeter-scale gutter casts (Fig. 3.8c). At El Realito Section (Figs. A.10 and 3.9a, b), the forced regression surface is characterized by big gutter casts, partially amalgamated with the overlying thickest sandstone (labeled FSST), and thin sandstone wedges resembling swaley cross-stratification are also common within the underlying storm-influenced (HST) deposits (Fig. 3.9b). At El Arpa canyon, nearby El Realito (Fig. 3.9c), meter-scale gutter casts at the bottom of the unit labeled stacked upper shoreface FSST also scour into the underlying deeper muddy lower shoreface to offshore HST deposits (Fig. 3.9d).

The term gutter cast includes several scour-and-fill structures previously described as large groove casts, elongated flute casts, parallel scour-structures, erosional channels or runnel casts (Whitaker, 1973). However, the term is more frequently applied to U- or V-shaped sand-filled channels up to 10 cm wide and deep, which protrude into the underlying fine-grained sediments. They are thought to be produced by the scouring effect of moving water along helicoidal paths, possibly aided by the "blast effect" of sand carried by the flow (Collison and Thomson, 1989). Boggs (2001) groups these of U- or V-shaped erosional sedimentary structures into channels and scour-and-fill structures. The latter consists of small asymmetrical troughs, few centimeters in size, filled either by coarser-grained or finer-grained material than the substrate.

The sand-filled channel-shaped gutter casts observed at several locations in the study area are attributed to the lowermost facies of the thick upper shoreface sandstone labeled FSST (Figs. 3.8b and 3.9 b, d). These structures interpreted to be developed in the upper shoreface, scoured into the finer-grained substrate of deeper lower shoreface facies (HST deposits) mostly composed of mudstone, swaley, hummocky cross-stratified sandstone, and storm deposits (Fig. 3.8b and 3.9b, d). The gutter casts are interpreted as erosional structures produced by the action of seaward-moving currents perpendicular to the shoreline

(rip currents) induced by waves. They were probably originated when the shallow sand-rich facies belts of the upper shoreface migrated basinward, overlapping the deeper muddy lower shoreface facies of the underlying HST as a consequence of the forced regression resulting from a relative sea level fall.

The meter-scale size of the channel-shaped gutter casts shown in Fig. 3.8b, suggests erosive action of rip currents close to the shoreline where their energy was still able to confine the water flow and scour the sea floor. Boggs (2001) suggests that rip currents are primarily, a seawater surface phenomena whose sediment transport capacity gradually wanes from proximal to distal shoreface settings. However, he adds that rip currents can transport considerable quantities of sediment when moving through the breaker zone out into the shoaling wave zone (Fig. 3.3). Channels 1 to 3 m deep can be scoured on the seafloor of the breaker zone by rip currents whose velocities range from about 1 m/s to over 5 m/s in severe storms (King, 2000).

The identification of a sequence boundary in outcrop requires the recognition of a facies dislocation characterized by the superposition of relatively proximal facies, overlying significantly more distal facies without the preservation of the intermediate facies. Forced regressions commonly produce facies dislocations and develop sharp erosional surfaces and unconformities that grade seaward of the shoreline into their correlative submarine conformities (Plint and Nummedal, 2000; Posamentier and Morris; 2000). In shallow marine settings, facies dislocations are often associated with and abrupt increase in grain size (Emery and Myers, 1996). The forced regression surface (FRS) of the upper Cañón del Tule Formation meets all of the previously mentioned stratigraphic features and is, therefore, proposed as a sequence boundary (SB). The surface represents an erosional truncation within a normal vertical succession of facies in which the gradual stacking of shallowing facies predicted by Walther's law is interrupted by an unconformity.

Plint and Walker (1987); Plint (1988); Hadley and Elliot, 1993; Hunt and Gawthorpe (2000), among others, describe examples of forced regressive deposits. Forced regression surfaces similar to the one of the Cañón del Tule Formation have also been described at the base of nearshore deposits of important hydrocarbon reservoirs (Posamentier *et al*., 1992). The surfaces have been interpreted to be produced by submarine erosion of the seafloor. During the process, the underlying facies are gradually exposed to the action of waves while the shoreline and coarse-grained facies belts migrate and stack seaward in response to relative sea level lowering (Posamentier *et al*., 1992). The major features in most of the documented examples are the abrupt occurrence of coarser and more proximal sediments in distal marine settings and sharp-based shoreface deposits, commonly containing gutter casts, overlying shale (Plint, 1988; Posamentier *et al*., 1992; Hadley and Elliot, 1993).

In the central Parras Basin, the forced regression surface (FRS) is a diachronously developed unconformity and sequence boundary (Fig. 3.2b). The surface originated during a sea level fall that exceeded the subsidence rate, reduced accommodation space in nearshore proximal settings, and forced the shoreline and facies belts to migrate basinward. It is interpreted that during the forced regression, the shoreline and facies belts migration produced a successive stacking of sharp-based sandstone bodies bounded at their bottoms by a regressive surface of submarine erosion (Fig. 3.2 a, b). Consequently, the FRS is a complex surface originated by the amalgamation of multiple surfaces of submarine erosion that partially removed the deep HST deposits and cannibalized much of the laterally equivalent FSST deposits (yellow-green FSST unit, Fig. 3.2b). The sediments eroded during the forced regression are represented in the idealized sedimentary model of the central Parras Basin by an erosional vacuity below the FSST sandstone unit in orange (Fig. 3.2b). The mechanisms that controlled the depositional architecture of the sharp-based upper shoreface

sandstone (FSST) of the uppermost Cañón del Tule Formation are discussed in the next subchapter.

3.3 UPPERMOST CAÑON DEL TULE FORMATION

3.3.1 Falling Stage Systems Tract (FSST)

Sharp-based Upper Shoreface to Foreshore Sandstone

Plint and Nummedal (2000) proposed the *falling stage systems tract* (FSST) to group the stratal units deposited during the initial stage of a relative sea level fall. This relatively new term in sequence stratigraphy is herein adopted to include the rocks of the study interval interpreted to be deposited during a forced regression, in a regime of relative sea level fall. Those FSST deposits include the shoreface to foreshore sandstone (orange unit, Fig. 3.2b) and their contemporaneous deeper-water deposits (lower shoreface) subjected to cannibalization during the seaward migration of facies (yellow-green unit, Fig. 3.2b). Within a completely marine section of similar lithologic characteristics, it was not possible to define a boundary to differentiate the HST deposits (green unit in Fig. 3.2) from the cannibalized FSST deposits (Fig. 3.2). The FSST also includes the coastal plain red deposits of the lower Las Imágenes Formation (red dotted unit, Fig. 3.2b) contemporaneous and laterally contiguous to the shallow-marine deposits of the uppermost Cañón del Tule Formation. Only the latest shallow-marine deposits are described in these paragraphs, the FSST strata of the lower Las Imágenes Formation are described ahead in the subchapter 3.4.

The FSST deposits of the uppermost Cañón del Tule Formation (Fig. 3.2) include a thick, ridge-forming, sharp-based sandstone that overlie the forced regression surface (FRS+SB), interpreted to be deposited in upper shoreface to foreshore environments (Figs. 3.7-3.9). This interpretation is based on: 1) the high proportion of sand (and discrete amounts of mud), which suggests a high-energy sand-dominated environment; 2) the occurrence of the previously described

meter-scale gutter casts facies association observed at its bottom, which suggest an environment subjected to the action of strong rip currents; and 3) sedimentary structures such as trough cross-bedding, horizontal to gently inclined planar lamination, multidirectional cross-lamination (Fig. 3.10), and wave ripples, common in upper shoreface to foreshore environments. Additional features that support the interpreted depositional environment are the low proportion of bioturbation and the scarcity of marine fossils (ammonite impressions); as well as thickness (tens of meters) and lateral distribution (kilometers) along dip and strike directions. The stratigraphic position of the FSST sandstone in the middle part of an overall regressive vertical succession of facies, underlain by deeper lower shoreface to offshore deposits and overlain by coastal plain red deposits is also supporting evidence. Baker (1970) previously recognized that the Upper Member of the Cañón del Tule Formation was deposited during a regressive phase and interpreted the capping sandstone as beach or forebeach deposits on the basis of its low clay content, stratigraphic position, and rare occurrence of cross-bedding.

The FSST sandstone of the uppermost Cañón del Tule Formation is a complex unit composed by thick-bedded stacked sandstone beds. The FSST sandstone unit thins and pinches out eastward and to a lesser degree northward. It is 58, 33, and 15 m thick at El Saucillo, El Realito, and La Florida sections, respectively (Figs. 3.11, 3.9 and 3.8a); and less than 2 m thick at the Altamira section (Fig. 3.12; see also cross sections A.17 to A.19). The ridge-forming sandstone is internally subdivided into at least two and up to ten stacked, upward-thickening individual sandstone beds bounded at their bottoms and tops by discrete very thin horizons of gray-yellowish, oxidized, silty mudstone (Fig. 3.11). Many beds contain wave ripples at the tops, suggesting shoaling and short breaks in sedimentation characterized by fine-grained muddy deposition. In some outcrops, short interruptions in deposition are also suggested by the occurrence of undulated amalgamation surfaces with chert pebbles.

Figure 3.10 Common sedimentary structures of the FSST deposits. Upper shoreface to foreshore (FSST) sandstones commonly display multidirectional cross-lamination (a, b) and planar lamination (c, d). The dashed arrows show sets of laminae differently oriented. Photograps (a) and (c) are from La Florida Section; (b) and (d) from outcrops observed along Highway 57 nearby Las Imágenes, Coahuila. Stick is subdivided every 10 cm; scorpion is 6 cm long.

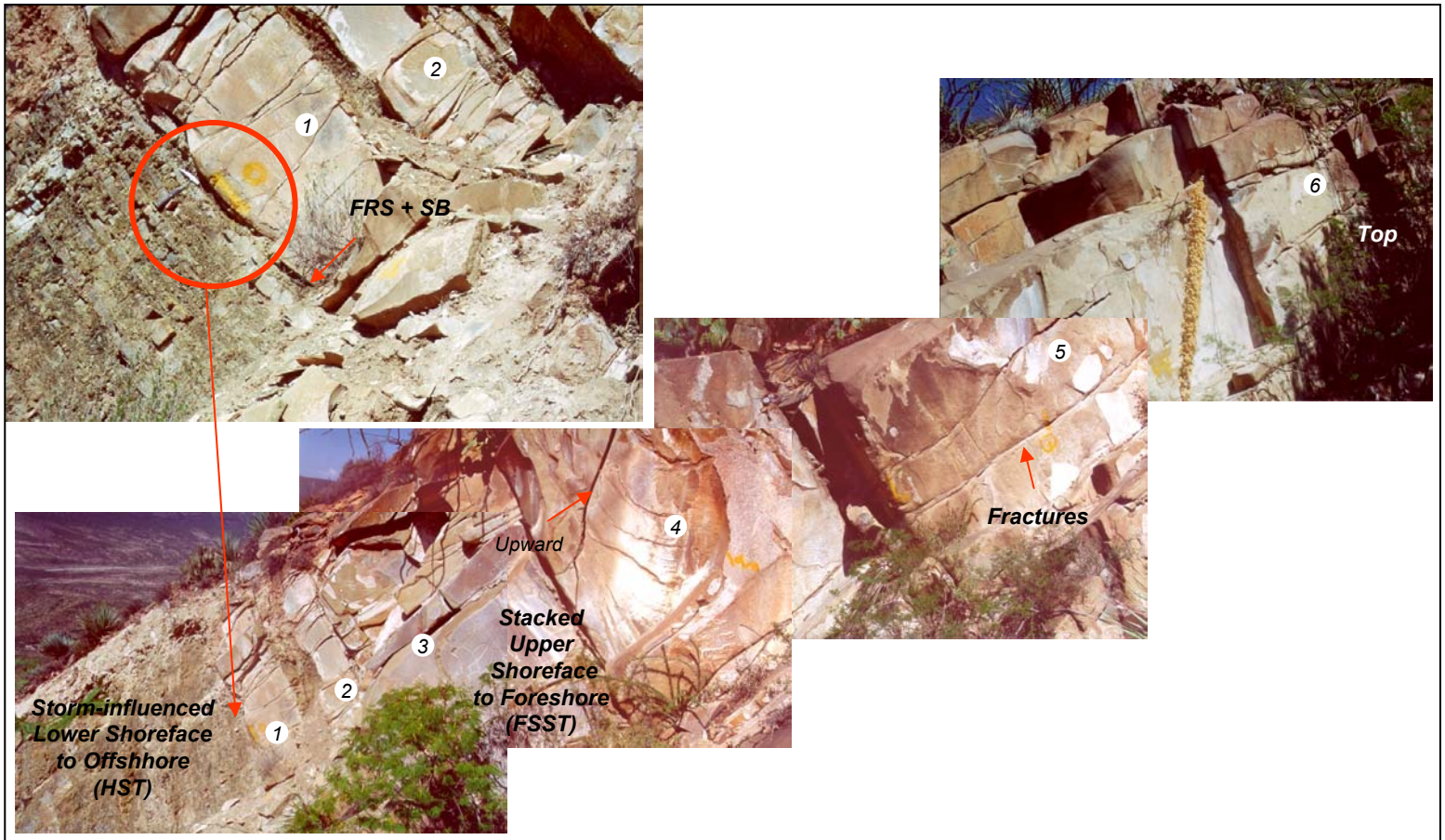

Figure 3.11 Sharp-based stacked upper shoreface to foreshore (FSST) sandstone and forced regression surface (FRS+SB) at El Saucillo Section. The upper shoreface to foreshore (FSST) sandstone deposits sharply overlie deeper lower shoreface to offshore muddy strata (HST). At this section, the forced regression surface is a sharp and almost flat surface without gutter casts (upper left detail). The FSST deposits can be subdivided into ten upward-thickening sandstone beds (see Fig. A.12). Only the lower six beds, which include 17 m of section, are labeled and shown in the photomosaic. The FSST deposits include a total of 58 m of sandstone at this proximal location and are reduced to to almost 2 m at the more distal Altamira Section (Fig. 3.12). The distance between El Saucillo and Altamira sections is 15.5 km.

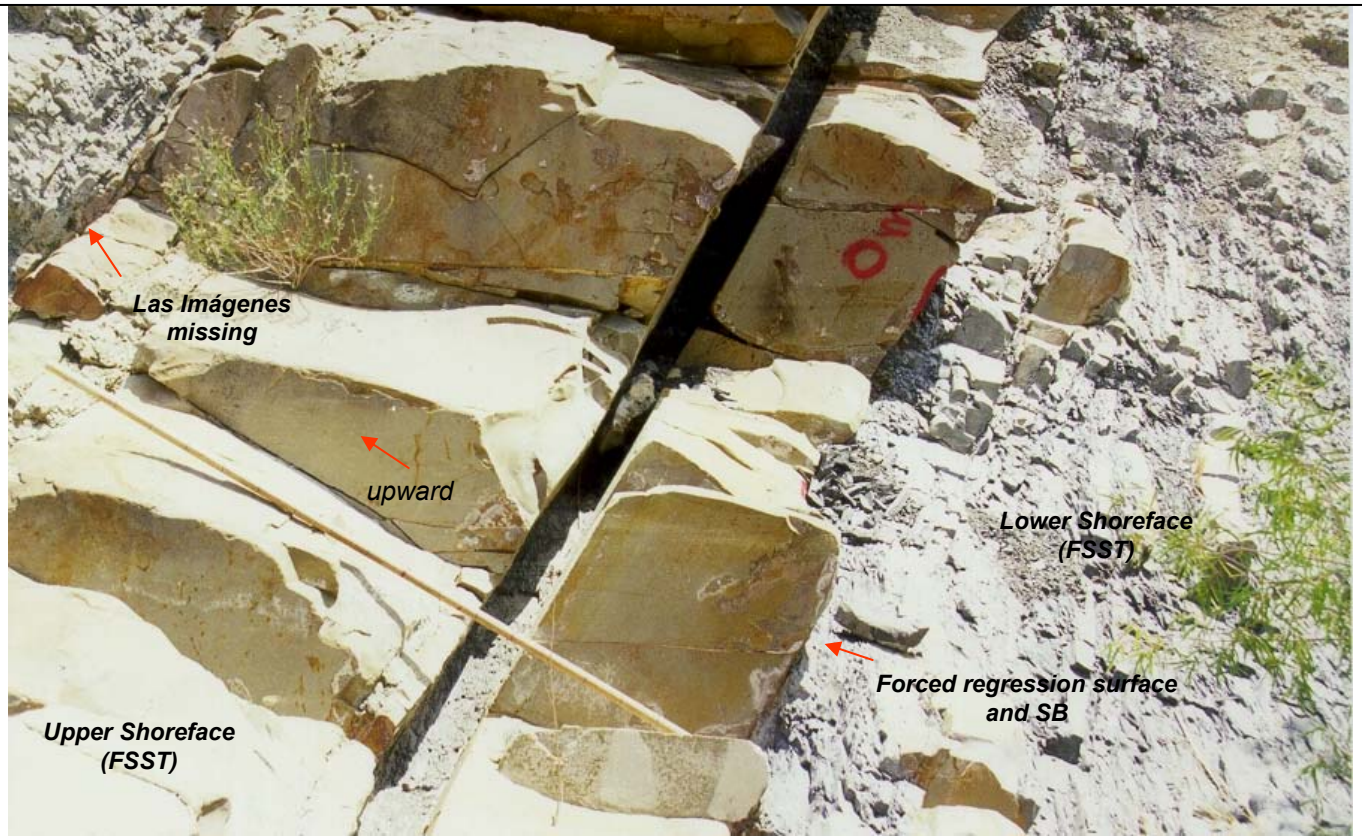

Figure 3.12 Easternmost distal expression of the sharp-based FSST sandstone of the uppermost Cañón del Tule Formation, Altamira Section. The ridge-forming sandstone whose maximum measured thickness is 58 m to the southwest at El Saucillo Section, is reduced to almost 2 m at this location (Altamira Section, Fig. A.2). It is interpreted that in this area the lower shoreface FSST muddy deposits were cannibalized during the forced regression process. Note that the sharp and erosional character of the forced regression surface still remains. At this location the coastal plain red beds of Las Imágenes Formation have pinched out. The differentiation between the marine units Cañón del Tule and Cerro Grande is difficult eastward of this location where the ridge-forming FSST sandstone unit pinches out completely. Stick is 2 m long.

Overall, the sharp-based upper shoreface to foreshore sandstone (FSST) can be stratigraphycally subdivided into three parts (lower, middle, and upper), recognizable in most of the studied sections. Each part is characterized by sandstone beds with similar sedimentary structures. At El Saucillo, the most complete and thickest section (Figs. A.12 and 3.11), the lower part of the FSST ridge-forming sandstone includes very fine- to medium-grained trough cross-bedded gray sandstone with horizontal to gently inclined planar lamination. This lower part includes seven stacked, upward-coarsening and thickening sandstone beds labeled from 1 to 6 (Fig. 3.11). Individual cross-bedded sandstone beds may be separated by amalgamation surfaces with chert pebbles, or by very thin horizons of gray-yellowish, oxidized, and hardened mudstone. Badly preserved impressions of ammonites are rare, especially at the bottom, and mud clasts are commonly distributed throughout the beds.

At El Saucillo Section, the gutter casts that characterize the forced regression surface (FRS+SB) in multiple locations were not observed. In this section, the lower boundary of the FSST sandstone is a sharp, erosional surface shown in the upper left detail in Figure 3.11. The photomosaic in the same figure only shows the lowermost six upward-thickening, stacked sandstone beds distributed along 17 m of section. The uppermost 41 m of section, include four sandstone beds (not shown in the photomosaic) that lie on top of the bed 6. At the same El Saucillo Section (Fig. A.12), the middle part of the FSST deposits includes a thick, massive, medium-grained gray sandstone bounded at its bottom by 1-m-thick bed of gray-yellowish oxidized mudstone. Sedimentary structures were not observed due to a thick weathered layer that covers the external surfaces of sandstone beds. The upper part of the FSST sandstone includes medium-grained greenish and reddish massive sandstone that contains traces of reddish material and grades upward into the red beds of Las Imágenes Formation. The contact between the Cañón del Tule and Las Imágenes formations is described later in this subchapter.

Along Highway 57 nearby Las Imágenes, Coahuila (Fig. 2.8), the sharp-based sandstone of the uppermost Cañón del Tule Formation (FSST) is 17 m thick (Fig. 3.13). The lower part of the FSST deposits is a fine-grained sandstone with multidirectional cross-lamination, horizontal and low-angle planar-lamination (Fig. 3.10), wave ripples, and mud clasts on top (Fig. 3.13c). The upper part is an intensively fractured cross-bedded very fine-grained sandstone bounded at its bottom by a thin interval of silty mudstone and silty very fine-grained sandstone (Fig. 3.13b). In this outcrop, the contact of the FSST sandstone unit with overlying red beds of Las Imágenes is covered, but it is exposed at Las Trancas-Palo Blanco Section (Fig. A.16), where the uppermost sandstone of the Cañón del Tule Formation becomes progressively reddish upward (Fig. 3.13d).

Progressive stacking of upward-thickening sandstone beds separated by thin horizons of silty mudstone suggests that the forced regression process induced by a falling relative sea level was characterized by basinward migration of the shoreline, basinward shift of coarse-sediment facies belts, and deposition of sandstone. The overall falling of relative sea level, however, was punctuated by higher frequency pulses of sea level risings that produced alternate periods of renewal of accommodation space controlled by subsidence. These short periods of deepening or drowning conditions initially produced fine-grained deposition and the subsequent infilling of the available accommodation space by coarse sediments. Deposition of 57 m of sand in upper shoreface to foreshore environments at El Saucillo Section is explained by the mechanism previously described. In this proximal section, the FSST deposits are characterized by the stacking of 10 upward-thickening cycles separated by thin horizons of silty mudstone (Fig. A.12). Figure 3.11 only shows the lowermost six cycles overlying the forced regression surface. Differentiation between upper shoreface from foreshore deposits was not possible, but it is inferred that every individual cycle might be capped by foreshore facies.

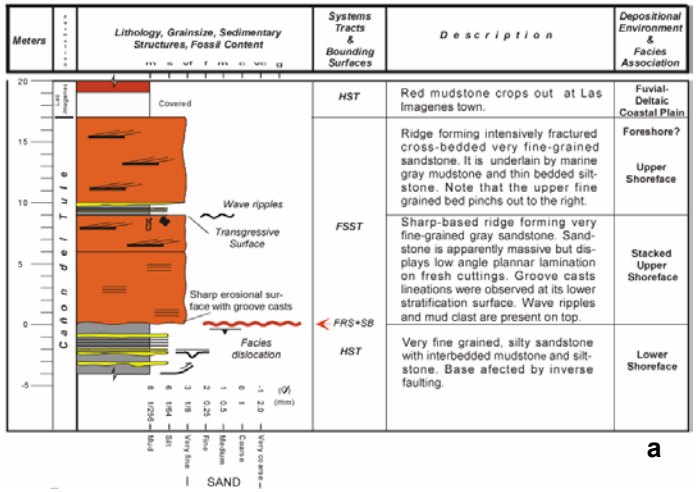

Figure 3.13 The FSST sandstone deposits on Highway 57 nearby Las Imágenes, Coahuila. At this location, the FSST deposits are subdivided into two sandstone beds separated by a thin interval of silty mudstone and a silty sandstone wedge (a, b). The lower subunit displays horizontal and low-angle planar lamination, wave ripples, and mud clasts on top (c). At Las Trancas-Palo Blanco Section (d), the uppermost gray greenish sandstone of the Cañón del Tule Formation contains traces of red material and grades into red mudstones of Las Imágenes Formation. Stick is 2 meters long.

The same stratigraphic relationship of thick sandstone bodies separated by thin to laminar mudstone or amalgamation surfaces was observed in most of the studied sections, where the sharp-based uppermost sandstone of the Cañón del Tule Formation was described (see sections La Casita, La Florida, El Realito and San Miguel; Figs. A.4, A.6, A.10, and A.11). Even at the distal Altamira Section (Fig. A.2), the forced regressive sandstone (FSST) is subdivided into two parts by a thin horizon of gray marine mudstone (Fig. 3.12). At this location, the ridge-forming sandstone, whose maximum thickness is 57 m at El Saucillo Section, is reduced to almost 2 m. However, its sharp-based character remains.

Discussion on Forced Regressions and Falling Stage Systems Tract (FSST)

Transgression and regression refers to the landward and seaward migration of the shoreline. Regression occurs at stable or rising sea level when sediment supply exceeds the rate at which accommodation space is created or during a sea level fall independently of sediment supply. In this second instance, regression occurs regardless of how much or how little sediment is delivered to the shoreline. This type of regression, forced by relative sea level fall and independent of sediment influx is termed forced regression (Posamentier *et al*., 1992; Posamentier and Morris, 2000).

Lowering of relative sea level results in successive lowering of fair-weather wave base, cannibalization of the substrate, and scouring of the sea floor in advance of the prograding shoreface (Posamentier *et al*., 1992). The shoreface deposits associated with forced regressions are commonly characterized by a sharp base, which defines an unconformity or sequence boundary (Posamentier *et al*., 1992; Posamentier and Morris, 2000). The major feature of forced regressions is the abrupt occurrence of coarser and more proximal sediments in distal marine settings. The surface underlying forced regressions deposits is

erosional in its proximal part grading seaward to a conformable contact (Posamentier *et al*., 1992). In nearshore areas, the lower boundary of forced regression deposits is the first surface of submarine erosion that commonly contains gutter casts (Plint and Nummedal, 2000).

The strata deposited during a forced regression either are grouped within the lowstand systems tract (Posamentier and Morris, 2000) or are included within a newly proposed *falling stage systems tract* (FSST; Plint and Nummedal, 2000). In other words, forced regression deposits are intrinsically assigned to lowstand by simple definition since their deposition occurred during the initial stage of relative sea level fall. The falling stage systems tract (FSST) is attributed to deposition during a relative sea level fall and is considered as the logical counterpart of a transgressive systems tract (Plint and Nummedal, 2000). FSST deposits lie above the highstand systems tract, their top is defined as a subaerial surface or a sequence boundary, and are overlain by the lowstand systems tract (LST). FSST deposits may be an undifferentiated sedimentary package without a differentiated internal structure or it may contain internal erosional surfaces of submarine erosion and ravinement surfaces. These latest surfaces record higher-frequency sea level falls and rises superimposed on an overall lower frequency sea level fall (Plint and Nummedal, 2000).

It was previously stated that the forced regression surface of the uppermost Cañón del Tule was initially developed by wave erosion of the underlying highstand and subsequently, while the regression progressed, by cannibalization of the deep-water FSST deposits (Fig. 3.2b). The erosional surface defines a facies truncation characterized by relatively deeper muddy sediments below (storm influenced lower shoreface to offshore) from shallower and coarser sediments above (sharp-based stacked upper shoreface to foreshore sandstone). The intermediate middle shoreface facies association is missing (Figs. 3.7 to 3.9, and 3.11). Additionally, the forced regression surface has a

regional expression and is characterized by an undulatory relief. Erosional structures such as tool marks, small gutter casts, and sand-filled meter scale channel-like deposits scouring the underlying HST deeper-water mudstone, were observed associated with the surface. These stratigraphic and sedimentologic features are commonly observed in forced regressive deposits. Therefore, the sharp-based sandstone of the uppermost Cañón del Tule Formation is interpreted as FSST deposits composed of individual forced regressive subunits (Fig. 3.2). It is interpreted that the deposition of the upper shoreface to foreshore sandstone occurred at the initial lowstand stage of sea level fall. Thus, the new terminology proposed by Plint and Nummedal (2000) for the initial lowstand deposits is adopted here, and the unit is assigned to a falling stage systems tract (FSST).

High rates of subsidence and accommodation space generation have been interpreted for the proximal Parras Basin on the areas adjacent to the SMO structural front (Ye, 1997; Halik, 1998). Soegaard *et al*. (*in press*) estimate extremely high subsidence rates of 1 m /1000 yr. Thus, a lowering in sea level within such a subsiding Parras Basin can only be explained assuming that eustasy overwhelmed and exceeded subsidence reducing accommodation space in proximal areas. Consequently, sediments supplied into the shoreline and nearshore facies were gradually deposited basinward. However, in the study area, the resultant change in sea level was not a continuous nor an "extended" sea level drop since the FSST shoreface are not overlain by lowstand deposits (see Plint and Nummedal´s Fig. 2, p. 9, 2000). In other words, the case studied here does not exactly match the Plint and Nummedal´s model or their FSST definition.

In some documented cases, lowstand (LST) deposits in proximal settings characterized by a sequence boundary, fluvial entrenchment, and sediment bypass, lie on top of forced regressive (FSST) deposits (Mellere and Steel, 2000; Gawthorpe *et al*., 2000; Plint and Nummedal, 2000). However, in the study herein

described, neither a sequence boundary associated with an unconformity, nor lowstand deposits overlie the FSST sandstone of the uppermost Cañón del Tule Formation. Here, the FSST deposits are transitionally overlain by coastal plain red beds of Las Imágenes Formation (FSST). It is interpreted that during the forced regression in the central Parras Basin, the shoreline migration was not associated with significant fluvial incision of the underlying shallow-marine sediments. It is assumed that high rates of subsidence lowered the coastal plain equilibrium profile preventing the fluvial systems to incise over the underlying marine rocks. Therefore, the contact between the Cañón del Tule and Las Imágenes formations is gradational and instead of an unconformity and a sequence boundary, the contact records a smooth shoreline regression and gradual deposition of coastal plain sediments over shoreface deposits. The transitional contact between the Cañón del Tule and Las Imágenes Formation is described in the subchapter 3.3.2.

In other words, there is no evidence to consider Las Imágenes Formation to be lowstand (LST) deposits simply because a continuous and extended sea level fall did not occur after the deposition of the forced regressive deposits (FSST). Consequently, an unconformity and sequence boundary on top of the shallow-marine FSST deposits was not developed. Posamentier and Allen (1999) suggest that one of the most common factors causing a lowering of fluvial equilibrium profile is tectonic tilting, that results in an increment of accommodation on the fold-and-thrust belt side of foreland basins. Tectonic tilting and subsidence is the major cause of accommodation, and for this reason, fluvial deposits commonly form thick accumulations toward the orogenic belt in foreland basins. The typical aggradational depositional architecture of the lower Las Imágenes Formation, its anomalously thickness in the western study area, and the absence of a sequence boundary at its bottom is attributed to the mechanisms suggested by Posamentier and Allen (1999).

It is still in debate whether a sequence boundary must be placed on top or at the bottom of the forced regressive deposits. Posamentier and Morris (2000) argue that it must be placed at the bottom of forced regressive deposits since this surface has chronostratigraphic significance. Additionally, its nature is consistent with the initial definition of sequence boundaries; it can be expressed, in part, as an unconformity and, at distal positions, as a correlative conformity. Plint and Nummedal (2000) suggest placing the sequence boundary on top of forced regressive deposits, where erosional processes related with the sea level fall and subsequent transgressive stage produce an unconformity. They argue that this unconformity can be easily recognized, has wide expression, and is a most readily mapable surface. In the case herein described, there is only one option. The unique candidate for a sequence boundary is the sharp erosional surface at the bottom of the forced regressive deposits of the uppermost Cañón del Tule Formation. This surface involved a process of sea level fall, facies dislocation, and basinward shift in facies.

In conclusion, adopting the terminology proposed by Plint and Nummedal (2000), the sharp-based sandstone of the uppermost Cañón del Tule is interpreted as falling stage systems tract deposits (FSST). It is also interpreted that eustasy was involved in the sea level fall process that produced the forced regression, in which eustasy overwhelmed and temporarily exceeded subsidence reducing dramatically accommodation space in proximal settings and forcing facies belts to move basinward. It is proposed, that the sea level fall that produced the forced regressive deposits was punctuated by short periods of sea level risings and renewal of accommodation space controlled by subsidence.

Discussion on Attached and Detached Forced Regressive Deposits

Posamentier and Morris (2000) apply the term *attached* forced regressive deposits to those shoreface deposits whose successive shoreface regressive units are in contact with each other. In this attached stratigraphic arrangement, there is not a significant zone of lateral separation between each successive regressive unit. The term attached also implies that forced regressive deposits lie directly over the immediate underlying highstand deposits. Posamentier and Morris (2000) also state that the development of attached forced regressive deposits is favored by low rates of relative sea level fall, high rates of sediment supply, and high-energy nearshore environments in relatively sharply inclined shelves.

At low rates of relative sea level fall, the rate at which the shoreline is forced to move basinward is also low, assuming a constant sediment supply. In this case, slow shoreline regression allows the successive forced regressive units to migrate basinward and deposit in contact with each other. These deposits are also attached in the sense that they lie directly over the underlying highstand deposits. When the rate of relative sea level fall is high, the shoreline migrates rapidly seaward. Only if the rate of sediment supply is high enough to keep up with the rapid rate of regression, regressive deposits will be in contact with each other; and attached deposits will develop. If the rate of sediment supply is not sufficient to keep up with the rate of shoreline regression, each successive regressive unit will be deposited separately, at a certain lateral distance basinward from the previous one. Then, detached regressive deposits will be produced. In this case, each successive regressive unit is isolated (detached) from the previous one, and a zone of offshore/prodelta muds separates the forced regressive units (Posamentier and Morris, 2000).

In the central Parras Basin, diagnostic features of forced regression were recognized at locations over 23 km in an east-west direction (El Realito-Altamira, Fig. A.18), and 15 km in a southwest-northeast direction (El Saucillo-La Casita, Fig. A.19; see also Fig. 2.8). This extensive areal distribution of sharp-based forced regression deposits within the study area suggests at least 23 km of shoreline displacement within a wide and shallow, gently inclined ramp-type depositional setting, characterized by minor lateral environmental variations and facies distribution. The internal architecture of the forced regressive sandstone deposits of the uppermost Cañón del Tule Formation reveals that the forced regressive subunits are stacked and separated by thin muddy-silty horizons (Fig. 3.11). Additionally, forced regressive deposits lie over the underlying highstand lower shoreface to offshore deposits. This stratigraphic arrangement is typical of the deposits that have been referred as "attached" forced regressive deposits by Posamentier and Morris (2000).

3.3.2 Contact Cañón del Tule / Las Imágenes Formation

Baker (1970) describes the contact between the Upper Member of the Cañón del Tule Formation and the overlying Las Imágenes rocks as a planar surface represented by an abrupt lithologic change. According to his observations, there is no trace of red material within the Cañón del Tule and there is no evidence of erosion. However, in several sections studied in this work, the uppermost unit of the Cañón del Tule Formation is a massive sandstone that fines, contains traces of red material, becomes gradually reddish upward, and grades into red mudstones of Las Imágenes Formation (El Saucillo Section, Fig. A.12). The same gradational character was observed at La Campana and Las Trancas-Palo Blanco sections (Figs. A.2, A.16 and 3.13d). In none of the studied sections does fluvial incision occur between Las Imágenes channelized deposits and the underlying shallow marine shoreface sandstone of the uppermost Cañón del Tule Formation, as Baker (1970) suggests. McBride *et al*. (1975) also point

out that nowhere in several localities in the Parras and La Popa basins do they observe major channels cutting into the shallow marine sediments of the Difunta Group.

It was observed in this work, that there are traces of red material within the uppermost sandstone of the Cañón del Tule Formation. The zone of transition is several meters thick and is characterized by gray greenish grains mixed with reddish material within the same sandstone beds (El Saucillo Section, Fig. A.12). It is assumed that rivers flowing in the coastal plain partially eroded the reddened coastal deposits and transported red sediments to the shoreline, where they were mixed with green and gray shallow marine foreshore to upper shoreface sediments. The gradational character of the contact between the Cañón del Tule and Las Imágenes formations suggests a slow and smooth shoreline regression and progressive advance of the coastal plain (FSST red deposits) over shallow marine (FSST) foreshore to upper shoreface environments (Fig. 3.2). This transitional contact is interpreted as a process characterized by sediment supply exceeding the accommodation space generation and coastline regression without significant fluvial erosion.

3.4 LOWER LAS IMAGENES FORMATION

Falling Stage Systems Tract (FSST)

3.4.1 Coastal Plain Red Mudstone, Siltstone, and Sandstone

Besides the shallow-marine shoreface deposits of the uppermost Cañón del Tule Formation, the FSST includes the contemporaneous and laterally contiguous red bed deposits of the lower Las Imágenes Formation deposited in the adjacent coastal plain (red dotted unit, Fig. 3.2b). This lower part of the formation is interpreted to be deposited in a regime of relative sea level fall, following the basinward migration of the shoreline during the forced regression described in the preceding subchapters. In west to east direction, the seaward-

advancing red beds never extended farther the intermediate area between the Temporal and the Altamira sections (Fig. 2.8; cross section A.18). From south to north the fine-grained red beds never extended farther than the town of Fraustro located in northern Parras Basin (Soegaard *et al*., 1997), 10 km northward of La Florida Section (Figs. 2.8 and A.6).

The best exposures of the FSST deposits of the lower Las Imágenes Formation are located in outcrops of difficult access in the western sector of the study area, nearby El Potrero and El Realito sections (Fig. A.10; cross section A.18). At El Realito, the thickest measured section of Las Imágenes Formation, the FSST deposits include 425 m of mostly aggradational fluvial floodplain overbank deposits. Overall, the section includes a major proportion of varicolored massive mudstone and less amounts of ripple cross-laminated mudstone and siltstone. The coarse-grained deposits include thin-bedded brown reddish sandstone and channel-fill deposits that interrupt the monotonous fine-grained red deposits.

The FSST red deposits of the lower Las Imágenes Formation are lithologically similar to their transgressive (TST) counterpart of the upper part of the formation (Fig. 3.2; cross section A.18). Regardless of the limited stratigraphic coverage of the FSST red strata, it can be pointed out that the most significant difference of this unit with the overlying Early TST deposits is their fossil content. Overall, the FSST includes a monotonous red succession in which fossils were not found. In contrast, the overlying Early TST red bed deposits contain charophytes, ostracods, and fossils that evidenced marine influence (rotalid-type and other benthonic foraminifers, oyster deposits, echinoderm plates). All the red strata of the lower Las Imágenes Formation deposited below the first fossiliferous charophyte-bearing interval are grouped within the falling stage systems tract (FSST) (Fig. 3.2; cross sections A.17 to A.19). The charophyte-bearing interval thus represents the lowermost part of the transgressive (Early TST) deposits and

the first signals of an intermittent transgression within a highly subsiding coastal plain (Fig. 3.2). The charophyte-bearing interval is described in the following paragraphs.

3.5 UPPER LAS IMAGENES FORMATION

Early Transgressive Systems Tract (Early TST)

The Early Transgressive Systems Tract (Early TST) groups the red beds of the upper Las Imágenes Formation, including the charophyte-bearing interval and all the overlying coastal plain deposits (Fig. 3.2). Within a coastal plain, different depositional settings were interpreted for the red bed deposits of the upper Las Imágenes Formation. The associated deposits to these environments include lacustrine and lagoonal charophyte-bearing deposits, overbank fluvial floodplain fine-grained red beds, channel-fill sandstone, strand plain (?) sheet sandstone, and non-red fluvial conglomerates.

The Early TST also includes the shallow marine deposits of the lowermost Cerro Grande Formation (Fig. 3.2). These strata are described later in the subchapter 3.6.

3.5.1 The charophyte-bearing interval

Lacustrine and Lagoonal Charophyte-bearing Deposits

The coastal plain deposits in the middle part of Las Imágenes Formation (Fig. 3.2; cross sections A.17 to A.19) contain fossil remains of charophytes, aquatic plant-like organisms with genetic affinity to green algae. The fossil charophytes include remains of branchlets and abundant excellently preserved gyrogonites that in some sections are associated with thin-shelled ostracods or benthonic foraminifers (Plate 11). G*yrogonite* or lime shell are terms applied to spherical to ovoidal particles less than 2 mm in size that constitute the fossilized

female reproductive organs of charophytes (Plates 7-10). The most important charophyte concentrations within strata of Las Imágenes Formation occur in hard calcite-cemented beds or white clays interbedded with red mudstone.

The charophyte deposits are confined to the middle part of Las Imágenes Formation, within a 40-m-thick interval (cross section A.17 to A.19). Charophyte gyrogonites were recovered from samples collected approximately of the same stratigraphic position at El Potrero, El Realito, El Saucillo, La Campana, La Florida, and La Casita sections, distributed within the study area (Fig. 2.8). Charophytes were also collected nearby the Doce the Diciembre Section (Fig. A.5) from deposits of the middle part of Las Imágenes Formation. In the western study area covered by El Realito and El Potrero sections, the regionally extended ridge-forming sandstones provide a reference for the stratigraphic control of the charophyte deposits. In the east-central area, these deposits were recognized due to their unmistakable stratigraphic position a few meters above the contact between Las Imágenes and the sharp-based (FSST) shallow marine sandstone of the uppermost Cañon del Tule Formation (Fig. 3.2).

Most of the charophyte deposits are isolated and laterally restricted bodies of white charophyte-bearing clays or well-cemented charophyte banks, encased within fine-grained floodplain red deposits (Fig. 3.2; cross sections A.17 to A.19). Charophyte deposits are commonly a few centimeters to 3 m thick and up to 50 m wide. Charophytes in these beds are commonly associated with thin-shelled ostracods and remains of charophyte branchlets. Lithology, thickness, the isolated character of these deposits, and the fossil association observed, suggest that charophytes grew in laterally restricted bodies of fresh water (small lakes or ponds) located within an extensive and rapidly subsiding Las Imágenes coastal plain.

In contrast, the charophytes recovered from La Casita Section (Fig. A.4) are associated with abundant benthonic foraminifers and thin-shelled ostracods

(Plates 10 and 11), within intensively bioturbated mudstone with branched burrows resembling *Thalassinoides.* A complete destruction of primary sedimentary structures within the interval suggests intense biogenic activity at low rates of deposition in quiet conditions that let aquatic organisms dig into the muddy substrate. The intense bioturbation and the association of fossils (charophytes, benthonic foraminifers, and ostracods), suggest a quiet muddy depositional brackish water environment such as a marginal lagoon or bay. The benthonic foraminifers clearly indicate marine water influence since these organisms are not able to survive in fluvial or any other restricted internal continental environment. Crawley (1975) interprets that some gray beds of Las Imágenes were deposited in poorly drained lower delta-plain and inner delta-fringe environments. He adds that depositional environments include fresh to saline marshes, lagoons or bays, and smaller distributary and tidal channels.

The fine-grained Early TST coastal plain deposits commonly display intense bioturbation (Fig. 3.14a). Some interbedded green horizons are composed of accumulations of broken oysters, diverse shell fragments, and hematitized benthonic foraminifers (El Potrero Section, Figs. A.8 and 3.14b). This assemblage of fossil charophytes and associated marine fossils is interpreted as the beginning of an intermittent marine transgression that favored the development of charophytes within a set of marginal marine environments (marshes, small lakes or ponds, and lagoons). The occurrence of benthonic foraminifers and echinoderm fragments within red sandstone upward in Las Imágenes Formation also supports this interpretation (Puerto La Cuesta Section, Fig. A.9, cross section A.18).

The charophyte-bearing interval was useful as a level of reference and correlation due to its restricted stratigraphic and regional distribution (Fig. 3.2;

Figure 3.14 Sedimentary structures and fossil content within the transgressive (Early TST) red bed deposits of the upper Las Imágenes Formation. Fine-grained coastal plain deposits of the upper Las Imágenes Formation are commonly bioturbated (a). Some Early TST deposits are accumulations of broken oysters (b), which are brackish-water faunas. Thin sections of these rocks contain hematitized benthonic foramaminifers. Current ripples (c) and plant debris (d) are also common. Outcrops shown in (a), (c) and (d) are from the Puerto La Cuesta Section (Fig. A.9), (b) from El Potrero Section (Fig. A.8).

cross sections A.17 to A.19). The interval is a stratigraphic boundary useful to differentiate the coastal plain red strata deposited during a sea level fall regime (FSST) from the overlying transgressive (Early TST) red beds deposited within an overall rising in relative sea level stage (Fig. 3.2). Consequently, the bottom of the charophyte-bearing deposits is interpreted an early marine transgressive surface developed during the initial stage of an intermittent marine transgression that preceded the major marine transgression of the lower Cerro Grande Formation (Fig. 3.1 and 3.2).

Charophyte oogonia were described to be locally contained in the finer-grained beds of Las Imágenes (Murray *et al*., 1962; McBride, 1974; Crawley, 1975). However, the charophytes have never been formally described nor illustrated in previous studies of the Parras Basin. Their excellent preservation, abundance, and diversity as well as their value for stratigraphic correlation and paleoenvironmental interpretation are considered important reasons to dedicate Chapter 4 to their description and illustration. The chapter includes a brief introduction to the morphology, reproduction, and taxonomy of modern charophytes and deals with different aspects regarding their habitat and environmental distribution.

3.5.2 Overbank Fluvial Floodplain Deposits

Monotonous successions of varicolored mudstone, mostly red and less purple, green, gray, and white-greenish, constitute the major proportion of the Early TST aggradational deposits of Las Imágenes Formation (Fig. 3.15). McBride *et al*. (1974) estimated that 70 percent of Las Imágenes deposits are mudstone and 30 percent sandstone and siltstone. Approximately the same proportion was observed in the sections measured in this study. Based on their aggradational character, fine-grained size, thickness, lateral and vertical association with fluvial channel-fill and lacustrine deposits, these intervals are interpreted as overbank

Figure 3.15 Aggradational Early TST coastal plain red bed deposits of Las Imágenes Formation. (a) monotonous interbedding of, varicolored, mostly red, less purple, and green massive mudstone at El Saucillo Section. (b) ripple cross-laminated red and purple mudstone, siltstone, and thin-bedded red sandstone at La Florida Section. At this location, besides charophyte gyrogonites, the red silty deposits contain badly preserved plant fragments (c-d).

fluvial floodplain deposits. Floodplain aggradation occurs when the river's water column mostly containing suspended-load sediments, overflow the river banks and spill sediment-laden water across interchannel areas. The resultant layer-by-layer aggradational accumulation of sediments between interdistributary channels may spread out several kilometers and reach few centimeters in thickness per year (Galloway and Hobday, 1996).

The most continuous exposures of the Early TST deposits of Las Imágenes Formation may reach 50 to 80 m of continuous and monotonous accumulations of sediments without a defined vertical grain-size trend (Las Trancas-Palo Blanco Section, Fig. A.16). Ripple cross-laminated mudstone, siltstone, and thin-bedded brown reddish sandstone commonly interrupt the overbank floodplain deposits. Interbedded sandstones are commonly lenticular, a few centimeters thick in the middle part and a few meters of lateral distribution. Some of them are very low relief channel-shaped bodies that may represent deposits of temporal channelized flow of shallow water during river floodings. Overbank floodplain fine-grained deposits commonly contain impressions of small plant branches, palm-like leaves (Fig. 3.15c) and abundant plant debris (Fig. 3.15d).

3.5.3 Channel-fill Deposits

Lenticular sandstone bodies a few meters thick and tens of meters wide commonly interrupt the continuous exposures of overbank floodplain deposits of Las Imágenes Formation (Fig. 3.16). Four of these sandstone units locally incise the fine-grained floodplain red deposits exposed along the 148-m-thick Las Trancas Section (Fig. A.16), and several were observed at El Saucillo Section (Fig. A.12). Based on their geometry, erosional relationship with the lateral and underlying fine-grained sediments, and their internal framework composed mostly of sandstone, these lenticular sandstone are interpreted as channel-fill deposits.

Figure 3.16 Channel-fill and overbank red deposits of Las Imágenes Formation. The channel is almost 70 m wide and 6 m thick in its middle part (note the standing person for scale). Channel-fill is composed of four stacked planar-laminated and trough cross-bedded reddish sandstone (labeled 1 to 4) that pinch out and seem to be laterally accreted over the encasing red and green fine-grained overbank deposits. Mud drapes are abundant at the low-relief basal surface that cuts into the underlying massive green mudstone. Sandstone in channel-fills and fine-grained floodplain deposits suggest a mixed-load probably meandering (?) fluvial system. At least four channels of variable size incise along 148 m of overbank floodplain deposits in this section; similar deposits are 550 m thick at El Realito Section. Outcrop of the lowermost channel-fill at Las Trancas-Palo Blanco Section (Fig. A.16).

Most commonly observed channels include lenticular sandstone bodies internally composed of tabular stacked beds of planar-laminated and trough cross-bedded reddish sandstone. In the vicinity of the type locality of Las Imágenes Formation, Crawley (1975) also observed channel-fill, levee, or crevasse-splay deposits. He describes that channel-lag deposits consists of mudstone and claystone intraclasts and wood fragments, and reports that extrabasinal pebbles are absent in the channel-fill deposits. Caliche nodules derived from soils are common, especially at the base of some channel-lag deposits (McBride *et al*., 1974; Crawley, 1975).

The best exposed channel-fill was observed at the lower part of Las Trancas Section (Fig. A.16), where the outcrop wall roughly cuts perpendicular to the northeast paleocurrent flow direction (Fig. 3.16). The channel-fill is composed of four individual lenticular sandstone beds (labeled 1 to 4) that reach 6 m of maximum thickness in the middle part of the channel. These sandstones pinch out and merge laterally within the green and red mudstone of the encasing overbank floodplain deposits (Fig. 3.16). The channel is about 70 m wide; the lowermost sandstone (1) contains abundant mud drapes and displays planar lamination and a low-relief basal surface that cuts into the underlying massive green mudstone. The uppermost sandstone (4) is covered by green and purple burrowed mudstone and interbedded thin laminar siltstone. Channel geometry, low relief basal surface, and lithology suggest a wide and shallow mixed-load fluvial system flowing on a low gradient coastal plain mostly composed of fine-grained sediments. Very fine- to fine-grained sand transported as a bedload settled to form the channel-fill deposit itself. When rivers overflowed their low-relief banks, suspended-load fine-grained sediments were spilled out of the channels and deposited on extensive floodplain areas. Note in Figure 3.16 that the sandstones labeled 2-3 seem to be laterally accreted on one flank of the channel (right side of the photograph) which suggests a meandering stream.

The channel-fill deposits of Las Imágenes Formation seem to have a discrete lateral and stratigraphic distribution. Channel-fill deposits are most commonly exposed on the southwestern portion of the study area covered by the sections El Saucillo, Las Trancas-Palo Blanco, Doce de Diciembre, and Puerto La Cuesta (see cross sections A.17 and A.19). Fluvial channels are less abundant or are totally absent in the east-central part of the area covered by the sections La Campana, Santo Domingo, Temporal, and La Casita Section (Fig. 2.8). In the west, where Las Imágenes Formation reaches its maximum thickness, channels are confined within the middle and upper portion of the formation. The lower to middle part of Las Imágenes Formation in the west and the middle to upper part in the east are fine-grained fluvial plain overbank where channel-fill deposits are almost absent.

Additionally, the channel-fill deposits of the middle portion of Las Imágenes Formation, such as those described at Las Trancas-Palo Blanco Section (Fig. A.16), are lithologically different from those described in the upper part of the same formation and the lower Cerro Grande Formation. The lower channel-fill deposits consist of fine-grained sandstone, whereas those described from the upper part contain conglomerate deposits, either as channel lags of chert pebbles (Fig. 3.17a, b), intraformational conglomerates, or forming the channel-fill deposit itself. On the other hand, the gravelly upper channels incise into fine-grained floodplain red sediments intensively bioturbated (Fig. 3.14a) and are interbedded with sheet sandstone deposits that contain benthonic foraminifers and echinoderm fragments, which clearly suggest marine influence. The upward occurrence of gravels within channel-fill deposits of Las Imágenes Formation and the fossil content of the associated deposits, suggest that with time, streams increased their transport capacity. Coarse gravel sediments supplied by rivers eventually reached the shoreline where they were redistributed and mixed with sand by marine processes.

Figure 3.17 Channel-fill deposits of the upper Las Imágenes Formation (Early TST) at Puerto La Cuesta Section. Channel-fills are characterized by trough cross-bedded fine-grained sandstone (c), and lenticular channel lag deposits composed of varicolored chert pebbles, siltstone, and mudstone fragments (a, b). The red circle in (a) indicates the detail of the channel lag shown in (b). Note that the channel lag pinchs out to the left toward the channel margin. The lower sandstone of the upper photograph is almost 1 m thick. All photographs taken from the middle part of the Puerto La Cuesta Section (interval pc+85 to pc+90; Fig. A.9).

3.5.4 Strand Plain (?) Sheet Sandstone

The best exposures of the strand plain (?) sheet sandstone are confined to the western study area between El Realito and El Potrero sections, where Las Imágenes reaches about 550 m in thickness (Fig. A.18). These red deposits include very fine- to fine-grained ridge and mesa-forming sheet sandstones that extend laterally along strike up to 15 km and 10 km in an east-west dip direction (Fig. 3.18). Sheet sandstone ridges are interbedded with deposits that reach 50 to 80 m of monotonous red mudstone, thin sandstone, and siltstone attributed to overbank fluvial floodplain deposits. Sheet sandstone ridges are 10 m thick on average, but some display variable thickness along strike.

In El Realito area (Fig. 2.8), some sheet sandstone ridges thicken locally for about 100 m and laterally reduce their thickness until they pinch out and merge within the encasing red mudstone, several kilometers away. It is interpreted that these lenticular thicker portions were channelized deposits and that they were amalgamated with laterally extended sheets of sand once these channelized sediments reached the shoreline. Redistribution of sediments along the coast was produced by the action of waves and longshore currents. The occurrence of abundant benthonic foraminifers and echinoderm plates in samples collected from one of these sheet sandstones supports this interpretation. These marine fossils were observed in thin sections of red sandstones from the Puerto La Cuesta Section (Fig. A.9; sample PC+68, Plate 13). Green horizons containing hematitized benthonic foraminifers, whole oyster shells, gastropod fragments, and diverse shell fragments debris were also observed within a green horizon at the base of El Potrero Section (Fig. 3.14b), within the charophyte interval (Fig. A.18).

In summary, geometry, remarkable strike extension, and fossil content, suggest that the sheet sandstone bodies of the upper Las Imágenes Formation represent accumulations of redistributed sediments. Interbedding of these

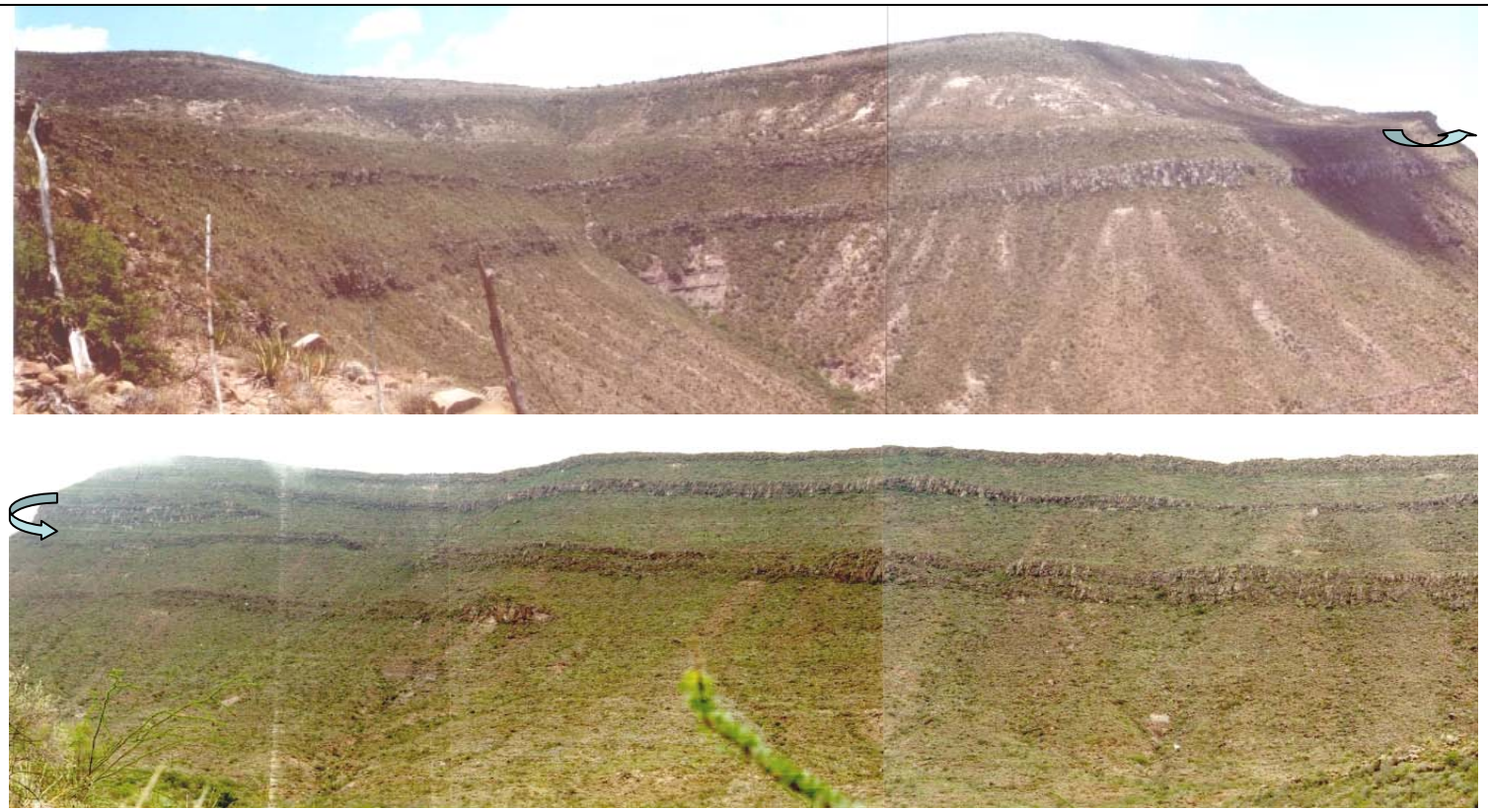

Figure 3.18 Prominent ridge-forming sheet sandstone deposits (Early TST) of the upper Las Imágenes Formation nearby El Realito and El Potrero sections. The ridges extend up to 10 km along strike and up to 15 km in a west to east dipping direction. Some sandstone ridges pinch out within the fine-grained coastal plain red deposits. These widely extended sheets of sand are thought to be fluvial deposits that were redistributed along the coastline by waves and longshore currents within a wave-dominated strand plain (?). Ridges thicken locally probably where channelized deposition occurred. Interbedding of sediments of fluvial character with marine-influenced red sediments was observed at the Puerto La Cuesta Section, where some red sandstone ridges contain rotalid-type benthonic foraminifers and diverse biogenic fragments of clear marine origin. The photograph below covers the hidden portion back of the ridges shown in the upper photograph.

redistributed sheet sandstone bodies with other deposits of fluvial character suggests intermittent marine incursions over a subsiding coastal plain. The Maastrichtian coastal plain of Las Imágenes seems to have been drained by mixed-load meandering rivers that did not develop typical fluvial-dominated deltas. It is proposed that sediments supplied by rivers were redistributed by either waves or longshore currents that developed strand plain deposits similar to those of cuspate wave-dominated deltas. Once the sediments reached the shoreline, redistribution processes precluded the development of typical progradational delta front facies and mouth bars. According to Crawley (1975), there is no evidence that any large rivers formed a deltaic center in the Cerro Grande outcrop area. He suggests that "the deltaic coast was a relatively straight coast, perhaps with small cuspate deltas, and was formed of coalesced beach and beach-ridge deposits, much like the modern Tabasco and Nayarit coasts of Mexico" (Crawley, 1975, p. 200).

In wave-dominated deltas, most bed-load sediments deposited at distributary mouths are reworked and redistributed by waves and longshore currents along the delta front (Galloway and Hobday, 1996). Redistribution results in coalescent beach ridges and a smooth cuspate to arcuate delta front. The Rhone, Magdalena, Tiber, Nile, Orinoco, among others, are modern examples of wave-dominated delta systems. The modern Rhone, for instance, has prograded basinward more than 16 km and has produced a strike-elongated delta front composed of beach-ridges complexes of sand up to 10 m thick, and 50 km by 20 km in areal extent. Intense redistribution processes in wave-dominated deltas such as the Rhone may produced widespread dispersal of suspended sediments and, consequently, thick and localized mud and silt deposits may be absent in the delta front facies (Galloway and Hobday, 1996).

3.5.5 Fluvial Conglomerates

In the western part of the study area, gravelly deposits occur locally as discrete layers of chert pebbles within thick-bedded sandstone beds of the upper Las Imágenes Formation (Puerto La Cuesta Section; Figs A.9 and 3.19a). Conglomerates are gradually abundant upward in this formation. The upper Doce de Diciembre Section (Fig. A.5) is composed of fine-grained trough cross-bedded channel-fill sandstone (Fig. 3.19b), light brown fine-grained overbank fluvial deposits, and interbedded non-red conglomerates that become the framework of channel-fill deposits (Fig. 3.19c, d). Conglomerates are composed of varicolored red, green, and black chert pebbles and cobbles. These fluvial conglomerates are grouped within the Early TST deposits that preceded the subsequent transgressive event and deposition of Late TST marine deposits of the lower Cerro Grande Formation (Fig. 3.2). They are attributed to the final stage of fluvial deposition and are assigned to the upper Las Imágenes coastal plain deposits by the following reasons.

Crawley (1975), who studied the stratigraphy and sedimentology of the Cerro Grande Formation, used the resistant, cliff- or ridge forming sandstone units to recognize the bottom and the top of this formation. He established the contact between Las Imágenes and Cerro Grande formations at the base of the first thick-bedded, laterally persistent, gray sandstone bed overlying the red beds of Las Imágenes Formation. He also suggested including within the Cerro Grande Formation all the gray-brown rocks of "apparent marine origin" that lies stratigraphically between the red beds of Las Imágenes and Las Encinas Formation (see Crawley, 1975, p. 16). However, in the western study area, the resistant or ridge-forming sandstone used by Crawley is absent, and the first non-red deposits overlying the red beds of Las Imágenes Formation are fluvial sandstone and conglomerates (Doce de Diciembre and Puerto La Cuesta sections, Figs. A.5 and A.9; cross section A.18). Consequently, in this area,

Figure 3.19 Conglomeratic deposits of the upper Las Imágenes Formation. In the uppermost Las Imágenes Formation, pebbles and cobbles occur as channel lags or discrete horizons within sandstone beds (a). Cross-bedded sandstone (b) and channel-fill non-red fluvial conglomerates (c, d) were observed in the upper part of the Doce de Diciembre Section (upper interval in Fig. A.5). Photographs (a) is from the Puerto La Cuesta Section (interval pc+65.3, Fig. A.9).

Crawley's criterion for identifying the lithostratigraphic contact between Las Imágenes and the overlying Cerro Grande Formation is not applicable. The change from red to green-gray coloration cannot be used to distinguish the stratigraphic contact between these two formations. Although it is a distinctive feature of Las Imágenes Formation, the use of the red color as a stratigraphic boundary is inappropriate because such red color boundaries are of diagenetic origin and cut across lithosomes (E. F. McBride, written comm., 2003).

Consequently, the conglomerates that overlie the uppermost red mudstone of Las Imágenes Formation in the upper Doce de Diciembre and Puerto La Cuesta sections (Fig. A.18) are assigned to Las Imágenes Formation. These non-red conglomerates do not contain marine fossils and their fluvial origin suggests more affinity with the fluvial character of the coastal plain (Early TST) red deposits of Las Imágenes Formation. At the Doce de Diciembre Section (Fig. A.18), the contact between Las Imágenes and Cerro Grande formations undoubtedly lies several meters above the conglomerates, at the first stratigraphic horizon that contains gastropods and bivalves. Covered intervals and poor stratigraphic coverage made difficult the accurate identification of the contact in the western study area.

The conglomerate deposits of the upper Las Imágenes Formation suggest that the transport capacity of fluvial streams increased in time. These more powerful streams drained across the coastal plain and transported gravels that eventually reached the shoreline. Coarser deposits may have been produced by uplifting of the source area before the covering of the central Parras Basin by the shallow marine transgressive sediments of the lower Cerro Grande Formation. A similar interpretation is formulated by Crawley (1975), who suggests that streams quickened in response to tectonics adjustments transported pebbles to the Cerro Grande coast. The fluvial conglomerates of the upper Las Imágenes Formation probably have the same origin.

3.5.6 Transgressive Surface (TS 3)

In the central study area, the transgressive surface (TS 3) on top of the Early TST deposits roughly coincides with the lithostratigraphic contact between Las Imágenes and Cerro Grande formations (Figs. 3.1, 3.2 and A.19). The surface TS 3 was observed in most of the sections, but the best exposures occur at the sections La Campana, La Florida, and Las Trancas-Palo Blanco (Fig. 2.8). At La Campana Section (Fig. A.3), a thick ridge-forming red sandstone encased in non-bioturbated red mudstone characterizes the uppermost Las Imágenes Formation (Fig. 3.20a, b). The uppermost red mudstone is directly overlain by a gray greenish mudstone interpreted to be the initial transgressive deposits of the Cerro Grande Formation, where the transgressive surface TS 3 was tentatively placed (Fig. 3.20c). Successively upward, a first 1-m-thick massive sandstone contains small flute casts at its base (Fig. 3.20d), and a 1.5-m-thick second sandstone contains shell fragments on top. The sequence deepens upward grading into bioturbated muddy deposits with ammonite fragments and rare hematitized benthonic foraminifers (Fig. A.3, interval LC+128.8). The flute casts at the bottom of the first prominent ridge-forming sandstone of the lowermost Cerro Grande Formation (Fig. 3.20 c, d) and scarce marine fossils in the overlying highly bioturbated fine-grained sediments, suggest deposition in shallow marine environments. Flute casts are attributed to the scouring action of currents moving over an unconsolidated mud bottom (Selley, 2000).

At Las Trancas-Palo Blanco Section (Fig. A.16), 5 km southwest of La Campana Section, the transgressive surface occurs at a similar stratigraphic position on top of Las Imágenes Formation (Fig. 3.21). The uppermost red strata are overlain by approximately 30 cm of gray greenish mudstone and successively by 1-m-thick bioturbated massive sandstone. At its base, the sandstone contains a discrete pebble lag made of black chert pebbles and small bivalves (Fig. 3.21a,

Figure 3.20 The transgressive surface (TS 3) on top of Las Imágenes Formation at La Campana Section. In this section (Fig. A.3), Las Imágenes deposits predominantly consist of red and less green mudstone, thin-bedded siltstone and sandstone (a). The bed in (b) is the thickest and unique ridge-forming red sandstone, 1.6 m thick, encased within red strata almost at the top of the formation. The red dashed line in (c) represents an option to place the transgresive surface TS 3, but the surface may lie somewhere within the 1.6-m-thick interval of gray-greenish mudstone with lenticular sandstone wedges or at the bottom of the first 1-m-thick sandstone bed (above the dashed line), which contains small flute casts at its bottom (d). The 1.5-m-thick upper sandstone bed in (c) contains shell fragments on top. The sequence deepens upward grading into muddy deposits (see Fig. 3.22) with ammonite fragments and hematitized benthonic foraminifers.

Figure 3.21 The transgressive surface (TS 3) on top of Las Imágenes Formation at La Florida and Las Trancas-Palo Blanco sections. The uppermost red bed of Las Imágenes Formation at Las Trancas-Palo Blanco Section (a) is overlain by a 30-cm-thick interval of green bioturbated mudstone, by an amalgamated marine sandstone bed shown in (b). The bottom of the sandstone contains a lag of black chert pebbles and shell fragments. The upper part of the bed is of massive character and is overlain by biotubated gray mudstone. At La Florida Section (c, d) the uppermost red bed deposits of Las Imágenes Formation are directly overlain by intensively bioturbated gray mudstone with *Glossifungites* (d), commonly observed at firm grounds of transgressive surfaces.

b). Here, the transgressive surface (TS 3) is interpreted to be at the bottom of the first marine sandstone containing the pebble lag (Fig. 3.21b).

At La Florida Section (Fig. A.6), marine highly bioturbated green mudstone directly overlies the uppermost red mudstone without any sandstone or pebble lag (Fig. 3.21c). However, the lowermost gray mudstone contains branched burrows and *Glossifungites* (Fig. 3.21d), commonly described of firm grounds of transgressive surfaces (Posamentier and Allen, 1999). Whole specimens of *Exogyra costata* also appear a few meters upward in the section, and thin sections of the gray mudstone contain benthonic foraminifers and few badly preserved charophyte gyrogonites. The transgressive surface (TS 3) was inferred to lie at the bottom of the bioturbated gray mudstone (Fig. 3.21d).

At the distal Altamira Section (Fig. A.2), the red deposits of Las Imágenes are absent since the unit pinched out about 3 km west of this section (Figs. 3.2 and A.18). Consequently, the sediments of the lower Cerro Grande Formation lie directly above the forced regressive deposits (FSST) of the uppermost Cañón del Tule (Fig. 3.12). Theoretically, the transgressive surface (TS 3) lies on top of the FSST deposits, but no evidence of transgression other than a marine mudstone overlying the FSST deposits was observed. The precise position of the transgressive surface (TS 3) in the eastern region of the study area needs to be established.

In the western study area, the transgressive surface (TS 3) was inferred to lie at the bottom of the first marine rocks that contain gastropods and bivalves. This marine fossil-bearing interval lies several meters above the uppermost red beds and above the channel-fill fluvial conglomerates of the upper Las Imágenes Formation (Fig. 3.2). Covered intervals and poor stratigraphic coverage made difficult the accurate identification of the transgressive surface (TS 3) in this area (Fig. A.18).

3.6 LOWER CERRO GRANDE FORMATION

3.6.1 Early and Late Transgressive Systems Tract (TST)

Upper, Middle, and Lower Shoreface

The Early Transgressive Systems Tract (Early TST) groups the red beds of the upper Las Imágenes and the laterally equivalent shallow-marine deposits of the lowermost Cerro Grande formations (Fig. 3.2). The shallow marine deposits of the Cerro Grande Formation, apparently not equivalent to any red beds in the study area and deposited immediately below the MFS 3 (Fig. 3.2b), are conventionally named in this study as Late TST deposits. The charophyte and associated Early TST coastal plain red deposits that contain benthonic foraminifers, ostracods, oyster shell, and echinoderm fragments, suggests marine incursions and signals of an intermittent transgression over a rapidly subsiding coastal plain. It is proposed that the marine transgressive sediments (Early and Late TST) of the lower Cerro Grande were diachronously deposited over the Early TST strata of Las Imágenes Formation. Consequently, it was not defined a boundary to differentiate the Early from the Late TST deposits of the lower Cerro Grande Formation (Fig. 3.2b).

Crawley (1975) reports to have measured 168 m of Las Imágenes Formation in the vicinity of its type locality. He describes that "the lower 78 m is predominantly red-colored rock in contrast to the upper 90 m of non-red rock" (Crawley, 1975, p. 28). He adds that a 1.5-m-thick gray sandstone unit that abruptly overlies red mudstone marks the base of the non-red gray lithosome. However, in a section measured in the same type locality area (Las Trancas-Palo Blanco Section; Fig. A.16), the base of the non-red lithosome described by Crawley is characterized by a thick-bedded sandstone with a pebble and shell lag at its bottom, interpreted as a transgressive lag (Fig. 3.21a, b). Additionally, above the sandstone, the section rapidly grades upward into fine-grained sediments including black and gray mudstone and siltstone that contain mollusks specimens

identified as *Stantonella* sp., *Idonarca* sp., *Anomia* sp. (F. Vega, written comm., 1998), and unidentified ammonite fragments. Therefore, the non-red rocks above the uppermost red mudstone of Las Imágenes Formation (Fig. 3.21a, b), included by Crawley as the lowermost part of the 90-m-thick non-red rocks of Las Imágenes Formation, are interpreted here as the lowermost transgressive deposits of the Cerro Grande Formation. These strata were deposited in upper to middle shoreface environments. In other words, the first thick-bedded gray sandstone with a pebble and shell lag is considered the lower boundary of the Cerro Grande Formation (Fig. 3.21a, b).

Crawley (1975) points out that although the abrupt base (of the non-red deposits) suggests a channel-fill surface, the 1.5-m-thick sandstone at the bottom may be a transgressive shore zone deposit, which is more consistent with the environment interpreted here. He adds that the lowermost non-red sandstone was not considered the lower boundary of the Cerro Grande Formation because a much thicker and more persistent sandstone unit, higher in the section, that has definite shore zone sedimentary characteristics, was preferred (see Crawley, 1975, p. 32).

The transgressive (Early TST) deposits of the lower Cerro Grande Formation were also studied at La Campana and Altamira sections (Figs., A.3 and A.2; cross sections A.18 and A.19). At La Campana Section (Fig A.3), the lowermost transgressive strata of the lower Cerro Grande Formation include two beds, 1 and 1.5 m thick, of massive planar-laminated sandstone interpreted as upper shoreface deposits (Figs. 3.20c, d and 3.22a). The section rapidly fines upward and is mostly composed of marine highly bioturbated mudstone, silty mudstone (Fig. 3.22b-d), and very fine-grained thin sandstone interpreted as middle to lower shoreface deposits (Fig. A.3). Badly preserved fragments of ammonites are common. Thin sections of some samples contain isolated broken chambers and hematitized benthonic foraminifers. Above the first marine

Figure 3.22 Fine-grained transgressive deposits (Early TST) of the lower Cerro Grande Formation at La Campana Section. (a) shows the Early TST deposits of the Cerro Grande Formation above the transgressive surface TS 3 on top of Las Imágenes Formation. The section becomes fine-grained and deepens upward, grading into a thick section of highly bioturbated marine silty shale and black mudstone (b-d). The mudstone and siltstone beds in (d) contains *Skolitos* (vertical burrows close to the hammer). The muddiest deposits of the lower Cerro Grande Formation above the MFS 3 contains ammonites, benthonic foraminifers, echinoderm and other biogenic fragments (see Plate 14).

transgressive sandstone overlying the uppermost red horizon of Las Imágenes Formation (Figs. 3.20c, 3.22a), the section becomes muddier upward reaching the maximum interpreted depth at the maximum flooding surface (MFS 3).

The lowermost transgressive (Early TST) deposits at the Altamira Section (Fig. A.2) includes 2 to 4-m-thick beds of mudstone and 20-cm-thick sandstone beds. The upper part contains thick beds of siltstone with abundant *Exogyra.* Some siltstone beds that alternate with gray mudstone and thin-bedded sandstone reach 9 m in thickness.

3.6.2 Upper Maximum Flooding Surface (MFS 3)

In none of the studied sections, (La Campana and Altamira, Figs A.2 and A.3), does the transgressive deposits (TST) of the lower Cerro Grande Formation display a clearly defined retrogradational and fining-upward stacking pattern. Consequently, the position of the MFS 3 was inferred to lie below the interval characterized by a clear progradational and thickening upward depositional architecture. At La Campana Section, the maximum flooding surface (MFS 3) was tentatively placed at a fossiliferous gray mudstone that contains abundant rotalid-type benthonic foraminifers, echinoderm spicules, and a discrete lag of chert pebbles (Plate 14). Above this interval, there is a clear change to a progradational stacking pattern that suggests shallowing-upward depositional conditions.

The MFS 3 at the Altamira Section is inferred to lie somewhere within a 65-m-thick covered interval, below the upper part of the Altamira Section characterized by shallowing-upward progradation deposition. The maximum flooding surface (MFS 3) constitutes the upper boundary of the study interval.

3.6.3 Highstand Systems Tract (HST)

Lower and Middle Shoreface Mudstone and Siltstone;
Upward-thickening Upper Shoreface Sandstone

Above the maximum flooding surface (MFS 3), there is an increase in sandstone content and cycles capped progressively by thicker sandstone and siltstone beds. These are interpreted as sets of progradational parasequences (Figs. 3.1, 3.2 and A.3). The progradational succession above the flooding surface (MFS 3), is assigned to a highstand (HST), and is interpreted to be deposited at conditions of sediment supply exceeding the rates of accommodation space generation. The highstand deposits (HST) are well exposed at La Campana and at the more distal Altamira Section (Figs. A.2 and A.3).

At the Altamira Section (Figs. A.2 and 3.23a), the interval between 170 and 177 m partially illustrates the progradational stacking pattern typical of the HST deposits of the lower Cerro Grande Formation. The cycles in this succession are characterized by interbedding of mudstone and thin-bedded sandstone capped by medium- to thick-bedded upward-thickening sandstone (Fig. 3.23a). Upward in the section, between 297 and 330 m, sandstone beds reach almost 1 meter in thickness (Figs. A.2 and 3.23b). Above this interval, mudstone sections are thicker and sandstones coarsen and thicken upward reaching 4 m and more in thickness. *Exogyra* and some bivalves specimens are scattered throughout a moderately bioturbated mudstone. Individual mostly planar and ripple cross-laminated sandstone beds displays groove casts and small gutter casts at their bases. The progradational upward-thickening and shallowing-upward interval from the MFS 3 to the top of the section is interpreted as lower, middle, and upper shoreface deposits. However, the section above the referred surface resembles delta flank or delta front deposits due to its distinctive progradational character.

Figure 3.23 Progradational upward-thickening shoreface sandstone (HST) of the lower Cerro Grande Formation. At the Altamira Section, the HST includes cyclic deposits of mudstone with *Exogyra* and planar-laminated sandstone with small groove casts and gutter casts. This interval in the section is characterized by a distinctive progradational character (170 to 177 m, Fig. A.2). Sandstone beds gradually thicken upward in the section reaching 30 cm to 1 m in thickness (b). The top of the section contains 4-m-thick sandstone beds. These strata in the Altamira Section resemble delta front or delta flank deposits and are similar to the delta-fed turbidites that characterize the Previous HST deposits (Fig. 3.2).

At La Campana Section (Fig A.3), the interval above the maximum flooding surface (MFS 3) also displays a well-defined shallowing-upward, upward thickening, and progradational depositional architecture. In this section, the lower part of the HST deposits mostly contains bioturbated and fossiliferous gray mudstone and thin-bedded sandstone (lower shoreface). The fossil assemblage in this interval includes rotalid-type and other diverse benthonic foraminifers, echinoderm spines (Plate 14), gastropods and bivalves including whole specimens of *Exogyra* sp. (Plate 4). An ammonite fragment identified as *Sphenodiscus* sp. (Plate 4) indicates an upper Campanian to Maastrichtian age (A. Villaseñor, personal comm., 2002). However, all the strata overlying the HST deposits of the Upper Cañón del Tule (Fig. 3.2) are interpreted to be Upper Maastrichtian in age, since they overlie the strata that contain *Coahuilites sheltoni* and *C. cavinsi*.

At La Campana Section (Fig. A.3), the muddy and fossiliferous interval above the MFS 3, grades upward into a succession characterized by equal proportions of mudstone and siltstone beds (middle shoreface) that thicken and increase upward (Fig. A.3). The uppermost strata on top of the section include very thick and very fine-grained silty sandstone beds that may reach up to 12 m in thickness. The cyclic succession of parasequences capped by upward-thickening siltstone and thick sandstone beds suggests deposition in upper shoreface settings. However, its well-defined progradational character resembles delta front or delta flank deposits. It is assumed that this progradational stacking pattern remains upward within the upper Cerro Grande Formation, successively overlain by Las Encinas red beds that closed the cycle SC 3 on top of the section (Fig. 3.1).

3.7 DISTAL DEPOSITS OF THE UPPER CAÑON DEL TULE, LOWER CERRO GRANDE, AND TANQUE FORMATIONS

Offshore Outer Shelf (?) Deposits

At the Altamira Section (Fig. A.2), the red deposits of Las Imágenes are absent, since the red unit pinched out about 3 km west of this section (Figs. 3.2 and A.18). Consequently, the shallow marine sediments of the Cerro Grande Formation (TST) lie directly above the FSST deposits of the uppermost Cañón del Tule (Fig. 3.12). Lithology of these two formations is similar and their differentiation is only possible in this section based on their relative position with the forced regressive ridge-forming sandstone and partially on their characteristic stacking patterns; progradational for the upper Cañón del Tule and retrogradational and fining-upward for the Cerro Grande Formation (Fig. A.2). At the Altamira Section, the FSST deposits of the uppermost Cañón del Tule Formation are less than 2 m thick (Fig. 3.12), but the erosional surface at the bottom of the unit can be observed at this distal position. Even gutter casts occur on top of the lower shoreface to offshore mudstone below the surface.

Eastward of the Altamira Section, the FSST deposits of the upper Cañón del Tule and the transgressive (Early TST) deposits of the lower Cerro Grande formations grade rapidly into thick muddy successions (Fig. 3.24). Consequently, in the area covered by the sections Los Ojitos and Tanque (Figs. A.7, A.14, cross section A.18) the differentiation between these two formations is difficult due their similar lithology. With the aid of air photographs, the contact was tentatively placed in the middle part of Los Ojitos Section. The contact was laterally projected from the Altamira toward Los Ojitos Section following the general strike direction of the forced regressive ridge-forming sandstone.

Distal deposits at Los Ojitos and El Tanque sections are characterized by thick monotonous intervals of mudstone interrupted by thin sheets of sandstone

Figure 3.24 FSST offshore to outer shelf (?) deposits laterally equivalent to the upper Cañón del Tule Formation. In the easternmost Tanque Section, the upper Cañón del Tule Formation grades laterally into distal cyclic successions of thick massive mudstone and very thin layers of sandstone, whose cyclicity resembles outer shelf or prodelta deposits. At this location, the red beds of Las Imágenes Formation and the forced regressive sandstone of the uppermost Cañón del Tule have pinched out completely, and the differentiation between the Cañón del Tule and Cerro Grande marine formations is not possible. The stratigraphic position of these outcrops was controlled by air photographs. These deposits were described as Tanque Formation by McBride *et al*. (1974).

whose cyclicity resembles the most distal outer shelf or prodelta deposits (Fig. 3.24). At Los Ojitos Section (Fig. A.7), the lower part of the section contains stratified and bioturbated mudstone with *Exogyra*. The middle part of the section consists of interbedded massive mudstone, siltstone, and thin-bedded sandstone. Ball and pillow structures and thin calcite-cemented hardgrounds interpreted as sediment starvation surfaces are common. The upper part of the section is an aggradational succession of massive, burrow-homogenized fossiliferous mudstone and thin-bedded siltstone. Unidentified ammonite fragments, rotalid-type benthonic foraminifers, and a few bivalves are sporadic. Hematitized nodules, intervals of microlaminated mudstone, and muddy-silty lenses with abundant shell debris are also common.

The stratigraphic interval measured at El Tanque Section (Fig. A.14) includes a monotonous succession of massive gray mudstone interbedded with very thin-bedded to laminar sandstone. No fossils were observed in this section other than plant debris. The analysis of six samples of mudstone from different intervals of Los Ojitos and El Tanque sections indicated that the analyzed samples are devoid of calcareous nannofossils (M. A. Sánchez-Rios and P. Padilla, written comm., 2000). The sediments studied at these two sections were described as Tanque Formation by McBride *et al.* (1974).

The unconformity and sequence boundary (FRS+SB) widely extended in the central and western study area grades laterally from west to east into its equivalent conformity (Figs. 3.2 and A.18). It is interpreted that the surface overlaps the transgressive surface (TS 3) at the base of the Cerro Grande Formation. However, stratigraphic coverage in this area was not enough to support this interpretation. Detailed description of distal sediments and identification of major sequence stratigraphic surfaces might be the objectives of future research in the easternmost central Parras Basin.

CHAPTER 4

CHAROPHYTES

4.1 Introduction

Charophyte deposits of Las Imágenes Formation occur at eight locations distributed throughout the study area. Due to their restricted stratigraphic distribution, the charophyte-bearing interval is a valuable stratigraphic interval of reference and correlation (Figs. A.17 to A.19). Besides charophytes gyrogonites, the processed samples contain remains of charophyte branchlets and ostracods; and benthonic foraminifers are associated with charophytes at one location (La Casita Section, Fig. A.4). The gyrogonites from all of the samples are excellently preserved and are morphologically diverse (Plates 7-8).

Previous studies in the Parras Basin have never described the charophyte assemblage of Las Imágenes Formation. For this reason, and due to their excellent preservation, abundance, and diversity, this chapter is dedicated to their description and illustration. The following paragraphs first contain a brief introduction to the morphology, reproduction, and taxonomy of modern charophytes and deals with different aspects regarding their habitat and environmental distribution. This is followed by a brief review of the literature about their fossil record. The next part describes the general morphology of the charophyte gyrogonites of Las Imágenes Formation, and a morphological comparison of one identified specimen with specimens described in the literature. Finally, there is a brief discussion about the paleoenvironmental interpretations of the charophytes and the origin of the white clay deposits in which the charophytes are contained.

The charophyte fossil assemblage found in Las Imágenes Formation constitutes the appropriate material to perform more detailed statistical and morphological studies, as well as paleoenvironmental interpretations. It is possible that new species never described in the literature are present within such a diverse gyrogonites population. A more complete formal study and a systematical and statistical description of the assemblages will be conducted and published at a later time.

4.2 Definition and Habitats

Modern charophytes are structurally complex, fragile, and highly developed aquatic green algae that live entirely submerged in fresh and brackish water environments (Fig. 4.1). Due to their fragile structure (Fig. 4.1a), living charophytes are common colonizers of low-energy fresh water environments such as lakes, pools, and ponds and may survive in fluvial channels only in quite slow-moving streams (Peck, 1957; Johnson, 1961; Tappan, 1980). They may grow isolated, such as *Chara corallina* (Fig. 4.1a), but most commonly live associated and compete for space, light, and nutrients with aquatic plants (Fig. 4.1b). In equivalent low-energy conditions, some other modern species live in brackish coastal bays, swamps, estuaries, marshes, lagoons, and fjords, where water reaches up to two-thirds the salinity of seawater (Peck, 1957; Tappan, 1980). In all these environments, charophytes may occur from near shore to depths up to 30 m (Fig. 4.1c). However, because they largely depend on light availability and water transparency, most of them live at depths between 1 to 8 m in temperate zones (Johnson, 1961; Tappan, 1980). Charophytes appeared in the geologic record in the Silurian. Their remains have been found commonly associated with other fossils of known habitats such as crustaceans, aquatic fungi, and ostracods. Therefore, based on the observation of their occurrence with other fossils and

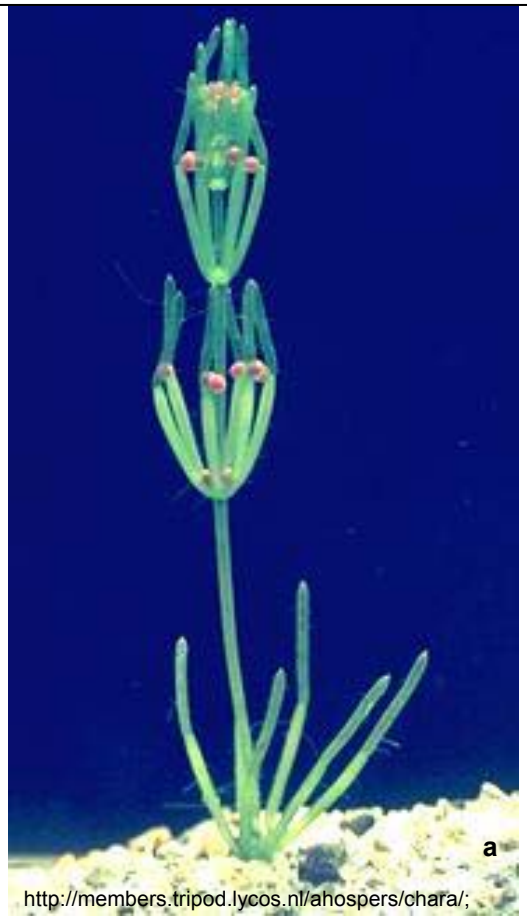

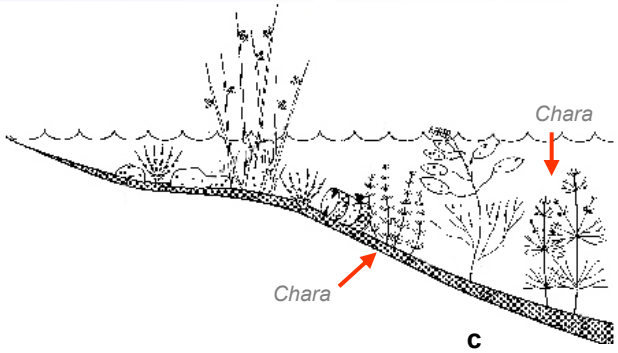

Figure 4.1 Living charophytes. (a) *Chara corallina* showing its fragile structure and small spheric redish reproductive organs. (b) shows a tank housing charophytes and native New Zealand aquatic plants. Modern charophytes live submerged and are common colonizers of fresh to brackish water environments where they compete for space, light and nutrients. (c) Charophytes may occur from near shore to depths up to 30 m. However, because they depend on light availability most of them live at depths between 1 to 8 m.

studies about the ecology of modern charophytes, it is assumed that their fossil forms occupied similar environments (Johnson, 1961; Wray 1977).

4.3 Morphology and Reproduction

Charophytes resemble real plants, but they develop rhizoids instead of roots to fix their structure to the substrate and absorb nutrients (Fig. 4.2a). They do not have true leaves or stems, nor develop vascular water- and nutrient-conductive structures typical of higher plants (Tappan, 1980; Darley, 1991). They are bushy and intricately branched, ranging in average from 15 to 30 cm and up to 2 m in height. Charophytes possess a branched structure composed of branches and branchlets, which are subdivided into long internodal segments separated by nodes (Fig. 4.2a, b). It is at the nodes where reproductive sexual organs termed *gametangia* are situated (Wray, 1977; Tappan, 1980; Fig. 4.2c and 4.3).

Charophytes reproduce both vegetatively and sexually. In sexual reproduction, a single individual produces both a male sexual reproductive organ or *antheridium*, and a female reproductive organ termed *sporophydium* (Figs. 4.2c and 4.3). Once fertilized, the female reproductive organ or *sporophydium* is subject to a calcification process. Calcification begins in its inner wall and then consists of a gradual replacement of the original cell substance by alternated layers of organic matter and laminar calcite (Wray, 1977; Tappan, 1980; Figs. 4.2e-h). This calcification process allows these organs to be preserved in the sedimentary record (Tappan, 1980).

The fossilized female organs termed *gyrogonites* or *lime shells* constitute the most commonly fossilized particles of charophytes (Fig. 4.4). The study of the gyrogonites morphology in their apical, lateral, and basal views is the key for their

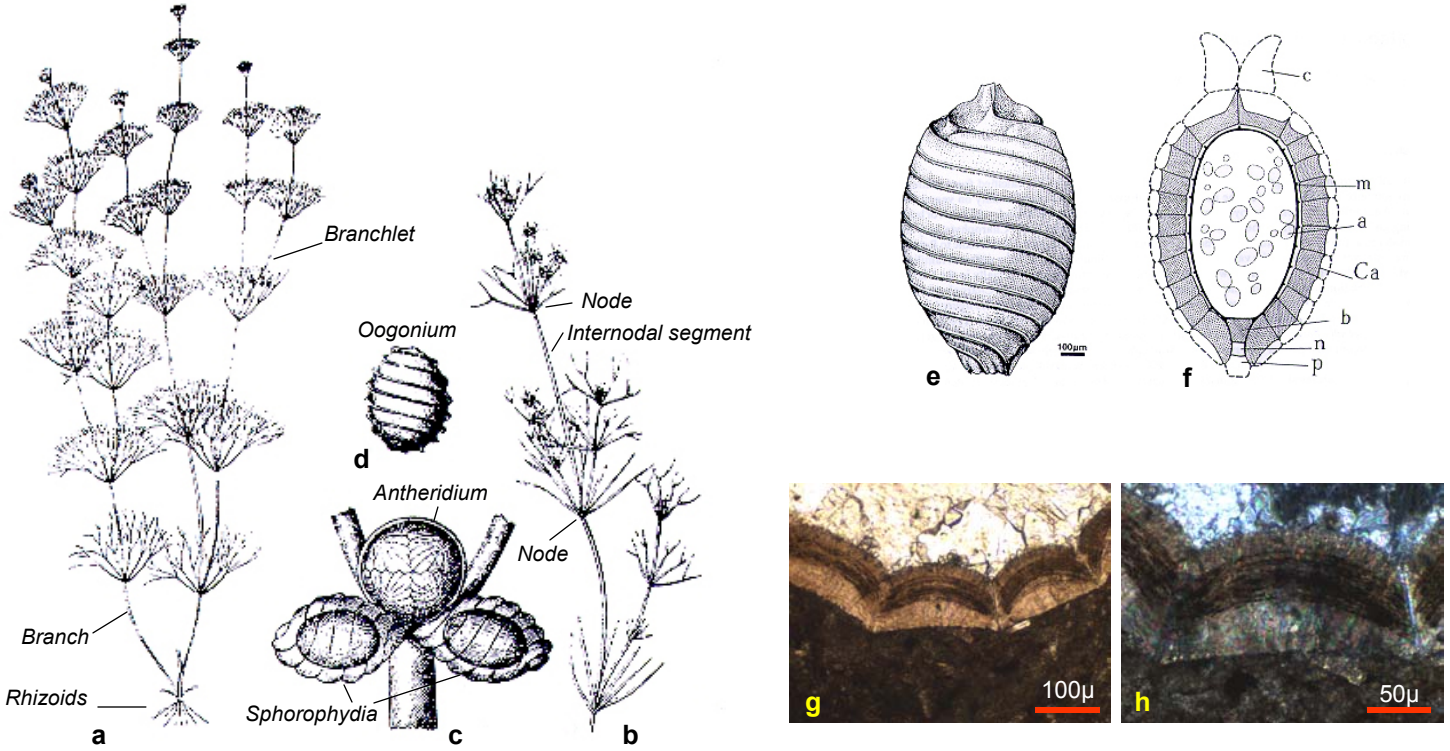

Figure 4.2 Morphology of a living charophyte. (a) Branchy structure of *Nitella gracilis* (Smith) Agardth, reduced. (b) A branch of *Nitella flexilis* (Linnaeus) Agardth, x1. (c) Fertile branch showing one spherical male reproductive organ or antheridium of shield plates; and the female organ or sphorophydia composed of two ellipsoidal oogonia, x30. (d) Partial calcification of the oogonium produces the lime shell or gyrogonite, *N. Flexilis,* x45 (Modified from Tappan, 1980). (e) Calcified oogonium or gyrogonite of a Recent specimen of *Chara hispida*. (f) The gyrogonite and its structure viewed in axial section showing the oospore membrane (m); starch grains(a); calcified part of the spiral cells (Ca); calcified sister-cell of the oospore or basal plate (b); nodal cell (n); basal pore (p). In dotted line, not preserved uncalcified part of the spiral and coronular cells (c). a-d modified from an original figure by Tappan (1980); e and f: from Feist and Grambast-Fessard (1991), from an original figure by Grambast (1958); unpublished thesis). (g-h) fossil gyrogonites in thin section showing details of the calcified spiral cells. Dark brown organic laminae alternate with clear laminar calcite; (g) paralell nicols, (h) crossed nicols. Microphotographs (g-h) taken from a thin section of the sample SLC+13, Las Imágenes Formation at La Casita Section.

Figure 4.3 Sexual reproductive organs (gametangia) of living charophytes. Both the spherical male organ (antheridium) and ovoidal female organ (sphorophydium) develop from the nodes during fertile stages of the charophyte. After fertilization, only the female reproductive organ calcifies which allow these particles to be preserved in the sedimentary record. **(a-c)** *Chara* sp., (c) only shows the female gametangium or sporophydium. **(d)** *Chara zeylanica. Sources:* (a-c) from hhttp://www.biol.tsukuba.ac.jp/~inouye/ino/g/char/charophytes.html; web site maintained by the Institute of Biological Sciences, University of Tsukuba: Tsukuba Ibaraky 305, Japan. Images and resources from this web site can be used for educational purposes without permission. (d) from the web site: http://members.tripod.lycos.nl/ahospers/chara/chschier.htm

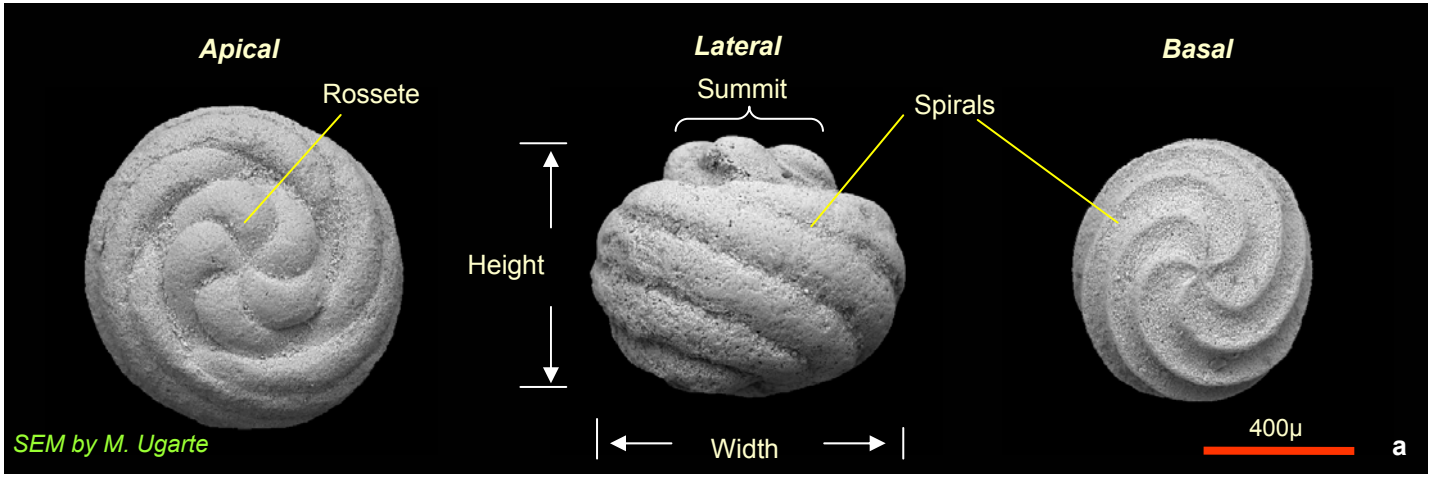

Figure 4.4 SEM views of fossil charophyte gyrogonites and their morphology. (leftt) apical view showing a five-element prominent and well differentiated rossete and deep furrows; (center) lateral view showing six convex spirals and a prominent summit; (right) five concave spirals on the basal view. Generic and specific identification of charophyte gyrogonites is based on shape, size (width to height ratio), rossete shape, character and number of spirals. Specimens from El Potrero Section (sample -15.5EP), Las Imágenes Formation, Coahuila, northeastern México.

generic and specific classification (Fig. 4.4 a-c). Charophyte gyrogonites may be abundant and some of them may constitute extremely valuable stratigraphic markers and paleoenvironmental indicators for non-marine to marginal continental strata. Charophytes have such continuous stratigraphic record that has allowed the subdivision of sedimentary successions into precise zonation schemes. Charophyte zonations have been correlated with those of other fossil groups especially ammonites, nannofossils, mammals (Riveline *et al*., 1996), and foraminifera (Martín-Closas *et al*., 1999). Detailed studies about their morphological evolution from the Paleozoic to Recent have been also performed for decades (Grambast, 1974; Feist and Grambast-Fessard, 1991).

4.4 Taxonomy

Charophytes, and in general all algae, have both structural and metabolic features in common as well as remarkable differences with animals and plants. Algae, for instance, contain the green pigment chlorophyll and can therefore carry out photosynthesis to produce their own food as plants do. Cellulose considered basic in the wall of plant cells is absent in many algae species; yet some algae also ingest food particles as animals (Darley, 1991). Consequently, the taxonomic classification of algae has always been problematic; whereas some biologists group them along with the widely distributed kingdom of plants; the same organisms are included in the kingdom Protactist in modern classifications. Studies on the structure and cellular wall composition and the nature of food reserves storage suggest that charophytes have genetic affinity with chlorophytas. In terms of number of species, chlorophyta is one of the most important algae groups (Darley, 1991).

4.5 Ecology of Living Charophytes

Studies on the habitat of living charophytes suggest that their individual distribution and development is strongly controlled by several factors including, environmental energy, water salinity, light availability, water transparency, organic matter content, and oxygenation. The fragile structure of charophytes restricts their development to low-energy environments. According to Johnson (1961), charophytes are abundant in abandoned stream channels of former glacial areas of North America and Europe, and Tappan (1980) points out that they can grow in fluvial running water only when stream movement is slow. Darley (1991) suggests that the high energy of waves in shallow water environments might be a limiting factor for charophyta colonization and that their absence in powerful fluvial streams might be a consequence of their fragile structure. In low energy and appropriate environmental conditions, living charophytes such as *Chara* and *Nitella* commonly occur in widely spread colonies forming meadows (Fig. 4.5).

Charophytes are common colonizers of fresh and brackish water environments. Studies on the habitat of living charophytes suggest that their individual distribution is strongly controlled by water salinity. Johnson (1961) observed that charophytes grow in brackish water of salinities no greater than 18 ppm NaCl. Tappan (1980) points out that brackish waters in which charophytes live, may reach up to two-thirds the salinity of the seawater (about 24 ppm of NaCl).

Organic matter, lime content, oxygenation, pH, and water transparency are also important limiting factors for charophyta development. Modern charophytes, for instance, are sensitive to phosphorous and ammonia dissolved in water (Bornette and Arens, 2002). They are abundant in lime-rich (CaO) substrates and well oxygenated waters with low organic matter content, where the concentration of phosphorous is less than 20 μg per liter (Tappan, 1980).

Figure 4.5 Charophyte meadow of *Chara* and *Nitella*. In low energy and appropriate environmental conditions, living charophytes such as *Chara* and *Nitella* commonly occur in widely-spreaded colonies. Charophyta distribution and development is strongly controlled by water energy and salinity, lime and organic matter content, oxygenation, pH and light availability. They are water-clarifying agents. Accumulations of large amounts of charophyte remais on recent and ancient lake bottoms are commercial sources of lime (CaO). Photo from the web site http://www.thekrib.com/Plants/ Plants/ NZ/)

According to Shaw and Rabenhorst (1997), some modern species tolerate extremely high concentrations of calcium carbonate dissolved in water (75-100g /100g of $CaCo_3$). Most living charophyte species only grow in alkaline water at pH conditions ranging from 7.0 to 8.0 (Peck, 1957; Wray, 1977); acidic waters are less favorable for them (Johnson, 1961; Olsen, 1944 *in*: Tappan, 1980).

Charophytes are not only dependent on water transparency but they also exert a strong positive impact on it (Tappan, 1980; Van den Berg, 1999). The water-clearing effect is due to the fact that some charophyta species such as *Chara vulgaris* may deposit significant amounts of lime (CaO) or calcium carbonate onto its branchy structure (Tappan, 1980). For this reason, charophytes are also known as stoneworts (Darley, 1991). The role of charophytes as calcium carbonate providers for sedimentary rocks cementation is unknown. However, some studies report that important amounts of charophyte remains accumulated on ancient lake bottoms and recent accumulations are exploited as commercial sources of lime (CaO) and cement (Wray, 1977; Shaw and Rabenhorst, 1997).

4.6 Fossil Record

Organic remains of the structural elements of charophytes other than gyrogonites are rarely preserved since only the female *gametangium* calcifies (Peck, 1957; Wray, 1977; Tappan, 1980). There are, however, a few exceptions of silicified fossil male *gametangium*, casts, or impressions (Tappan, 1980) as well as branches, branchlets, and rhizoids preservation due to particular mineralization processes (Martín-Closas, 1999). Therefore, the fossil female *gametangia* or gyrogonites are the most valuable remains for charophyte study and classification (Fig. 4.4).

Fossil charophytes have a continuous record from the Upper Silurian to Recent (Grambast, 1974; Feist and Grambast-Fessard, 1991). Although the

number of species have never been significant at any single time, the limited stratigraphic range and wide geographic distribution of most taxa allows these fossils to be used as stratigraphic markers for non-marine deposits. Initial zonations based on charophytes were proposed for upper Silurian to Recent rocks (Grambast, 1974; Feist and Grambast-Fessard, 1991). In other cases, zonation schemes of Mesozoic strata have been successfully used worldwide in correlating non-marine sediments (Peck, 1957; Grambast and Gutiérrez, 1977; Peck and Forester, 1979; Kumar and Grambast-Fessard, 1984; Jaillard *et al*., 1994; Schudack and Herbig, 1995). More recently, Riveline *et al*. (1996) proposed a detailed biostratigraphic zonation for Mesozoic to Cenozoic charophytes of Europe.

On the American continent, Peck (1957) described and illustrated charophytes from several Jurassic and Cretaceous localities of the Rocky Mountains area (Piper, Morrison, and Kootenai formations). Kumar and Grambast-Fessard (1984) reported charophyte gyrogonites from the Maastrichtian Slippery Rock Formation of Jamaica, and Jaillard *et al*. (1993) described the charophytes from the Upper Cretaceous Vilquechico Group of southern Perú (Fig. 4.6). Some of the species reported by Kumar and Grambast-Fessard (1984) and Peck and Forester (1979) from an unnamed Upper Cretaceous unit in Coahuila, México, were also found in Las Imágenes Formation (Fig. 4.6).

Figure 4.6 shows that several of the Campanian-Maastrichtian species from Perú, Bolivia, and Jamaica have a short stratigraphic distribution. The stratigraphic position of three species found in Las Imágenes Formation is shown for comparison. It is unknown if the charophytes described by Peck and Forester from an unnamed Upper Cretaceous unit in Coahuila, México, were collected from Las Imágenes, Cerro Huerta, or Las Encinas formations. The stratigraphic

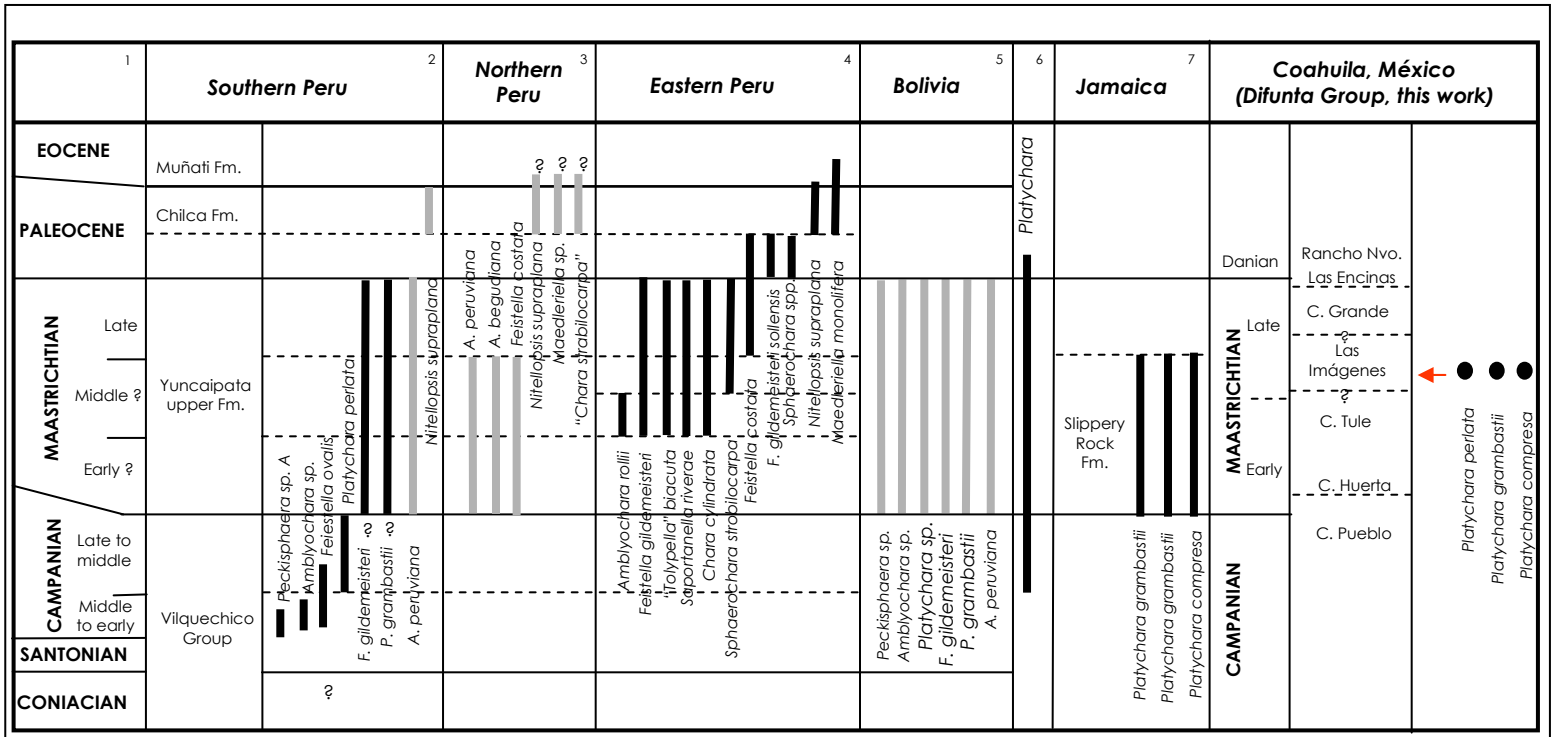

1-5: FromJaillard *et al*., 1994
6: Grambast-Fessard(1980), Peck and Forester (1979)
7: Kumar and Grambast-Fessard (1984)

Figure 4.6 Stratigraphic distribution of the main charophyte species in the Peruvian Andes, Bolivia, and Jamaica. Note that *Platychara* occurs in the Campanian to Early Tertiary and *Platychara perlata* (Peck and Recker, 1947) has been reported from the upper Campanian in southern Perú. In Las Imágenes Formation, *P. perlata* and other species were found above shallow marine strata that contain *Coahuilites sheltoni*, an ammonite of the lower part of the Upper Maastrichtian. It is unknown if the same species found in this work in Las Imágenes also occur in the Cerro Huerta Formation below or in Las Encinas Formation above. These three red bed units were deposited in similar coastal plain depositional environments.

distribution of the charophytes within the Difunta Group needs to be investigated in future research.

4.7 Charophytes of Las Imágenes Formation

It was previously mentioned that charophyte gyrogonites were recovered from several samples and different locations within the study area. All the fossiliferous samples lie within an interval approximately 40 m thick within the redbeds of Las Imágenes Formation. This particular stratigraphic distribution of charophytes provided a valuable stratigraphic interval of reference and regional correlation (Fig. 3.2; cross sections A.17 to A.20).

The charophyte-bearing horizons at five out of eight locations distributed within the central Parras Basin are confined within white-greenish, sticky-to-tongue clays interbedded with fine-grained red overbank deposits (Fig. 4.7). The soft nature of this clay material allowed the recovery of free forms of gyrogonites, thin-shelled small ostracods, and debris material, which seems to be remains of the charophyte branchlets. Diverse gyrogonites were totally isolated from the containing sediment from samples collected at El Potrero (Plates 7 and 8) and El Realito sections (Figs. A.8 and A.10) and two locations nearby the town Doce de Diciembre, northeast of San Martin de Las Vacas, Coahuila (Fig. 4.7). Gyrogonites from one horizon at La Florida (Fig. 4.8) and one from La Casita Section (Fig. 4.9) were studied in thin sections due to the hard nature of the rock in which they are contained (Figs A.4 and A.6; Plates 9-10).

4.7.1 Morphology of Recovered Specimens

The morphology described in the following paragraphs is based on the gyrogonite population recovered from El Potrero Section (Fig. A.8; Plates 7-8). Description is based on the morphological elements including shape, size (width

Figure 4.7 Charophyte-bearing white greenish clays of Las Imágenes Formation. Outcrop in (a) nearby the Doce de Diciembre Section. (b) El Potrero Section; (c) El Realito Section. Photograph in (d) shows an small channel located 20 m above the horizon shown in (c). Charohyte gyrogonites are commonly associated with thin-shelled ostracods in all these localities.

Figure 4.8 Charophyte bank within coastal floodplain red deposits of Las Imágenes Formation. Charophyte bank in (a) is 20 to 50 cm thick and extends laterally for about 50 m. In thin section (c), the bank is almost exclusively composed of spherical to ovoidal charophyte gyrogonites and quartz fragments cemented by calcite. Associated within the same intervals, low-relief lenticular sadstone bodies suggest temporal channelized flow (b), and muddy calcite-cemented laminar horizons of short lateral distribution were probably produced by desiccation of shallow bodies of water (d). All potographs are from La Florida Section, (c) from sample -31LF.

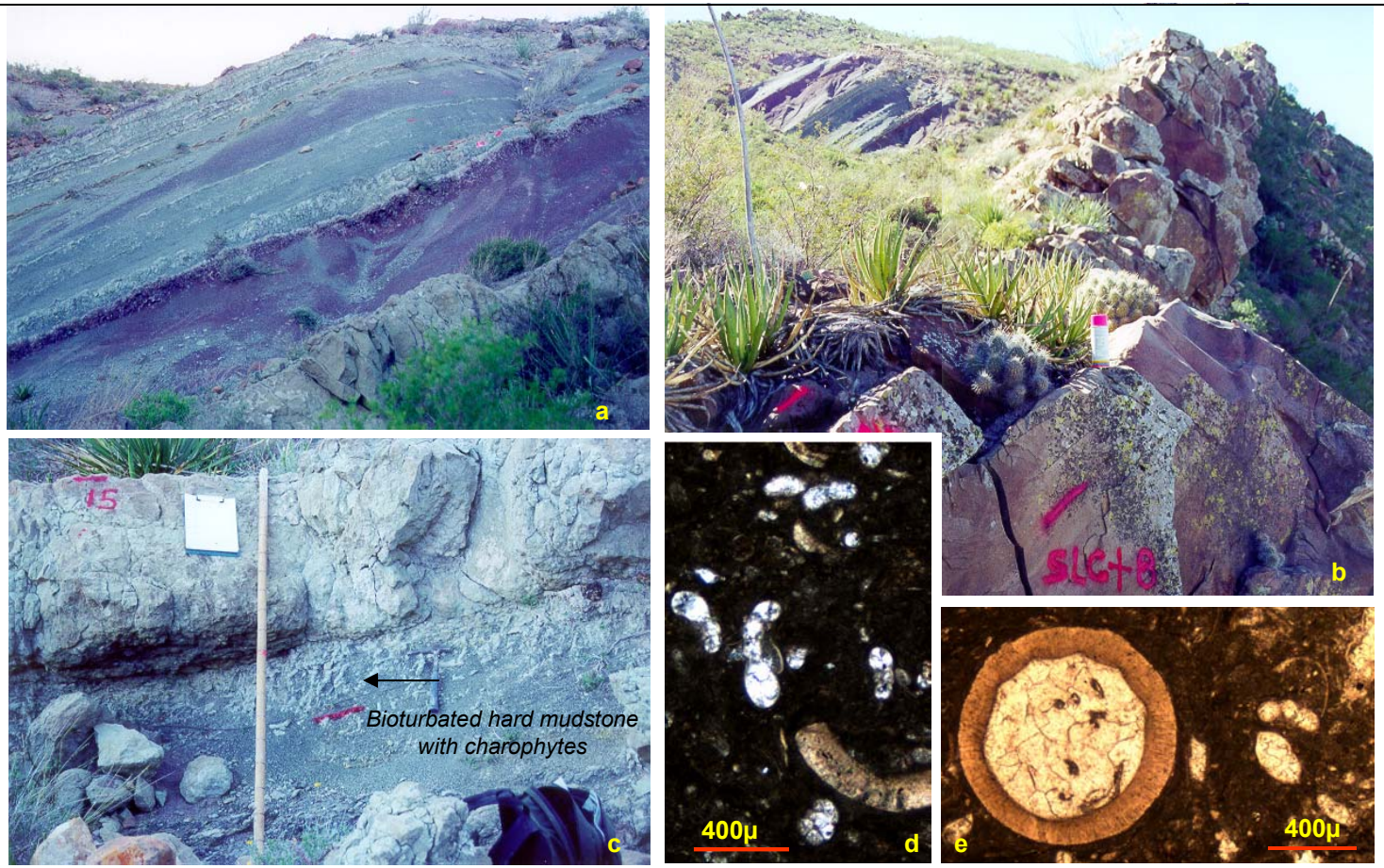

Figure 4.9 Charophytes, ostracods, and bethonic foraminifers of Las Imágenes Formation at La Casita Section. (a) Panoramic view of the red, purple, and green deposits of Las Imágenes Formation. (b) ridge forming upper shoreface sandstone of the uppermost Cañón del Tule Formation and overlying red beds. Detail in (c) shows the charophyte-bearing horizon with branched burrows resembling *Thalassinoides*; (d) shows several specimens of benthonic foraminifers. (e) association of a gyrogonite (spheric), benthonic foraminifers, and ostracods in thin section (sample SLC+13).

to height ratio), rosette shape, character, and number of spirals (Fig. 4.4). All these morphological features are basic for identification and classification of fossil charophytes. Statistical studies of gyrogonites populations focused on their morphology allow their generic and specific identification.

Hundreds of gyrogonites were obtained from 500g of sampled material from strata of El Potrero Section (Fig. 4.6b; sample -15.5 EP, Fig. A.8). A quick estimation might be that roughly 95% of the gyrogonites are subspherical to ovoidal (Plate 7; Figs. 1-6 on Plate 8) with a minority ellipsoidaly-shaped forms (Figs. 7-12 on Plate 8). All the individuals without exception are left-coiled. The spherical to ovoidal forms ranges in size from 600 to 950 μ, most of them showing convex and rarely concave spirals. Their summits on lateral views are variable, some of them are very well defined and prominent (Figs. 2, 5, 8, 9 on Plate 7). Only a few forms have a completely flat to slightly depressed summits that define individuals of flattened periphery (Figs 4-6 on Plate 8).

On apical views, most of the specimens display variable-shaped rosettes of five "petals" (left column on Plate 7). Some rosettes are formed by straight, tear drop- to digitated-shaped "petals" separated by straight and deep sutures. In these forms, the rosette surrounded by deep furrows appears to be completely isolated and without connection with the peripheral spirals that produce each petal in the rosette (Fig. 1 on Plate 7). In other forms, fan-shaped rosettes also isolated by deep furrows are defined by curved sutures for each "petalum", which is wider at the rosette center but decreasing its width to the periphery (Figs. 4 and 7 on Plate 7). A third rosette shape is that one in which the "petals" extend to the periphery, where they join and merge with the spirals (Fig. 10 on Plate 7).

The ellipsoidal forms are variable in size. The largest recovered gyrogonite is 997μ high by 771μ wide (Fig. 11 on Plate 8), but most of the ellipsoidaly-shaped gyrogonites of the population are on average 768μ to 478μ high by 771μ

to 321μ wide (Figs. 7 and 12 on Plate 8). Within the entire studied population of El Potrero (sample -15.5 EP), almost all of the specimens display five-petalum rosettes on apical views. There is only one remarkable and rare exception of a gyrogonite with a six-petalum rosette (Figs. 1-3 on Plate 8). Whether this gyrogonite is a new genera or species, or it is simply a rare aberrant form is not yet clear at this moment. Only two gyrogonites with six-petalum rosettes from the whole population of El Potrero, composed by hundreds, have been found. Undoubtedly, the abundant material of several localities needs a formal study including a complete systematical and statistical description and illustration. A formal description of the charophyte gyrogonite assemblages obtained from several localities of Las Imágenes Formation will be published later.

4.7.2 Identification of Charophyte Gyrogonites

A process of selection and preliminary identification was performed to facilitate the generic or specific identification of the charophyte gyrogonites of Las Imágenes Formation. The most abundant and representative specimens of the gyrogonites population were grouped according to their major morphological features and subsequently compared with Upper Cretaceous specimens described in the literature (Peck and Forester, 1979; Kumar and Grambast-Fessard, 1984). This process of study and morphological comparison allowed the identification of *Platychara perlata* as one of the most abundant species of the El Potrero population (Fig. 4.10 and Plate 7).

The specimens of *P. perlata* recovered from Las Imágenes Formation (Fig. 4.10 d-f) are almost identical to the specimens described by Peck and Forester (1979; Plate II) from an unnamed Upper Cretaceous Unit in Coahuila, México (Fig. 4.10a-c). Only some minor variations are evident between them. Basal views of *P. perlata* for instance (Fig. 4.10a, d), show five wide spirals separated by deep furrows. In apical views (Fig. 4.10b, c), the spirals converge

Figure 4.10 Comparative mophology of *Platychara perlata* (Peck and Recker, 1947). From left to right: basal, apical, and lateral views. (a), (b) and (c) are reproductions at their original size of the illustrations provided by Peck and Forester (1979), from specimens of an unnamed Upper Cretaceous unit in Coahuila, México. Note the similar morphology of the upper specimens with those of Las Imágenes Formation shown in (d), (e), and (f) collected at El Potrero Section (sample -15.5 EP). The scale applies for all the illustrations. See the text for additional explanation.

rom the periphery toward the interior of the gyrogonite, but every spiral is interrupted by a depression that separates the ending spiral from their respective petal in the rosette. This remarkable interruption produces the appearance that the rosette is isolated in the center of the gyrogonite. In the compared specimens (b) and (e), the rosette is composed of five petals and only a slight difference between a fan-shaped (e) against a flower-shaped rosette (b) is perceptible.

The fan-shaped rosette of the Las Imágenes specimen (Fig. 4.10e) is more prominent than the smaller rosette in the Peck and Forester´s specimen (see also lateral views c and f). In lateral views, the only difference is the number of spirals; seven in the first case (f) against eight spirals in the specimen (c) illustrated by Peck and Forester (1979). The specimens of Las Imágenes are also slightly wider; the illustrated specimen is 825 μ wide. All the differences between the compared specimens lie within common intraspecific variations. For instance, *Platychara perlata* may contain between 6 to 9, but most commonly 7 to 8 concave to strongly convex spirals. Size may be also variable ranging from specimens of 590 to 800μ high and 700 to 1000μ wide according to Peck and Forester's description (1979). They also remark that the specimens from México have strongly convex spirals, well-developed peripheral furrows and prominent rosettes, features also recognized in Las Imágenes specimens.

Some other gyrogonites were compared with specimens described in the literature following the same procedure. Other specimens markedly resemble *Platychara grambastii* (Figs. 4-6 on Plate 8) and *Platychara compressa.* (Figs. 7-9 on Plate 7) according to the descriptions and illustrations provided by Kumar and Grambast-Fessard (1984), and Peck and Forester (1979), respectively. At least three different species of *Porochara* sp. were also identified (Figs. 7-12 on Plate 8). The specimens collected from several localities within the Las Imágenes Formation display, however, intraspecific variabilities and their study in more

detail will allow their accurate and proper identification. It is possible that there exists here new species never described in the literature.

The specimens of *Platychara perlata* described by Peck and Forester, (1979) were extracted from samples collected by R. C. Robeck from an unnamed Upper Cretaceous unit in Coahuila, México. The location lies along Highway 75 (?) in a section located 171.5 km from Piedras Negras, Sabino area, Coahuila. *P. Perlata* has been also reported from the Campanian of the Peruvian Andes (Jaillard *et. al.*, 1994). *Platychara grambastii* was originally described from shales of the Maastrichtian of Jamaica (Peck and Forester, 1979) and reported later from the Maastrichtian Slippery Rock Formation from the same country. *Platychara compresa* has been reported from the Upper Cretaceous part of the North Horn Formation, which crops out in Wales Canyon, Utah, USA; and from the Paleocene (member E) Willow Creek Formation in Alberta, Canada (Peck and Forester, 1979). Figure 4.6 compiles the stratigraphic distribution of several charophyte species reported in some of the previously mentioned works. Note that *Platychara perlata*, identified in samples of Las Imágenes Formation, has been also reported from the Maastrichtian Yuncaipata Formation of southern Perú.

4.7.3 Paleoenvironmental Interpretations of Charophyte Deposits

The charophyte-bearing clays of Las Imágenes are laterally restricted deposits encased within fine-grained fluvial-deltaic plain sediments that mostly include red mudstone (Figs. 4.7 and 4.8). Some clay deposits extend tens of meters merging and pinching out within the red mudstone (Fig. 4.7a). Their thickness is variable, ranging between 20 to 100 cm in some locations (Fig. 4.7b) and up to 3 m in other locations (Fig. 4.7a). In two locations, the charophyte clay deposits are right above one another, separated by red fine-grained overbank deposits. It is noteworthy, that the charophyte deposits are frequently associated

with deposits of fluvial origin. Small channels such as the one shown in Figure 4.7d were commonly observed interbedded with charophyte deposits.

At La Florida Section, charophytes occur within a calcite-cemented bank, which is 20 to 50 cm thick and extends laterally for about 50 m (Fig. 4.8a). The bank is almost exclusively composed of spherical to ovoidal charophyte gyrogonites and quartz fragments cemented by calcite (Fig. 4.8c). At the same section, a few meters above the charophyte bank, a low relief channel-shaped lenticular sandstone body again suggests flow of water within a shallow channel no wider than 10 m (Fig. 4.8b). Some other associated deposits include calcite-cemented muddy horizons composed of alternating laminae of dark mud and calcite (Fig. 4.8d). These deposits also have a short lateral distribution and are no more than 30 cm thick. They probably formed in ponds or shallow and temporal accumulations of calcium carbonate-rich waters exposed to high rates of evaporation.

Chrarophyte gyrogonites from El Potrero (Fig. A.8, Plates 7-8), El Realito, Doce de Diciembre, and La Florida sections were recovered and observed associated in the same sampled material with well preserved thin-shell ostracods. Smooth, poorly ornamented shells and valves that remained joined after deposition suggests that these ostracods lived in environments where low-energy water conditions prevailed (M. Aguilar, personal comm., 2002). Whole, joined valves and well-preserved thin-shell delicate ostracods would not have been preserved in high-energy conditions subject to the action of waves or powerful fluvial streams. Oyster concentrations and benthonic foraminifers in horizons below the charophyte bearing clay at El Potrero Section (Fig. 3.14b) suggest environments close to the shoreline eventually subject to marine influence. Moreover, the presence of branchlet material in the processed samples suggests deposition *in situ* within bodies of water, which could be inferred to be small interfluvial lakes or ponds situated between interdistributary channels. Field

observations, such as the association of channelized deposits at La Florida Section, and the restricted lateral distribution of charophyte-bearing clay deposits also support this interpretation.

Charophytes from La Casita Section (Fig. A.4), are associated with abundant benthonic foraminifers and thin-shell ostracods (Fig. 4.9 and Plates 10 and 11). The charophyte-bearing interval is an intensively bioturbated gray mudstone with branched burrows resembling *Thalassinoides* (Fig. 4.9c). The interval is characterized by a complete destruction of primary sedimentary structures produced by intense biogenic activity at low rates of deposition and quiet conditions that let aquatic organisms dig into the muddy substrate. Low energy conditions are also supported by the excellent state of preservation of thin and fragile ostracod valves. Observe on Plate 11 that both delicate valves of two ostracod specimens remained together (Figs. 4 and 6 on Plate 11). Charophytes associated with benthonic foraminifers and ostracods, suggest deposition in a quiet muddy brackish water environment such as a marginal lagoon. The benthonic foraminifers clearly indicate marine water influence since these organisms are not able to survive in fluvial or any other restricted internal continental environment.

4.7.4 Origin of Charophyte-bearing Clays

For a particular reason, charophyte gyrogonites are mainly confined in the white clays. The interbedded red horizons are devoid of charophytes or contain few, isolated, and poorly preserved specimens. An initial working hypothesis is that the white clays might represent volcanic ash deposits. However, the fossiliferous clay bodies do not have a continuous and uniform lateral distribution, or a uniform thickness; all of them are encased and pinch out within overbank red bed deposits (Fig. 4.7). In addition, thin sections of the clay material did not reveal the occurrence of remnants of minerals to support a volcanic origin.

SEM observations and X-ray analysis revealed that charophyte-bearing clays are composed of a mixture of illite and montmorillonite. It is unknown, however, whether the white clay deposits of Las Imágenes Formation have a genetic relationship with the development of charophytes in the interpreted lacustrine environments. It has been observed that modern charophytes fix small particles suspended in water onto their branchy structure. However, there are no clues to suggest that the fossil charophytes of Las Imágenes Formation selectively fixed clay particles to produce such high concentration and pureness of clay in which they are confined.

There are few examples that show the relationship between the development of charophytes and a particular kind of sediment. Shaw and Rabenhorst (1997), for instance, studied freshwater marl deposits, which occur adjacent and along several streams in the Great Limestone Valley, in the western portion of Maryland and Virginia. They conclude that calcium carbonate, which occurs in high concentration in marls (60-100 g/100 g of sediment), was produced through inorganic and biogenic processes. According to Shaw and Rabenhorst (1997), the marl was formed in ponds, as evidenced by the presence of algae, gastropods, and bivalves. Based on grain analysis and micromorphological evidence, they also conclude that "certain algae (*Chara* sp.), capable of accumulating carbonate internally and externally, were largely responsible for forming the marl" (Shaw and Rabenhorst, 1997, p. 41). These deposits have been mined throughout the last century for lime materials.

An additional question regarding the charophyte-bearing clays is their white color. It is noteworthy that the white clays are included within thick successions of red sediments. According to McBride *et al*. (1975) and Walker (1976), red coloration of sediments is of diagenetic origin produced by post-depositional alteration of iron-bearing minerals and dehydration of hydrous iron oxides in stages of lowering of water table. If Las Imágenes deposits acquired

their red coloration through this diagenetic process, it is unknown why the charophyte-bearing clays did not acquire the characteristic red coloration of the surrounding deposits. One possible explanation might be that charophyte deposits remained white due to their high content in organic matter produced by branches and branchlets structures of charophytes. High concentrations of organic matter and plant debris prevent oxidation of iron-bearing minerals and therefore, preclude sediments from reddening (McBride, 1974). Red sediments may even suffer a bleaching process due to the action of organic acids produced by the roots of plants.

4.8 Summary

In conclusion, the charophyte deposits of Las Imágenes Formation provided a useful stratigraphic level of reference for stratigraphic correlation. The species identified have a wide stratigraphic distribution that extends from the Campanian-Maastrichtian and some of them may even occur in the Paleocene (Fig. 4.6). However, the occurrence of individuals with a precise or more restricted chronostratigraphic distribution should be investigated through the detailed study of the widely extended, well preserved, and diverse charophyte assemblage. It is possible that new species never described in the literature are present in the charophyte deposits of Las Imágenes Formation.

Although the charophytes of Las Imágenes do not provide a particular age, their association with other microfossils was useful to interpret particular depositional environments. Based on the fossil assemblage, field observations, and the habitats in which modern charophytes develop, the charophytes of Las Imágenes Formation are interpreted to have grown in some cases within shallow and laterally restricted bodies of fresh water. Small coastal plain lakes or ponds in areas of intermittent water spilling from distributary streams are interpreted for El Potrero, El Realito, Doce de Diciembre, La Campana, and La Florida deposits.

The association of charophytes with ostracods and benthonic foraminifers in La Casita deposits (Fig. 4.9) suggest a marginal marine brackish water environment such as a lagoon at this location. Some issues regarding the occurrence of the charophytes of Las Imágenes remain unsolved and the search for a convincing response will be the objectives of future research in the central Parras Basin.

CHAPTER 5

DEPOSITIONAL HISTORY

5.1 Introduction

The following paragraphs describe the sedimentary history of the study interval. The chapter is subdivided into three parts: the first one intends to set the study area within a regional geologic context, the second one concentrates on the sedimentary history of the study interval, and the final part includes three discussions. The second part includes a chronological narration of the sedimentary events and contains an interpretation on the role that sediment supply, eustasy, and tectonics exerted on the depositional architecture of units and facies distribution through time. Description is supported with the generalized stratigraphic column of the middle Difunta Group at La Campana Section (Fig. 3.1) and the sequence stratigraphic model of the study interval (Fig. 3.2). Stratigraphic cycles are based on the nomenclature proposed by Halik, (1998; Fig. 2.7 and 3.1). Figure 3.2 resembles the stratigraphic geometry of the central Parras Basin in an east to west direction and illustrates the interpreted systems tracts, bounding surfaces, facies associations, and main lines of correlation. Although the study interval does not include the lower and middle Cañón del Tule Formation, these intervals are included to place the description within an overall sequence stratigraphic context.

5.2 Regional Geologic Context

In the Late Cretaceous an inland-migrating magmatic arc (Fig. 2.4) developed in northwestern México as a consequence of subduction processes along the Pacific coast (Dickinson, 1981). Compressional stresses associated with subduction gradually produced regional uplift and deformation in

northwestern México, while the advancing orogenic front that later will produce the Sierra Madre Oriental (SMO) fold and thrust belt migrated eastward (Fig. 2.4). In the meantime, large amounts of coarse volcaniclastic sediments were eroded from the plutonic-volcanic complex and deposited in adjacent extensive alluvial-fluvial systems (Crawley, 1975; Goldhammer and Johnson, 2001). In the Campanian-Maastrichtian the shoreline, situated eastward of the SMO deformation front (Fig. 2.4), migrated regionally roughly in the same direction, but oscillated producing transgressive and regressive episodes.

The regional eastward migration of the shoreline during the Campanian-Maastrichtian was associated with extensive fluvial-deltaic and shallow marine sedimentation in the Parras, La Popa, and Sabinas basins (McBride *et al*., 1974; Crawley, 1975; Warning, 1977; Ye, 1997; Halik, 1998) and Ojinaga basin (Araujo y Estavillo, 1985). Deposition occurred along the ancient coastline of the Gulf of México (Fig. 2.4), within a remnant southward extension of the Cretaceous Western Interior Seaway (Williams and Stelck, 1975; Crawley, 1975; Nations, 1989). The main source of sediments for the clastic units of the Difunta Group in the Parras and La Popa basins was an ancient volcanic arc active during the latest Cretaceous in western México (Crawley, 1975; Arney, 1998; Garrick, 1999). Paleogeography of northern México for the Maastrichtian (Fig. 2.4) suggests that the Alisitos Magmatic Arc was most probably the original source of sediments for the Parras and peripheral basins developed eastward of the SMO orogenic front (Goldhammer and Johnson, 2001).

Eastward migration of the shoreline in northeastern México was not a uniform and continuous process. In the central Parras Basin, the general regressive trend alternated with transgressive (T) episodes (Fig. 1.2). Regressive episodes (R) developed after flooding events (MFS), were characterized initially by progradational shallow-marine sedimentation, and closed by mostly aggradational deposition of red beds in coastal plain transitional environments.

Red bed wedges (Cerro Huerta, Las Imágenes, and Las Encinas formations) were transgressed at different times and finally overlapped by shallow-marine sediments. This alternating process of landward and seaward shoreline migration produced at least three major transgressive-regressive cycles (TR) recorded by the clastic deposits of the Difunta Group (Fig. 1.2). Sedimentation that produced such complex stratigraphy and facies associations occurred under an interaction of factors, including relative sea level variation and shoreline migration that involved clastic sedimentation in coastal plain and shallow marine environments. Renewal of accommodation space in the central Parras Basin was controlled by eustasy and localized extremely high rates of subsidence. Combined, all these factors produced a stratal geometry characterized by thicker stratigraphic units in the southwestern portion of the study area (northwest of Saltillo), and thinner units northward and eastward (Figs. 1.3, 3.2, cross sections A.17 to A.19).

5.3 Depositional History of the Study Interval

5.3.1 Lower- Middle Cañón del Tule Formation

TST and Previous HST (Sub Cycle SC 2.1)

In the early Maastrichtian, fluvial-deltaic red beds of the Cerro Huerta Formation record the closure of one of the major aggradational cycles (Figs. 1.2 and 3.1). Upward, retrogradational deposition of the lower Cañón del Tule Formation indicates transgression that produced overlapping of shallow-marine sediments and deepening-upward conditions (lower part of subcycle SC 2.1; Fig. 3.1). Maximum depth was reached at the maximum flooding surface (MFS 2.1) within thick muddy outer shelf deposits in the lower Cañón del Tule Formation (Halik, 1998). This major flooding event within the formation marks the beginning of a progradational shallowing-upward trend of deposition (HST) that culminates at the transgressive surface (TS 2.2) on top of subcycle SC. 2.1 (Fig. 3.1). The HST deposits conventionally labeled in this work as Previous HST, consists on cyclic turbiditic successions that grade upward into middle to upper shoreface

sandstone and mudstone (Figs. 3.1 and 3.4). Tool marks and flute casts in this succession indicate paleocurrent direction flows between north 75° east and south 75° east (Soegaard *et al*., 1997; Halik, 1998; this work), which are consistent with the paleocurrent data collected by McBride *et al*. (1975).

5.3.2 Upper Cañón del Tule Formation
TST and HST (lower part of Sub Cycle SC 2.2)

After the development of the surface of marine transgression (TS 2.2), depositional conditions in the area deepened and finer-grained sediments were deposited as part of the overlying transgressive (TST) systems tract (Fig. 3.1 and 3.2). The developed transgressive succession is characterized by a retrogradational stacking pattern that includes lower shoreface strata below grading into offshore muddy deposits above. Retrogradational deposition developed during relative sea level rise, up to the maximum flooding surface (MFS 2.2), which represents the lower bounding surface of the study interval. Subsequently, sediment supply exceeded the rate of relative sea level rise and shallowing-upward conditions and coarsening-upward HST deposits prograded again into the basin (green lower unit in Fig. 3.2).

The sediments deposited as part of the highstand systems tract (HST), between the maximum (MFS 2.2) and the forced regressive surface (FRS+SB), include offshore deposits below and storm-influenced lower shoreface deposits above (Fig. 3.1 and 3.2). Gastropods, bivalves, ammonites (Plates 1-3, 5-6), benthonic foraminifers and diverse microfossils (Plate 12), typical of shallow marine environments, occur in this interval. Swaley cross-stratification suggests that deposition of the upper part of the HST, occurred under the influence of storm processes (Figs. 3.3 and 3.6). Meter-scale sandstone units that commonly contain shell fragment lags at their bottoms suggest that high-energy conditions periodically predominated. Wave energy during storms appears to have produced

reworking of nearshore sediments and breakage of mollusk shells, which were later mixed and concentrated in layers several centimeters thick (Fig. 3.6). Highly bioturbated mudstone on top of individual sandstone beds suggests deposition in quiet conditions, after the storm processes waned, and fair weather conditions returned (Fig. 3.6).

Lithology, sedimentary structures, intensity of bioturbation, and fossil content suggest that deposition of the upper Cañon del Tule Formation occurred in shallow marine nearshore environments subject to the action of waves, storms, rip and longshore currents (Fig. 3.3). Minor lateral variations of facies in an west to east direction suggests a ramp-type depositional setting whose distal areas were located eastward and northward of the study area. More exactly, deposition in proximal areas in the central Parras Basin occurred in offshore, shoreface, and foreshore environments (Fig. 3.3). Storm processes did not affect the deepest muddy offshore deposits above the maximum flooding surface (MFS 2.2). On the eastern study area, eastward of the Altamira Section (Fig. A.18), the HST deposits dramatically change to distal muddy sediments described as Tanque Formation by McBride *et al*. (1974). The region around Los Ojitos and El Tanque sections (Fig. A.18), were subjected to fine-grained deposition characterized by considerably thick intervals of mudstone with lesser amounts or almost devoid of sand (Fig. 3.24).

The interval between the transgressive surface TS 2.2 and the forced regression surface (FRS+SB), which includes the TST and HST deposits (Fig. 3.1 and 3.2), is lower Upper Maastrichtian in age based on the occurrence of the index ammonites *Coahuilites sheltoni* and *C. cavinsi* (Cobban and Kennedy, 1995; Kennedy *et al*., 1996; Plates 1, 3). *C. sheltoni* occurs right above the transgressive surface TS 2.2 at the Altamira Section (Fig. A.2 and A.18), and 19 m below the forced regression surface (FRS) at La Florida Section (Figs. 3.8c and

A.6, Plate 1). Associated gastropods and bivalves are typical assemblages of the Early Maastrichtian (F. Vega, written comm., 1998; Plates 5-6).

5.3.3 Uppermost Cañón del Tule Formation
Falling Stage Systems Tract (FSST)
(Middle part of Sub Cycle SC 2.2)

Following the highstand (HST) deposition described above, sedimentation patterns in the basin underwent a drastic and abrupt change produced in a stage when the rates of eustatic fall exceeded and overwhelmed the rates of subsidence. Accommodation space was reduced in proximal settings forcing the shoreline and coarse-grained shoreface facies belts to migrate basinward in response to a relative sea level fall (forced regression). Consequently, relatively deeper muddy offshore HST deposits were overlain directly and sharply by FSST (falling stage systems tract) upper shoreface to foreshore sandstones (Figs. 3.2, 3.6 to 3.9). The erosional vacuity below the FSST sandstones (Fig. 3.2b) represents a diachronously developed unconformity (forced regression surface) and sequence boundary (FRS+SB) produced by multiple surfaces of submarine erosion that partially removed the deep HST muddy deposits and cannibalized much of the laterally equivalent FSST deposits. The FSST groups the strata deposited during the initial stage of relative sea level fall. Thus, the terminology proposed by Plint and Nummedal (2000) for this kind of deposits was here adopted.

The relative sea level-fall in the Late Maastrichtian had a regional influence in facies distribution, produced wave scouring, and developed a sharp erosional forced regression surface (FRS) with a meter-scale undulatory relief (Figs. 3.2, 3.7 to 3.9). The surface represents a facies truncation in which the intermediate middle shoreface facies association is missing. Thus, the forced regression surface of the upper Cañón del Tule Formation represents an abrupt

interruption of normal regressive sedimentation in which the gradual stacking of shallowing facies predicted by Walter's law was truncated by a marine erosional unconformity. Submarine erosion of the sea floor substrate was characterized by the development of erosive structures such as groove casts, and channel-like meter-scale gutter casts (Figs. 3.8 and 3.9).

The regional relative sea level fall that produced the forced regression was gradually attenuated within a subsiding Parras Basin. It is interpreted that accommodation space was constantly renewed in proximal areas, adjacent to the orogenic front, by the effect of high rates of subsidence (1m/1000 yr according to Soegaard *et al., in press*). The general relative sea level fall was punctuated by small pulses of sea level rises. This interpretation is based on the internal stratigraphic architecture of the FSST sandstone, which can be subdivided into at least two and up to ten sandstone subunits. Every stacked upward-thickening sandstone is separated by thin horizons of marine mudstone or amalgamation surfaces with chert pebbles. It is interpreted that every rising pulse produced an increase in water depth and that every thin horizon of marine mudstone was deposited in these periods of deepening. Subsequently, thick columns of nearshore sand occupied most of the renewed accommodation space still available. The FSST sandstone deposits display variable thicknesses ranging from 2 m on the distal sections eastward of the study area, and up to 58 meters in proximal areas of the southwest (Figs. 3.11 and 3.12). The area nearby El Saucillo Section (Fig. 2.8), where the forced regressive deposits reach their maximum measured thickness (58 m), is interpreted as the region of the highest rates of subsidence and sediment supply at this period of deposition.

In the central Parras Basin, the forced regression process produced submarine erosion along 24 km in a west to east direction (Fig. A.18). Forced regressive deposits described in the northern Parras and La Popa basins (Ye, 1997; Soegaard *et al*., 1997) suggest that in a north to south direction the surface

extends for at least 170 km (Fig. 5.1). Field observations, similar stratigraphic relationships, and stratigraphic position of the forced regressive surface support the interpretation of its regional distribution. Most important is the fact that the surface is interpreted as the result of a forced regression controlled by a regional sea level fall. Its regional distribution beyond the boundaries of the Parras and peripheral basins might be the objective of future research.

5.3.4 Lower Las Imágenes Formation
Falling Stage Systems Tract (FSST)
(Upper part of Sub Cycle SC 2.2)

While the forced regression progressed and FSST rocks of the upper Cañón del Tule were deposited in shallow marine environments, over the adjacent coastal plain, thick, mostly aggradational red deposits of the lower Las Imágenes Formation (FSST) accumulated. During the basinward migration of the shoreline, red sediments eroded from the coastal plain were transported into nearshore environments and mixed in low proportion with green and gray sediments of the uppermost Cañón del Tule. The uppermost sandstone of this unit contains traces of red material in some locations and records a gradational process characterized by deposition of intervals of variable thickness of bicolored mixed, gray/green and red silt and clay. The contact between the coastal plain FSST red deposits and the underlying shallow marine FSST sandstone is gradational and suggests a smooth shoreline regression, which did not involve fluvial incision, erosion, or sequence boundary development. Eventually the FSST red beds of the coastal plain extended to the east and northeast, reaching their maximum areal distribution. In a west to east direction, the red beds never extended farther than the intermediate area between the Temporal and the Altamira sections (Figs 2.8 and A. 18). From south to north the same coastal red deposits never extended farther than the town of Fraustro located in northern Parras Basin, 10 km northward of La Florida Section (Soegaard *et al*., 1997; Fig.

5.1). Theoretically, the contact between the Cañón del Tule and Las Imágenes Formation is diachronous, probably older to the west and relatively younger eastward (Fig. A.18). However, no evidence other than the wedge-shaped geometry of Las Imágenes Formation (Fig. 5.1) and the interpretation of a shoreline migration process can be provided.

High rates of subsidence in the southwestern central Parras Basin produced an accentuated generation of accommodation space. In the western region covered by El Realito and the Doce de Diciembre sections (Figs. 2.8 and A.18 to A.19), extremely high rates of subsidence favored sedimentation of almost 550 m of FSST coastal floodplain deposits.

5.3.5 Upper Las Imágenes Formation
Early Transgressive Systems Tract (Early TST)
(Lower part of Sub Cycle SC 2.2)

Following the maximum east and northeast distribution of the FSST red deposits, the interaction between subsidence and eustasy created an equilibrium and finally produced a discrete rising or still stand position of relative sea level. Consequently, the shoreline began to migrate landward while wide (70 m) and shallow (6 m), mixed-load, probably meandering fluvial systems flowed on a low-gradient coastal plain and transported sand as bedload and fine-grained sediments is suspension (Fig. 3.16). In adjacent areas, thick monotonous successions of aggradational deposits of mudstone and siltstone accumulated in the coastal floodplain (Fig. 3.15). These fine-grained deposits commonly contain abundant plant debris, impressions of small plant branches, and palm-like leaves (Fig. 3.12c, d). Diagenetic processes acting soon after deposition eventually produced the reddening of these sediments typical of Las Imágenes Formation (see discussion at the end of this subchapter).

The lower horizons of the Early TST deposits contain benthonic foraminifers, ostracods (Fig. 4.9 and Plate 11), and broken oyster shell deposits encased in highly bioturbated red beds (Figs. 3.14a, b). Additionally, an abundant, diverse, and well-preserved assemblage of fossil charophytes occur in laterally restricted bodies of white charophyte-bearing clays or well-cemented charophyte banks (Fig. 4.7-4.9) that lie within a 40-m-thick interval in the middle part of Las Imágenes Formation. The association of charophytes and marine fossils suggest the beginning of an intermittent marine transgression across a rapidly subsiding coastal plain, whose initial transgressive pulses favored the development of charophytes within diverse marginal marine environments (marshes, small lakes or ponds, and lagoons; Figs. 4.7 to 4.9). The occurrence of benthonic foraminifers and echinoderm fragments within widespread sheets of red sandstone, upward in Las Imágenes Formation (Plate 13), is also supporting evidence of intermittent signals of transgression (Puerto La Cuesta Section, Fig. A.9, cross section A.18).

The regional distribution of charophytes in the middle part of Las Imágenes Formation, suggest that they were widespread in the central Parras Basin approximately after the time when the red beds reached their maximum distribution eastward (Figs. 3.2 and A.18). It is interpreted that the transgressive process was characterized by intermittent marine incursions controlled by the interaction between the rate of sediments supplied to the coastline and relative rise in sea level produced by subsidence.

At the final stage of deposition of Las Imágenes Formation, rivers flowing on the western study area increased their transport capacity. Streams transported and deposited gravels as channel lags and channel-fills (Fig. 3.17). Gravels eventually reached the shoreline where they were redistributed, mixed with sand, and deposited as intraformational conglomerates in strand plain (?) sheets of sandstone (Fig. 3.18). Some sheet sandstone deposits of the upper Las

Imágenes Formation contain benthonic foraminifers and echinoderm plates (Plate 13), which clearly suggest deposition in marine-influenced environments.

Sheet sandstones are extensive in the western study area. They are interpreted as accumulations of sediments redistributed along shallow marine environments. Interbedding of the sheet sandstone bodies with deposits of fluvial character, their geometry characterized by along strike extension, and their content of benthonic foraminifers, suggest deposition in a strand plain (?). While the transgressive process advanced covering the marginal continental environments, waves and longshore currents redistributed sediments supplied by rivers along the coastline. Redistribution of sediments along the shoreline precluded the development of the typical progradational delta-front facies and mouth bars.

Crawley (1975), who studied the Cerro Grande Formation, found no evidences of any large rivers in the Cerro Grande outcrop area. He suggests that the coast was relatively straight, formed of coalesced beach and beach-ridge deposits, perhaps with small cuspate deltas similar to those of the modern Tabasco and Nayarit coasts of México. The depositional environments interpreted for the study interval support the development of a straight coast with marginal lagoons bounded by wide extensively extended shoreface and offshore environments for this part of the Late Maastrichtian Gulf Coast of México. An analog is probably the modern coast of Texas, Tamaulipas, and Veracruz, where meandering rivers flowing on a wide coastal plain, discharge large amounts of sediments into a roughly straight coast.

Finally, after the stage of intermittent marine transgression that characterized the Early TST red deposits, shallow seas definitively covered the region. Depositional conditions deepened again, developing fining-upward

sedimentary successions characterized by a retrogradational depositional architecture (Early and Late TST; lower Cerro Grande deposits).

5.3.6 Lower Cerro Grande Formation
Early and Late TST (lower part of Cycle SC. 3)

After the maximum distribution of red beds, the shoreline began its migration landward and shallow marine sediments of the Cerro Grande Formation gradually covered the red sediments of Las Imágenes Formation (Figs. 3.20-3.22). Overlapping of marine sediments was apparently a diachronous process that produced a transgressive surface and deposition of sediments relatively older on the eastern study area and younger westward (Fig. 3.2 and A.18). It is interpreted that eastward migration of the shoreline until the maximum areal distribution of red beds was produced as a consequence of sediment supply exceeding the rate of accommodation space generated. As soon as the rate of sediment supply decreased, transgression began, and shallow marine deposits of the Cerro Grande Formation gradually covered the Early TST coastal plain red deposits of Las Imágenes Formation. Direction of transgression is difficult to determine but most probably was overall from east to west producing a diachronous transgressive surface in the same direction.

Exposures of the transgressive surface TS 3 (Figs 3.1 and 3.2) are limited to few outcrops of restricted lateral extension. In the eastern-central portion of the study area at La Campana Section (Fig. A.3), the surface roughly coincides with the lithostratigraphic contact between Las Imágenes and the Cerro Grande formations (Figs. 3.20-3.22). The surface lies a few centimeters above the uppermost red mudstone, which is overlain by gray highly bioturbated mudstone and thick beds of upper shoreface sandstone. At La Campana Section, the initial transgressive sandstone contains small flute casts at their bottoms (Fig. 3.20d). In other locations, a chert pebble lag and marine fossils that occur a few meters

above characterizes the transgressive surface (TS 3). *Exogyra costata* and diverse gastropods and bivalves also occur upward in some sections (i.e., La Florida and Las Trancas-Palo Blanco sections). In the western area covered by the sections Doce de Diciembre and Puerto La Cuesta, the transgressive surface TS 3 is difficult to identify, but undoubtedly lies above the non-red fluvial conglomerates of the uppermost Las Imágenes Formation (Figs. 3.2 and 3.19c, d).

The transgressive (Early TST) deposits of the lower Cerro Grande Formation define an upward-fining and deepening succession of retrogradational sets of parasequences that reach the maximum mudstone content up to the maximum flooding surface MFS 3. The MFS 3 constitutes the upper bounding surface of the study interval (Figs 3.1 and 3.2).

5.3.7 Lower Cerro Grande Formation
HST (upper part of Cycle SC. 3)

Above the transgressive surface MFS 3, stacking of beds is characterized by shallowing-upward and upward-thickening HST deposits. This progradational interval was studied at La Campana and Altamira sections. At the Altamira Section, the HST deposits display a well-defined cyclic succession of parasequences composed by interbedded mudstone, siltstone, capped by upward thickening sandstone beds deposited in lower to upper shoreface environments. These cyclic succession of beds resemble delta front or delta flank deposits due to their progradational character. It is assumed that this progradational character remains until the deposition of Las Encinas red beds that closed the cycle SC 3 on top (Fig. 1.2).

5.4 Discussions

5.4.1 Development of Type-1 Sequence Bounding-unconformities and Forced Regressions in Ramp-type Foreland Settings

In tectonically active settings such as foreland basins, rates of subsidence commonly increase landward toward the orogenic belt (Posamentier and Allen, 1993; Fig. 5.1). At any specific region across the foreland basin profile, the resultant relative sea level change depends of the interaction between the rates of flexural subsidence and eustasy. Based on these assumptions, Posamentier and Allen (1993) suggest that a foreland ramp-type basin can be subdivided into zones A and B. In zone A, subsidence always exceeds the rate of eustatic fall. Therefore, no relative sea-level fall occurs and type-2 sequence boundaries develop. In the distal zone B, eustatic sea level fall periodically exceeds the rate of flexural subsidence. In this zone, the resultant relative sea level fall produces type-1 sequence-bounding unconformities and forced regressions. The equilibrium point that divides zone A from zone B is defined as the position across the profile where the rate of eustatic change equals the rate of subsidence (Fig. 5.1). When eustatic fall accelerates, the equilibrium point migrates landward in the direction of the highest subsidence. If eustatic fall is significantly greater than subsidence rate, type-1 sequence bounding-unconformities and forced regressions will develop as well in proximal settings close to the orogenic front.

The forced regression surface of the uppermost Cañón del Tule Formation is interpreted to be a type-1 sequence-bounding unconformity developed in proximal settings (zone A of Posamentier and Allen's model; 1993; Fig. 5.1). The surface is interpreted to be the result of a regional relative sea level fall produced in a stage when the rate of eustatic fall overwhelmed the rate of subsidence (see discussion in Chapter 3, Fig. 3.2). Although the Posamentier and Allen's model (1993) predicts the development of type-1 sequence boundaries in proximal settings, based on the same model, Ye (1997) interpreted only type-2 sequence

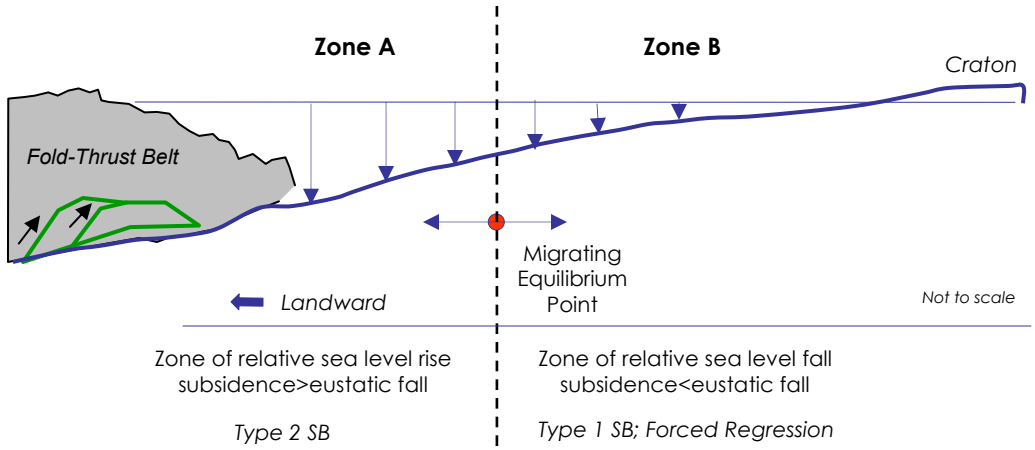

Figure 5.1 Schematic representation of the tectonostratigraphic zones in a foreland ramp-type basin. In proximal zone A subsidence commonly exceeds the rate of eustatic fall. Thus, no relative sea-level fall occurs and type 2 sequence boundaries are developed. In contrast, in those basins where shorelines develop within zone B are characterized by type 1 sequence-bonding unconformities and forced regressions since the region is influenced by relative sea level falls. When the rate of eustatic fall exceeds the rate of subsidence, the equilibrium point migrates landward in the direction of higher subsidence. Consequently, the generation potential of type 1 sequence boundaries and forced regressions on the tectonically active side of the foreland basin is favored by the landward migration of the equilibrium point. (Modified from Posamentier and Allen, 1993).

boundaries in the proximal zone of the south central Parras Basin (see Ye´s Fig. 2-5, p. 24, 1997). His interpretations are not consistent with the identification of the type-1 sequence boundary and forced regression surface (FRS+SB) identified at the bottom of the uppermost FSST sandstone of the uppermost Cañón del Tule Formation (Fig. 3.2).

5.4.2 Regional Stratigraphic Expression of the Forced Regression Surface (FRS+SB)

In the central Parras Basin, the forced regression process produced submarine erosion for at least 24 km in a west to east direction. In a south to north direction, the forced regression surface occurs at El Saucillo and La Florida sections separated by a horizontal distance of 13 km (Fig. 2.8). However, field observations and previous works suggest that the surface extends farther north into the northern Parras, La Popa, and southern Sabinas basin. Halik (1998) describes stacked upper shoreface sandstone of the Cuchilla Tongue/Las Imágenes Formation (Fig. 5.2), sharply overlying outer shelf and lower shoreface mudstone of the Potrerillos Formation (sections Huisachal, San Bernabé, Anhelo, Reata, and Fraustro; Halik´s Appendix C). At the Fraustro Section, shallow marine sandstone sharply overlies outer shelf mudstone of the Cañón del Tule Formation (Fig. 5.2). According to Halik (1998) and Soegaard *et al.* (1997), both in the Fraustro and Reata sections the stacked upper shoreface sandstones are separated from the underlying deep muddy sediments by a regressive surface of submarine erosion.

Ye (1997) points out that in the La Popa Basin, the Cuchilla Tongue, which consists of stacked erosive-based shoreface parasequences, sharply overlies offshore/prodelta deposits of the Potrerillos Formation (Ye´s Plates XVIIa and XVIIb). He also states that the forced regression surface at the bottom of the Cuchilla Tongue is a type-I sequence boundary and mentions that the surface

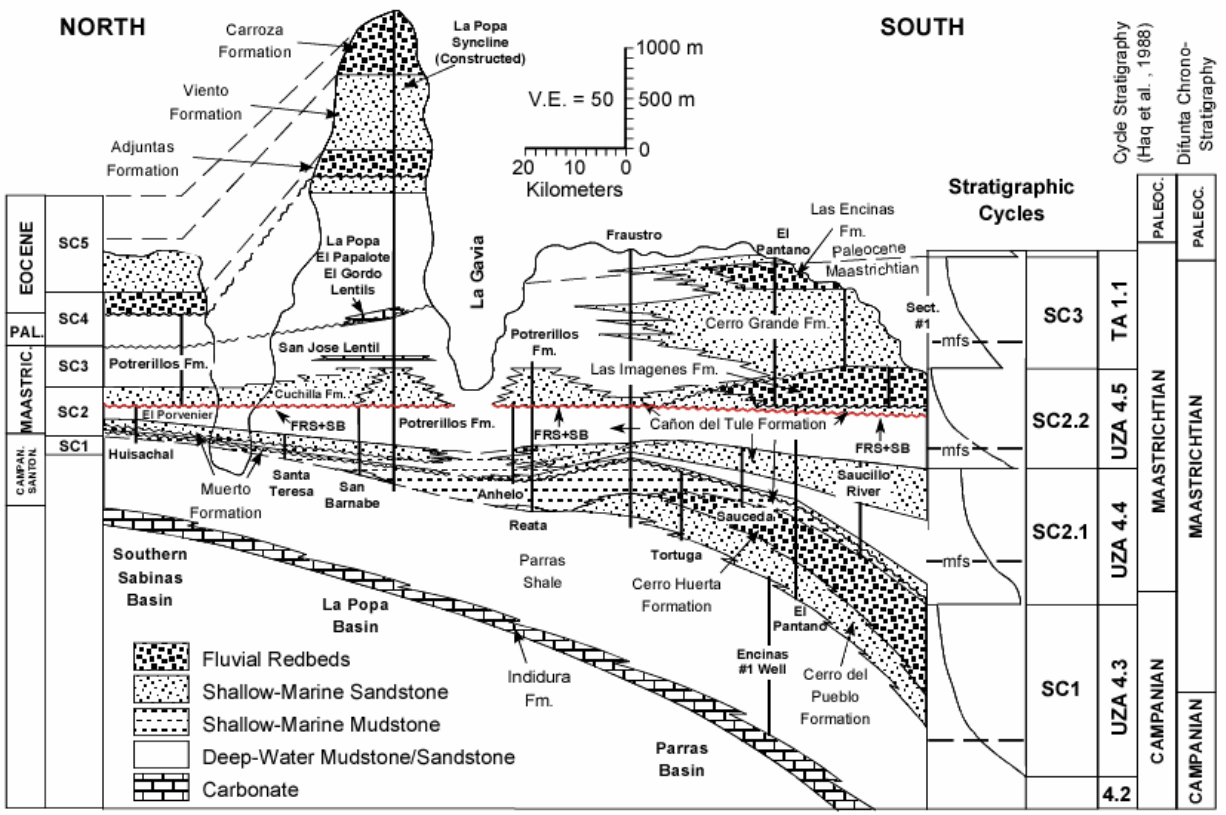

Figure 5.2 Regional distribution of the forced regression surface and sequence boundary (FRS+SB) in the Parras, La Popa, and south Sabinas basins. The Difunta Group is sudivided into five stratigraphic cycles, overall progradational units, whose boundaries coincide with the top of fluvial redbeds overlain by fossil-bearing marine sediments. The wavy surface in red is the forced regression surface and sequence boundary (FRS+SB) hat extends across the Parras, La Popa and south Sabinas basins. The surface extends for at least 170 km in a south to north direction. The forced regressive surface was redrawn and colored on the original figure from Soegaard *et al*. (1997). The stratigraphic cycles nomenclature was proposed by Halik (1998). This figure was modified and reproduced under the kind permission of Dr. Kristian Soegaard.

extends southward into the northern Parras basin. He adds that this sequence boundary and forced regression surface can be traced along Highway 57 at the Fraustro Section (see Ye´s plates XIXb and XXb). In the Fraustro Section (Fig. 5.2) “The base of Las Imágenes Formation is an excellent example of a sharp, erosionally based shoreface caused by a forced regression during a relative sea-level fall” (Soegaard *et al*., 1997, p. 8).

Note on the north side of Figure 5.2 the red wavy surface at the base of the Cuchilla Formation, almost in the middle part of the sub cycle SC 2. This wavy line represents the regressive surface of submarine erosion described by Soegaard *et al.* (1997), Ye (1997), and Halik (1998). The surface extends southward to the Fraustro Section. At El Pantano Section, an erosional surface was interpreted by Soegaard *et al*. (1997) at the base of Las Imágenes Formation. However, it was previously stated (sub chapter 3.3.2) that the contact between the Cañón del Tule and Las Imágenes Formation is gradational. Instead of fluvial incision and an unconformity, the contact records a smooth shoreline regression and deposition of coastal plain red beds over shallow marine sediments. It was observed here that the unconformity and sequence boundary in reality occurs below, at the base of the stacked upper shoreface (FSST) deposits of the uppermost Cañón del Tule Formation. Consequently, the wavy line (forced regression surface) at the base of Las Imágenes Formation must be placed below, at the base of the uppermost sandstone of the Cañón del Tule and Cuchilla formations (Fig. 5.2). This change makes an almost horizontal surface represented by a wavy line (FRS+SB) colored in red, almost in the middle part of the sub cycle SC 2.2.

Based on the previous descriptions and own field observations, it is concluded that the upper shoreface sequences referred by Ye (1997), Halik (1998), and Soegaard *et al*. (1997) are in reality equivalent to the uppermost sharp-based FSST shoreface sandstone of the uppermost Cañón del Tule

Formation (Fig. 5.2). In other words, the forced regression surface at the bottom of the Cuchilla Tongue in the southern Sabinas and La Popa basins is the same forced regression surface that crops out on Highway 57 nearby Fraustro and in most of the measured sections in the central Parras Basin (this study). The forced regression surface (FRS+SB) extends along 170 km across the Parras-La Popa (Fig. 5.2) and the southern Sabinas basin (Halik´s Huisachal Section, 1998). The distribution of the surface (FRS+SB) and associated FSST deposits beyond the boundaries of these basins may be the objective of future research.

5.4.3 Timing and Environmental Significance of Red Deposits

According to McBride *et al.* (1975) and McBride (1974), reddening of Las Imágenes sediments occurred by diagenetic processes soon after deposition, during dry seasons and stages of lowering of water table. Red coloration is due to pervasive hematite coatings produced by post depositional alteration of iron-bearing minerals and dehydration of hydrous iron oxides. They also point out that erosion of the already reddened substrate is evident by the presence of red mudstone clasts in channel-fill deposits.

It was previously mentioned (subchapter 3.2.2) that the stratigraphic contact between the Cañón del Tule and Las Imágenes formations is characterized by a transitional interval several meters thick of mixed green and reddish sandstone. It is interpreted that the traces of red material on top of the uppermost FSST sandstone deposits of the upper Cañón del Tule were eroded by rivers from the laterally contiguous coastal plain FSST deposits of Las Imágenes Formation. After erosion and transportation, sediments preserved their red coloration.

Erosion of red sediments and later transportation into shallow marine environments has been documented for the lower Juniata (Late Ordovician)

Formation of southwestern Virginia. Based on primary sedimentary structures and traces of marine fossils, Dorsch and Driese (1992) suggest that marine red beds of the lower Juniata Formation attained their red coloration during storage on alluvial plains. They conclude that even after erosion, hematite coatings of sediments were preserved and sediments retained their red coloration until their final deposition in shallow marine shoreface to inner shelf depositional environments. It must be noted that the red coloration *per se* should not be considered as an indicative character of non-marine deposition (Dorsch and Driese, 1992).

CHAPTER 6

SUMMARY AND CONCLUSIONS

1. Sequence stratigraphic concepts were used to develop a sequence stratigraphic model to synthesize and interpret the depositional history of the study strata (Fig. 3.2 and 3.2). The study interval includes 900 m of Maastrichtian rocks deposited in coastal plain and shallow marine environments in the central Parras Basin. It includes rocks of the upper Cañón del Tule, Las Imágenes, and lower Cerro Grande formations.

2. Basic analysis of lithology, vertical grain-size trends, bed thickness, sedimentary structures, fossil content, and stacking patterns at sixteen stratigraphic sections, allowed placing the stratal units within a sequence stratigraphic frame of reference. This analysis allowed the identification of sequence stratigraphic bounding-surfaces, which were used to subdivide the study interval into transgressive (TST), highstand (HST), and falling stage systems tracts (FSST) based on their retrogradational, aggradational, and progradational depositional architectures. The study interval consists of one major relative sea level cycle bounded by the maximum flooding surfaces MFS 2.2 below and the MFS 3 above.

3. The vertical stratigraphic succession recognized within the studied interval from bottom to top includes:

   a) Highstand (HST) deposits of the upper Cañón del Tule Formation, bounded at its bottom by a maximum flooding surface (MFS 2.2) and at the top by a forced regression surface and sequence boundary (FRS+SB).

b) Falling stage systems tract (FSST) deposits that includes the red beds of the lower Las Imágenes Formation; and the stacked sharp-based FSST sandstone of the uppermost Cañón del Tule Formation and the laterally equivalent cannibalized deposits. Both the FSST sandstone deposits of the uppermost Cañón del Tule Formation and the FSST red beds of the lower Las Imágenes Formation lie above the forced regression surface and are bounded on top by an early marine transgressive surface characterized by a charophyte-bearing interval and marine fossils. The cannibalized FSST shallow marine deposits of the upper Cañón del Tule Formation lie below the forced regression surface.

c) Transgressive (Early TST) coastal plain red deposits of the lower Las Imágenes Formation that lie between the early marine transgressive surface and the transgressive surface TS 3. Transgressive (Early and Late TST) shallow marine strata of the lower Cerro Grande Formation lie between the transgressive surface (TS 3) below and the maximum flooding surface (MFS 3) above.

4. The highstand (HST) deposits of the upper Cañón del Tule Formation above the MFS 2.2 include a progradational shallowing- and coarsening-upward sedimentary succession composed of muddy offshore deposits that grade upward into storm-influenced lower shoreface mudstone, siltstone, and sandstone. Minor lateral variations of facies suggest that the deposition of this interval occurred in a ramp-type depositional setting, whose distal areas were located eastward and northward of the study area. Deposition occurred during a period of relative sea level rise and sediment supply exceeding the rate of accommodation space, which produced progradation of sediments into the basin.

5. The highstand (HST) rocks that lie above the MFS 2.2, as well as the underlying transgressive (TST) deposits, contain a rich assemblage of gastropods and bivalves frequently found in Lower Maastrichtian strata. However, the occurrence of the index ammonites *Coahuilites sheltoni* and *C. cavinsi* restricts their age to the lower part of the Upper Maastrichtian. Therefore, the TST and HST deposits of the upper Cañón del Tule Formation and all strata that lie above this interval, including Las Imágenes and Cerro Grande formations, can be accurately assigned to the Upper Maastrichtian by stratigraphic position. The Lower/Upper Maasthichtian boundary could not be established, since it is unknown if the referred index ammonites also occur below the study interval.

6. In the Late Maastrichtian, the final stage of shallow marine sedimentation of the upper Cañón del Tule Formation was characterized by a drastic and an abrupt change in the sedimentation patterns. The change was the result of an eustatic sea level fall that exceeded and overwhelmed the rates of subsidence. In this stage, accommodation space was reduced in proximal settings, forcing the shoreline and coarse-grained shoreface facies belts to migrate basinward in response to a relative sea level fall (forced regression).

7. The forced regression in the central Parras Basin had a regional impact in facies distribution, produced submarine erosion of the sea floor substrate by wave scouring, and the development of a sharp, erosional, forced regression surface (FRS) characterized by a meter-scale undulatory relief and associated erosional structures. Meter-scale channel-like gutter casts associated to this surface are attributed to the erosive action of strong rip currents.

8. The forced regression surface (FRS) of the uppermost Cañón del Tule Formation:

   a) separates relatively deeper muddy lower shoreface deposits below (HST) from coarser and shallower upper shoreface to foreshore sandstone above (FSST). This vertical association of rocks is identified as a facies truncation in which the intermediate middle shoreface facies association is missing.

   b) represents an abrupt interruption of normal regressive sedimentation in which the gradual and continuous stacking of upward-shallowing facies predicted by Walter's law is truncated by a marine erosional unconformity.

   c) is a diachronously developed unconformity and type-1 sequence boundary produced by the amalgamation of multiple surfaces of submarine erosion. Wave scouring of the seafloor substrate, and rip and longshore currents partially removed the deep HST muddy deposits and cannibalized much of the laterally equivalent FSST strata during the forced regression process. Groove casts and channel-like meter-scale gutter casts that scour the underlying highstand (HST) muddy deposits are the most characteristic associated erosional structures.

   d) has a regional distribution and constitutes a valuable stratigraphic horizon of reference and correlation. In the central Parras Basin, the forced regression surface extends for at least 24 km in a west to east direction. In a south to north direction, the same surface extends for at least 170 km across the central Parras, La Popa, and southern Sabinas basins. Its regional distribution beyond the boundaries of these basins should be investigated.

9. The FSST deposits of the uppermost Cañón del Tule Formation include a prominent, ridge-forming, sharp-based sandstone deposited in upper

shoreface to foreshore environments. The area nearby El Saucillo Section, where these deposits reach their maximum measured thickness (58 m), was the region of the highest rates of subsidence and sediment supply during this period of sedimentation. The FSST sandstone unit thins and pinches out eastward and to a lesser degree northward. It is 33 and 15 m thick at El Realito and La Florida sections, repectively, and les than 2 m thick at the Altamira Section, located 15.5 km eastward of El Saucillo Section.

10. The FSST deposits are composed at least two and up to ten stacked upward-thickening sandstone beds separated by thin horizons of silty hardened mudstone. This internal stratigraphic architecture suggests that the regional relative sea level fall that produced the forced regression in the central Parras Basin, was attenuated and punctuated by small high-frequency pulses of sea level risings controlled by subsidence. These short periods of deepening or drowning conditions initially produced fine-grained deposition, which was followed by infilling of the available accommodation space by fine- to medium-grained sand.

11. While the forced regression progressed and the FSST strata of the upper Cañón del Tule were deposited in shallow marine environments, thick, mostly aggradational red deposits of the lower Las Imágenes Formation (FSST) accumulated on the adjacent coastal plain. During the basinward migration of the shoreline, red sediments eroded from the coastal plain were transported into nearshore environments and mixed in low proportion with shallow marine sediments of the uppermost Cañón del Tule Formation. The uppermost interval of this unit is massive sandstone that contains traces of red material at the top and grades into red mudstones of Las Imágenes Formation.

12. The gradational character of the contact between the Cañón del Tule and Las Imágenes formations suggests a slow shoreline regression and progressive

advance of the coastal plain (FSST red deposits) over shallow marine (FSST) foreshore to upper shoreface environments. The transitional contact was developed in a stage characterized by sediment supply exceeding the accommodation space generation that produced a smooth shoreline regression, which did not involve significant fluvial incision, erosion, or sequence boundary development.

13. The FSST coastal plain red beds of the lower Las Imágenes Formation extended to the east and northeast, reaching their maximum areal distribution. In a west to east direction, the red beds extended to the intermediate area between the Temporal and the Altamira sections. From south to north, the same coastal red beds never extended farther than the town of Fraustro, located in northern Parras Basin. In the western region of the central Parras Basin, high rates of subsidence produced an accentuated generation of accommodation space that favored sedimentation of almost 550 m of FSST coastal plain red deposits.

14. Following the maximum east and northeast distribution of the FSST red deposits, the interaction between subsidence and eustasy reached equilibrium and finally produced a discrete rising or still stand position of relative sea level. Consequently, the shoreline began to migrate landward. Evidences of an initial intermittent marine transgression occur in the lower horizons of the Early TST deposits, in the middle part of Las Imágenes Formation. These deposits contain benthonic foraminifers, ostracods, and broken oyster shell deposits encased in highly bioturbated red beds with *Ophiomorpha* and *Thalassinoides*.

15. An abundant and well-preserved assemblage of fossil charophyte gyrogonites occurs in laterally restricted bodies of white clays or well-cemented charophyte banks. The charophyte-bearing deposits lie within a 40-m-thick

interval in the middle part of Las Imágenes Formation. Their distribution within this particular interval provides a valuable horizon for stratigraphic reference and correlation. The charophytes in the middle part of Las Imágenes Formation:

a) are abundant and have a regional distribution, which suggest that they were widespread in the central Parras Basin approximately after the time when the FSST red beds reached their maximum distribution eastward.

b) did not grow inside the fluvial channels of Las Imágenes Formation characterized by a high suspended-load of fine-grained sediments. Studies on habitats of modern charophytes indicate that they require conditions of high water transparency, oxygenation, and light availability to survive. Some living species tolerate extremely high concentrations of calcium carbonate dissolved in water (75-100g /100g of $CaCo_3$). Due to their fragile structure, charophytes preferentially colonized low-energy fresh and brackish water environments.

c) are associated with marine fossils. This association suggests a transgressive process characterized by intermittent marine incursions controlled by the interaction between the rate of sediments supplied to the coastline and the relative rise in sea level produced by subsidence. It is interpreted that the initial marine transgressive pulses across a rapidly subsiding coastal plain, favored the development of charophytes within diverse marginal marine environments (marshes, small lakes or ponds, and lagoons). The association of benthonic foraminifers and echinoderm fragments within widespread sheets of red sandstone, upward in Las Imágenes Formation, is also supporting evidence of intermittent signals of transgression.

d) are excellently preserved and are morphologically diverse. The charophyte assemblage constitutes the appropriate material to perform detailed statistical and morphological studies. Within such a diverse gyrogonites population, it is possible that new species never described in the charophyte literature are present.

16. Transgressive (Early TST) red deposits of the lower Las Imágenes Formation are characterized by thick aggradational successions of mudstone, siltstone, and sandstone deposited on a low-gradient and rapidly subsiding coastal plain. Wide (70 m) and shallow (6 m), mixed-load, probably meandering fluvial systems transported sand as bedload and fine-grained sediments in suspension. In adjacent interfluvial areas, thick monotonous successions of aggradational fine-grained deposits also accumulated. Diagenetic processes acting soon after deposition eventually produced the reddening of these sediments.

17. At the final stage of deposition of Las Imágenes Formation, rivers flowing in the western study area increased their transport capacity. Streams transported and deposited gravels as channel lags and channel-fills on the coastal plain. Some gravels eventually reached the shoreline.

18. The sheet sandstone deposits of the upper Las Imágenes Formation are extensive in the western study area. Interbedding of the sheet sandstones with deposits of fluvial character, their geometry characterized by along strike and dip extension, and their content of benthonic foraminifers and echinoderm fragments, clearly suggest deposition in marine-influenced environments (strand plain?). While the transgressive process advanced covering the marginal continental environments, waves and longshore currents redistributed sediments supplied by rivers along the coastline.

19. The Late Maastrichtian coastal plain of Las Imágenes Formation seems to have been drained by mixed-load probably meandering rivers that did not develop typical fluvial-dominated deltas. It is proposed that sediments delivered by rivers to the shoreline were redistributed by either waves or longshore currents, developing strand plain deposits similar to those of cuspate wave-dominated deltas. Once the sediments reached the shoreline, redistribution processes precluded the development of typical progradational delta-front facies and mouth bars. Previous studies found no evidences of any large rivers in the Cerro Grande outcrop area and suggest that the coast was relatively straight, formed of coalesced beach and beach-ridge deposits, perhaps with small cuspate deltas similar to those of the modern Tabasco and Nayarit coasts of México.

20. The depositional environments interpreted for the studied strata support the development of a straight coast with marginal lagoons bounded by widely extended shoreface and offshore environments for this part of the Late Maastrichtian Gulf Coast of México. Some analogs are probably the modern coasts of Texas, Tamaulipas, Veracruz, and Tabasco, where meandering rivers flowing on a wide coastal plain, discharge large amounts of sediments into a roughly straight coast with the occasional development of small cuspate deltas (i.e., the rivers Grijalva in Tabasco or the Tecolutla in Veracruz).

21. After the stage of intermittent marine transgression that characterized the Early TST red deposits, relative sea level rise finally exceeded the rate of sediment supply, the shoreline began its migration landward, and shallow seas definitively covered the region. Depositional conditions deepened again developing fining-upward sedimentary successions characterized by the retrogradational depositional architecture of the transgressive deposits of the lower Cerro Grande Formation (Early and Late TST).

22. The transgressive surface TS 3 at the bottom of the lower Cerro Grande Formation lies a few centimeters above the uppermost red mudstone of Las Imágenes Formation. The transgressive surface is characterized by a pebble and shell lag at the bottom of a thick-bedded marine sandstone and mudstone that contain gastropods and bivalves, such as *Exogyra*. At La Florida Section, the surface underlies gray mudstone with *Glossifungites*, commonly observed at firm grounds of transgressive intervals. The transgressive succession reaches a maximum depth at the upper maximum flooding surface MFS 3, at the top of the study interval.

23. Above the maximum flooding surface MFS 3, shallowing- and thickening-upward successions characterize the progradational HST deposits of the lower Cerro Grande Formation. These strata display a well-defined cyclic arrangement of parasequences composed of interbedded mudstone, siltstone, capped by upward-thickening sandstone beds. It is assumed that this progradational character continues upward to the top of the Cerro Grande Formation, which is overlain by the red beds of Las Encinas Formation.

P L A T E S

Plate 1

Ammonites

Upper Cañón del Tule Formation

Figures 1-6. *Coahuilites sheltoni* (Böse, 1927).

(1-3) from a specimen collected at La Florida Section (Fig. A.6), sample labeled (-20LF).

(4-6) from a specimen of La Campana Section (Fig. A.3), sample labeled (-42.2 LC).

(1) Right lateral view. (0.8x)

(2) Detail showing the suture lines on the right lateral side. (0.85x)

(3) Ventral view. (0.8x)

(4) Right lateral view. (0.75x)

(5) Ventral view. (0.75x)

(6) Axial view showing the quadratic section and the keeled venter in the inner whorl. (x 0.75)

C. sheltoni is restricted to the *Holploscaphites birkelundi* Zone, the lowermost zone of the Upper Maastrichtian (Cobban and Kennedy, 1995; Kennedy *et al*., 1996).***** Both specimens were collected from the highstand (HST) deposits of the upper Cañón del Tule Formation (Fig. 3.2).

***** The author of this dissertation is grateful to Dr. Keith Young of The University of Texas at Austin who identified most of the illustrated specimens in Plates 1-4.

The identification of some ammonite specimens and support for the preparation and illustration of the fossil material in plates 1-4 was kindly provided by Ma. Eugenia Gómez (M. Sc.) and Geol. Daniel Olvera García (Instituto Mexicano del Petróleo) and by Dra. Ana Bertha Villaseñor (Instituto de Geología, UNAM), to whom the author is also thankful by their helpful advising.

Plate 1

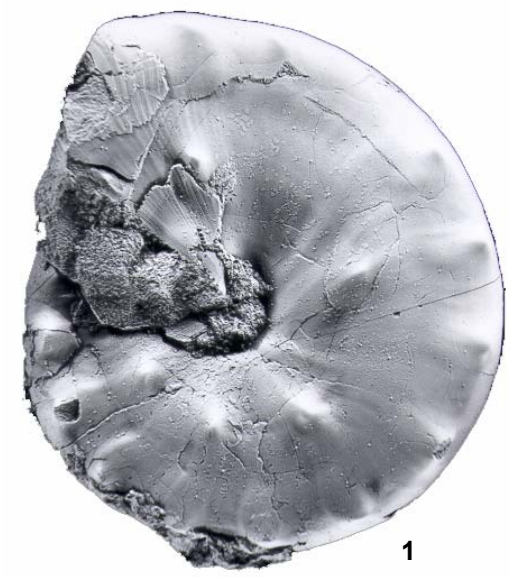

1

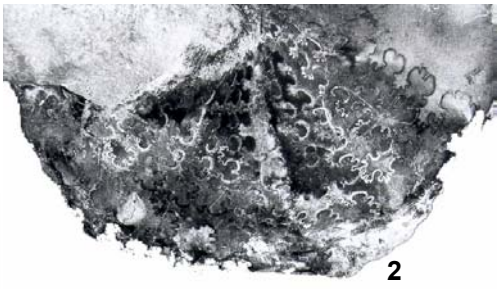

2

3

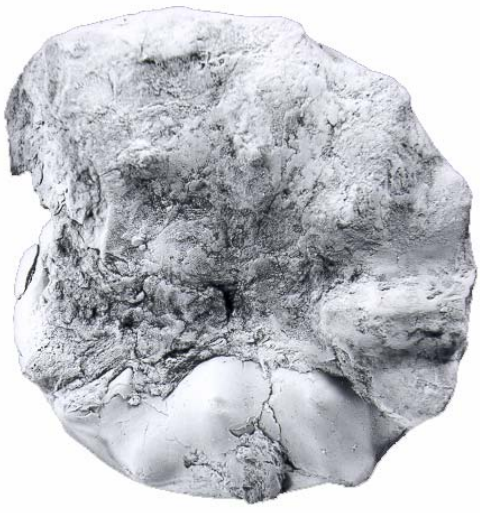

4

5

6

Plate 2

Ammonites

Upper Cañón del Tule Formation

Figures 1-3. *Eutrephoceras planoventer* (Stephenson, 1941). Specimen labeled (-62 LC) collected at La Campana Section (Fig. A.3) from the highstand (HST) deposits of the upper Cañón del Tule Formation.*

(1) Oblique lateral view also showing partially the ventral section (0.95x).

(2) Axial section showing the inner whorls with the suture line (0.95x).

(3) Ventral view showing the characteristic striae (0.95x).

Figure 4. *Eutrephoceras planoventer* (Stephenson, 1941). Specimen collected *ex situ* ? from the interval between -130 to -136.5 meters at La Campana Section (Fig. A.3). The fossiliferous interval lies within the transgressive (TST) deposits of the upper Cañón del Tule Formation.*

(4) Axial section showing the remarkable involving whorl (0.75x).

Figure 5. *Sphenodiscus intermedius* (Böse, 1927). Right lateral view showing the bulla in the upper part of the flank. Ammonite collected at La Campana Section (sample -50 LC, specimen a) from the highstand (HST) deposits of the upper Cañón del Tule Formation (0.9x).

*Both the transgressive (TST) and highstand (HST) deposits of the upper Cañón del Tule Formation (Fig. 3.2) contain *Coahuilites sheltoni* Böse and *C. cavinsi*, which are index ammonites of the lower part of the Upper Maastrichtian.

All specimens identified by Dr. Keith Young.

Plate 2

1

2

3

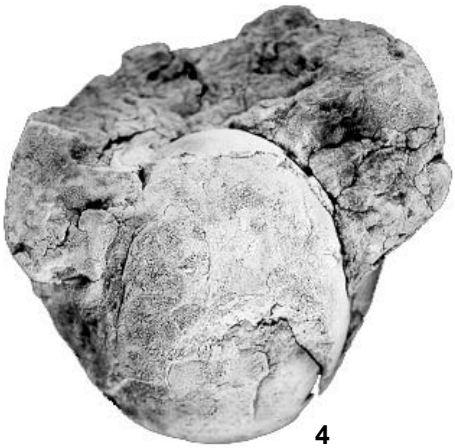

4

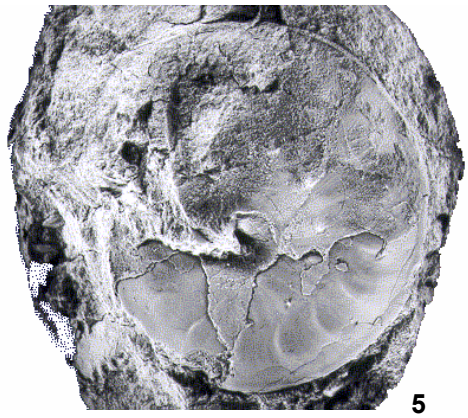

5

Plate 3

Ammonites

Upper Cañón del Tule Formation

Figure 1-2. *Sphenodiscus intermedius* (Böse, 1927). Specimen from La Campana Section (Fig. A.3), sample labeled (-49.8 LC), collected from the highstand (HST) deposits of the upper Cañón del Tule Formation.*

(1) Ventral view. Natural size.

(2) Left lateral view. Natural size.

***Figure 3-4** *Coahuilites cavinsi* (Böse, 1927). Specimen collected *ex situ*? at La Campana Section (Fig. A3) from the interval between -130 and -142.5 meters. Specimen b labeled (-130/-142.5LC) from transgressive (TST) deposits of the upper Cañón del Tule Formation.*

(3) Ventral view partially showing the right lateral view (0.97X)

(4) Left lateral view (0.97X)

****Figure 5**. *Coahuilites sheltoni* (Böse, 1927). Collected at La Campana Section, sample -50LC, specimen b, from highstand (HST) deposits of the upper Cañón del Tule Formation.

(5) Left lateral view (0.95X)

* Identified by M. Sc. Ma. Eugenia Gómez. According to Cobban and Kennedy (1995), *Coahuilites sheltoni* and *C. cavinsi* are synonymous of the same individual. They selected the unique name *sheltoni* for the species. *C. sheltoni* is restricted to the *Holploscaphites birkelundi* Zone, the lowermost zone of the Upper Maastrichtian (Cobban and Kennedy, 1995; Kennedy *et al*., 1996).

** Identified by Dra. Ana Bertha Villaseñor.

Plate 3

1

3

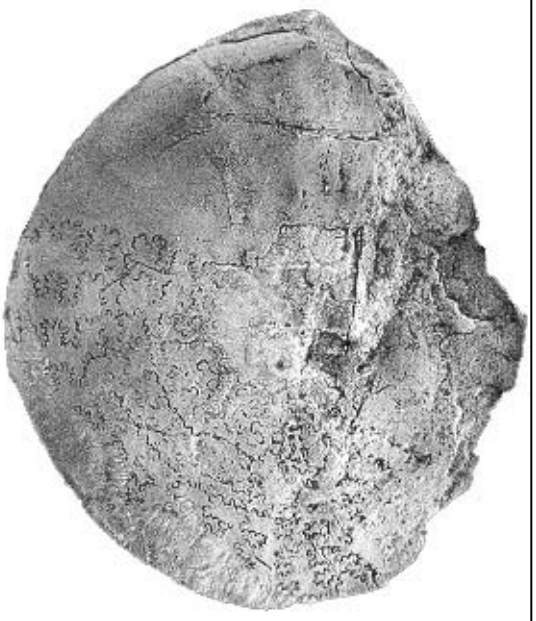

2

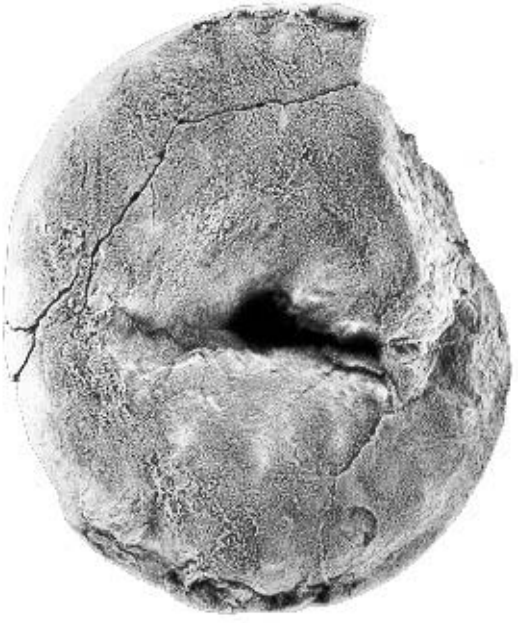

4

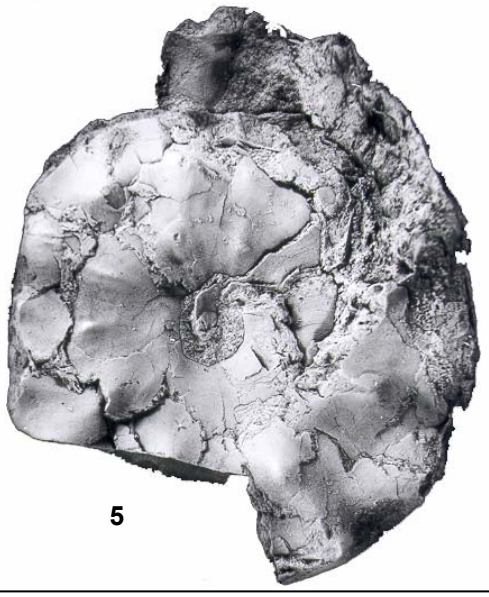

5

Plate 4

Bivalves and Ammonites

Lower Cerro Grande Formation

Figure 1. *Exogyra* sp. Sample labeled (LC+254).

(1-2) Left valve (0.55 X)

*__Figure 2-3__. *Sphenodiscus* sp. Sample labeled (LC+267.5).

(3) Left lateral view (0.75 X)

(4) Ventral view (0.75X)

The illustrated fossils were collected from highstand (HST) deposits of the lower Cerro Grande Formation (La Campana Section, Fig. A.3).

*Specimen identified by Dra. Ana Bertha Villaseñor. *Sphenodiscus* sp has a stratigraphic distribution that includes the Upper Campanian to Maastrichtian (A. Villaseñor, personal comm., 2001)

Plate 4

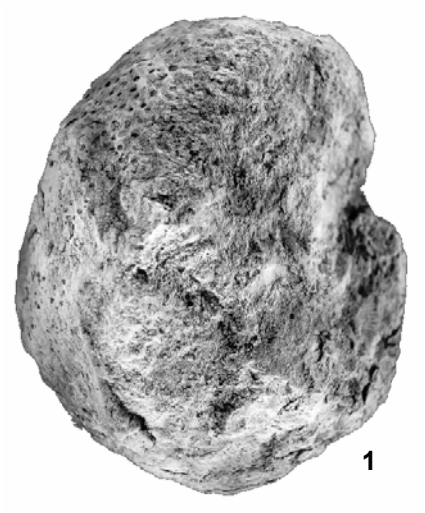

1

2

3

Plate 5

Bivalves and Gastropods

Upper Cañón del Tule Formation

Figure 1. *Veniella* sp. Left valve, (0.75X). Collected where the dirt road from San Miguel to La Campana crosses an unnamed creek, nearby San Miguel village, Coahuila.

Figure 2. *Trachycardium* sp. Left valve, (0.75X). Sample -50 LC, La Campana Section.

Figure 3-4. *Exogyra costata* Say. Left valves (0.75X). La Campana Section (Fig. A.3). Both specimens collected from the fossiliferous horizon (-152.5 LC)

Figures 5-6. *Stantonella* sp. (0.75X). Sample -62 LC, La Campana Section.

Specimens 1,2,5 and 6 collected from highstand (HST) deposits of the upper Cañón del Tule Formation. Specimens 3 and 4 from the underlying transgressive (TST) deposits of the same formation.

The author of this dissertation is sincerely grateful to Dr. Francisco Vega Vera and Biol. Roberto Cozátl (Instituto de Geología, UNAM) for the identification and illustration of the fossil material shown in Plates 5-6. The illustrated specimens are housed in the museum of that institution in Ciudad Universitaria, México, D.F.

Plate 5

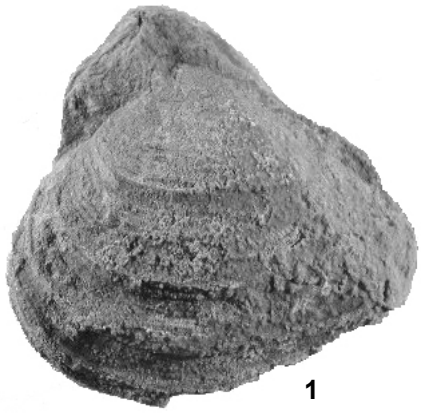

1

3

2

4

6

5

Plate 6

Bivalves and Gastropods

Upper Cañón del Tule Formation

Figure 1-2. *Pholadomya occidentalis* Morton.

(1) Left valve (0.75X)

(2) Right valve (0.75X). Sample -51 LC, La Campana Section.

Figure 3.- *Pholadomya* sp. Left valve (0.75X), sample (-51LC).

Figure 4.- *Trachycardium eufaulense* (Conrad). Right valve (0.75X), sample (139-8 LC).

Figure 5-6. *Periplomya sulcatina* (Shumard).

(5) Left valve (0.75X)

(6) Right valve (0.75X). La Campana Section, sample(-139.8 LC),

Specimens 1-3 collected from highstand (HST) deposits of the upper Cañón del Tule Formation. Specimens 4-6 from the underlying transgressive (TST) deposits of the same formation.

Plate 6

1

2

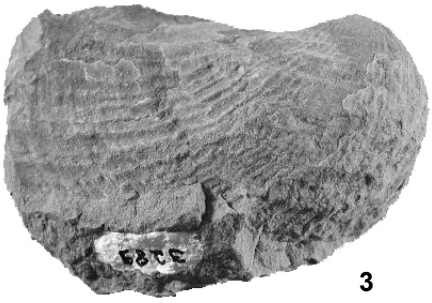

3

4

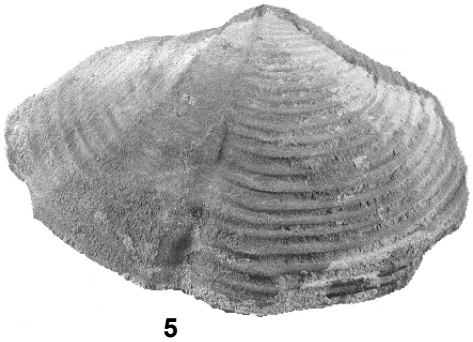

5

6

Plate 7

Charophyte Gyrogonites

Las Imágenes Formation

The left column in this plate shows apical views of charophyte gyrogonites. Note the different shaped rosettes: (**1**) shows a five-element drop-shaped rosette whose "petals" are divided by deep and straight divisions. The rosette appears to be isolated from the outer spirals by deep furrows. (**4**) shows also a five-element rosette whose fan-shaped "petals" are wider in the central area and progressively narrower toward the periphery. The rosette elements appears to be separated and isolated from the forming spirals. Specimen in (**7**) also shows a fan- five-element rosette whose "petals" are completely isolated from the outer spirals by deep furrows. Note also the concave spirals better exposed in lateral view (**8**). Illustration in (**10**) shows a specimen in which the rosette elements are an extension of the outer spirals. Note the ellipsoidaly-shaped outer periphery.

The middle column displays lateral views of charophyte gyrogonites. Note the prominent rosettes in specimens (**2**) and (**5**) in contrast to specimens less prominent in (**8**) and (**11**) and the angle of inclination of spirals, highest in the specimen (**2**).

The basal views on the right column show invariably five left-coiled spirals. Note the ovoidal periphery of the specimen (**9**) and the remarkable concave spirals in the specimen (**12**).

(**1-3**) specimens have not been found so far reported in the available literature. It is here informally named "*Platychara? rectirosetta*" due to its straight drop-shaped petals. (**4-6**) views absolutely resemble the *Platychara perlata* species described and illustrated by Peck and Forester (1979, Plate II, Figures 5, 7-8) from a sample collected from an "unnamed upper Cretaceous unit in Coahuila, Mexico". (**7-9**) resembles *Platychara compressa* according to the description provided by Peck and Forester (1979). The forms in (**10-12**) are referred here also provisionally and informally as *Platychara? obesa* by its particular thick spirals and size and since also appears to be a new species. Tappan (1980) suggests that, depending on the degree of the calcification attained, the spirals may be concave, smooth, or convex, resulting in a variety of apparent surface characteristic and wall thickness. Therefore, the concave or convex spirals nature might depend on seasonal changes in the calcium carbonate content in the aqueous environment in which the charophyte lives. The red bar on the plate defines the scale for all the specimens.

The charophyte gyrogonites shown in this plate were obtained of samples collected from the Early TST coastal plain deposits of the upper Las Imágenes Formation. Charophyte-bearing interval at El Potrero Section (Fig. A.8), sample -15.5 EP.

The SEM pothographs of the charophyte gyrogonites were made at the Laboratorio de Petrografía y Diagénes, Instituto Mexicano del Petróleo, with the kind support and technical assistance of Marcela Ugarte to whom the author is deeply grateful.

Plate 7

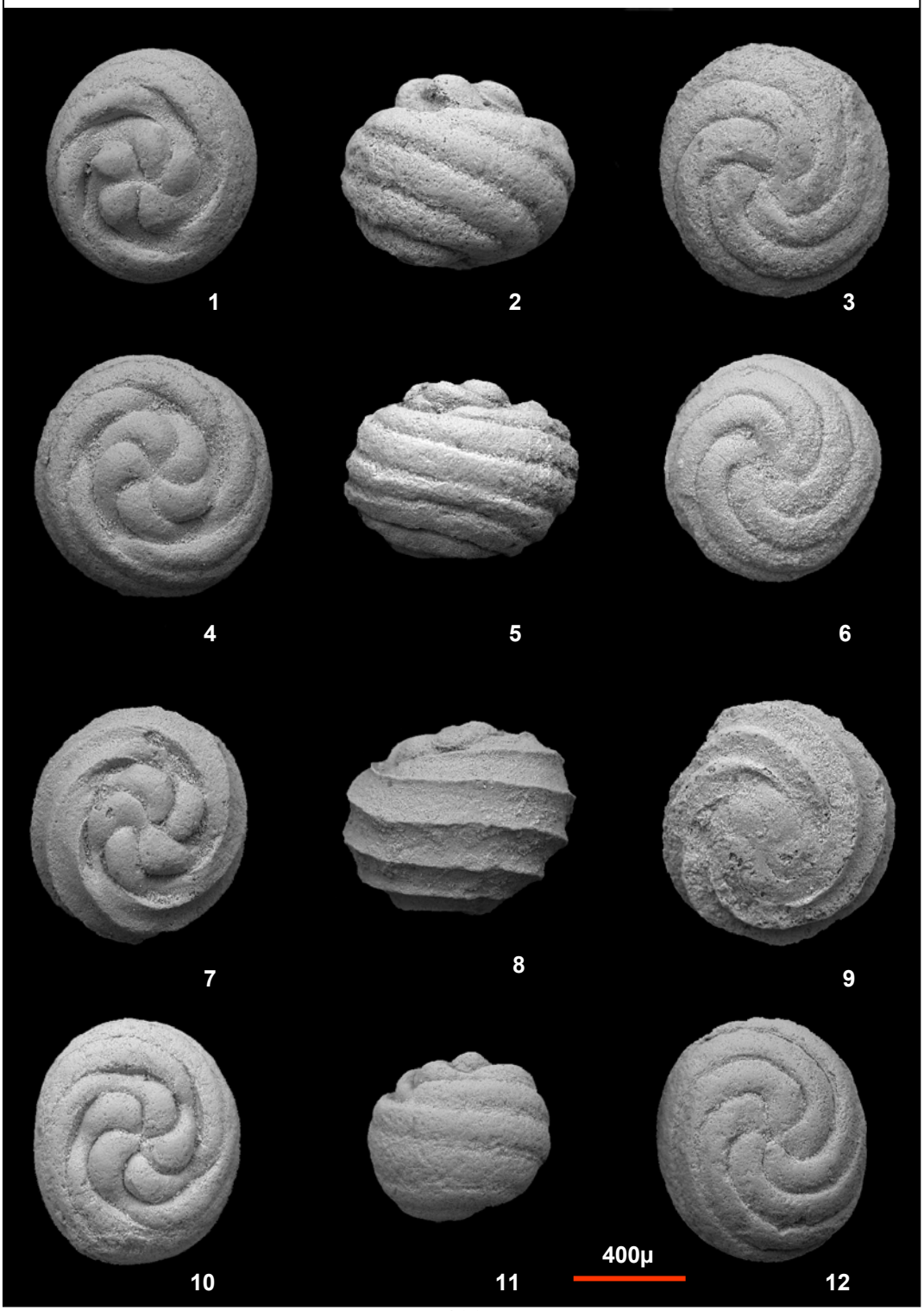

Plate 8

Charophyte Gyrogonites

Las Imágenes Formation

(**1-3**) within the entire assemblage gyrogonites of El Potrero Section (sample -15.5 EP) most of the specimens display five-element rosettes on apical views with only one remarkable and rare exception of a gyrogonite with a six-element rosette. Wheter this gyrogonite is a new genus or species or it is simply a rare and aberrant form is not yet clear at this moment. What it is too clear is that El Potrero charophyte population needs an statistical and formal description following the established nomenclature codes. The six-petalum rossete specimen is here informally named *Platychara? chicoase.* "Chicoase" is the given name to the number six in the ancient Náhuatl Mexican language. In honor to the ancient mexicans we would like to this name be preserved in any formal description in the future. (**3**) shows a detail of the six-element rossete of the same specimen showed in (**1**) and (**2**). The horizontal rosette´s diameter is 480µ wide.

(**4-6**) show a gyrogonite with a flat summit and not prominent rossette with deep furrows on apical view (**4**). It slighly resembles in apical view to the *Platychara grambastii* specimen illustrated by Kumar and Grambast-Fessard (1984, Plate 1, Fig. 6); the lateral view on (**5**) shows six concave spirals bounded by prominent ridges. (**6**) also displays five spirals on the basal view. The three views are from different specimens with the same morphological features. No basal pore or plate was observed in any sub-spherical to ovoidal form within the entire El Potrero assemblage.

(**7-9**) show respectively apical, lateral, and basal views of three different specimens of *Porochara* sp. (**7**) shows five left-coiled spirals and a pore; (**8**) an ellipsoidal individual with nine flat to slighly convex spirals on lateral view; and five spirals and pore on basal view (**9**). The external outline displayed by the specimen in (**9**) highly resembles the specimen showed in the Plate 10, Figure 4. This latter might be a non complete axial section of the specimen that does not cut exactly the basal pore.

(**10-11**) views were taken from the same specimen, the bigger one found from the entire El Potrero assemblage. (**10**) displays six concave spirals and a rounded external periphery without or with an obstructed apical pore. (**11**) shows nine concave spirals which extend to the summit forming slighly prominent tips. Specimen not yet identified.

(**12**) shows the lateral view of an ellipsoidal gyrogonite with eight concave spirals bounded by prominent ridges which extend to the summit forming prominent tips instead of "petals". Note the apical pore slighly visible on lateral view. It is not clear if the basal pore is sealed by calcitic material or is absent. *Porochara*? sp.

The red bar on the plate defines the scale for all the specimens except for the detail in (**3**).

The charophyte gyrogonites shown in this plate were obtained of samples collected from the Early TST coastal plain deposits of the upper Las Imágenes Formation, within the charophyte-bearing interval (El Potrero Section, Fig. A.8).

Plate 8

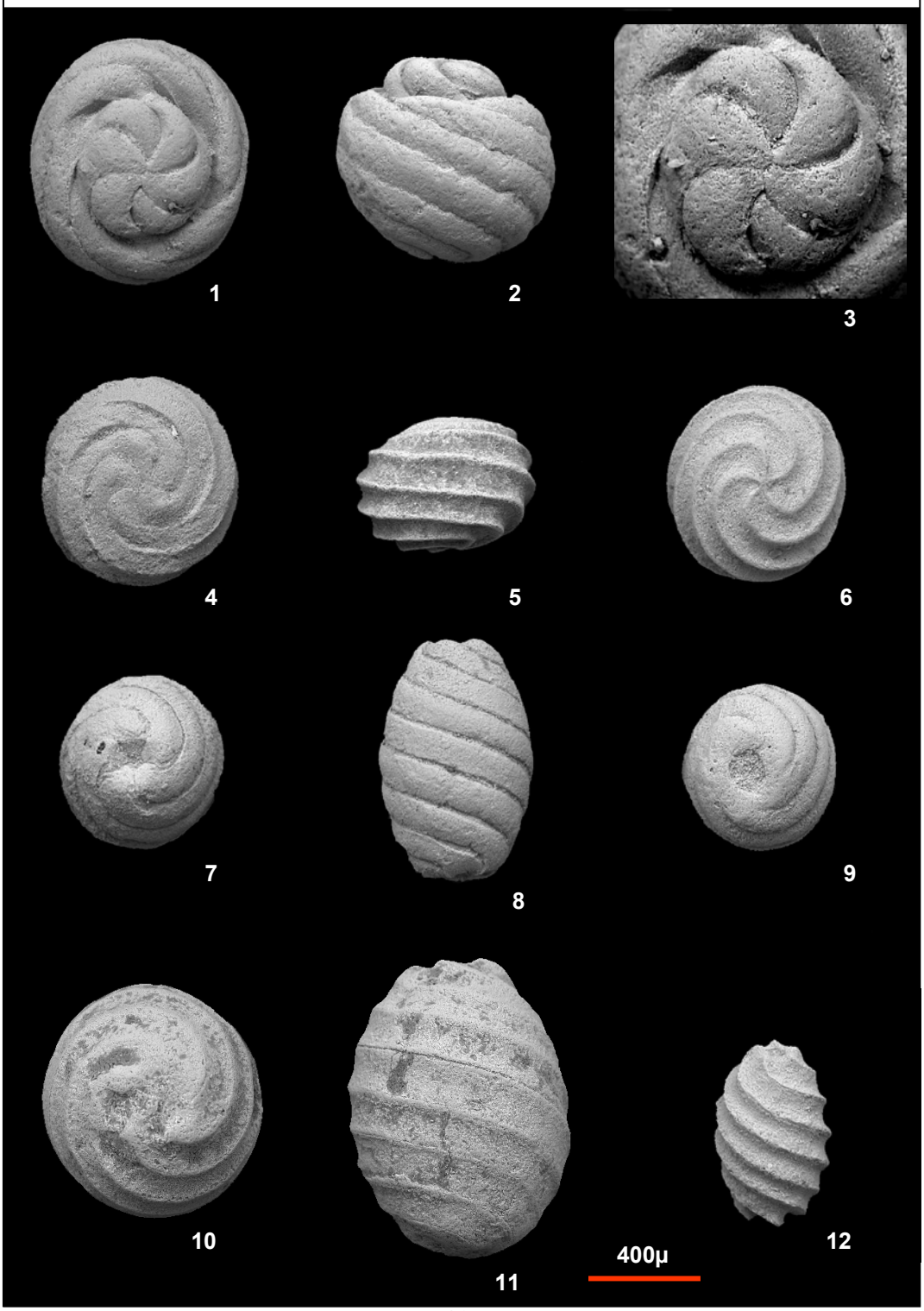

Plate 9

Charophyte Gyrogonites in Thin Section.

Las Imágenes Formation

(**1**) shows several charophyte gyrogonites randomly sectioned whose interior is filled with clear crystals of calcite. (**2**) shows the mineral components of the charophyte-containing muddy rock composed mainly by silt-size fragments of angular quartz (Qz), plagioclase (Pl) and chert (Ch) embedded in a pervasive clay matrix and calcite cement (Ca). (**3, 5, 7**) show axially sectioned gyrogonites whose wall has the aspect of a continuous arrangement of trapezoidal "bricks". The equatorial sections (**4,6**) cut just one spiral producing the ring-shaped form clearly defined in (**4**). The picture in (**8**) shows a detail of the gyrogonite wall composed of the trapezoidal-shaped "bricks" which in reality are the calcified spirals seen in section. The calcification process of the gyrogonite wall occurs in the living charophyte and consists of adding of alternated layers of organic material and laminar calcite (Tappan, 1980).

All the photographs were taken in crossed nicols using a blue filter. The charophyte gyrogonites shown in this plate were obtained of samples collected from the Early TST coastal plain deposits of the upper Las Imágenes Formation, within the charophyte-bearing interval (La Florida Section, Fig. A.6, sample LF+31).

Plate 9

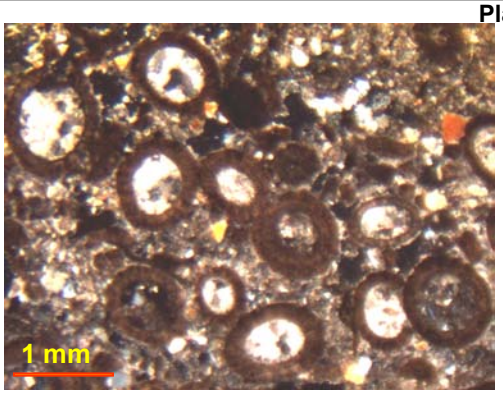

1

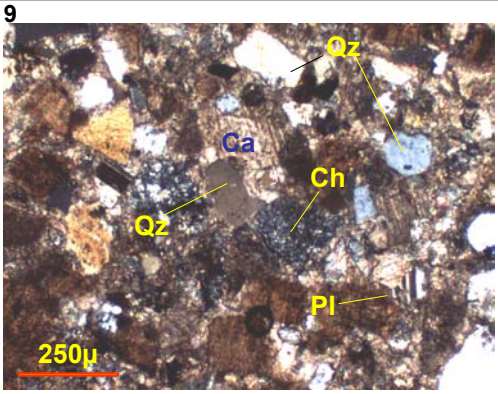

2

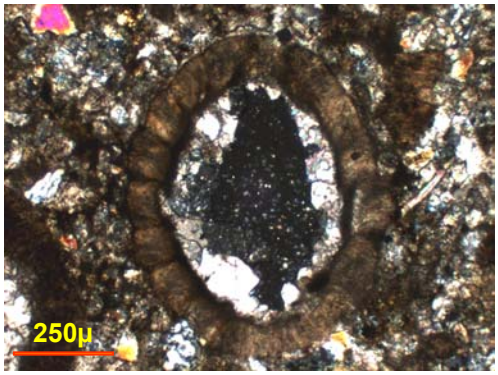

3

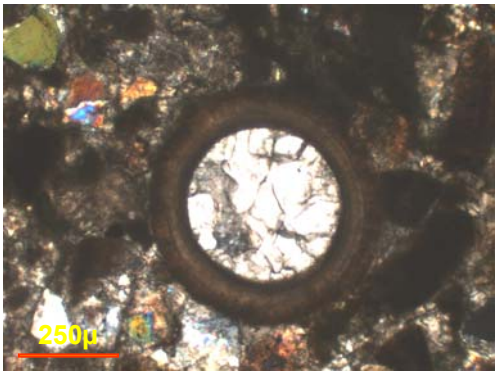

4

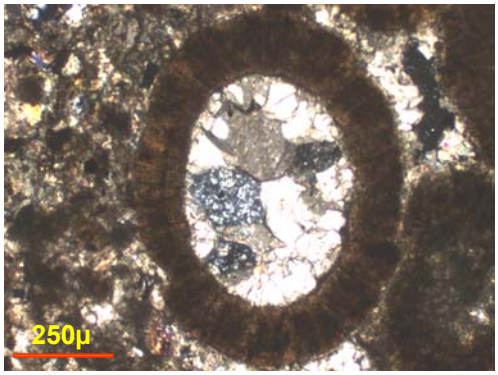

5

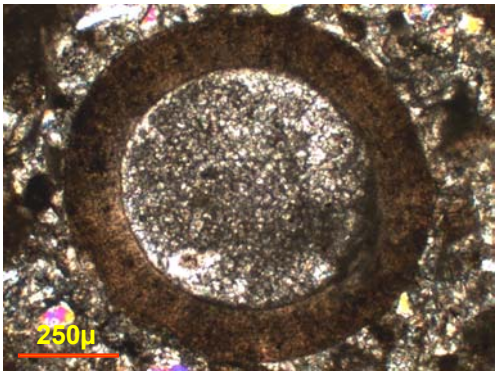

6

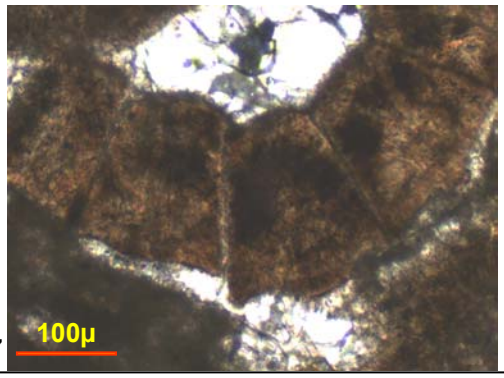

7

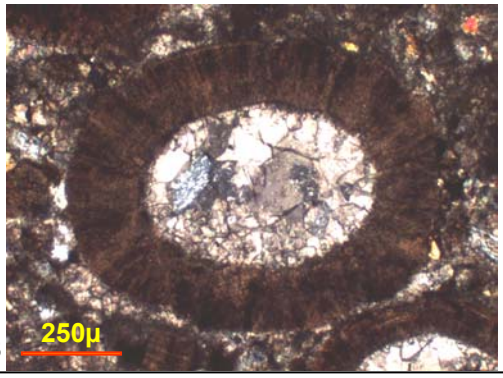

8

Plate 10

Charophyte Gyrogonites in Thin Section.
Las Imágenes Formation

(**1-8**) Differently oriented sections of gyrogonites of variable shape. The hard pelitic charophyte-bearing horizon is overlaid by an intensively burrowed light brown mudstone, encased within red and purple mudstone. The same fossiliferous horizon overlies a 9 meter-thick sharp-based shallow marine sandstone interpreted to be upper shoreface to foreshore? deposits (see Fig. A.4).

The charophyte gyrogonites are associated in the studied sample to thin-shelled ostracods (**1**) and benthonic foraminifers (**2,6**). An axial spherical section of a gyrogonite with its interior cemented by clear crystals of calcite is shown in (**3**). Note that this excellently preserved specimen displays an upper pore; the calcified spirals of its wall are defined by trapezoidal segments individually formed by alternated layers of organic material and laminar calcite. (**4**) shows an axial section of a ellipsoidally-shaped specimen with an upper pore which resembles the three dimensional specimen shown in the Figure 8, Plate 7, from the El Potrero Section, located 15.6 Km northwest of La Casita Section. One can imagine the orientation of the gyrogonite section by looking at the three dimensional forms illustrated in Plates 6 and 7. (**5**) shows a gyrogonite with a basal extension and slightly prominent summit whose interior is also cemented by calcite. Specimen (**7**) similar to the previous one has also an extension at its basal region but has a thinner wall and concave spirals. (**8**) only shows a gyrogonite of different shape than others surrounded by pelitic dark sediment.

All the pictures were taken with a soft blue filter in crossed nicols, except (**1**), (**2**) and (**6**) in parallel nicols.

The charophyte gyrogonites shown in this plate were obtained of samples collected from the Early TST coastal plain deposits of the upper Las Imágenes Formation, within the charophyte-bearing interval (La Casita Section, sample SLC+13; Fig. A.4).

Discussion

The association of charophytes, benthonic foraminifers, and thin-shelled ostracods (see the Plate 11), as well as and the intense biogenic activity in the charophyte-bearing horizon, suggest a quiet, muddy, brackish water depositional environment (i.e., lagoon). The benthonic foraminifers clearly indicate marine influence.

Plate 10

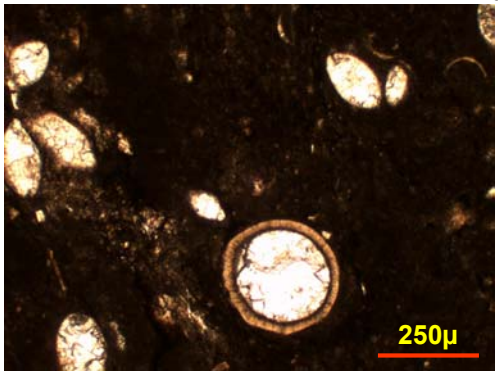

1

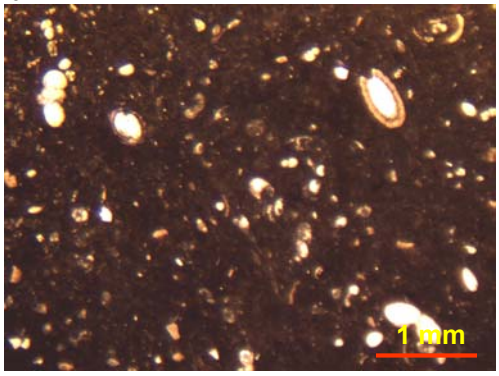

2

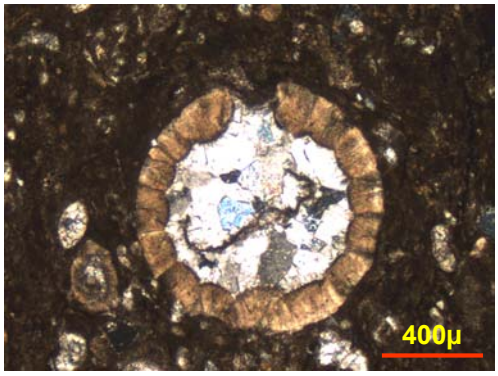

3

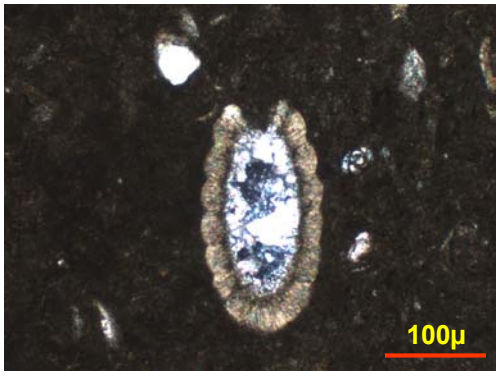

4

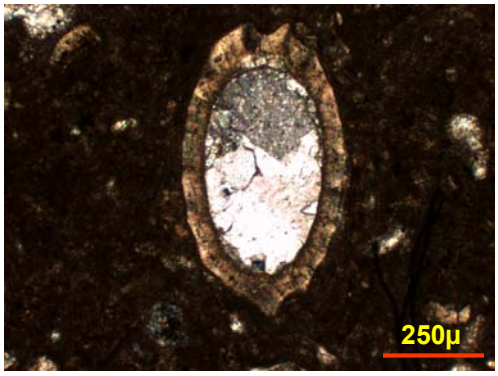

5

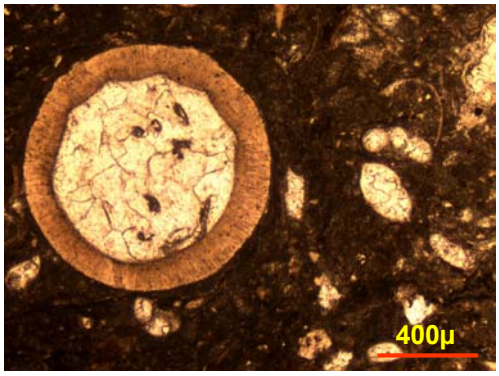

6

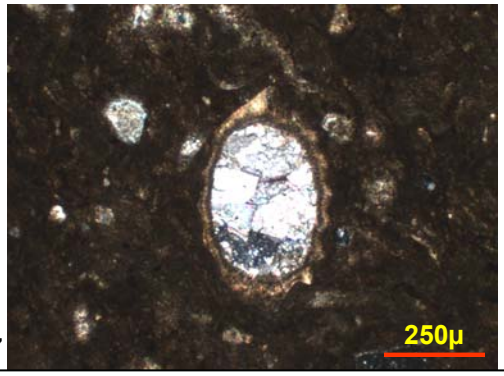

7

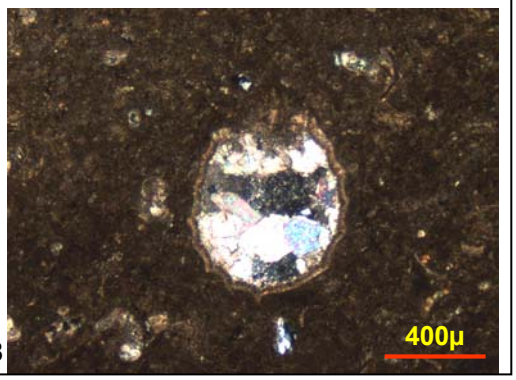

8

Plate 11

Benthonic Foraminifers and Ostracods in Thin Section
Las Imágenes Formation

Photographs (**1-8**) illustrate details of the foraminiferal assemblage and ostracods associated to the diverse charophyte gyrogonites population. (**1**) shows several unidentified thin-walled axial sections of benthonic foraminifers, one of them is detailed in (**3**). Four axial sections of unidentified benthonic foraminifers appear in the photograph (**2**). Observe in details (**4**) and (**6**) that the two valves of two different delicate ostracods specimens remained together, which suggest their shells were not subject to high-energy water conditions. (**5**) show an axial section of an unidentified benthonic foram of spherical chambers, triangular- to trapezoidally-shaped in (**7**). Observe in the upper middle area of the specimen the juvenile initial globular chambers. The picture in (**8**) shows an equatorial section of a left-coiled foram specimen viewed on its spiral side. Note also the initial juvenile chambers on its right side.

All the pictures were taken with a soft blue filter in parallel nicols, except (**1,3,5**) in crossed nicols.

The microfossils shown in this plate were obtained of samples collected from the Early TST coastal plain deposits of the upper Las Imágenes Formation, within the charophyte-bearing interval (La Casita Section, sample SLC+13; Fig. A.4).

Discussion

Paleontologist Victoria Gómez, expert in Upper Cretaceous planktonic foraminifers, carefully observed in thin section the foraminiferal assemblage shown in this plate. She concluded have not been found any Maastrichtian planktonic foraminifera and that no one of the fossil forms even resemble the well-known and characteristic index planktonic Upper Cretaceous foraminifera. Her observations made us conclude that some of the forms we initially thought might be planktonic, are in reality unidentified benthonic forms which deserve a formal and detailed study.

Mrs. Gómez works at the Escuela de Ciencias de la Tierra (Earth Sciences School) of the Instituto Politécnico Nacional (IPN) at México City. The author appreciates her interest and willingness to review the thin-sectioned material.

Plate 11

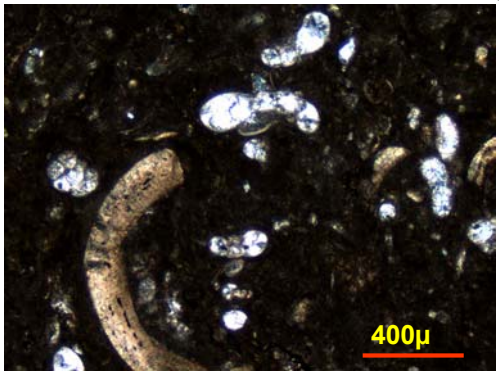

1

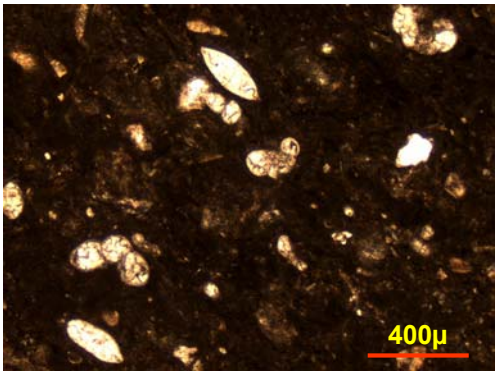

2

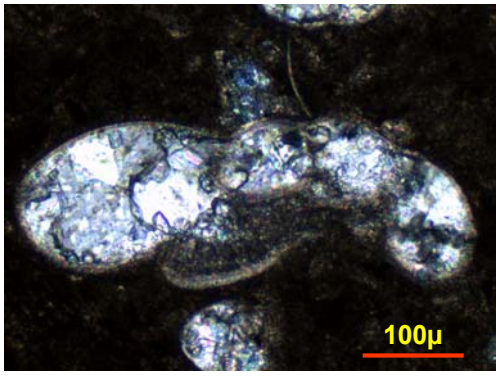

3

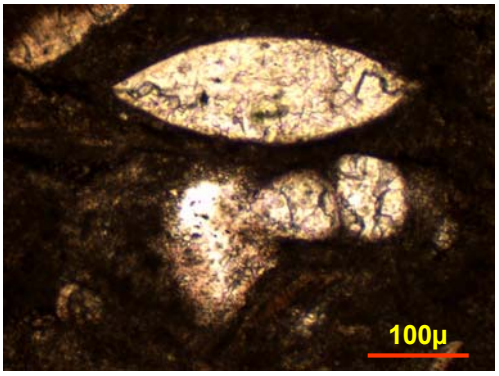

4

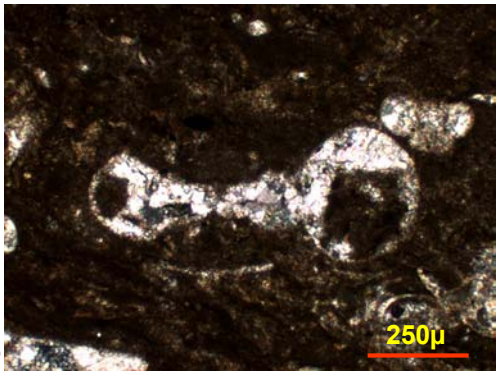

5

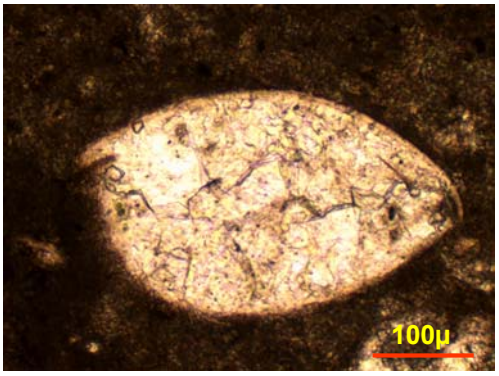

6

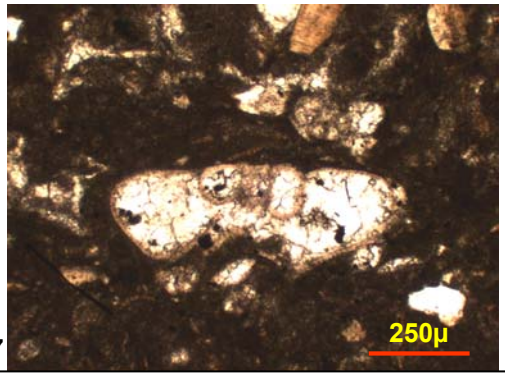

7

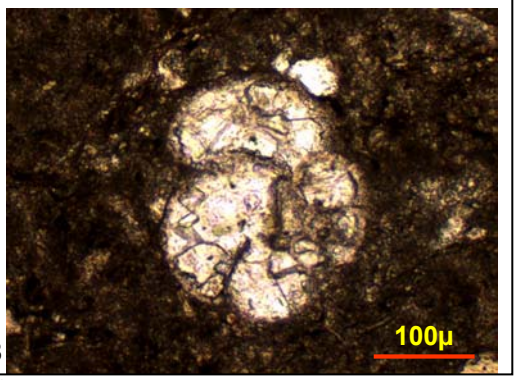

8

Plate 12

Benthonic Foraminifers and Diverse
Microfossils in Thin Section.
Upper Cañón del Tule Formation

(**1**) small gastropods and diverse shell debris material within a gray silty mudstone. Most of the silt grains are subangular quartz fragments but some volcanic rock fragments can be distinguished in (**2**). An equatorial section (right) and an axial section (left) of two benthonic foraminifera are shown in (**3**) and one of them detailed in (**5**). Axial sections of benthonic foraminifers are also shown in (**4**) and a benthonic foraminifer with a biserial chamber arrangement in (**7**). Note that in all the cases the foraminifera chamber interior is partially or completely hematitized. (**6**) and (**8**) illustrate two different specimens of ostracods. The sample was collected from the highstand (HST) deposits of upper Cañón del Tule Formation (La Florida Section, Fig. A.6, sample -5.6LF).

Plate 12

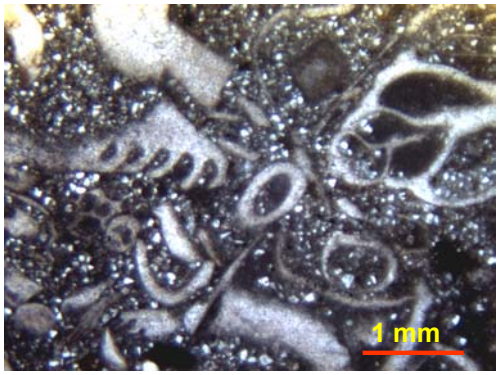

1

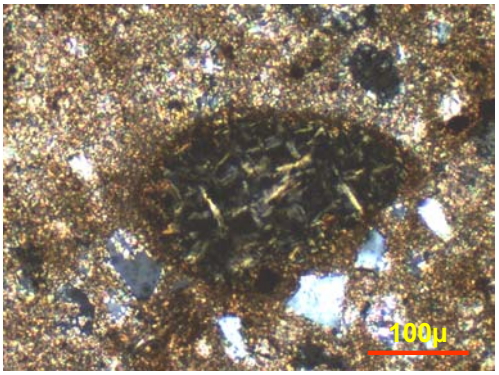

2

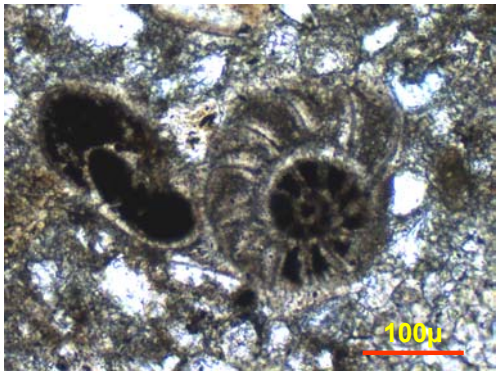

3

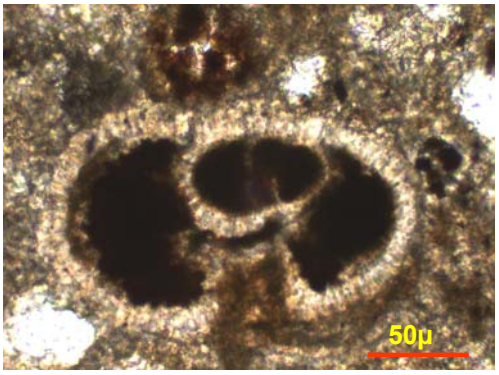

4

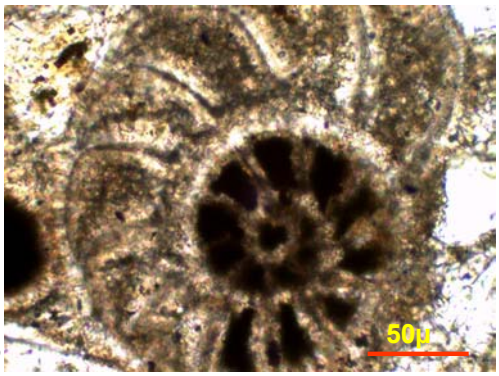

5

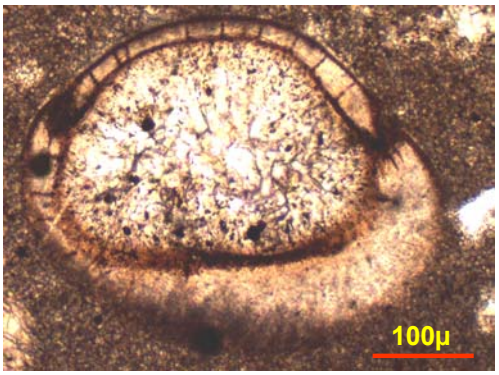

6

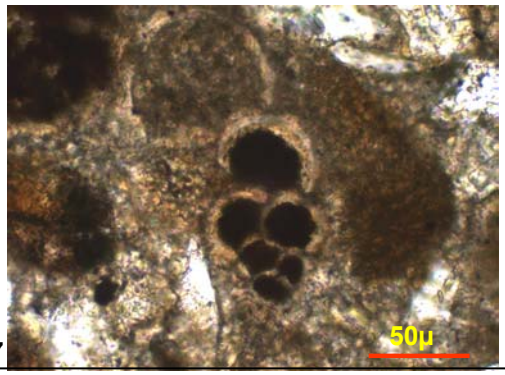

7

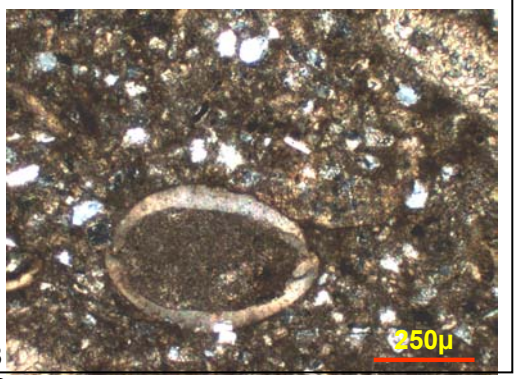

8

Plate 13

Rock and Fossil Fragments
Las Imágenes Formation

All the pictures were taken from a thin section of a fine to medium-grained red sandstone interbedded with channel-fill and sheet sandstone of the Early TST coastal plain red deposits of the upper Las Imagenes Formation (see Fig. A.9). The abundant fragments of rotalid-type benthonic foraminifera (**1,2,6,7**) and echinoderm plates (**3**) clearly suggest marine influence. The upward-coarsening grain size trend, the abundance of plant fragments, and current ripples, suggest deposition within a strand plain (?). Field observations showed that this sandstone deposits (Fig. A.9, horizon PC+68) are several kilometers long and wide, and about 10 m thick. Their remakable extension and content of marine fossils suggest that these sheets of sandstone were deposited under the influence of longshore currents and waves that redistributed the sediments supplied by streams along the coastline. The sandstone framework is mainly composed of angular fragments of quartz, sedimentary rock fragments with foraminifers (**5, 8**), and volcanic rock fragments (**4**). See the Plate 15 for more petrographic information.

All the photographs were taken with a soft blue filter in parallel nicols, except (**1**) in crossed nicols. The material shown in this plate was obtained from the Puerto La Cuesta Section, Fig. A.9; sample PC+68).

Plate 13

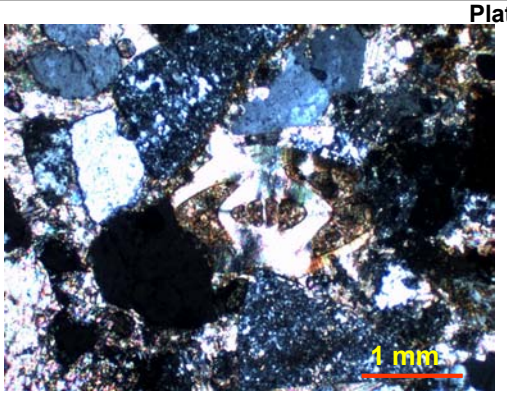

1

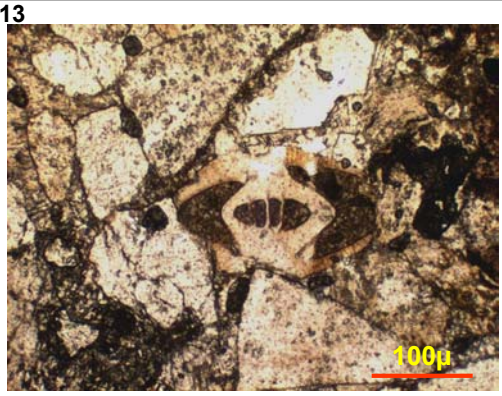

2

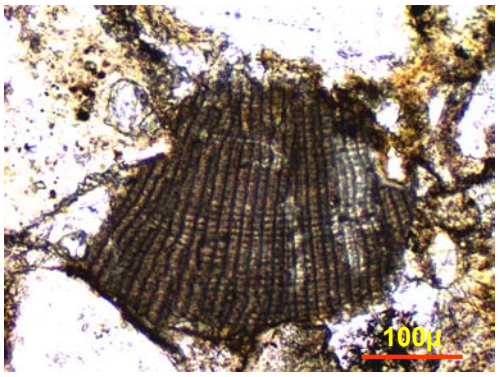

3

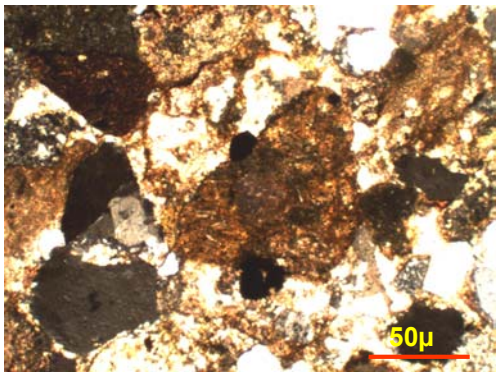

4

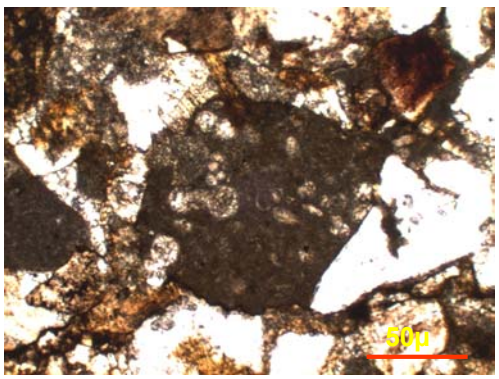

5

6

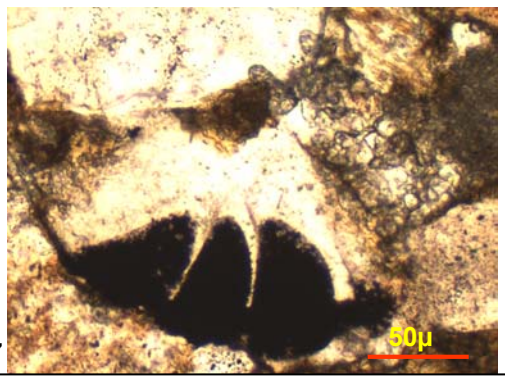

7

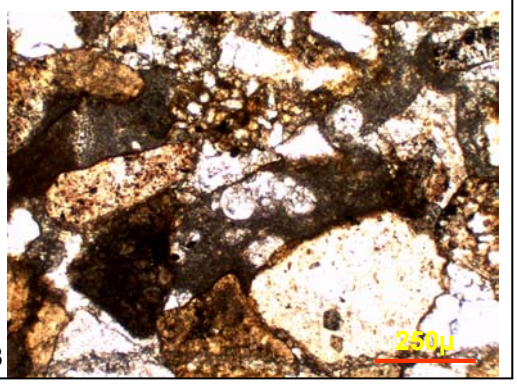

8

Plate 14

Benthonic Foraminifers and Diverse
Microfossils in Thin Section
Lower Cerro Grande Formation

Photograph (**1**) shows an ecuatorial section and (**2-4**) axial sections of rotaliform benthic forams of the Superfamily *Rotaliacea* Ehrenberg (1939). The thin-shelled specimens of low trochospire and pectinated wall are characteristic features of the Family *Calcarinidae* Schwager (1876), whose primitive forms appeard in the late Santonian-Campanian and evolved to more complex forms in the Maastrichtian. The sections (**2-3**) probably represent new species of calcarinid forams not yet described in literature (M. Aguilar, written comm.). Caus and Serra Kiel (1992) point out that the fossil siderolites, whose structure is analogous to the living calcarinids, occur in high-energy and shallow marine environments. Photograph (**5**) shows the embrionary chambers of a benthic foram.
Photograph (**6**) illustrates an axial section of a rotalid benthic foram. The section possibly represents a specimen not yet described of the genus *Pararotalia*. The benthic forams illustrated in this plate need to be studied in detail. Only a morphological study and comparison with European forms, currently more studied, might determine if some of these are new species and contribute to the knowledge of their stratigrahic distribution (M. Aguilar, written comm.).
The circular and radial structure shown in (**7**) is a transversal section of a echinoderm spicule, (**8**) shows two longitudinal sections.

All the pictures taken in parallel nicols except (**6**) in crossed nicols. The microfossils shown in this plate were observed in thin section of the sample LC+254 collected from the highstand (HST) deposits of the Cerro Grande Formation at La Campana Section (Fig. A.3).

Plate 14

1

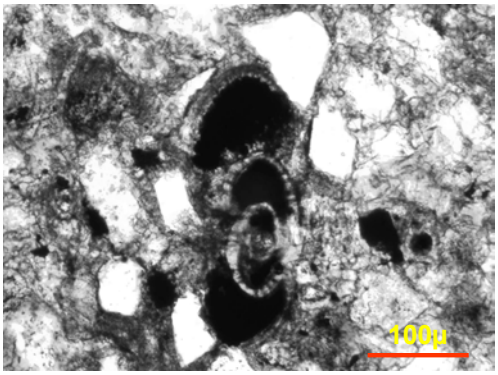

2

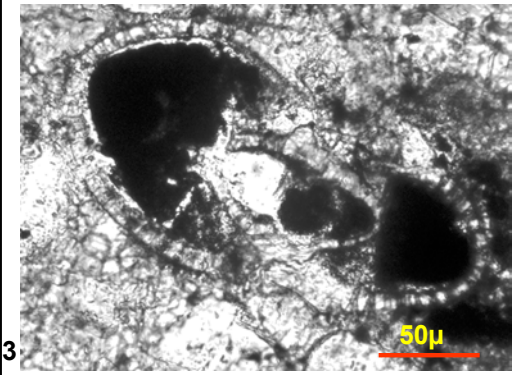

3

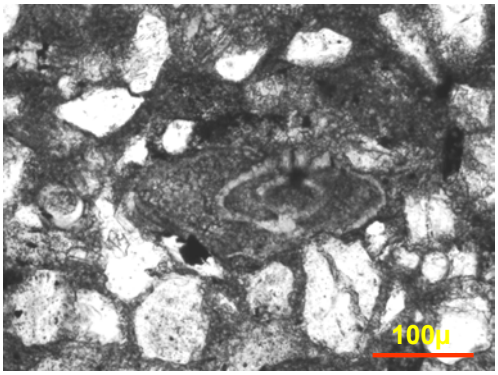

4

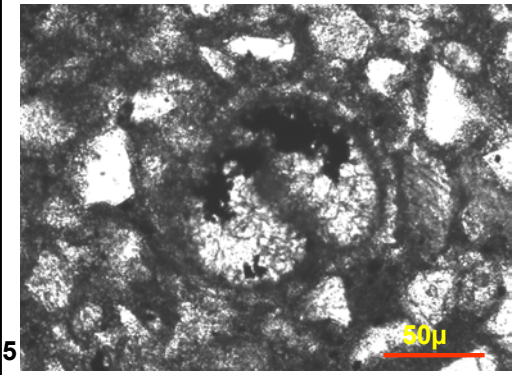

5

6

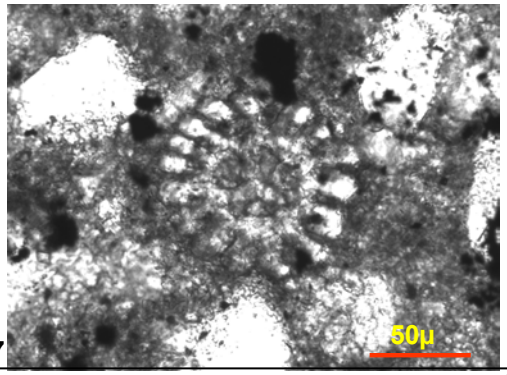

7

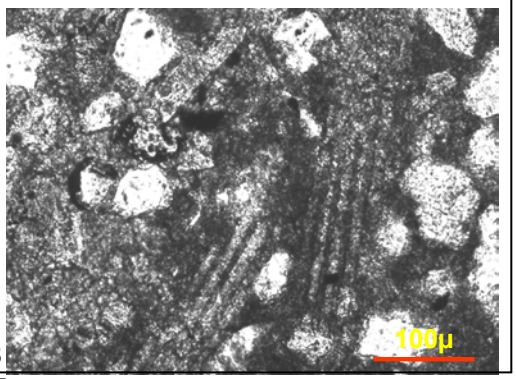

8

Plate 15

Petrographic Framework of Sandstones
Las Imágenes Formation

All the photographs taken from a fine to medium-grained red litharenite (Folk, 1968) composed by angular fragments of common quartz, rounded chert (**3**), volcanic (**4**) and sedimentary rock fragments. (**1**) shows a microcline fragment detailed in (**2**), angular quartz and chert. A volcanic rock fragment surrounded by calcite cement is shown in (**4**), and chalcedony in (**5**). Note the well-rounded quartz fragments of plutonic origin with quartz overgrowths in (**6-8**) and the tiny fluid inclusions in (**7**), detailed within the small square.
Microcline (**2**) is mainly of plutonic origin as other observed feldspars. Their occurrence suggest a plutonic source of sediments different to that one which provided the well rounded chert fragments since feldspars are in general weak and unstable components, from a survival point of view, more sensitive than quartz or chert (Pettijohn *et al*., 1987). Boggs (2001) suggests that small, rounded, highly weathered feldspar grains indicate a source of sediment supply of low relief and/or a warm, humid climate with a moderately intense chemical weathering. Most of the feldspar is destroyed by weathering where relief is low and rainfall high (Pettijohn *et al*., 1987). Therefore, a plutonic source of sediments other than the Sierra Madre Occidental suggested by McBride *et al*., (1975) must be somewhere in an unknown location.
The well rounded quartz fragment in (**6**) has a dark clay coating already hematized. Although the sandstone grains are cemented mostly by calcite, hematite coatings also cement the grains and provides the rock its typical pervasive red color (**8**).

All the pictures taken in crossed nicols except (**6**). (**8**) in parallel nicols and without any filter to remark the red coloration of the rock. The material shown in this plate was obtained from Early (TST) deposits of Las Imágenes Formation at the Puerto La Cuesta Section (Fig. A.9, sample PC+68).

Plate 15

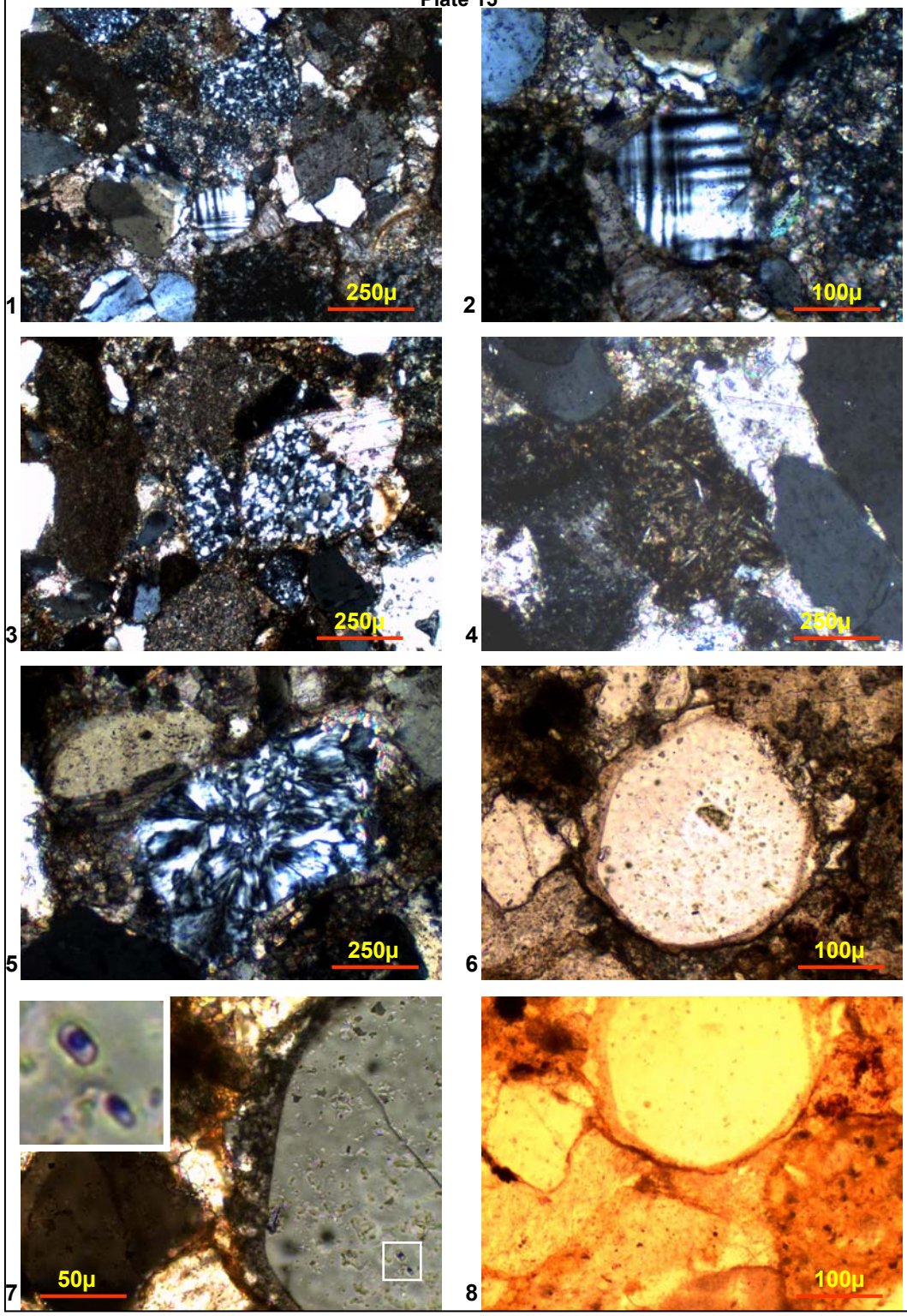

REFERENCES

Araujo, M. J., y Estavillo, G. C., 1985, Estudio estratigráfico sedimentológico del Cretácico Superior: Proyecto San Carlos, Chihuahua, Proyecto C-3000: Instituto Mexicano del Petróleo, unpublished technical report., 91 p., 50 pl.

Arney, J. W., 1998, Petrography and tectonic provenance analysis of late Cretaceous (Maastrichtian) Cañon del Tule-Muerto sandstones, Difunta Group, Parras-La Popa-South Sabinas basin, Nuevo León and Coahuila, Mexico: Masters thesis, University of Texas at Dallas, Richardson, Texas, 133 p.

Baker, R. A., III, 1970, Stratigraphy and sedimentology of the Cañon del Tule Formation (Upper Cretaceous), Parras Basin, NE Mexico: unpubl. Ph. D. dissertation, The University of Texas at Austin, Austin, Texas, 322 p.

Boggs, S. Jr., 2001, Principles of Sedimentology and Stratigraphy: Merrill Publishing Co., 3rd edition, 726 p.

Bornette, G., and Arens, M. F., 2002, Charophyte communities in cut-off river channels. The role of connectivity: Aquatic Botany 73, p. 149-162.

Böse, E., 1906, Excursion dans les environs de Monterrey et Saltillo: Internat. Geol. Cong., 10th sess., Mexico, Guide Excursion p. 29.

Böse, E., 1928, Cretaceous ammonites from Texas and northern Mexico: Univ. of Texas Bull. 2748, p. 143-312.

Burckhardt, C., 1930, Etude synthetique Sur le Mesozoique Mexican: Seconde Partie. Agh. Schweiz. Palaeon. Ges. Mem.; Soc. Paleon. Suisse, 50: 125-280.

Cobban, W. A. and Kennedy, W. J., 1995, Maastrichtian ammonites, chiefly from the Prairie Bluff Chalk in Alabama and Mississippi. Mem. Paleont. Soc. 44, 40 p., 23 figs.

Collison, J. D., and Thompson, D. B., 1989, Sedimentary Structures: Unwin Hyman, London, 2nd edition, 207 p.

Conrad, T. A., 1860, Description of new species of Cretaceous and Eocene fossils of Mississippi and Alabama: Acad. Nat. Sci. Philadelphia Jour., 2nd ser., v. 4, p. 275-298, pl. 46-47.

Crawley, R. A., 1975, Stratigraphy and Sedimentology of the Cerro Grande Formation (Upper Cretaceous), Parras Basin, Northeastern Mexico: Ph. D. dissertation, The University of Texas at Austin, Austin, Texas, 282 p.

Darley, W. M., 1991, Biología de las algas-enfoque fisiológico: LIMUSA, México, D.F., 236 p.

DeCelles, P. G., and Giles K. A., 1996, Foreland basin systems: Basin Research, v. 8, p. 105-123

Dickinson, W. R., 1981, Plate tectonic evolution of the southern Cordillera, in Dickinson, W.R., and Payne, W.D., (eds.), Relations of tectonics to ore deposits in the southern Cordillera: Arizona Geological Society Digest, v.14, p. 113-135.

Dillman, G. J., 1985, Structural investigation and tectonic history of the central Parras Basin, Saltillo, Coahuila, Mexico: Master thesis, University of Houston, Houston, Texas, 293 p.

Dillman, G. J., and Casey, J. F., 1985. Structural investigation and Tectonic history of east-central Parras Basin, Coahuila ., Mexico: AAPG Bull. v. 69, no. 9 (sept), p. 1419.

Dorsch, J., and Driese S. G., 1992, Marine red beds deposited in shoreface to inner offshore environments: The "Lower" Juniata formation of Southwestern Virginia. GSA Abstracts with programs, SE Section. v. 24, no. 2, p. 13.

Elliot, T., 1986, Siliciclastic shorelines. In: Sedimentary Environments and Facies, 2nd edn (ed. By H.G. Reading). Blackwell Scientific Publications, Oxford, p. 155-188.

Emery, D., and Myers, K. J., 1996. Sequence Stratigraphy: Blackwell Science Ltd, 297 p.

Feist, M., and Grambast-Fessard, N., 1991, The genus concept in Charophyta: evidence from Paleozoic to Recent: *In*: Riding, R. (ed.) Calcareous algae and stromatolites: Springer-Verlag, p. 189-203.

Freydier, C., Martinez, R. J., Lapierre, H. M., Tardy, and Coulon, C., 1996, The early Cretaceous Arperos oceanic Basin (Western Mexico). Geochemical evidence for a seismic ridge formed near spreading center: Tectonophysics, v. 259, p. 343-367.

Galloway, W. E. and Hobday, D. K., 1996, Terrigenous clastic depositional systems. Applications to fossil fuel and groundwater resources. Springer-Verlag Berlin Heidelberg ,New York, 2nd edition, 489 p.

Garrick, S. J., 1999, Petrography and tectonic provenance analysis of latest Cretaceous to early Tertiary Difunta Group sandstones, Delgado Syncline, Parras-La Popa Basins, northeast Mexico: Master thesis, University of Texas at Dallas, Richardson, Texas, 106 p.

Goldhammer, R. K., and Johnson, C. A., 2001, Middle Jurassic-Upper Cretaceous Paleogeographic evolution and sequence stratigraphic framework of the northwest Gulf of Mexico rim, *in* C. Bartolini, R.T. Buffler, and A. Cantú-Chapa, (eds.), The western Gulf of Mexico Basin: Tectonics, sedimentary basins, and petroleum systems: AAPG Memoir 75, p. 45-81.

Grambast, L., 1974, Phylogeny of the Charophyta: Taxon 23, 4:463-481.

Grambast, L. & Gutiérrez, L., 1977, Espèces nouvelles de Charophytes du Crétacé supérieur terminal de la province de Cuenca (Espagne): Paléobiologie Continentale, Montpellier, v. 8, n. 2, 34 p.,15 pl.

Hadley, D. F. & Elliot, T., 1993, The sequence-stratigraphic significance of erosive-based shoreface sequences in the Cretaceous Mesaverde Group of northwestern Colorado. *in* Posamentier, H.W., Summerhayes, C.P., Haq B.U. & Allen, G.P., (eds), Sequence stratigraphy and facies associations. International Association of Sedimentologists Special Publication, no. 18, Blackwell Scientific Publications, p. 521-535

Halik, N., 1998, Sequence stratigraphy of Upper Cretaceous (lower Maastrichtian) Cañon del Tule Formation, Difunta foreland basin, northeast Mexico: Ph. D. dissertation, University of Texas at Dallas, Richardson, Texas, 238 p.

Hampson, G. J., and Storms, J. E., 2003, Geomorphological and sequence stratigraphic variability in wave-dominated, shoreface-shelf parasequences: Sedimentology 50, p. 667-701

Hardenbol, J., Thierry, J., Farley, M. B., Jacquin, T. De Graciansky, P. C., and Vail, P. R., 1998, Cretaceous Sequence Chronostratigraphy, Chart 4, *in* De Graciansky, P. C., Hardenbol, J., Jacquin, Th., and Vail, P. R., (eds). Mesozoic and Cenozoic Sequence Stratigraphy of European Basin, SEPM Special Publication 60 on CD.

Hill, R. T., 1891, Preliminary notes on the topography and geology of Northern Mexico, southeast Texas, and New Mexico: Am. Geologist, v. 8, p. 133-141

Howard, J. D., Dorjes, J., Frey, R. W., Gadow, S., Hertweck, G., Reineck, H. E., and Wunderlich, F., 1972, Usable beach-to-offshore model for tide-dominated shoreline; Sapelo Island, Georgia: Meeting abstract, v. 56, no. 3 (March), p 629.

Hunt D. & Gawthorpe, R.L., (eds) 2000, Sedimentary Responses to Forced Regressions: Geological Society, London, Special Publication, 172, 383 p.

Imlay, R. W., 1936, Evolution of the Coahuila Peninsula, Mexico. Part IV, Geology of the western part of the Sierra de Parras: GSA Bulletin, v. 47, p. 1651-1652.

Imlay R. W., 1937, Stratigraphy and paleontology of the Upper Cretaceous beds along the eastern side of Laguna de Mayran, Coahuila, Mexico: GSA Bulletin, v. 48, p. 1785-1872, 26 pl.

Jagt, W. M., and Kennedy, W. J., 1994, Jeletzkites dorfi Landman & Waage 1993, a North American ammonoid marker from the lower Upper Maastrichtian of Belgium, and numerical age of tre Lower/Upper Maastrichtian boundary: N Jb. Geol. Paläont Mh., p. 239-245.

Jaillard, E., Capetta, H., Ellenberger, P., Feist, M., Grambast-Fessard, N., Lefranc, J.P. and Sige B., 1993, Sedimentology, palaeontology, biostratigraphy and correlation of the Late Cretaceous Vilquechico Group of southem Peru: Cretaceous Research, v.14, p. 623-661.

Jaillard, E., Feist, M., Grambast-Fessard, N., and Carlotto, V., 1994, Senonian-Paleocene charophyte succession of the Peruvian Andes: Cretaceous Research, v. 15, p. 445-456.

Johnson, J. H., 1961, Limestone-building algae and Algal Limestones: Johnson Publishing Co., Boulder, Colorado, 297 p.

Kennedy, W. J., Cobban, W. A., and Landman, N.H., 1996, The Maastrichtian ammonites *Coahuilites sheltoni* Böse, 1928, and *Sphenodiscus pleurisepta* (Conrad, 1857), from the uppermost Pierre Shale and basal Fox Hills Formation of Colorado and Wyoming: Am. Mus. Novitates 3186, 14 p.

Kennedy, W. J., Landman, N. H., Chistensen, W. K., Cobban, W. A., and Hancock, J.M., 1998, Marine connections in North America during the late Maastrichtian: paleogeographic and paleobiogeographic significance of *Jeletzkytes nebrascencis* Zone cephalopod fauna from the Elk Butte Member of the Pierre Shale, SE South Dakota and NE Nebraska: Cretaceous Reseach 19, p. 745-775.

King, C., A., 2000, rip current: The Dictionary of Physical Geography (3rd edition). David S.G. Thomas and Andrew Goudie (*ed*), Blackwell Publishers Ltd, 610 p.

Kumar, A. and Grambast-Fessard, N., 1984, Maastrichtian charophyte gyrogonites from Jamaica: Micropaleontology, v. 30, p 263-267.

Laudon, R. C., 1975, Stratigraphy and petrology of the Difunta Group La Popa and eastern Parras basin, northeastern Mexico: Ph.D. dissertation, The University of Texas at Austin, Austin, Texas, 249 p.

Lawton, T. F., Vega, J., Giles, K .A., and Rosales-Domínguez, C., 2001, Stratigraphy and origin of the La Popa Basin, Nuevo León and Coahuila, Mexico, *in* C. Bartolini, R.T. Buffler, and A. Cantú-Chapa, (eds.) The western Gulf of Mexico Basin: Tectonics, sedimentary basins, and petroleum systems: AAPG Memoir 75, p. 219-240.

Martín-Closas, C., Serra-Kiel, J., Busquets, P. and Ramos-Guerrero, E., 1999, New correlation between charophyte and larger foraminifera biozones (Middle Eocene, southeastern Pyrenees): Geobios, v. 32, p. 5-18.

Martín-Closas, C., 1999, Epiphytic overgrowth of charophyte thalli by stromatolite-like structures and fungi in the Lower Cretaceous of the Iberian Ranges (Spain): Aust. J. Bot., v. 47, p. 305-313.

McBride, E. F., Weidie, E., and Wolleben, J. A., 1971, Deltaic Origin of Difunta Group (Late Cretaceous to Paleocene), Parras Basin, Coahuila and Nuevo Leon, Mexico: AAPG Meeting abstract, Bull. 55, no. 2 (February), p. 352.

McBride, E.F., Weidie, A. E., and Wolleben, J.A., and Laudon, R.C., 1974, Stratigraphy and structure of the Parras and La Popa basins, northeastern Mexico: Geological Society of America Bulletin, v. 84, p. 1603-1622.

McBride, E. F., 1974, Significance of color in red, green, purple, olive, brown, and gray beds of Difunta Group, northeastern Mexico: Journal of Sedimentary Petrology, v. 44, no. 3. (September), p. 760-773.

McBride, E. F., Weidie, A. E., and Wolleben, J. A., 1975. Deltaic and associated deposits of Difunta Group (Late Cretaceous to Paleocene), Parras and La Popa basins, northeastern Mexico, in M.L.S. Broussard (ed) Deltas: Houston Geological Society, p. 485-522.

Mellere D., and Steel, R., 2000, Style contrast between forced regressive and lowstand/transgressive wedges in the Campanian of south-central

Wyoming (Hatfield Member of the Haystack Mountains Formation). *in* Hunt D. & Gawthorpe, R.L., (eds) 2000, Sedimentary Responses to Forced Regressions: Geological Society, London, Special Publication, 141-160 p.

Morton, S. G., 1834, Synopsis of the organic remains of the Cretaceous group of the United States: Philadelphia Key and Biddle, 88 p., 19 pl.

Murray, G. E., Wolleben J. A., and Boyd, D.R., 1959, Difunta strata of Tertiary age, Coahuila, Mexico: American Association of Petroleum Geologists Bulletin, v. 43, No 10, p. 2493-2495.

Murray, G. E., Weidie, Jr. A. E., Boyd, D. R., Forde, R. H. and Lewis, Jr. P. D., 1962, Formational divisions of Difunta Group, Parras Basin, Coahuila and Nuevo León, Mexico: AAPG Bulletin, v. 46, no 3, p. 374-383.

Nations, J. D., 1989, Cretaceous History of Northeastern and East-Central Arizona. I*n* Jenney, J.P., and Reynolds, S.J., 1989, Geologic evolution of Arizona: Tucson, Arizona Geological Society Digest 17, p. 435-446.

Peck, R. E., 1957, North American Mesozoic Charophyta: U.S. Geological Survey Professional Paper 294-A, 44 p., 8 pl.

Peck, R. E., and Reker, C. C., 1947, Cretaceous and Lower Cenozoic Charophyta from Peru: American Museum Novitates, no. 1369, 6 p., 1 pl.

Peck, R. E., and Forester, R. M., 1979, The Genus *Platychara* from the Western Hemisphere: Review of Paleobotany and Palinology, v. 28, p. 223-236, 2 pl.

Pemberton, S. G., Spila, M., Pulham, A. J., Saunders, T., MacEachern J. A., Robbins, and., Sinclair, D. I., 2001, Ichnology & Sedimentology of Shallow to Marginal Marine Systems; Ben Nevis & Avalon Reservoirs, Jeanne d'Arc Basin: Short Course Notes Volume 15, Geological Association of Canada, 343 p.

Pettijohn, F. J., Potter, P. E., Siever, R., 1987, Sand and Sandstone: Springer-Verlag, New York Inc, 2nd Edition, p. 553.

Plint, A. G., Walker, R. G., 1987, Morphology and Origin of an erosion surface cut into the bad heart formation during major sea-level change, santonian of west-central Alberta, Canada: Journal of Sedimentary Petrology, v. 57, n. 4, p. 639-650.

Plint, A. G., 1988, Sharp-based shoreface sequences and "offshore bars" in the Cardium Formation of Alberta: Their relathionship to relative changes in

sea level. In: Wilgus, C.K., Hastings, B. S. Kendall, C.G. St. C., Posamentier, H. W., Ross, C.A. & Van Wagoner, J. C. (eds) Sea Level Changes- An Integrated Approach: Society of Ecomomic Paleontologists and Mineralogists, Special Publications, 42, 357-370.

Plint, A. G. & Nummedal, D., 2000, The falling stage systems tracts: recognition and importance in sequence stratigraphic analysis, *in* Hunt, D. & Gawthorpe, R. L. (eds). Sedimentary Responses to Forced Regressions. Geological Society, London, Special Publications, 172, p. 19-46.

Posamentier, H. W., and Vail, P. R., 1988, Eustatic controls on clastic deposition II-Sequence and systems tract models, In C. K. Wilgus, B.S. Hastings, C.G. St. C. Kendall, H.W. Posamentier, C.A. Ross, and J. C. Van Wagoner, (eds.), Sea Level Changes: An Integrated Approach: SEPM Special Publication 42, p. 125-154.

Posamentier, H. W., Allen, G. P., James, D. P., and Tesson, M., 1992, Forced regressions in a sequence stratigraphic framework: concepts, examples, and exploration significance: AAPG Bulletin, v. 76, p 1687-1709. *In* Posamentier, H.W., C.P. Summerhayes, B.U. Haq & G.P. Allen, 1993, (eds), Sequence stratigraphy and facies associations. International Association of Sedimentologists Special Publication 18, Blackwell Scientific Publications, 644 p.

Posamentier, H. W., Allen, G. P., James, D. P and. Tesson, M., 1992. Forced regressions in a sequence stratigraphic framework: concepts, examples, and exploration significance: AAPG Bulletin, v. 76, p. 1687-1709.

Posamentier, H. W., and Allen, G. P., 1993, Siliciclastic sequence stratigraphic pattern in foreland ramp-type basins: Geology, v. 21, p. 455-458.

Posamentier, H. W., and Allen, G. P., 1999, Siliciclastic Sequence Stratigraphy-Concepts and Applications, SEPM Concepts in Sedimentology and Paleontology # 7, 210 p.

Posamentier, H. W., and Morris, W. R., 2000, Aspects of the stratal architecture of forced regressive deposits. *in* Hunt D. & Gawthorpe, R.L. (eds) 2000. Sedimentary Responses to Forced Regressions: Geological Society, London, Special Publication, p.19-46.

Riveline, J., Berger, J. P., Feist, M., Martín-Closas, C., Schudack, M. and Soulié-Märsche, I., 1996, European Mesozoic-Cenozoic Charophyte Zonation: Bull. Soc. Geol. France, t. 167, n. 3, p. 453-468.

Rodriguez, A. B., Fassell, M. L. Anderson J. B., 2001, Variations in shoreface progradiation and ravinement along the Texas coast, Gulf of Mexico: Sedimentology 48, p. 837-853.

Say, T., 1820, Species of the zoophytes, etc., principally fossil: Am. Jour. Sci., 1st. ser., v. 2, p. 34-45.

Schudack, M. and Herbig, H. G., 1995, Charophytes from Cretaceous-Tertiary boundary beds in the Middle Atlas Mountains, Morocco: Géologie Méditerranéenne, Marseille, v. 22, p. 125-139.

Selley R. C., 2000, Applied Sedimentology: Academic Press, 2nd Edition, 523 p.

Shaw, J. N. & Rabenhorst, M. C., 1997, The geomorphology, characteristics, and origin of the freshwater marl sediments in the Great Limestone Valley, Maryland, USA: Elsevier Science B.V., Catena 30, p. 41-59.

Shumard, B. F., 1961, Descriptions of new Cretaceous fossils from Texas: Boston Soc. Nat. Hist. Proc., v. 8, p. 188-205.

Soegaard, K., Giles, K. A., Vega, F.J., and Lawton, T. F., 1997, Structure, stratigraphy, and paleontology of Late Cretaceous-Early Tertiary Parras-La Popa foreland basin near Monterrey, northeast Mexico: AAPG Annual Convention, Dallas, Texas, Field Trip # 10, 136 p.

Soegaard, K., 1997, Tentative revision of stratigraphic subdivision of Difunta Group in Parras, La Popa, and southern Sabinas basin, northeast Mexico. *in* K. Soegaard, K. Giles, F. Vega, and T. Lawton, 1997, Structure, stratigraphy and paleontology of late Cretaceous-early Tertiary Parras-La Popa foreland basin near Monterrey, northeast Mexico: AAPG Annual Convention, Dallas, Texas, Field Trip # 10, p. 78-81.

Soegaard, K., Ye, H., Halik, N., Daniels, A. T., Arney, J. & Garrick, S., Stratigraphic evolution of latest Cretaceous to early Tertiary Difunta foreland basin in northeast Mexico: influence of salt withdrawal on tectonically induced subsidence by the Sierra Madre Oriental fold-thrust belt. *in* Bartoloni, C. (ed). The Circum-Gulf of Mexico and Caribbean Region: Plate Tectonics, Basin Formation, and Hydrocarbon Habitats. AAPG Memoir *in press.*

Stephenson, L. W., 1941, The larger invertebrate fossils of the Navarro Group of Texas (Exclusive of Corals and Crustaceans, and exclusive of the fauna of the Escondido Formation: Texas Univ. Pub. 4101, 641 p., 95 pl.

Tappan, H., 1980, The paleobiology of plant protists, Chapter 11: Charophytes and Umbellinaceans: W.H. Freeman and Co., San Francisco, 1028 p.

Van den Berg, M. S., 1999, Charophyte colonization in shallow lakes: processes, ecological effects and implications for lake management: Thesis Abs.: From the web site: http://aslo.org/dialog/199903-2.html), Vrije Universiteit Amstardam, 137 p.

Van Wagoner, J. C., Posamentier, H. W., Mitchum, R. M., Vail, P. R., Sarg, J. K., Loutit, T. S. and Handerbol, J., 1988, An overview of the fundamentals of sequence stratigraphy and key definitions, in C. K. Wilgus, B.S. Hastings, C.G. St. C. Kendall, H.W. Posamentier, C.A. Ross, and J. C. Van Wagoner, (eds.) Sea Level Changes: An Integrated Approach: SEPM Special Publication 42, p. 39-45.

Vega-Vera, F. J., Mitre-Salazar, L. M., Martínez-Hernández, E., 1989, Contribución al conocimiento de la estratigrafía del Grupo Difunta (Cretácico Superior-Terciario) en el Noreste de México: Rev. Inst. de Geología, UNAM, v. 8, no. 2, p 179-187.

Vega-Vera, F.J., and Perrilliat, M. C., 1989, La presencia del Eoceno marino en la Cuenca de La Popa (Grupo Difunta, Nuevo León; Orogenia PostYpresiana: Rev. Inst. de Geología, UNAM, v. 8, no. 1, p 67-70.

Vega, F. J., and Perrilliat, M. C., 1992, Freshwater gastropods from Early Eocene Difunta Group, northeastern Mexico: Journal of Paleontology, v. 66, p. 603-609.

Vega, F. J., and Perrilliat, M. C., 1995, On some Paleocene invertebrates from the Potrerillos Formation (Difunta Group), northeastern Mexico: Journal of Paleontology, v. 69, p. 862-869.

Vega, F. J., Perrilliat, M. C., and Mitre-Salazar, L. M., 1999, Paleocene ostreoids from the Las Encinas Formation (Parras Basin, Difunta Group), northeastern Mexico; stratigraphic implications, *in* C. Bartolini, J. L. Wilson, and T. F. Lawton, (eds.), Mesozoic sedimentary and tectonic history of north-central Mexico: GSA Special Paper 340, p. 105-110.

Walker, T. R., 1976, Diagenetic origin of continental red beds, *in* H. Falke (ed.) the Continental Permian in Central, Westh an South Europe. p. 240-282

Warning, K. R., 1977, Transgressive-regressive deposits of Difunta Group (Upper Cretaceous-Paleocene), Parras Basin, northeastern Mexico: Masters thesis, University of Texas at Austin, Austin, Texas, 164 p.

Weidie, A. E., and Murray, G. E., 1961, Tectonics of Parras basin, states of Coahuila and Nuevo Leon, Mexico: Transactions, Gulf Coast Assoc. of Geol. Soc., v. XI p 47-55.

Weidie, A. E., Murray, G. E., Cameron, C. P., Long, J. J. Jr., and Ritchie, E. J., 1966, Stratigraphy and Structure of Parras basin and adjacent areas of northeastern Mexico: AAPG Bulletin v. 50, n. 3 (march), p. 639-640.

Weidie, A. E., and Murray, G. E., 1967, Geology of Parras basin and adjacent areas of northeastern Mexico: AAPG Bulletin, v. 51, p. 678-695.

Weidie, A. E., Jr., 1961, The stratigraphy and sedimentology of the Parras basin, Coahuila and Nuevo León, Mexico: Ph. D. dissertation, Louisiana State University, Baton Rouge, Louisiana, p. 294.

Whitaker, J. H., 1973, "gutter casts", a new name for scour-and fill structures: with examples from the Llandoverian of Ringerike and Malmoya Southern Norway: Geological Society, London, Special Publications, p. 129.

Williams, G. D. & Stelk, C. R., 1975, Speculations on the Cretaceous paleogeography of North America, *in* Caldwell, W.G.E., Ed., The cretaceous system in the Western Interior of North America: Geological Association of Canada, p. 1-20.

Wray, J. L., 1977, Calcareous Algae: Developments in Paleontology and Stratigraphy 4: Elsevier Scientific Publishing Co., New York, 185 p.

Ye, Hongzhuan, 1997, Sequence stratigraphy of the Difunta Group in the Parras-La Popa foreland basin, and tectonic evolution of the Sierra Madre Oriental, NE Mexico, Ph.D. Dissertation, The University of Texas at Dallas, Richardson, Texas, 197 p.

VITA

Juan Clemente Bermúdez Santana was born in Apaxtla de Castrejón, Guerrero, southern México, on March 28 of 1963. The third son of Juan Bermúdez and Cira Santana. In 1977, Juan attended the Instituto Politécnico Nacional (IPN) at México City. In 1979 concluded the high school and in 1987 he received the degree of Geologist Engineer from the Escuela Superior de Ingeniería y Arquitectura. In 1985, he married María Teresa Quintana; they currently have two children, Alan and Carlos.

In 1987, Juan began his professional work as field assistant geologist for the small private company CONCIT, doing field work and air photo interpretation for Petróleos Mexicanos (PEMEX). In 1988, he worked for the subsurface geology department of PEMEX at Villahermosa, Tabasco. In November of the same year, the Instituto Mexicano del Petróleo (IMP) hired him, being involved since then in biostratigraphic studies from several sedimentary basins of México. He has some publications.

In the summer of 1989, Juan returned to the IPN where he received a Master of Sciences degree in April of 1994. He entered the University of Texas' Department of Geological Sciences in the fall of 1996, under the advising of R. T. Buffler, and the financial support of the Instituto Mexicano del Petróleo. Two years later, he began to work in his project on the sequence stratigraphy of the central Parras Basin. Juan currently works for the research branch for exploration technologies of the IMP at México City.

This dissertation was typed by the author.

Permanent Address:
Av. Norte 100 Edif. 7-401
08100, México, D. F., MEXICO.

e-mail: jbermude@imp.mx

LEGEND

- SALTILLO — City (more than 500, 000 inhabitants)
- San Miguel — Towns (more than 500 inhabitants)
- El Potrero — Ranch
- Local Airport
- Federal Highway
- State Highway
- Dirt Road
- Railroad
- Gas Pipeline (PEMEX)
- Creek
- Anticline
- Syncline
- Strike Slip Fault
- Thrust Fault (dashed where inferred)
- Strike and Dip (measured in outcrop)
- Strike and Dip (from air photo)
- LC — Measured Section

- Alluvium
- Rancho Nuevo Formation
- Las Encinas Formation
- Cerro Grande Formation
- Las Imágenes Formation
- Cañón del Tule Formation
- Cerro Huerta Formation
- Cerro del Pueblo Formation
- Parras Shale Formation

Measured Sections:

A.2 Altamira (SA)
A.3 La Campana (LC)
A.4 La Casita (SLC)
A.5 Doce de Diciembre (DD)
A.6 La Florida (LF)
A.7 Los Ojitos (LO)
A.8 El Potrero (EP)
A.9 Puerto La Cuesta (PC)
A.10 El Realito (ER)
A.11 San Miguel (SM)
A.12 El Saucillo (SS)
A.13 Santo Domingo (SD)
A.14 Tanque (ST)
A.15 Temporal (TE)
A.16 Las Trancas- P. Blanco (LT-PB)

Cross Sections:

A.17 El Realito-Altamira (ER-SA)
A.18 El Potrero-Tanque (EP-ST)
A.19 El Saucillo-El Realito (SS-ER)
A.20 El Saucillo-La Casita (SS-SLC)

0 1 2 3 4 Km

Approximated Map Scale: 1: 75, 000

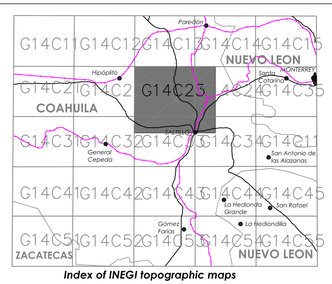

Index of INEGI topographic maps

Geographical Sciences

Bermúdez, J., 2003.

Figure A.1 Geologic Map of the Central Parras Basin

EXPLANATION: *The roadways, creeks, infrastructure and population centers were taken from the INEGI´s topographic maps (scale 1: 50,000) San Miguel (G14C23), Saltillo (G14C33), Ramos Arizpe (G14C24), and Arteaga (G14C34). The mapped units include the Parras Shale and the seven formations that integrate the Difunta Group in the central Parras Basin according to the stratigraphic nomenclature defined by McBride et al. (1974). Geologic mapping of units was developed using a set of INEGI´s air photographs included in the lines 145 to 151, scale: 1: 75: 000, taken in 1991 and 1994 in a north-south flight direction. This geologic map was also compiled with the support of the previous maps of McBride et al. (1974) and Soegaard et al (1997). See the text for additional explanations.*

Tie point: Top of sandstone
SA+38
Tie point: calcite-cemented horizon
SA+20
Las Imagenes missing.
Tie point: Thickest sandstone
SA+0.7
0m SA
Sharp erosional surface
Gutter cast
-1.5 SA
-19.5 SA
-29.1 SA
-51.5 SA
-106 SA
-144 SA
-148.5 SA
-189 SA
-202.2 SA
Coahuilites sheltoni
Cerro Grande
Del Tule Canyon

Early TST

Deepening Upward

Transgressive Surface

TS 3

FSST

Regressive Surface of Submarine Erosion (Forced Regression)+ Facies Dislocation ? + Sequence Boundary (SB)

FSST-HST *(Undifferentiated)*

HST

Shallowing Upward

Maximum Flooding Surface

MFS 2.2

Deepening Upward

Transgressive Surface

TS 2.2

TST

Previous HST

Massive gray mudstone, thin-bedded (15-10 cm) siltstone and very fine-bedded sandstone. This and the overlying unit display a well defined progradational stacking pattern defined by upward-thickening muddy-silty parasequences capped by thin-bedded sandstone or thick-bedded siltstone.

Lower Shoreface ?

Mostly bioturbated gray mudstone, less thin-bedded (10-20cm) very fine-grained sandstone and siltstone. *Ophiomorpha* and other unidentified burrows in sandstone and mudstone beds. A thin calcite-cemented horizon bounds this unit at its very top. Discrete arrangement of beds in discrete parasequences bounded on top by this sandstone beds.

Top: very fine-grained trough cross-bedded sandstone and light gray mudstone. At this location the red coastal fluvial-deltaic deposits of Las Imagenes Formation have pinched out and disappeared completely producing a non deposition gap that coincides with the transgressive surface TS 3 at the base of the Cerro Grande marine deposits. The stacked upper shoreface ridge-forming sandstone of the uppermost Cañon del Tule, continually exposed westward is condensed here to 1 to 1.5-meter thick layers. However, its sharp-based character and erosional features such as gutter cast still remain at this location (See Fig. 3.10).

Upper Shoreface

Mostly highly bioturbated gray mudstone and thin-bedded, sharp- and undulating-based planar-laminated or through cross-bedded very fine-grained sandstone. Poor fossil and shell debris content. Bed arrangement in discrete muddy parasequences capped by straight-crested wave-rippled sandstone beds.

Lower Shoreface

Predominantly massive fossiliferous gray mudstone and thin- to thick-bedded upward thickenning siltstone. Sandstone beds only at the bottom. Regular abundance of *Exogyra costata* and high shell debris content. Small hematized iron nodules at different levels. Stacking pattern characterized by muddy upward-thickenning progradational parasequences capped by upward-thickenning siltstone beds.
The maximum flooding surface at the bottom is placed within a muddy interval chracterized by a change from retrogradational to progradational stacking pattern.

Offshore

Predominantly massive fossiliferous gray mudstone and thin-bedded siltstone. Sandstone beds absent. Abundant *Exogyra costata;* rare ammonite fragments, gastropods, and bivalves. Horizons with high shell debris content, lenticular bodies of siltstone, and siltstone clasts distributed throughout the unit. Stacking arrangement in upward-thinning retrogradational muddy parasequences capped by siltstone.

Offshore

Mostly massive gray mudstone, interbedded thin-layered siltstone and very fine-grained sandstone. Some horizons within the mudstone are rich in shell debris and fossil fragments, other contain small hematized iron concretions. Beds arranged in muddy upward-thinning parasequences capped by low-angle and planar-laminated thin-bedded sandstone.

Lower Shoreface

Massive bioturbated gray mudstone and interbedded thin- to thick-bedded (10 to 100 cm) very fine sandstone. Beds cyclically arranged in upward-thickenning muddy parasequences. Some sandstone beds contain *Ophiomorpha* or undifferentiated burrows. Rare specimens of *Exogyra*.

Delta-Fed Turbidites

Mostly very fine-grained, planar-laminated or massive, medium to thick (40 to 200 cm) bedded, upward thickening silty sandstone and gray mudstone. Cyclic arrangement of sandstone beds which display flat and sharp tops and bases bounded by mudstone. Wave ripples and whole specimens of *Exogyra costata* on top of the unit.

Middle Shoreface

Φ (mm) — 8 1/256 Mud — 6 1/64 Silt — 3 1/8 Very fine — 2 0.25 Fine — 1 0.5 Medium — 0 1 Coarse — -1 2.0 Very coarse — -2 4.0 Granule — -6 64 Pebble — SAND

SA+250
SA+198
SA+161
SAR+40.8
SAR+36
Ball and pillow structures
Cerro Grande

HST

Predominantly massive gray mudstone and thick-bedded (50-400 cm) very fine-grained sandstone with rare *Ophiomorpha*. Shell debris concentration in some horizons, rare *Exogyra* and bivalves. Bed arrangement in a progradational upward-thickenning parasequence set. The section continues upward excellently exposed downstream.

Mostly very fine-grained, planar-laminated or massive, medium to thick-bedded (20 to 100 cm) sandstone. Upward-thickening very fine-grained tabular sandstone contain rare *Ophiomorpha*. Gray massive gray mudstone. Bed arrangement of muddy cycles capped by sandstone in well defined progradational upward thickening parasequence sets. Whole specimens of *Exogyra costata* on top of the unit.

Lower to Middle Soreface

Gray massive mudstone and very fine-grained, planar-laminated, medium-thick bedded (20-50 cm) sandstone. Muddy parasequences capped by tabular sandstone.

Massive black or dark gray mudstone and cyclically interbedded thin- to medium thick-bedded (10 to 50 cm) very fine, planar- or ripple cros-laminated sandstone. Rare gutter casts. Stacking pattern characterized by meter-scale stacked cycles of progradational parasequence sets. Rare whole specimens of *Exogyra costata.*

Delta Front

HST

Shallowing Upward

Mostly massive gray mudstone and very fine-grained, planar-laminated or massive, thin-bedded (10 to 40 cm) sandstone and less siltstone. Rare *Exogyra* specimens and ball and pillow structures. Tabular sandstone beds cyclically arranged in discrete muddy parasequences capped by sandstone and overlying mudstone (see Fig. 3.21).

Delta Front

?

Maximum Flooding Surface?

MFS 3

65 meters of covered section. The position of the Maximum Flooding Surface MFS 3 is uncertain, but it is is inferred to be within the covered interval since the lower unit displays a retrogradational stacking pattern whereas the upper one displays a well developed progradational, upward-thickenning with a remarkable increase in sand content.

Late TST

Massive siltstone, gray mudstone, and thin-bedded sandstone. Moderate abundance of *Exogyra* and bivalves. Beds stacked in a well defined upward-thickenning progradational parasequence set. This interval is not exposed on the creek, it was measured along the railroad and tied with the main measured section.

Middle Shoreface

Tie point: Top of sandstone

Meters	Formation	Samples	Lithology, Grainsize, Sedimentary Structures, Fossil Content (m s vf f m c vc g)	SEQUENCE STRATIGRAPHY: Cycles, Paraseq., Paraseq. Sets	SEQUENCE STRATIGRAPHY: Stacking Patterns	SEQUENCE STRATIGRAPHY: Systems Tracts Major Surfaces Water Depth	DESCRIPTION	DEPOSITIONAL ENVIRONMENT & FACIES ASSOCIATION
405								
400								
395								Upper Shoreface
390								
385								
380								

Depositional Architecture

Parasequence	Parasequence Sets	Water Depth, Grain Size and Facies Vertical Trends
Flooding Surface (fs) — Fine — Coarse — Flooding Surface (fs)	(a) (b) (c)	(a) (b) (c)
a) Retrogradational: net landward movement of the shoreline b) Agradational: no net movement of the shoreline c) Progradational: net basinward movement of the shoreline		a) Deepening Upward, Fining Upward, Distal Upward b) No net vertical trends. c) Shallowing Upward, Coarsening Upward, Proximal Upward

Legend

- Trough cross-bedding
- Bidirectional cross-bedding (planar foresets)
- Bidirectional cross-bedding (tangential foresets)
- Low angle tabular cross-bedding (straight foresets)
- Tabular cross-bedding (tangential foresets)
- Hummocky cross-stratification
- Undulating lamination
- Ripple cross-lamination
- Planar (horizontal) lamination
- Ball and Pillow structure
- Load structure
- Gutter cast
- Flute cast
- Current lineation
- Wave ripples
- Current ripples
- Siderite nodule
- Soft-sediment deformation
- Cemented horizon
- Mudstone clast
- Charophytes gyrogonites
- Palinomorphs
- Plant fragments
- Ammonoids
- Gastropods
- Bivalves
- *Exogyra*
- Equinoderm spicules
- Benthic forams
- Calcareous nannofossils
- Shell debris or shell concentration
- Bioturbation (undifferentiated)
- *Ophiomorpha*
- *Skolitos*
- *Thalassinoides*

1.5 Km to Zertuche — SOURCE: INEGI, 1997, Ramos Arizpe, G14C24, 1:50, 000

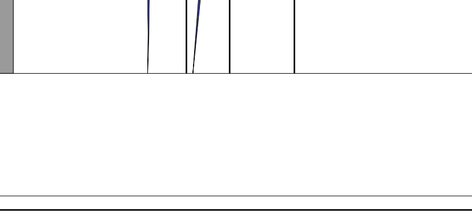

Section Location: Along unnamed tributary of La Encantada Creek, south of Zertuche Train Station.
GPS Geographic Coord.: At 0 meters N 25° 37' 41.2", W 100°59' 22.3". Interval from +39 to +86 meters measured along the railroad at N 25° 37' 49.2 ", W 100° 58' 55.0"
Formation: upper Cañon del Tule - lower Cerro Grande.
Measured by: J. Bermudez, August 1999.

Department of Geological Sciences

Figure A.2. Altamira Section (SA)
(composite)

Meters	Formation	Samples	Lithology, Grainsize, Sedimentary Structures, Fossil Content	SEQUENCE STRATIGRAPHY: Cycles, Paraseq., Paraseq. Sets	SEQUENCE STRATIGRAPHY: Stacking Patterns	SEQUENCE STRATIGRAPHY: Systems Tracts, Major Surfaces, Water Depth	DESCRIPTION	DEPOSITIONAL ENVIRONMENT & FACIES ASSOCIATION
370–365	Cerro Grande		Small dam wall on the Saucillo Creek.			HST	Massive gray mudstone with *Exogyra* and thick-bedded, massive coarse siltstone to very fine-grained sandstone on top of parasequences. Above the small dam wall the section is covered by the Saucillo Creek. Upward a covered interval, thick bedded sandtone are exposed.	Upper to Middle Shreface
365–305	Cerro Grande					HST	Thick, massive very fine-grained sandstone to coarse siltsone, siltstone and gray mudstone. Beds arrangement in a well defined upward thickenning progradational parasequence set.	Upper to Middle Shreface
305–290	Cerro Grande					HST	Covered and poorly exposed.	
290–270	Cerro Grande					HST	Predominantly bioturbated and fossiliferous gray mudstone, siltstone and less thin-bedded sandstone. Ball and pillow structures in the muddy intervals. Whole specimens of *Exogyra* sp. (see Plate) and ammonite fragments, gastropods and bivalves. Sample LC+254 contains an assemblage of abundant rotalid-type benthic forams and diverse microfossils fragments (see Plate). Beds arragement in meter-scale parasequences without a well-defined progradational stacking pattern trend. The maximum flooding surface may lay within the covered interval or tentatively within a pebble and shell lag.	Lower Shoreface
270–240	Cerro Grande	LC+267.6; LC+254	Rotalid-type benthic forams; *Exogyra* sp.; Pebbles, small gastropods and pelecypods, shell and other biogenic fragments.; calcite-cemented horizon (hardground)		Shallowing Upward; *Maximum Flooding Surface?*	*MFS 3*; Late TST	39 m presumibly of mudstone covered by El Saucillo Creek.	
240–195	Cerro Grande					Late TST	Mostly dark gray to black, intensively bioturbated and homogenized mudstone, thin bedded siltstone ocasionally with wave ripples on top and less sandstone. Rare ammonite and shell fragments, whole bivalves and *Exogyra*. Beds arragement in ten of meter- scale mud-richer upward parasequences without a well defined retrogradational upward thinning stacking pattern trend.	Lower to Middle Shoreface
195–185	Cerro Grande	LC+182				Early TST	Gray, slighly bioturbated silty mudstone and siltstone and interbedded, sharp-based, thick (120-160 cm) sandstone. Sandstone beds display small flute cast at the bottom, planar lamination and scattered shell fragments on top. Neither a lag nor a significant transgressive surface is evident. However, both litology and fossil content suggest submersion and deepening and a change from subaerial to shallow marine conditions. Rare hematized benthic forams were observed in thin section (sample LC+128.8). Beds arrangement in mud richer upward meter-scale parasequences.	Upper Shoreface
185–175	Cerro Grande	LC+173			Deepening Upward; *Transgressive Surface*	*TS 3*	Redish, thick-bedded (1.8 m) sharp-based sandstone encased in red and purple mudstone.	Foreshore to Coastal Plain Transition (?)
175–150	Cerro Grande	LC+161; LC+158	Deep gully				Mostly red massive mudstone, less green mudstone and siltstone, and rare thin-bedded very fine-grained redish silty sandstone. Seeds-saheped grains were obtaeined from a white greenish clay, sticky to tongue, which also contains charophyte branlets material (sample LC+53)	Coastal Floodplain
150–135	Cerro Grande		Ammonite fragments					
135–120	Cerro Grande	LC+128.8						
120–110	Las Imagenes	LC+110						
110–85	Las Imagenes	LC+107.5; LC+85						
85–55	Las Imagenes							
55–50	Las Imagenes	LC+53; LC+51	Seeds?			*Charophyte Interval*		
50–40	Las Imagenes		Covered			?	Covered and weathered, remnants of redish mudstone on soil.	

Aggradational

Meters	Formation	Samples	Lithology, Grainsize, Sedimentary Structures, Fossil Content	SEQUENCE STRATIGRAPHY: Cycles, Paraseq., Paraseq. Sets	SEQUENCE STRATIGRAPHY: Stacking Patterns	SEQUENCE STRATIGRAPHY: Systems Tracts, Major Surfaces, Water Depth	DESCRIPTION	DEPOSITIONAL ENVIRONMENT & FACIES ASSOCIATION
40–0	Canon del Tule / Las Imagenes		Covered			?	Covered and weathered, remnants of redish mudstone on soil.	
0–-28.5	Canon del Tule / Las Imagenes		Poorly exposed contact; LC+22; Sharp erosional surface; shell debris layers			FSST	Red and green mudstone on top of foreshore (?) sandstone.	
-28.5–-78	Canon del Tule / Las Imagenes	-28.5LC; -32.4LC; -33.5LC; -36LC; -37LC; -38LC; -39LC; -40.6LC; -40.7LC; -42.2LC; -42.5LC; -43.2LC; -45LC; -47LC; -49.8LC; -50LC; -51LC	*Trachycardium* sp.; *Periplomya* sp.; *Coahuilites sheltoni*; *Sphenodiscus intermedius*; *Coahuilites aff. cavinsi*; *Trachycardium* sp.; *Pholadomya occidentalis*			FSST; Shallowing Upward; *Regressive Surface of Submarine Erosion (Forced Regression) + Facies Dislocation + Sequence Boundary (SB)*	Very fine-grained sandstone becomes reddish and blueish purple at the top. Redish color produced by hematite coatings involving grains. Amalgamated massive fine to medium-grained sandstone. Ridge forming sandstone (see Fig. 3.7). Fine and very fine-grained stacked sharp-based sandstone, mostly massive with trough cross-bedding and hummocky cross-stratification. Lower bedding surfaces display current lineations on sharp, planar or undulating surfaces. At least six sandstone subunits were differentiated.	Stacked Upper Shoreface to Foreshore
-78–-104.4	Canon del Tule / Las Imagenes	-78LC; -80.8LC	Small black shells			HST	Mostly bioturbated gray mudstone and interbedded fine-grained sandstone and siltstone. Some sandstone layers pinch out laterally forming lense-type bodies encased within mudstone.	Storm-Dominated Lower Shoreface
-104.4–-139.8	Canon del Tule / Las Imagenes	-104.4LC				HST	Slighly bioturbated mudstone and very fine-grained medium to thick (20-60 cm) sandstone arranged in discrete meter-scale upward-coarsening cycles. Some sandstone layers display undulating erosive bottom and pinch out laterally. Common thin layers with high concentration of shell debris (storm deposits). Rare humocky cross-stratification. Bed arrangement in meter-scale parasequences. Diverse fossils were collected from the following horizons. **Bivalves:** *Trachycardium* sp. (-37,-40.6, -42.5, -50 and -51 LC); *Periplomya* sp. (-40.6 LC); *Scaphites* sp. (-50 LC); *Stantonella* sp. (-62 LC); *Pholadomya occidentalis* and *Pholadomia* sp. (-51 LC). **Ammonites:** *Coahuilites sheltoni* (-40.7, -42.2, -50 LC-b); *Coahuilites cavinsi* (-130/136.5 LC-b); *Coahuilites* aff. *cavinsi* (-50 LC-c); *Sphenodiscus intermedius* (-49.8, -50 LC-a); and *Eutrephoceras planoventer* (-62, -130/136.5 LC-a). Some specimens are illustrated in Plates 1-6.	
-139.8–-151.8	Canon del Tule / Las Imagenes	-139.8LC	*Trachycardium eufaulense*; *Periplomya sulcatina*; Covered			TST	Highly bioturbated gray mudstone and thin to medium thick-bedded siltstone. Early Maastrichtian gastropods and bivalves are particularly abundant. The index ammonite *Coahuilites sheltoni* precises the age of this interval to the lower Upper Maastrichtian. The clear retrogradational stacking pattern of the underlying unit, its change to progradational, progresively sand-riche upward parasequences, and the remarkable abundant fossil content were the main elements to proposed that the maximum flooding surface (MFS 2.2) position.	Offshore
-139.8–-151.8	Canon del Tule / Las Imagenes	-139.8LC	*Eutrephoceras planoventer*; *Coahuilites cavinsi*		Shallowing Upward; *Maximum Flooding Surface*	*MFS 2.2*	Mostly bioturbated gray mudstone and medium-bedded to massive (20cm-more than 1 m thick) fossiliferuos siltstone. Bed arrangement in discrete upward thinning muddy parasequences capped by siltstone, some of them with a high concentration of small black shells and shell debris. Ammonites identified as *Eutrephoceras planoventer* and *Coahuilites cavinsi* were collected ex situ? from the interval comprised beetween -130 to -136.5 LC. See Plate 2.	
-151.8–-167	Canon del Tule / Las Imagenes	-151.8LC; -152LC; -152.5LC; -157.3LC; -167LC	Abundant *Exogyra costata*; Badly preserved; *Exogyra costata*; *Exogyra costata*		Deepening Upward; *Transgressive (ravinement) Surface*	*TS 2.2*	Right and left valves of *Trachycardium eufaulense* and *Periplomya sulcatina* were collected from the horizon -139.8 LC (see Plate 6). Very fine-grained, thin-bedded (10-30 cm) sandstone, siltstone, and gray mudstone with abundant *Exogyra costata*, badly preserved ammonite fragments, and gastropods. Some sandstone layers with trough cross-bedding. Undefined bed arrangement but sand content decreases upward. Several specimens of *Exogyra costata* were collected from the horizons: -151.8, -152, -152.5, -157.3 and -167 LC (Plate 5).	Lower Shoreface
-167–-184.2	Canon del Tule / Las Imagenes	170-175 poorly exposed; 177-181 poorly exposed					Very fine-grained thin to thick-bedded (10-90 cm) sandstone beds and interbedded gray mudstone with *Exogyra costata*. Some sandstone layers with planar lamination. Bed arrangement in meter-sacele upward-thickening progradational parasequences.	Middle Shoreface
-184.2–-208.2	Canon del Tule / Las Imagenes	-184.2LC; -190.5LC; -201.3LC; -208.2LC	E-W Current Direction; Current Direction NE-SW 85; SE-NW 85			Previous HST	Highly bioturbated mudstone and very fine-grained medium to thick-bedded (20-100 cm) sandstone with *Ohiomorpha*. Lower and upper bedding surfaces in sandstone are sharp with current lineations, load casts, and planar lamination, particularly well-developed at its bottom. Some horizons contain gastropods, bivalves, and ammonite fragments. Rare hematite nodules. Bioturbation increases upward. Bed arrangement in meter-scale parasequences. An abundant and diverse assemblage of Micula (calacareous nannofossils) was observed in sediments of the samples (-190.5 LC) and (-211.2LC).	Proximal Delta-Fed Turbidites
-208.2–-211.2	Canon del Tule / Las Imagenes	-208.2LC; -211.2LC	Current Direction NE-SW 85; SE-NW 85			Previous HST	Very fine-grained, medium to thick (20-70 cm) sandstone and gray mudstone with rare bioturbation. Some single sandstone beds show plannar lamination, flute casts, and current lineations at its bottom (see Fig. 3.4) Bed arrangement in upward-thickening and shallowing progradational parasequences.	Distal Delta-Fed Turbidites
-211.2–-295	Canon del Tule / Las Imagenes	-211.2LC; -235; -240	Current Direction: SE 82		Shallowing Upward	Previous HST	Mostly gray mudstone with scattered very fine and very thin-bedded (5-20cm) silty sandstone layers.	Distal Delta-Fed Turbidites

COVERED

(Ø)	(mm)		
8	1/256	Mud	
6	1/64	Silt	
3	1/8	Very fine	SAND
2	0.25	Fine	
1	0.5	Medium	
0	1	Coarse	
-1	2.0	Very coarse	
-2	4.0	Granule	
-6	64	Pebble	

Depositional Architecture

Parasequence	Parasequence Sets	Water Depth, Grain Size and Facies Vertical Trends
Flooding Surface (fs); Fine; Coarse; (a) (b) (c)		
a) Retrogradational: net landward movement of the shoreline b) Agradational: no net movement of the shoreline c) Progradational: net basinward movement of the shoreline		a) Deepening Upward, Fining Upward, Distal Upward b) No net vertical trends. c) Shallowing Upward, Coarsening Upward, Proximal Upward

Legend

- Trough cross-bedding
- Bidirectional cross-bedding (planar foresets)
- Bidirectional cross-bedding (tangential foresets)
- Low angle tabular cross-bedding (straight foresets)
- Tabular cross-bedding (tangential foresets)
- Hummocky cross-stratification
- Undulating lamination
- Ripple cross-lamination
- Planar (horizontal) lamination
- Ball and Pillow structure
- Load structure
- Gutter cast
- Flute cast
- Current lineation
- Wave ripples
- Current ripples
- Siderite nodule
- Soft-sediment deformation
- Cemented horizon
- Mudstone clast
- Charophytes gyrogonites
- Palinomorphs
- Plant fragments
- Ammonoids
- Gastropods
- Bivalves
- *Exogyra*
- Equinoderm spicules
- Benthic forams
- Calcareous nannofossils
- Shell debris or shell concentration
- Bioturbation (undifferentiated)
- *Ophiomorpha*
- *Skolitos*
- *Thalassinoides*

SOURCE: INEGI, 1995. San Miguel, G14C23, 1:50, 000

Section Location: Along El Saucillo Creek, nearby La Campana, Coahuila.
GPS Geographic Coord.: At -45 meters N 25° 36' 50.6", W 101° 05' 07.4"
Formation: Canon del Tule-Las Imagenes-Cerro Grande.
Measured by: Juan C. Bermudez and Aaron del Valle, June and July 1998, June 1999.

Department of Geological Sciences

Figure A.3 La Campana Section (LC)

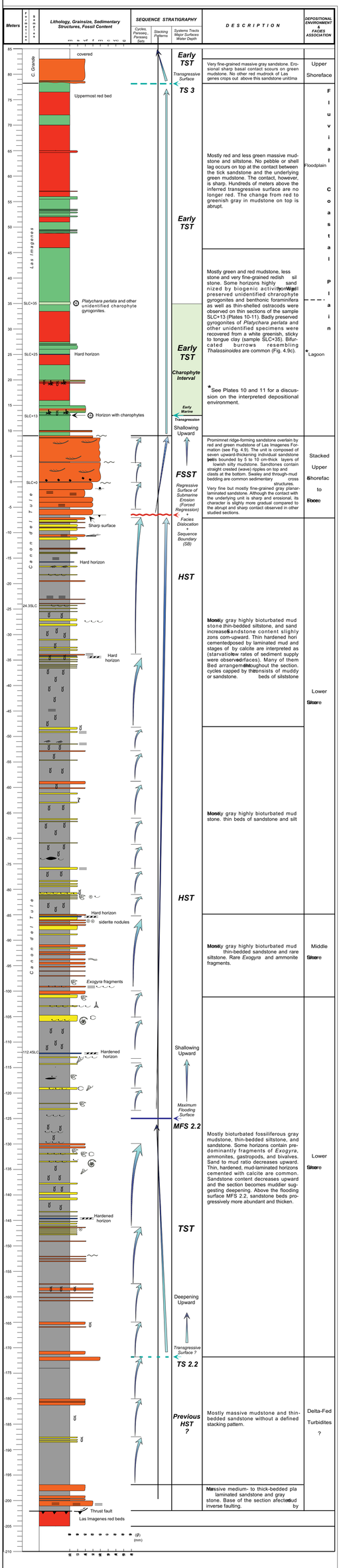

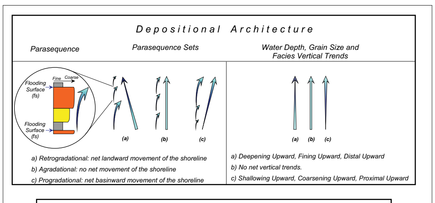

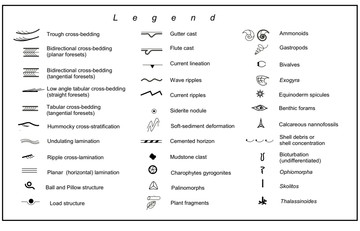

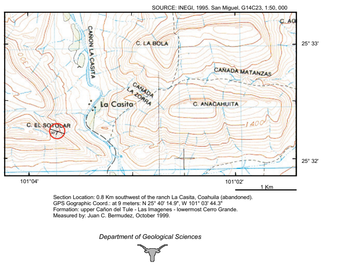

Section Location: 0.8 Km southwest of the ranch La Casita, Coahuila (abandoned).
GPS Gographic Coord.: at 9 meters: N 25° 40' 14.9", W 101° 03' 44.3"
Formation: upper Cañon del Tule - Las Imagenes - lowermost Cerro Grande.
Measured by: Juan C. Bermudez, October 1999.

Department of Geological Sciences

Figure A.4 La Casita Section (SLC)

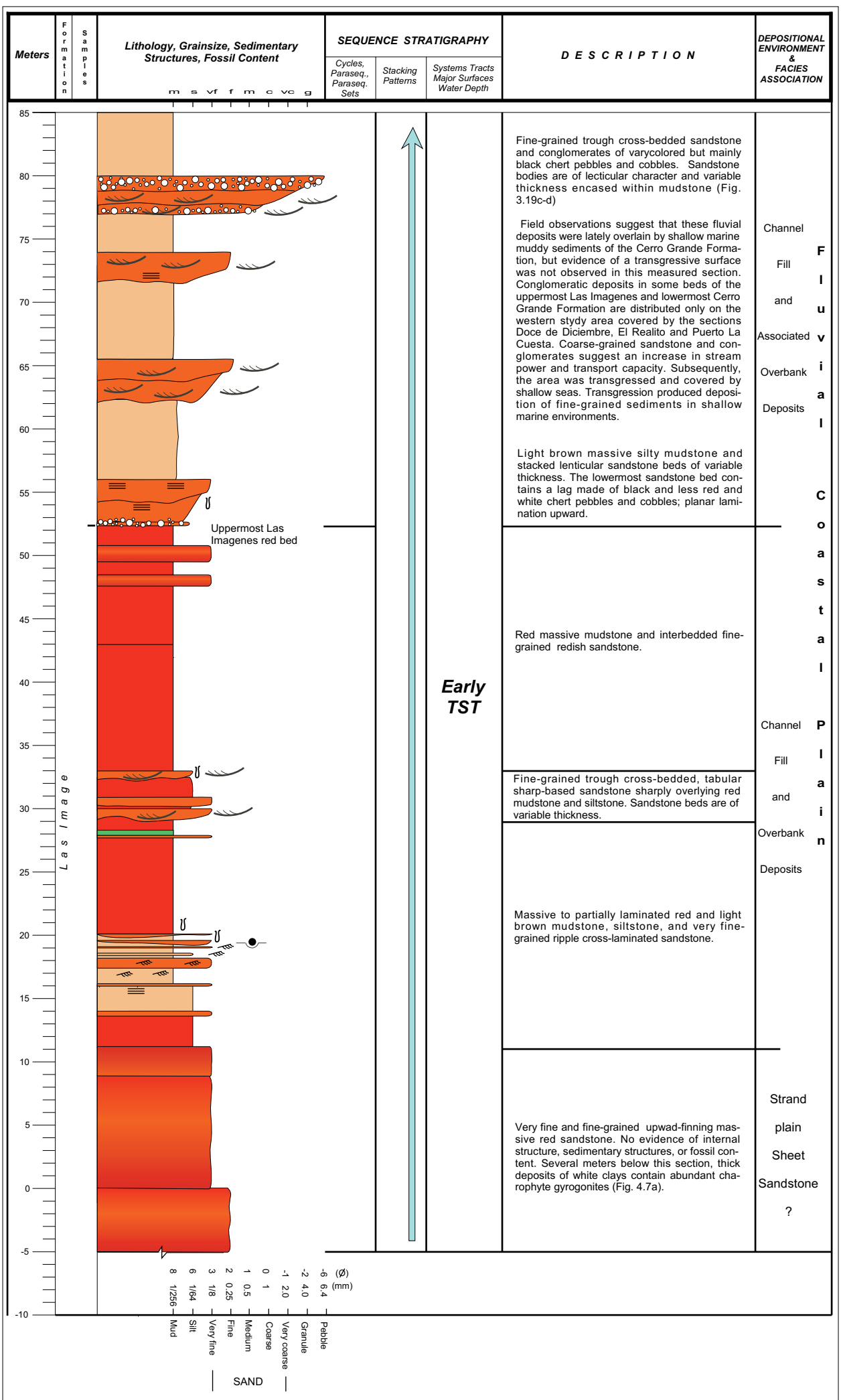

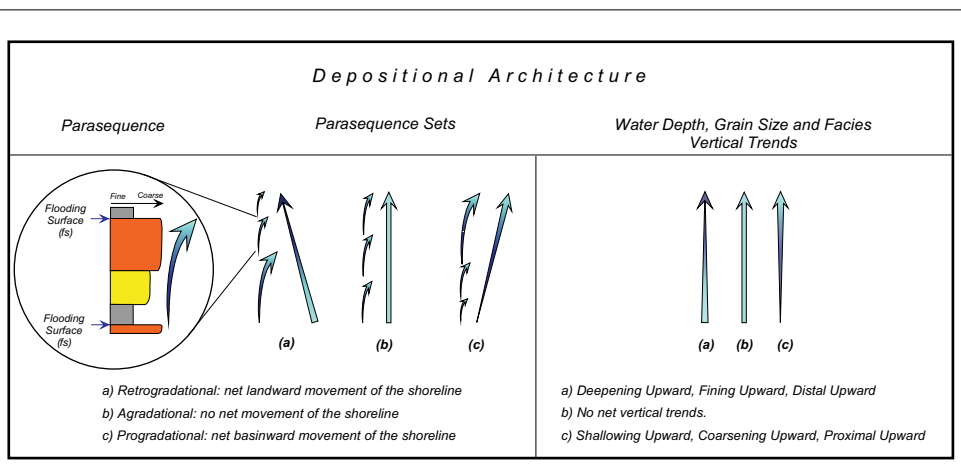

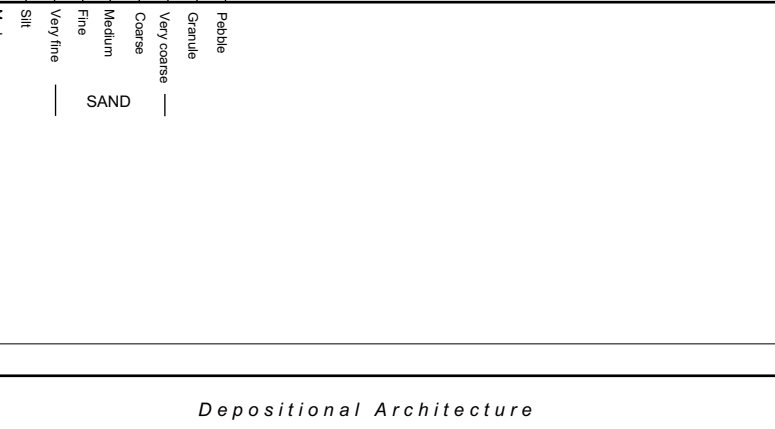

Section Location: 1.5 Km Northwest of 12 de Diciembre, CoahuiLa.
GPS Gographic Coord.: N 25° 35' 05.0", W 101°09' 57.1"
Formation: uppermost Las Imagenes- lowermost Cerro Grande?
Measured by: Juan C. Bermudez, October 1999.

Department of Geological Sciences

Figure A.5 Doce de Diciembre Section (DD)

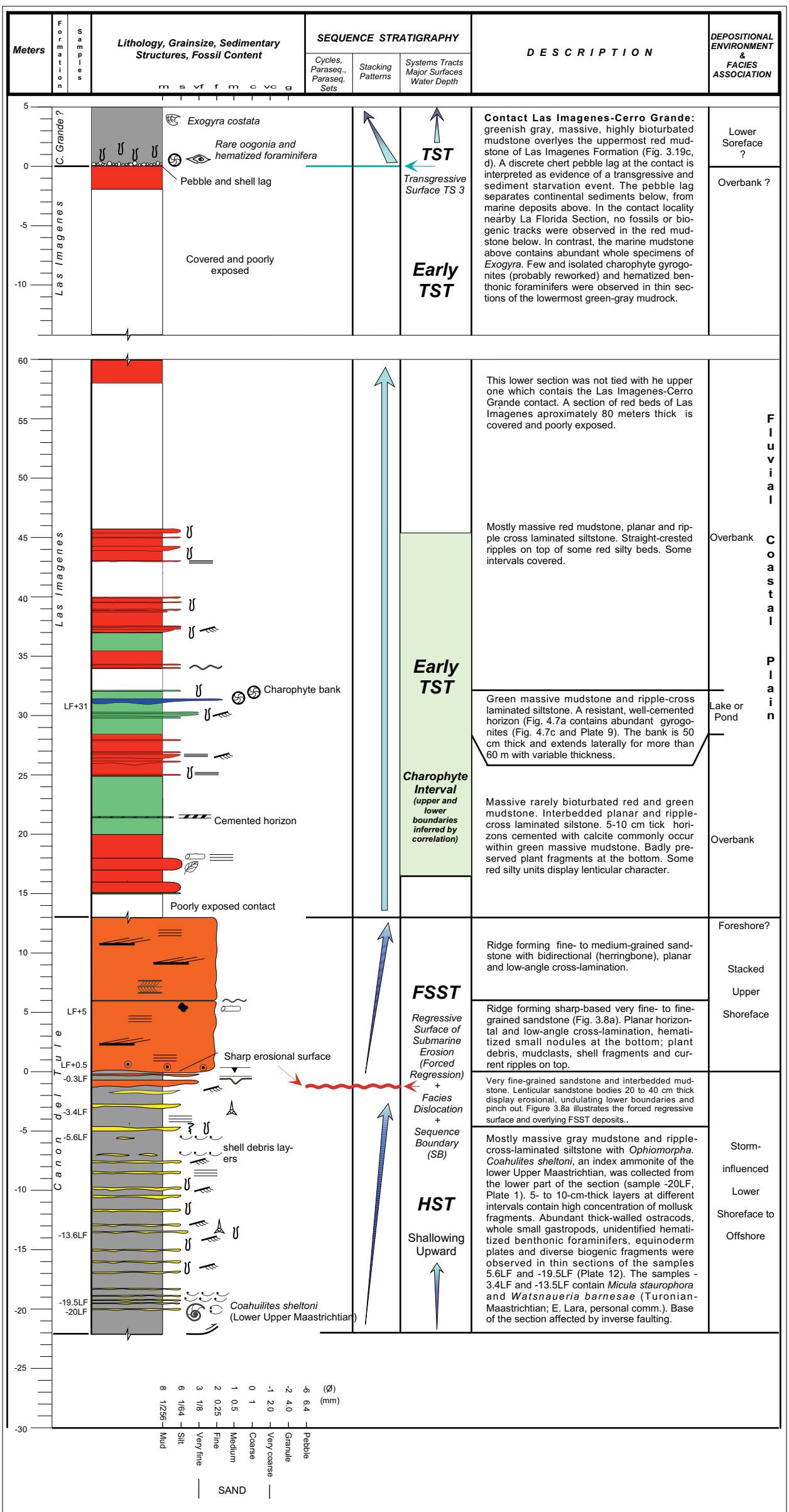

Depositional Architecture

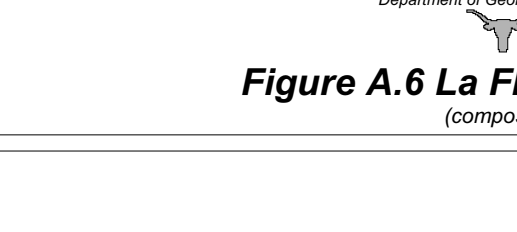

a) Retrogradational: net landward movement of the shoreline
b) Agradational: no net movement of the shoreline
c) Progradational: net basinward movement of the shoreline

a) Deepening Upward, Fining Upward, Distal Upward
b) No net vertical trends.
c) Shallowing Upward, Coarsening Upward, Proximal Upward

Legend

- Trough cross-bedding
- Bidirectional cross-bedding (planar foresets)
- Bidirectional cross-bedding (tangential foresets)
- Low angle tabular cross-bedding (straight foresets)
- Tabular cross-bedding (tangential foresets)
- Hummocky cross-stratification
- Undulating lamination
- Ripple cross-lamination
- Planar (horizontal) lamination
- Ball and Pillow structure
- Load structure
- Gutter cast
- Flute cast
- Current lineation
- Wave ripples
- Current ripples
- Siderite nodule
- Soft-sediment deformation
- Cemented horizon
- Mudstone clast
- Charophytes gyrogonites
- Palinomorphs
- Plant fragments
- Ammonoids
- Gastropods
- Bivalves
- *Exogyra*
- Equinoderm spicules
- Benthic forams
- Calcareous nannofossils
- Shell debris or shell concentration
- Bioturbation (undifferentiated)
- *Ophiomorpha*
- *Skolitos*
- *Thalassinoides*

SOURCE: INEGI, 1995. San Miguel, G14C23, 1:50, 000

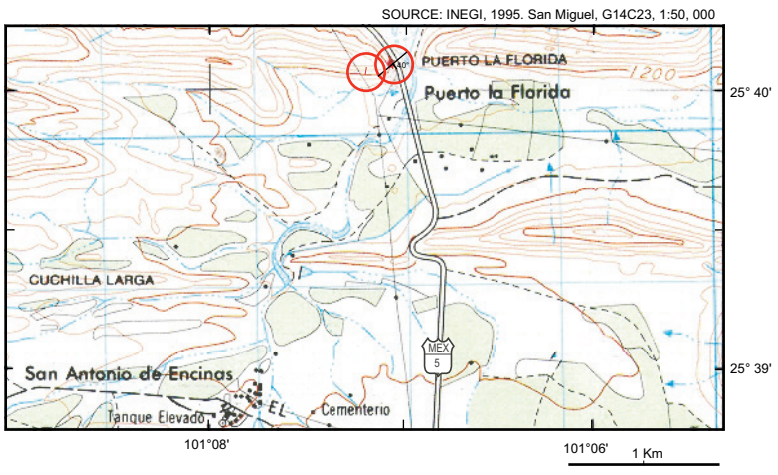

Section Location: Highway 57 Saltillo - Monclova, Coahuila.
Geographic Coord.: Interval from -22LF to LF+13 at N 25° 40' 7.8", W 101° 06' 46.5"; interval from LF+14 to LF+46 at N 25° 40' 4.2", W 101° 07' 29.0".
Measured by Juan C. Bermudez, October 1998.

Department of Geological Sciences

Figure A.6 La Florida Section

(composite)

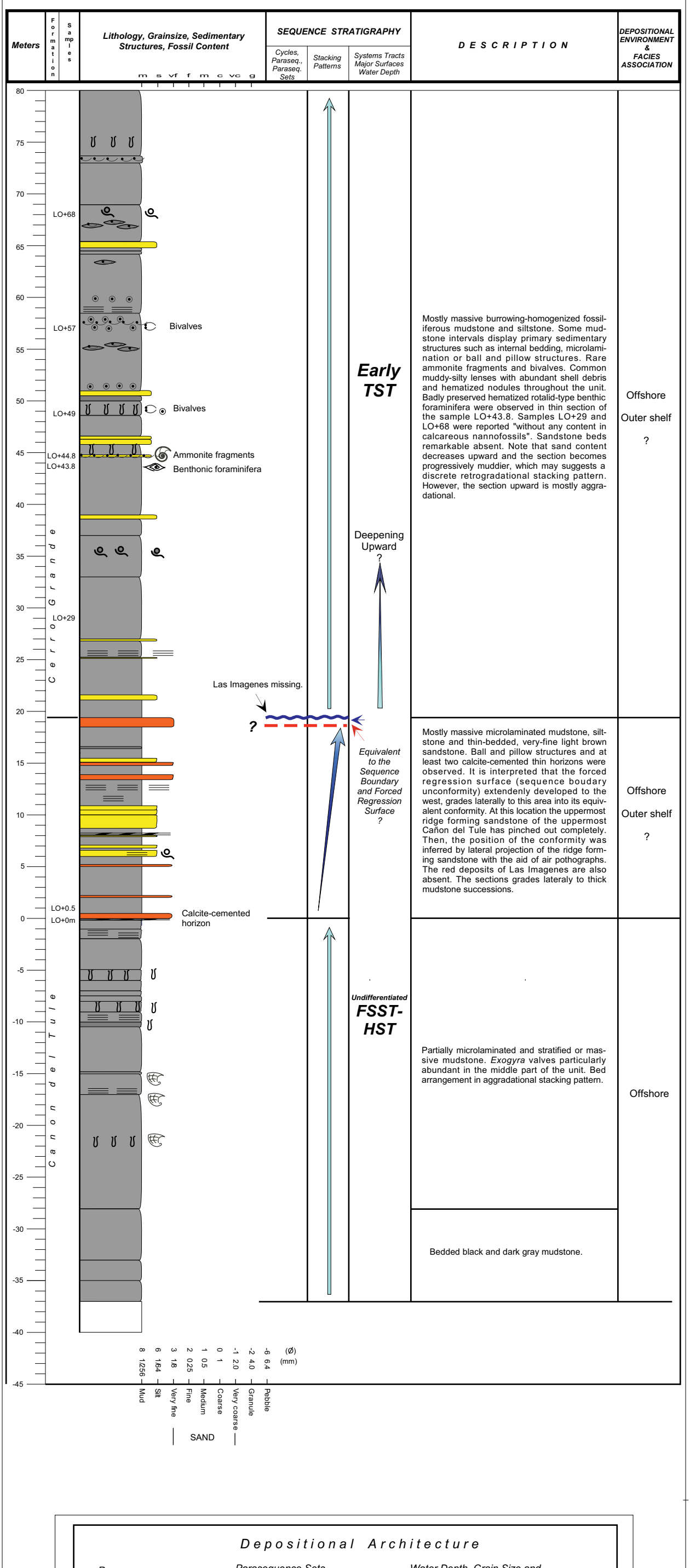

Depositional Architecture

a) Retrogradational: net landward movement of the shoreline
b) Agradational: no net movement of the shoreline
c) Progradational: net basinward movement of the shoreline

a) Deepening Upward, Fining Upward, Distal Upward
b) No net vertical trends.
c) Shallowing Upward, Coarsening Upward, Proximal Upward

Legend

- Trough cross-bedding
- Bidirectional cross-bedding (planar foresets)
- Bidirectional cross-bedding (tangential foresets)
- Low angle tabular cross-bedding (straight foresets)
- Tabular cross-bedding (tangential foresets)
- Hummocky cross-stratification
- Undulating lamination
- Ripple cross-lamination
- Planar (horizontal) lamination
- Ball and Pillow structure
- Load structure
- Gutter cast
- Flute cast
- Current lineation
- Wave ripples
- Current ripples
- Siderite nodule
- Soft-sediment deformation
- Cemented horizon
- Mudstone clast
- Charophytes gyrogonites
- Palinomorphs
- Plant fragments
- Ammonoids
- Gastropods
- Bivalves
- *Exogyra*
- Equinoderm spicules
- Benthic forams
- Shell debris or shell concentration
- Bioturbation (undifferentiated)
- *Ophiomorpha*
- *Skolitos*
- *Thalassinoides*

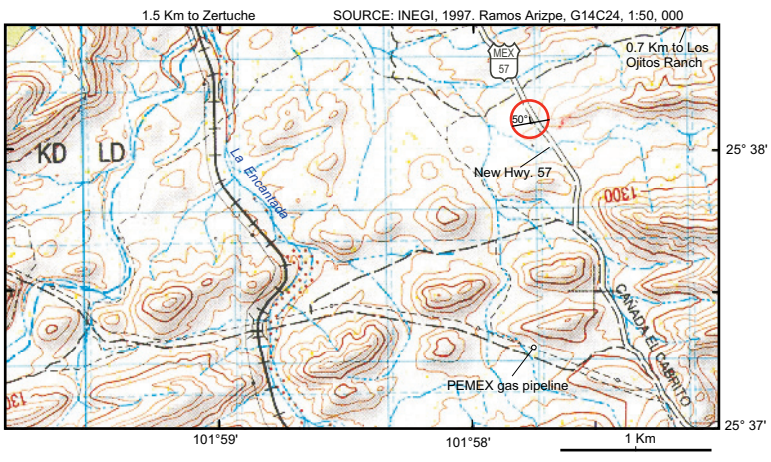

Section Location: New Highway 57 Ramos Arizpe-Monclova (segment Ramos Arizpe-Santa Cruz).
GPS Geographic Coord.: N 25° 38' 06", W 100°57' 46.4" NW10° 50°
Formation: upper Cañon del Tule - lower Cerro Grande.
Measured by: Juan C. Bermudez, October 1999.

Department of Geological Sciences

Figure A.7 Los Ojitos Section (LO)

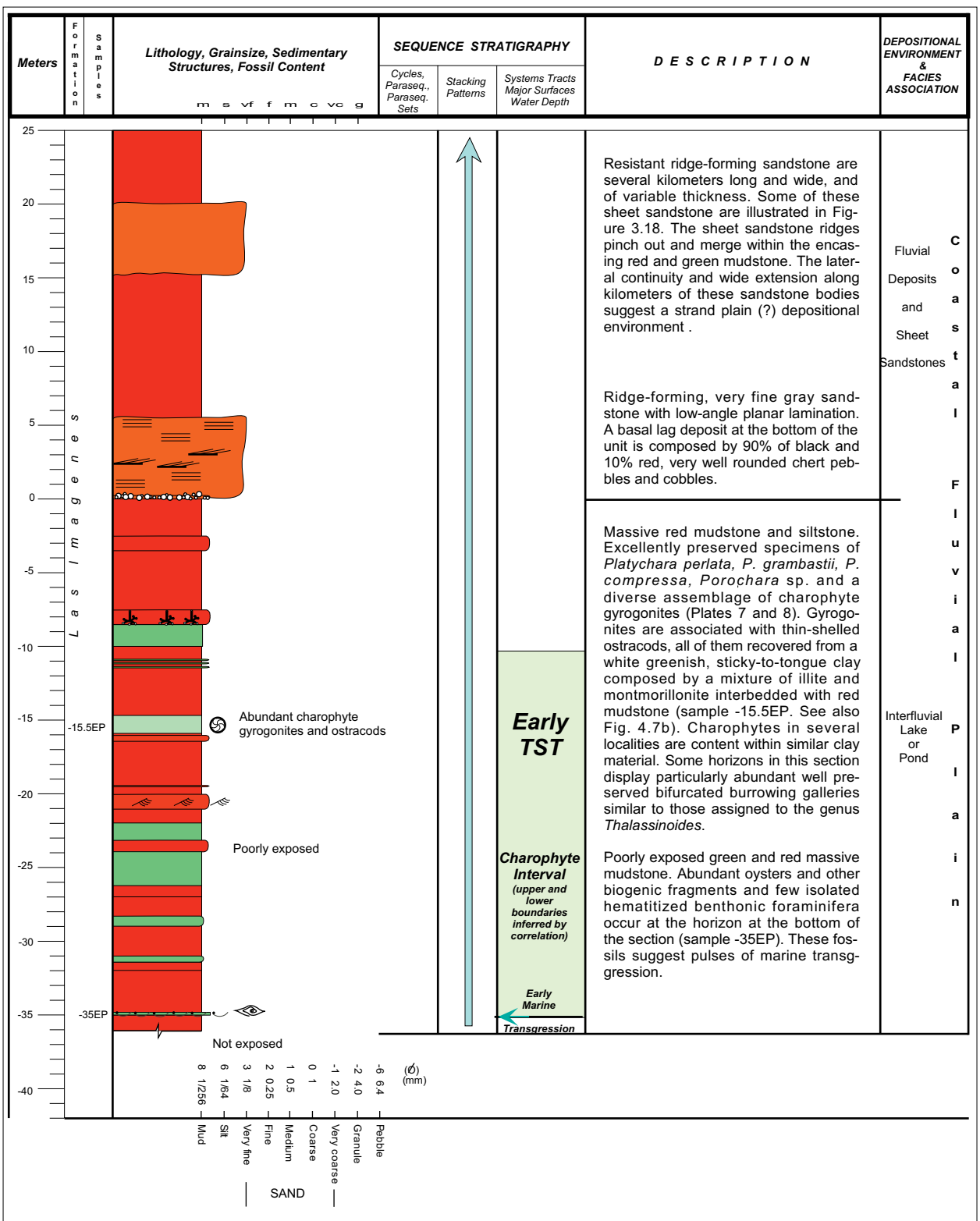

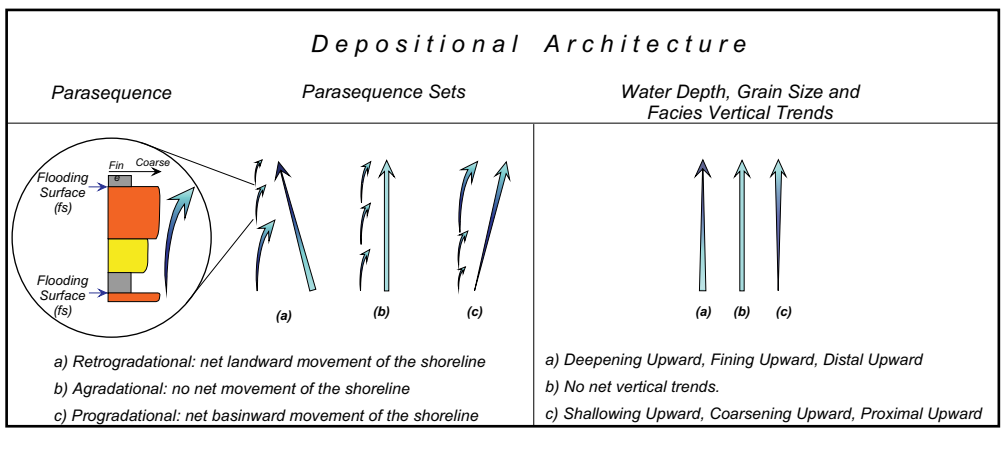

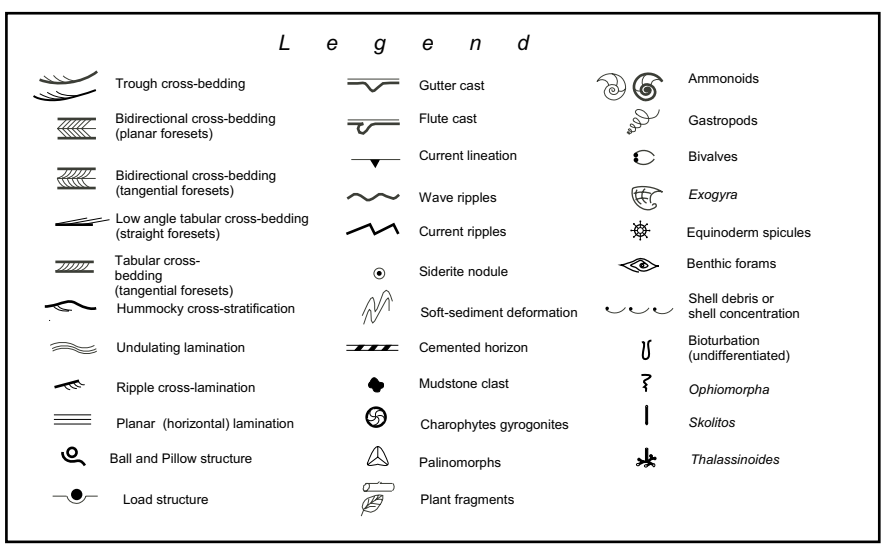

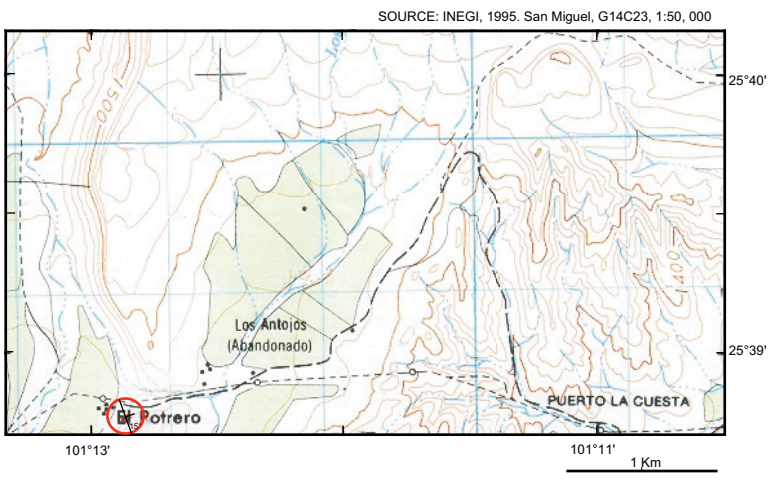

Section Location: El Potrero ranch, 18 Km West of Las Encinas, Coahuila.
Geographic Coord.: N 25° 38' 46.7", W 101° 12' 52.5"
Measured by: Juan C. Bermudez and R.T. Buffler, June 1999.

Department of Geological Sciences

Figure A.8 El Potrero Section (EP)

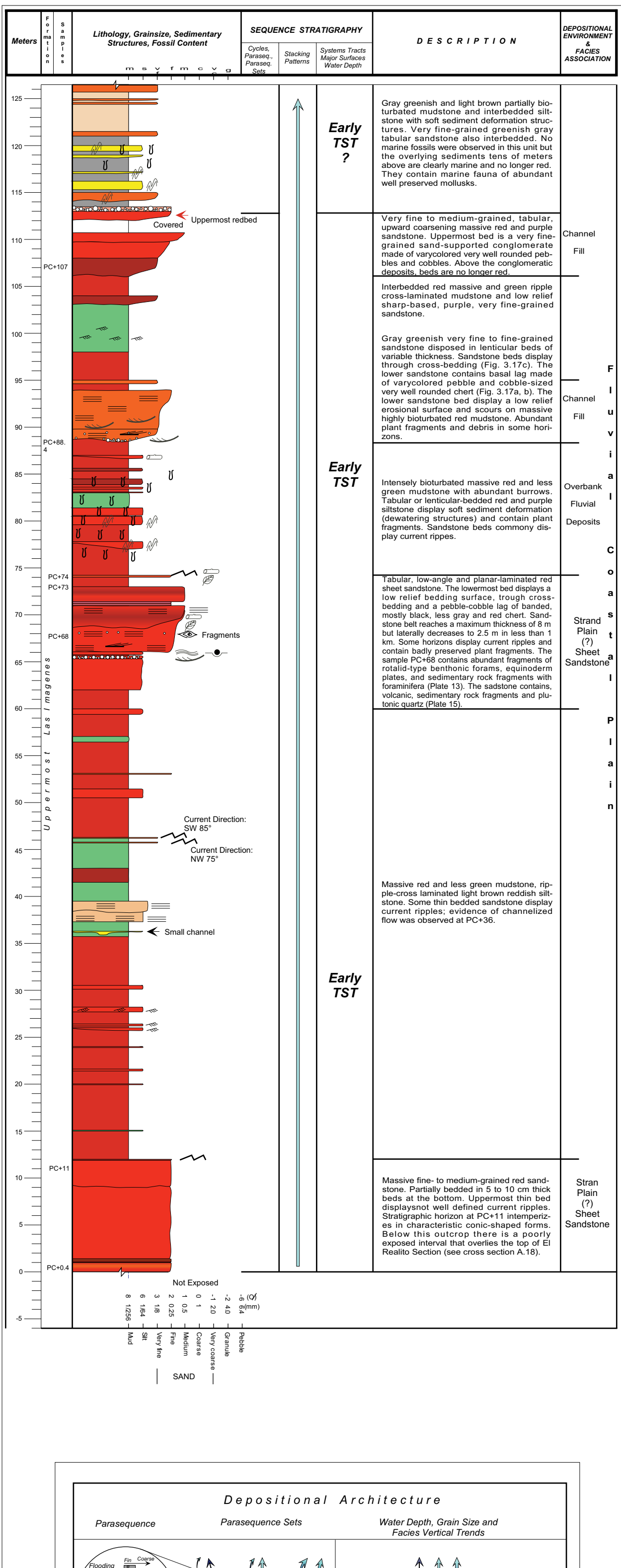

Depositional Architecture

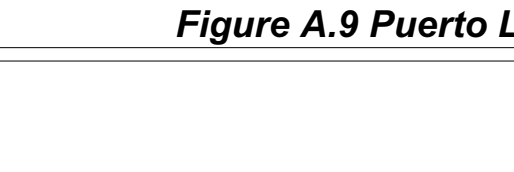

a) Retrogradational: net landward movement of the shoreline
b) Agradational: no net movement of the shoreline
c) Progradational: net basinward movement of the shoreline

a) Deepening Upward, Fining Upward, Distal Upward
b) No net vertical trends.
c) Shallowing Upward, Coarsening Upward, Proximal Upward

Legend

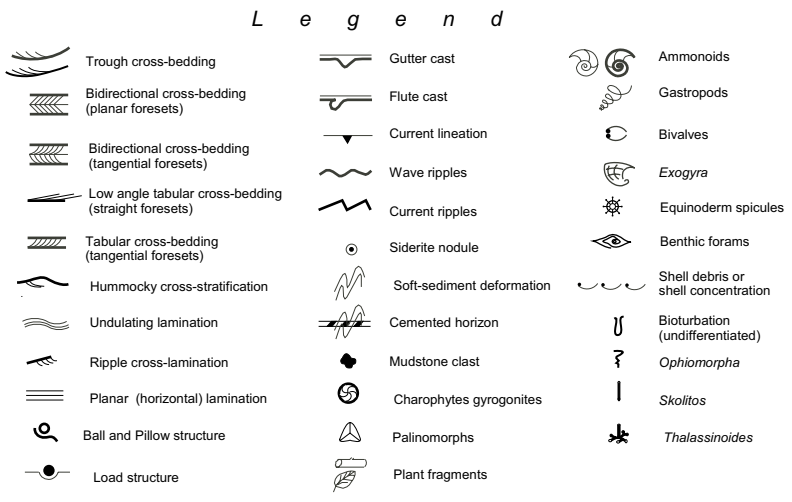

SOURCE: INEGI, 1995. San Miguel, G14C23, 1:50, 000

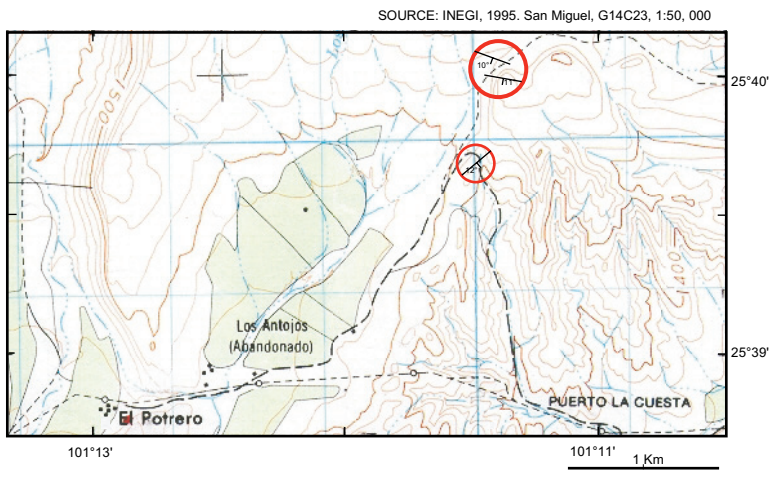

Section Location: Lower section at about 1.5 Km northwest of the most prominent bend on the dirt road Las Encinas-El Potrero. Upper section on the bend road.
Geographic Coord.: Lower section at N 25° 40' 06.4", W 101° 11' 25.6"
Measured by: Juan C. Bermudez and Adrian Quintana, July 2001.

Department of Geological Sciences

Figure A.9 Puerto La Cuesta Section (PC)

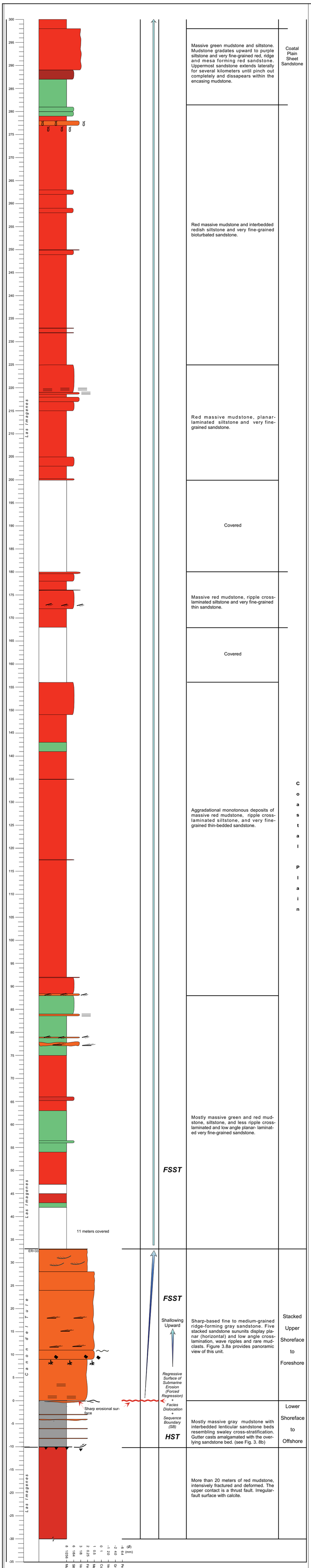

Massive green mudstone and siltstone. Mudstone gradates upward to purple siltstone and very fine-grained red, ridge and mesa forming red sandstone. Uppermost sandstone extends laterally for several kilometers until pinch out completely and dissapears within the encasing mudstone.

Coatal Plain Sheet Sandstone

Red massive mudstone and interbedded redish siltstone and very fine-grained bioturbated sandstone.

Red massive mudstone, planar-laminated siltstone and very fine-grained sandstone.

Covered

Massive red mudstone, ripple cross-laminated siltstone and very fine-grained thin sandstone.

Covered

Aggradational monotonous deposits of massive red mudstone, ripple cross-laminated siltstone, and very fine-grained thin-bedded sandstone.

Coastal Plain

Mostly massive green and red mudstone, siltstone, and less ripple cross-laminated and low angle planar- laminated very fine-grained sandstone.

Sharp-based fine to medium-grained ridge-forming gray sandstone. Five stacked sandstone sununits display planar (horizontal) and low angle cross-lamination, wave ripples and rare mudclasts. Figure 3.8a provides panoramic view of this unit.

Stacked Upper Shoreface to Foreshore

Mostly massive gray mudstone with interbedded lenticular sandstone beds resembling swaley cross-stratification. Gutter casts amalgamated with the overlying sandstone bed. (see Fig. 3. 8b)

Lower Shoreface to Offshore

More than 20 meters of red mudstone, intensively fractured and deformed. The upper contact is a thrust fault. Irregular-fault surface with calcite.

Coastal Plain

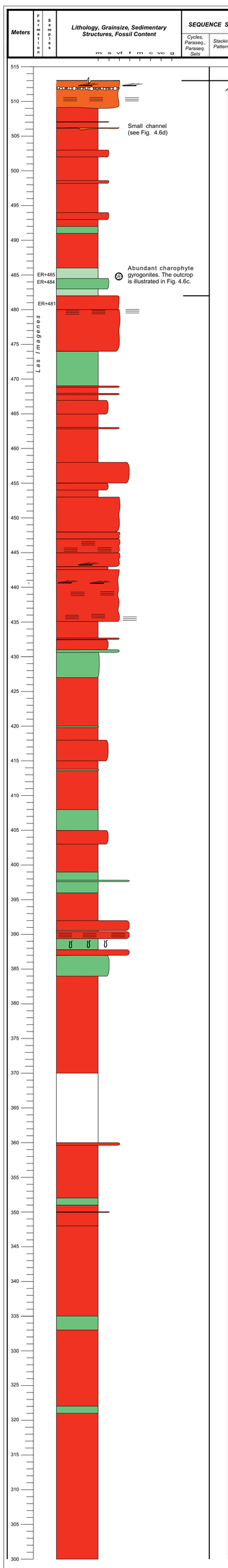

Meters	Formation	Samplings	Lithology, Grainsize, Sedimentary Structures, Fossil Content (m s vf f m c vc g)	SEQUENCE STRATIGRAPHY: Cycles, Paraseq., Paraseq. Sets	SEQUENCE STRATIGRAPHY: Stacking Patterns	SEQUENCE STRATIGRAPHY: Systems Tracts, Major Surfaces, Water Depth	DESCRIPTION	DEPOSITIONAL ENVIRONMENT & FACIES ASSOCIATION
						Early TST	**TOP**: Massive very fine-grained planar and low-angle cross-laminated sandstone. It forms a ridge several kilometers long aproximately equivalent to the uppermost sandstone ridge at El Potrero Section. El Realito is stratigraphically below the Puerto La Cuesta and Doce de Diciembre sections. Above the top of this section there is an interval less than 100 meters thick whick contaisn isolated outcrops with gravels and sandstone. In this section the red deposits of Las Imagenes Formation reach their maximum but uncomplete thickness.	Strand plain ? Sheet Sandstone
							Mostly red massive mudstone and siltstone and planar-laminated red sandstone. Abundant and well preserved charophyte gyrogonites were recovered from the white greenish sticky-to-tongue clay at the bottom of this unit. The charophyte-bearing interval is equivalent to the one of El Potrero Section. Specimens of *Platychara perlata*, *P. grambastii* and a diverse gyrogonites were recovered from the samples ER+484 and ER+485.	Lake or Pond
							Planar horizontally laminated red sandstone. It forms a wide mesa and extends laterally for more than 3 kilometres until pinch out completely southbound.	Sheet Sandstone
							Massive red and green mudstone, very fine-grained thin bedded sandstone and siltstone.	
						FSST	Stacked very fine-grained, planar and low angle cross-laminated red sandstone. Ridge forming unit that forms an extended mesa. Variable in thickness and extends laterally for several kilometers until pinch out within the encasing thick and monotonous successions of red mudstone.	Coastal Plain
							Massive red and green mudstone, interbedded redish siltstone, and rare thin-bedded sandstone.	Coastal Plain
							Burrowed green mudstone and massive siltstone. Interbedded fine-grained planar-laminated red sandstone.	
							Monotonous deposits of red and massive mudstone and sporadic thin-laminated sandstone.	

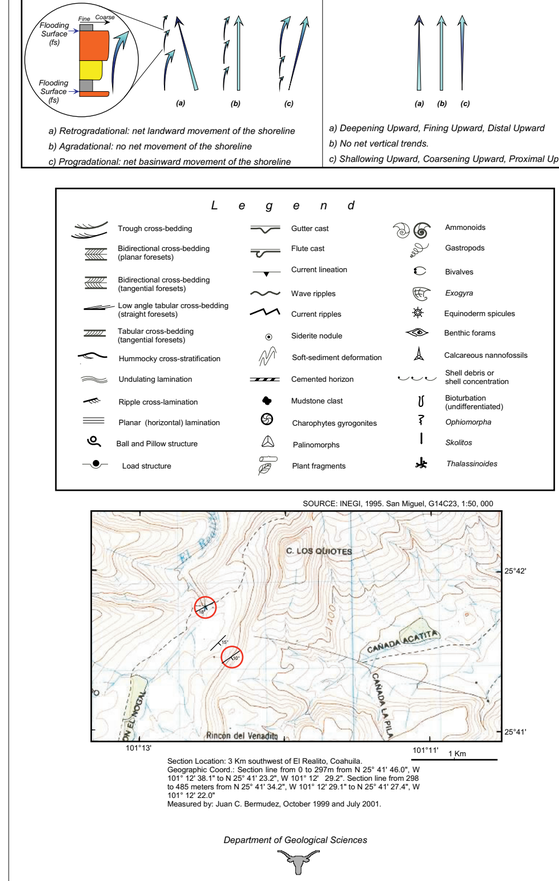

SOURCE: INEGI, 1995. San Miguel, G14C23, 1:50, 000

Section Location: 3 Km southwest of El Realito, Coahuila.
Geographic Coord.: Section line from 0 to 297m from N 25° 41' 46.0", W 101° 12' 38.1" to N 25° 41' 23.2", W 101° 12' 29.2". Section line from 298 to 485 meters from N 25° 41' 34.2", W 101° 12' 29.1" to N 25° 41' 27.4", W 101° 12' 22.0".
Measured by: Juan C. Bermudez, October 1999 and July 2001.

Department of Geological Sciences

Figure A.10 El Realito Section (ER)
(composite)

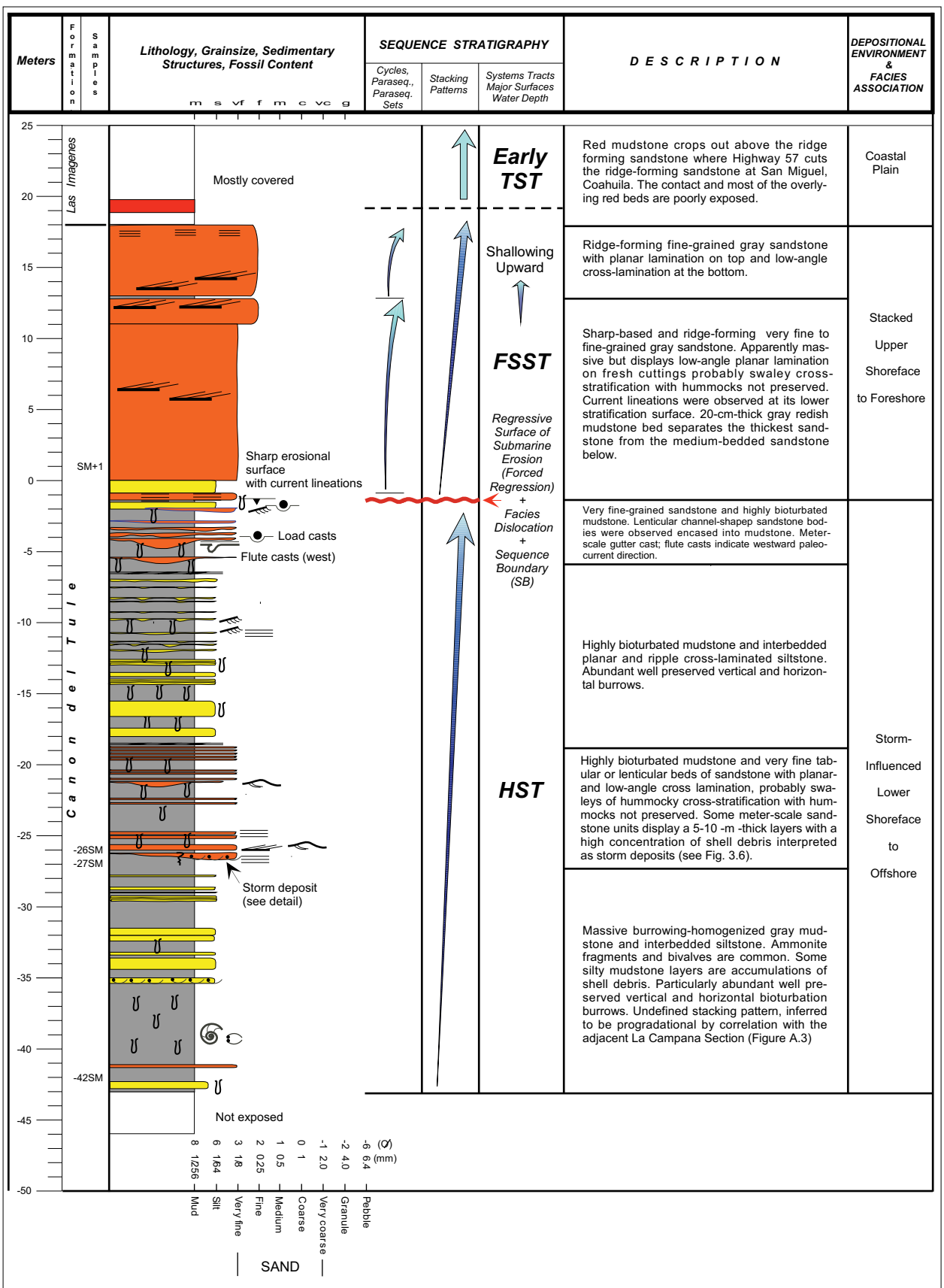

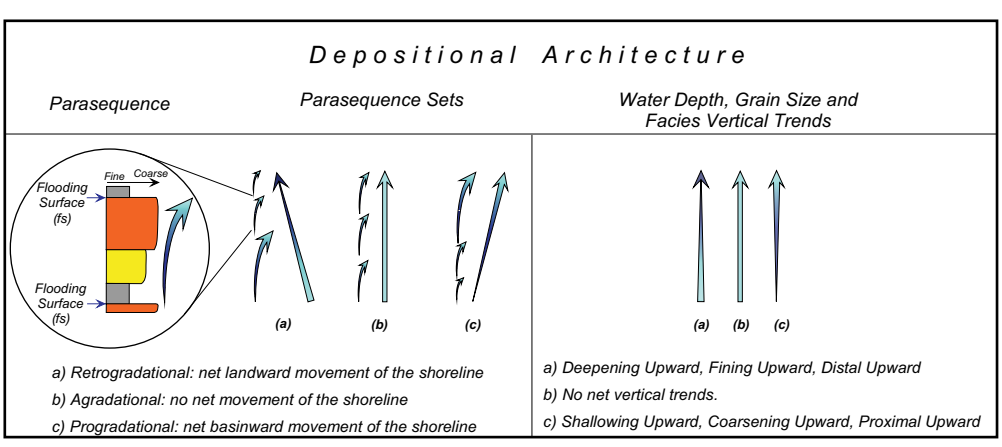

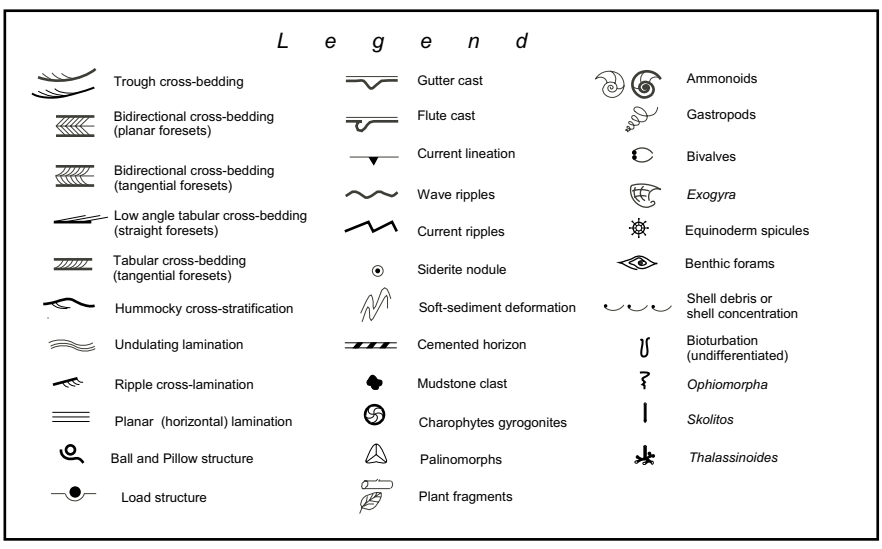

SOURCE: INEGI, 1995. San Miguel, G14C23, 1:50, 000

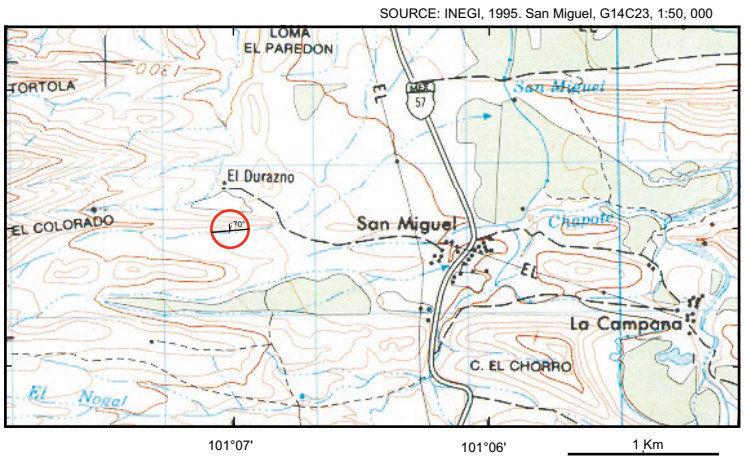

Section Location: Across the ridge-forming sandstone, west of San Miguel, Coahuila.
Geographic Coord.: Interval from -13SM to SM+18 at N 25° 36' 57.2", W 100° 07' 32.5". Lower interval at N 25° 36' 58.3", W 100° 07' 00.7".
Measured by: Juan C. Bermudez, October 1999.

Department of Geological Sciences

Figure A.11 San Miguel Section (SM)

(composite)

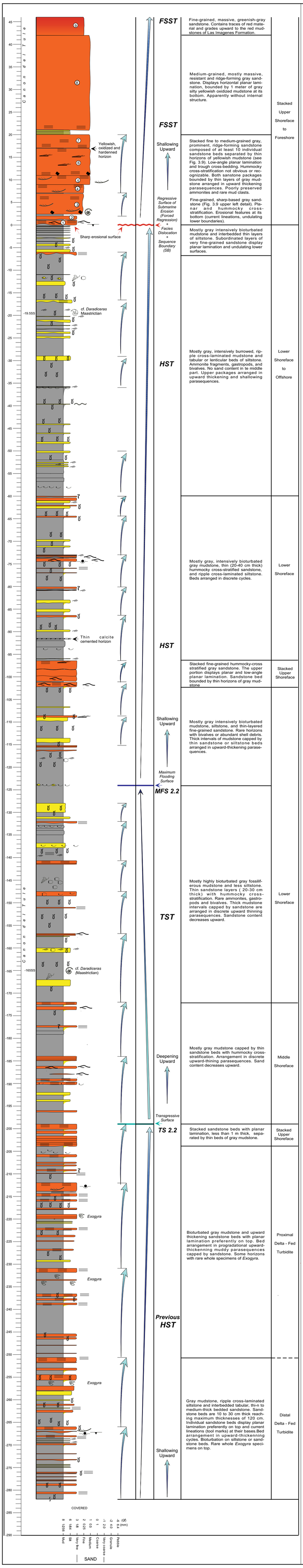

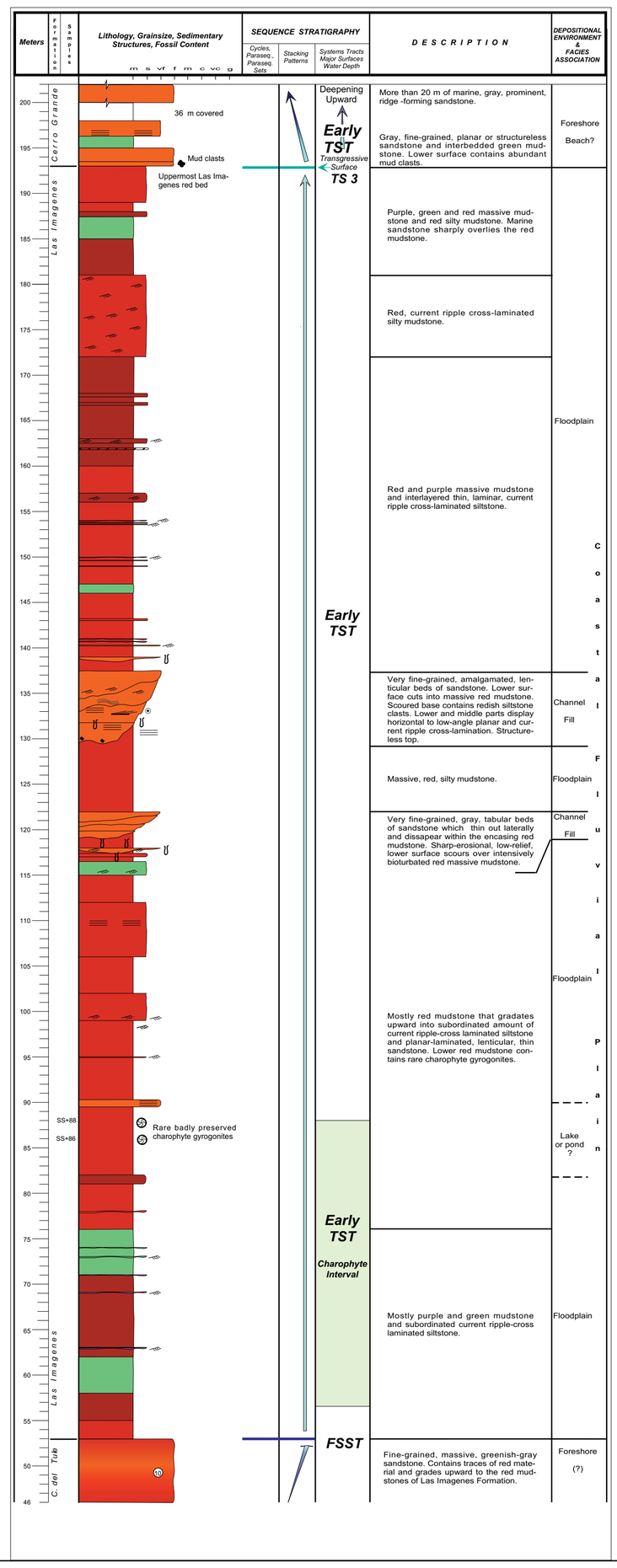

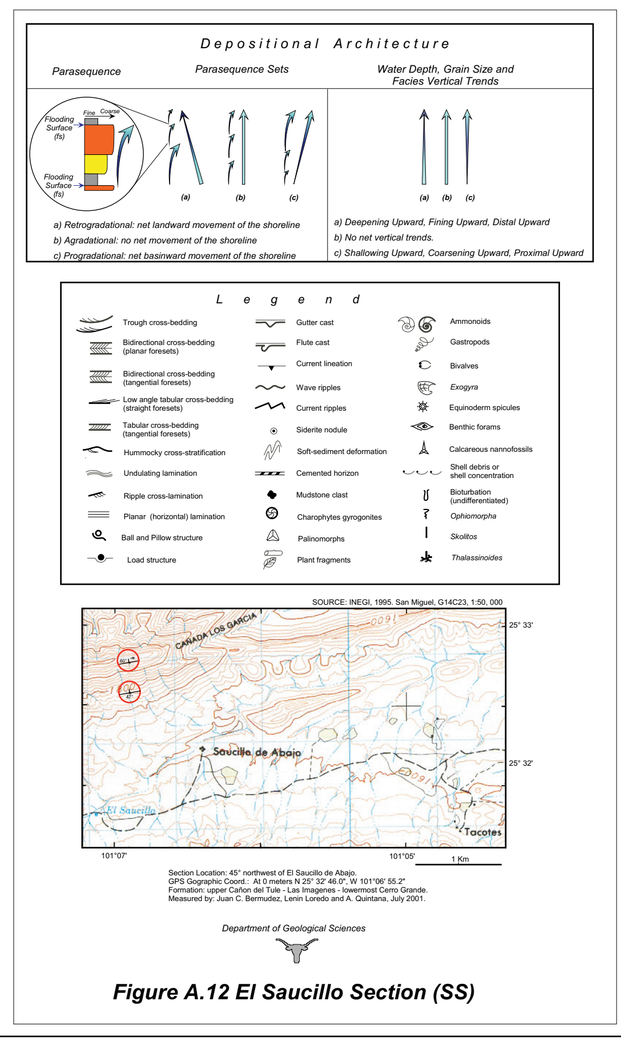

Figure A.12 El Saucillo Section (SS)

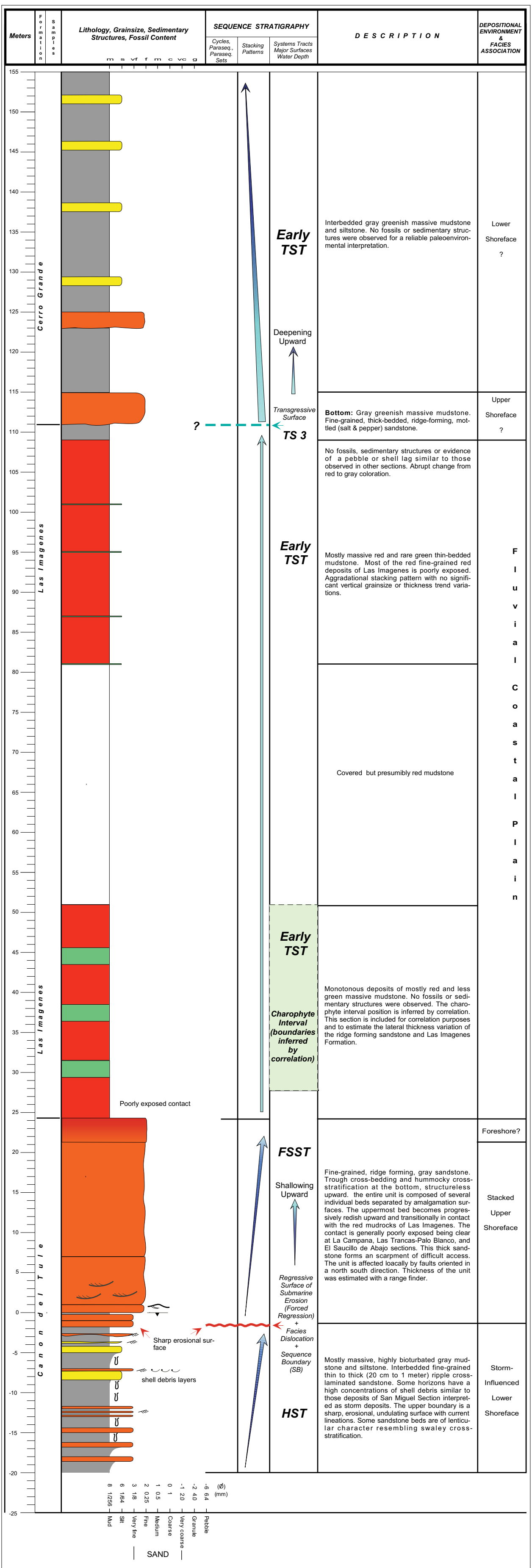

Depositional Architecture

Parasequence — *Parasequence Sets* — *Water Depth, Grain Size and Facies Vertical Trends*

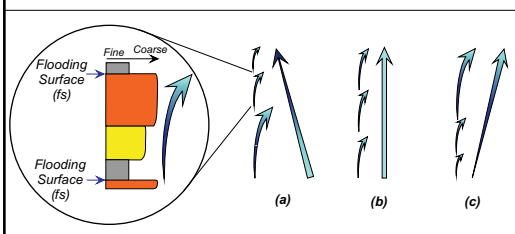

a) Retrogradational: net landward movement of the shoreline
b) Agradational: no net movement of the shoreline
c) Progradational: net basinward movement of the shoreline

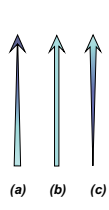

a) Deepening Upward, Fining Upward, Distal Upward
b) No net vertical trends.
c) Shallowing Upward, Coarsening Upward, Proximal Upward

Legend

- Trough cross-bedding
- Bidirectional cross-bedding (planar foresets)
- Bidirectional cross-bedding (tangential foresets)
- Low angle tabular cross-bedding (straight foresets)
- Tabular cross-bedding (tangential foresets)
- Hummocky cross-stratification
- Undulating lamination
- Ripple cross-lamination
- Planar (horizontal) lamination
- Ball and Pillow structure
- Load structure
- Gutter cast
- Flute cast
- Current lineation
- Wave ripples
- Current ripples
- Siderite nodule
- Soft-sediment deformation
- Cemented horizon
- Mudstone clast
- Charophytes gyrogonites
- Palinomorphs
- Plant fragments
- Ammonoids
- Gastropods
- Bivalves
- *Exogyra*
- Equinoderm spicules
- Benthic forams
- Shell debris or shell concentration
- Bioturbation (undifferentiated)
- *Ophiomorpha*
- *Skolitos*
- *Thalassinoides*

SOURCE: INEGI, 1995. San Miguel, G14C23, 1:50, 000

Section Location: 1.5 Km southwest of Santo Domingo, Coahuila.
GPS Geographic Coord.: N 25° 36' 52.6", W 101° 04' 07.3"
Formation: Canon del Tule-Las Imagenes-Cerro Grande.
Measured by: Juan C. Bermudez, August 1999.

Department of Geological Sciences

Figure A.13 Santo Domingo Section (SD)

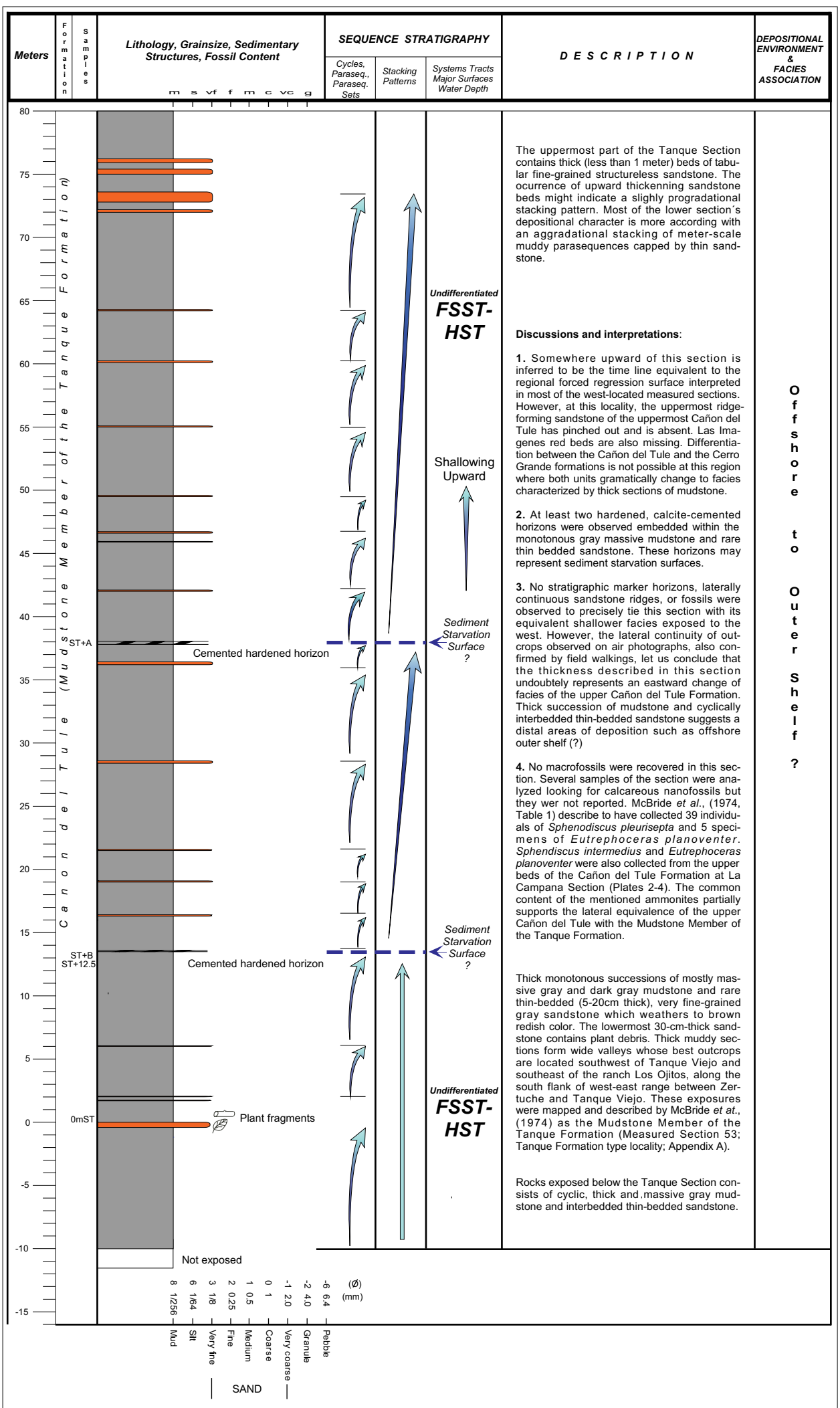

The uppermost part of the Tanque Section contains thick (less than 1 meter) beds of tabular fine-grained structureless sandstone. The ocurrence of upward thickenning sandstone beds might indicate a slighly progradational stacking pattern. Most of the lower section´s depositional character is more according with an aggradational stacking of meter-scale muddy parasequences capped by thin sandstone.

Discussions and interpretations:

1. Somewhere upward of this section is inferred to be the time line equivalent to the regional forced regression surface interpreted in most of the west-located measured sections. However, at this locality, the uppermost ridge-forming sandstone of the uppermost Cañon del Tule has pinched out and is absent. Las Imagenes red beds are also missing. Differentiation between the Cañon del Tule and the Cerro Grande formations is not possible at this region where both units gramatically change to facies characterized by thick sections of mudstone.

2. At least two hardened, calcite-cemented horizons were observed embedded within the monotonous gray massive mudstone and rare thin bedded sandstone. These horizons may represent sediment starvation surfaces.

3. No stratigraphic marker horizons, laterally continuous sandstone ridges, or fossils were observed to precisely tie this section with its equivalent shallower facies exposed to the west. However, the lateral continuity of outcrops observed on air photographs, also confirmed by field walkings, let us conclude that the thickness described in this section undoubtely represents an eastward change of facies of the upper Cañon del Tule Formation. Thick succession of mudstone and cyclically interbedded thin-bedded sandstone suggests a distal areas of deposition such as offshore outer shelf (?)

4. No macrofossils were recovered in this section. Several samples of the section were analyzed looking for calcareous nanofossils but they wer not reported. McBride *et al*., (1974, Table 1) describe to have collected 39 individuals of *Sphenodiscus pleurisepta* and 5 specimens of *Eutrephoceras planoventer*. *Sphendiscus intermedius* and *Eutrephoceras planoventer* were also collected from the upper beds of the Cañon del Tule Formation at La Campana Section (Plates 2-4). The common content of the mentioned ammonites partially supports the lateral equivalence of the upper Cañon del Tule with the Mudstone Member of the Tanque Formation.

Thick monotonous successions of mostly massive gray and dark gray mudstone and rare thin-bedded (5-20cm thick), very fine-grained gray sandstone which weathers to brown redish color. The lowermost 30-cm-thick sandstone contains plant debris. Thick muddy sections form wide valleys whose best outcrops are located southwest of Tanque Viejo and southeast of the ranch Los Ojitos, along the south flank of west-east range between Zertuche and Tanque Viejo. These exposures were mapped and described by McBride *et at*., (1974) as the Mudstone Member of the Tanque Formation (Measured Section 53; Tanque Formation type locality; Appendix A).

Rocks exposed below the Tanque Section consists of cyclic, thick and ,massive gray mudstone and interbedded thin-bedded sandstone.

Offshore to Outer Shelf ?

Depositional Architecture

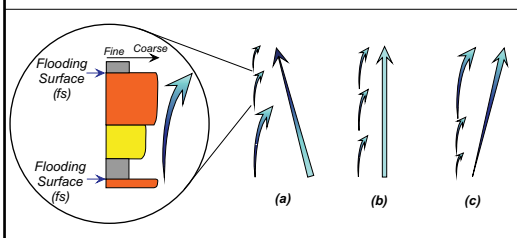

a) Retrogradational: net landward movement of the shoreline
b) Agradational: no net movement of the shoreline
c) Progradational: net basinward movement of the shoreline

a) Deepening Upward, Fining Upward, Distal Upward
b) No net vertical trends.
c) Shallowing Upward, Coarsening Upward, Proximal Upward

Legend

- Trough cross-bedding
- Bidirectional cross-bedding (planar foresets)
- Bidirectional cross-bedding (tangential foresets)
- Low angle tabular cross-bedding (straight foresets)
- Tabular cross-bedding (tangential foresets)
- Hummocky cross-stratification
- Undulating lamination
- Ripple cross-lamination
- Planar (horizontal) lamination
- Ball and Pillow structure
- Load structure
- Gutter cast
- Flute cast
- Current lineation
- Wave ripples
- Current ripples
- Siderite nodule
- Soft-sediment deformation
- Cemented horizon
- Mudstone clast
- Charophytes gyrogonites
- Palinomorphs
- Plant fragments
- Ammonoids
- Gastropods
- Bivalves
- *Exogyra*
- Equinoderm spicules
- Benthic forams
- Shell debris or shell concentration
- Bioturbation (undifferentiated)
- *Ophiomorpha*
- *Skolitos*
- *Thalassinoides*

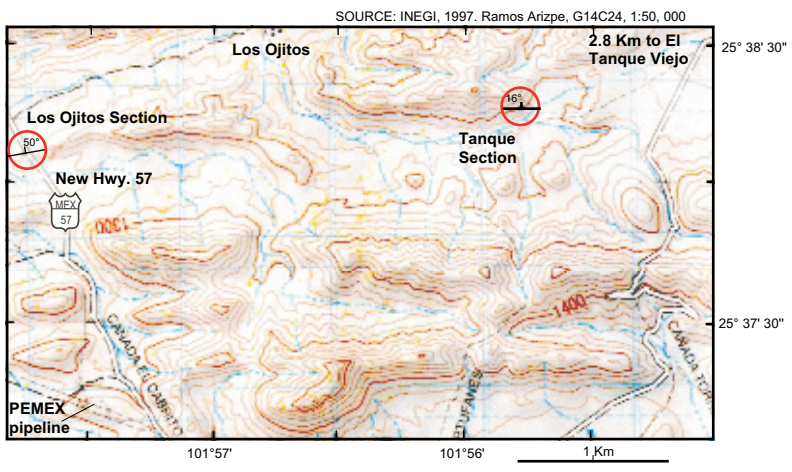

Section Location: 4.2 Km southwest of Tanque Viejo, Coahuila. 3.3 Km northeast of Los Ojitos Section located along the new Highway 57, segment Ramos Arizpe -Santa Cruz.
GPS Geographic Coord.: N 25° 38' 17.3", W 100°55' 46.9"
Formation: upper Cañon del Tule (Prodelta Facies, equivalent to the Mudstone Member of the Tanque Formation of McBride *et al*., 1974).
Measured by: Juan C. Bermudez and A. Quintana, October 1999; July 2001.

Department of Geological Sciences

Figure A.14 Tanque Section (ST)

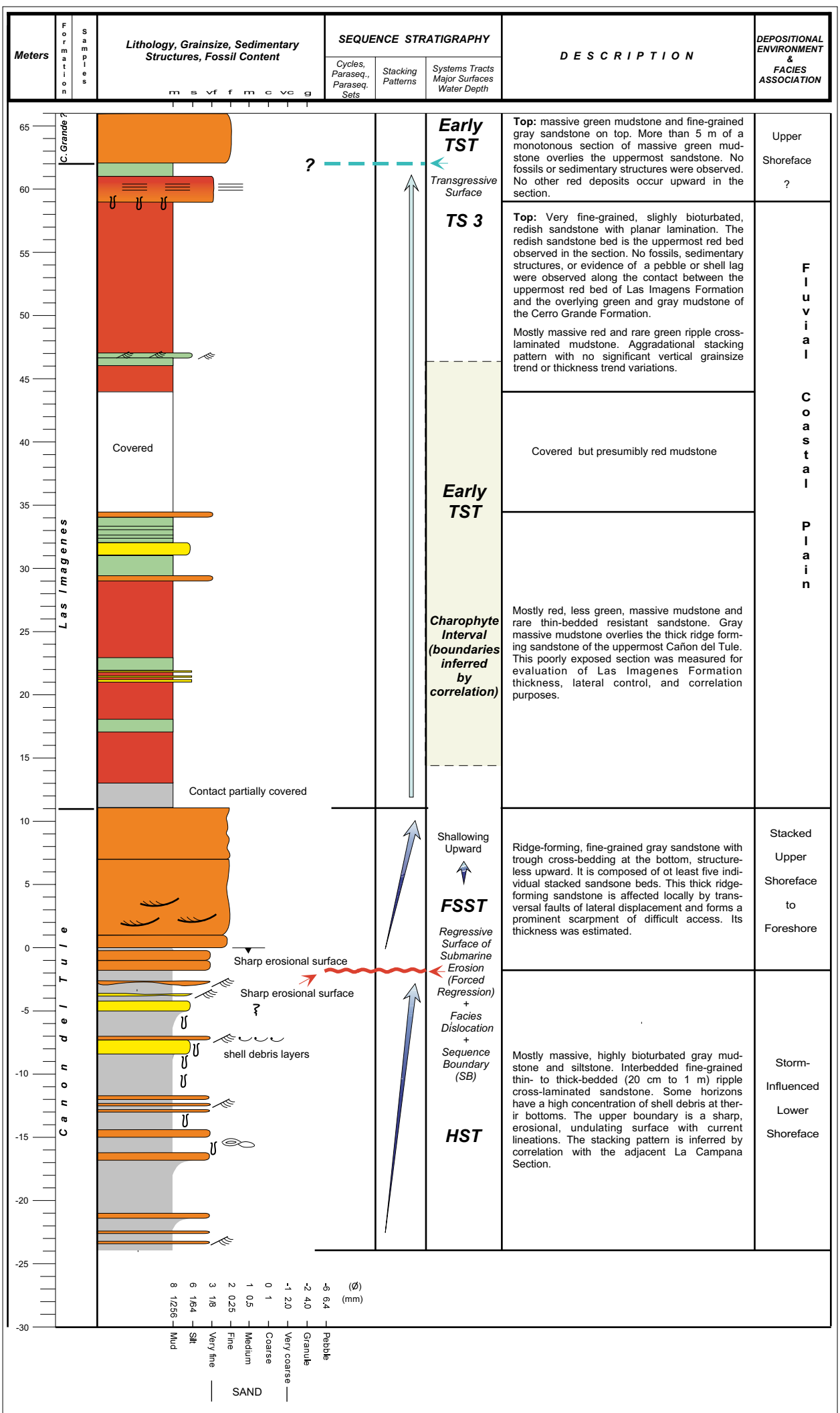

Depositional Architecture

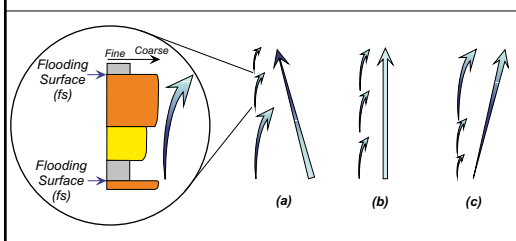

a) Retrogradational: net landward movement of the shoreline
b) Agradational: no net movement of the shoreline
c) Progradational: net basinward movement of the shoreline

a) Deepening Upward, Fining Upward, Distal Upward
b) No net vertical trends.
c) Shallowing Upward, Coarsening Upward, Proximal Upward

Legend

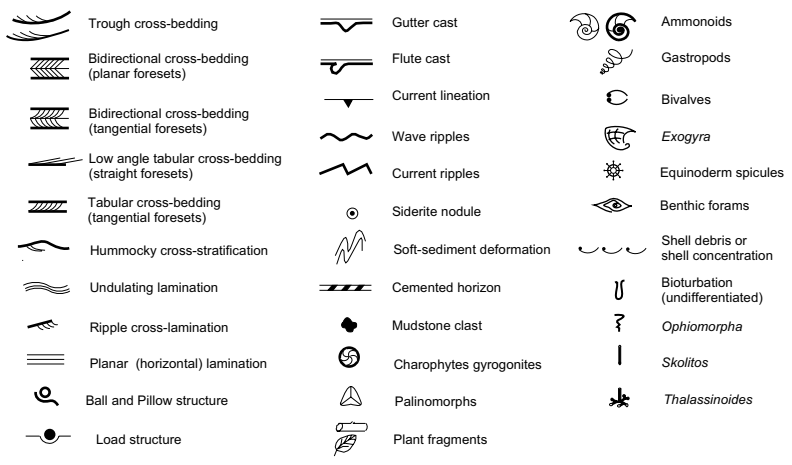

SOURCE: INEGI, 1995. San Miguel, G14C23, 1:50, 000

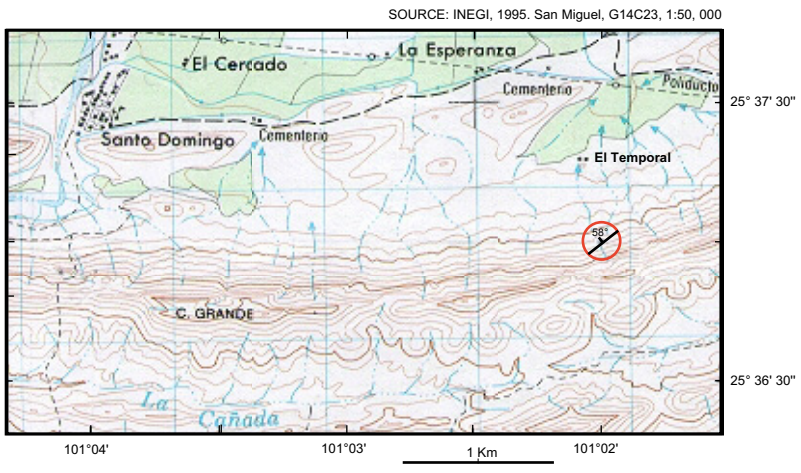

Section Location: 3.4 km southwest of Santo Domingo, Coahuila.
GPS Geographic Coord.: At TE+58 N 25° 37' 00", W 101°02' 00".
Formation: uppermost Cañon del Tule - Las Imagenes- lowermost Cerro Grande.
Measured by: Juan C. Bermudez, August 1999.

Department of Geological Sciences

Figure A.15 Temporal Section (TE)

Cerro Grande

Las Imagenes

Cañon del Tule

LT+170 *Stantonella* sp. *Idonarca* sp.

LT+162.5 *Anomia* sp. *Idonarca* sp.

LT+158.7

Pebble and shell lag

Amalgamation surfaces with chert pebbles

Sharp erosional surface with current lineations

Gutter casts

Covered

Cemented horizon @ -50m

Abundant shell debris and rare fish teeth @ -73.6 m

Exogyra fragments

Covered

(ø) (mm)

8 1/256 Mud
6 1/64 Silt
3 1/8 Very fine
2 0.25 Fine
1 0.5 Medium
0 1 Coarse
-1 2.0 Very coarse
-2 4.0 Granule
-6 64 Pebble

SAND

?

Maximum Flooding Surface

MFS 3

Covered by Las Trancas Creek. The Maximum Flooding Surface position is inferred by correlation with La Campana Section.

Late TST

Deepening Upward

Bioturbated mudstone, less siltstone and stacked lenticular sandstone bodies with ball and pillow and dewatering structures. Badly preserved ammonite fragments, bivalves and gastropods. The lowermost sandstone layer has a flat and sharp lower surface and contains black chert pebbles and small bivalves. Mudstone and siltstone clasts embedded within the mudstone (sample LC+158.7) contain rare isolated benthonic foraminifera. Figure 3.21a-b illustrates the contact between Las Imagenes and Cerro Grande Formation.

Middle Shoreface ?

Transgressive Surface

TS 3

Early TST

Mostly massive red mudstone and less siltstone in thin (20 cm) and thick (2 meters) layers. Moderate bioturbation was only observed on the upper part of this unit.

Through cross-bedded, fine-grained sandstone. Silty lower unit displays soft-sediment deformation and contains mudclasts at its bottom. The whole unit dissapears laterally in less than 5 m.

Channel Fill

Purple, massive mudstone and siltstone, fine and very fine-grained sandstone with planar and ripple cross-lamination. Through cross-bedding in the uppermost sandstone body. The lower contacts of the sandstone beds are sharp, undulating and erosional.

Channel Fill and Overbank

Tabular belts of amalgamated through cross-bedded and planar-laminated fine-grained sandstone. Sandstone bodies thin out and fine laterally to red limolite. Lower siltstone bed displays ripple cross-lamination and rare burrows.

Channel Fill

Mostly purple mudstone and ripple cross-laminated siltstone. Green, massive, rarely bioturbated mudstone.

Overbank

Fine-grained, trough cross-bedded sandstone. Slighly bioturbated siltstone with ripple cross-lamination, dewatering and ball and pillow structures. The unit thins out and interfingers with massive mudstone.

Channel Fill

Mostly red, purple, and green mudstone and less siltstone. Rare bioturbation.

Overbank

Charophyte Interval (boundaries inferred by correlation)

Top: tabular, amalgamated, through cross-bedded sandstone belts that stacked reach a maximum thickness of 6 m and a maximum width of about 70 m (with to depth ratio = 12). Sandstone belts pinch out laterally intil merge and disappear within green mudstone. Lower tabular sand belt contains abundant mud drapes, displays planar lamination and a low relief basal surface scouring massive green mudstone (see Fig. 3.16).

Channel Fill

Fluvial Floodplain

FSST

Massive, fine-grained, bicolored (green-redish) sandstone (see Fig. 3.13d).

Beach-Floodplain Transition

Shallowing Upward

About ten, massive, fine-grained individual sandstone beds stacked and separated by amalgamation surfaces with chert pebbles or thin laminar mudstone.

Stacked Upper Shoreface

Regressive Surface of Submarine Erosion (Forced Regression) + Facies Dislocation + Sequence Boundary (SB)

Amalgamated layers of fine-grained, sharp-based, planar-laminated sandstone. Amalgamation surfaces with pebbles. The sharp erosional surface displays current lineations.

Slighly bioturbated gray mudstone and siltstone. Very fine-grained, lenticular sandstone bodies form meter-scale gutter cast.(Fig.3.8b).

HST

Highly bioturbated gray mudstone and interbedded siltstone with wave ripples. Lots of vertical and horizontal burrows. Some horizons with high concentration of shell fragments (*Exogyra* and other bivalves) and rare fish teeth. Bed arrangement in not well-defined progradational parasequence set.

Lower Shoreface to Offshore

HST

Shallowing Upward

Fluvial Coastal Plain

Meters	Formation	Samples	Lithology, Grainsize, Sedimentary Structures, Fossil Content (m s vf f m c vc g)	SEQUENCE STRATIGRAPHY: Cycles, Paraseq., Paraseq. Sets	SEQUENCE STRATIGRAPHY: Stacking Patterns	SEQUENCE STRATIGRAPHY: Systems Tracts, Major Surfaces, Water Depth	DESCRIPTION	DEPOSITIONAL ENVIRONMENT & FACIES ASSOCIATION
280								
275								
270			LT+269.6					
265								
260								
255								
250								
245								
240								
235								
230								
225								
220								

HST

Bioturbated mudstone, siltstone and thin to medium-bedded sandstone.

Middle to Upper Shoreface ?

Covered by Las Trancas Creek. Presumibly mudstone

Planar-laminated sandstone. Conglomeratic at its bottom (black chert pebbles).

Upper Shoreface ?

Covered by Las Trancas Creek.

Very fine and fine-grained upward-coarsening trough-cross bedded and planar laminated sandstone. Medium-grained conglomeratic sandstone with gray and black chert pebbles.

Upper Shoreface

Shallowing Upward

Maximum Flooding Surface

MFS 3

Depositional Architecture

Parasequence — *Parasequence Sets* — *Water Depth, Grain Size and Facies Vertical Trends*

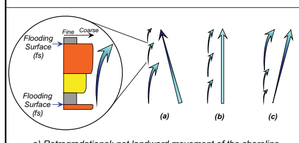

a) Retrogradational: net landward movement of the shoreline
b) Agradational: no net movement of the shoreline
c) Progradational: net basinward movement of the shoreline

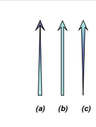

a) Deepening Upward, Fining Upward, Distal Upward
b) No net vertical trends.
c) Shallowing Upward, Coarsening Upward, Proximal Upward

L e g e n d

- Trough cross-bedding
- Bidirectional cross-bedding (planar foresets)
- Bidirectional cross-bedding (tangential foresets)
- Low angle tabular cross-bedding (straight foresets)
- Tabular cross-bedding (tangential foresets)
- Hummocky cross-stratification
- Undulating lamination
- Ripple cross-lamination
- Planar (horizontal) lamination
- Ball and Pillow structure
- Load structure
- Gutter cast
- Flute cast
- Current lineation
- Wave ripples
- Current ripples
- Siderite nodule
- Soft-sediment deformation
- Cemented horizon
- Mudstone clast
- Charophytes gyrogonites
- Palinomorphs
- Plant fragments
- Ammonoids
- Gastropods
- Bivalves
- *Exogyra*
- Equinoderm spicules
- Benthic forams
- Calcareous nannofossils
- Shell debris or shell concentration
- Bioturbation (undifferentiated)
- *Ophiomorpha*
- *Skolitos*
- *Thalassinoides*

SOURCE: INEGI, 1995. San Miguel, G14C23, 1:50, 000

Section Location: Upper Canon del Tule interval along the highway 57 at the large bridge over El Saucillo Creek. Las Imagenes-Cerro Grande interval along Las Trancas Creek and its afluent, nearby Las Trancas ranch.
Measured by: Juan C. Bermudez and Aaron del Valle, July 1998, August 1999.

Department of Geological Sciences

Figure A.16 Las Trancas - Palo Blanco Section (LT-PB)
(composite)

Figure A.17 El Realito (ER) - Altamira (SA) Cross Section

Northwest to southeast sequence stratigraphic cross section of the upper Cañon del Tule, Las Imagenes, and lower Cerro Grande formations, central Parras basin. The base of Las Imagenes coastal plain red beds (FSST) and the charophyte_bearing interval (Early TST) are used as the main correlation references. Coahuilites sheltoni is an index ammonite of the lower Upper Maastrichtian. The stacked upper shoreface to foreshore sandstone (FSST) is bounded at its bottom by the forced regression surface and sequence boundary (FRS+SB), interpreted to be produced during a forced regression in response to a relative sea level fall. The lower MFS 2.2 lies within a muddy fossiliferous interval on top of a transgressive systems tract (TST) characterized by a retrogradational stacking pattern; the upper maximum flooding surface MFS 3 within a muddy horizon that contains chert pebbles, small gastropods, bivalves, shell and diverse biogenic fragments (La Campana Section). The upper transgressive surface TS 3 roughly coincides with the contact between the red beds of Las Imagenes and the overlying shallow marine (TST) deposits of the Cerro Grande Formation. Pebble lags were observed at the transgressive surface TS 3 at Las Trancas-Palo Blanco and El Saucillo sections. The horizontal distances among the columns are structurally unrestored. See the stratigraphic sections in Appendix A for outcrop description and the text for additional explanations.

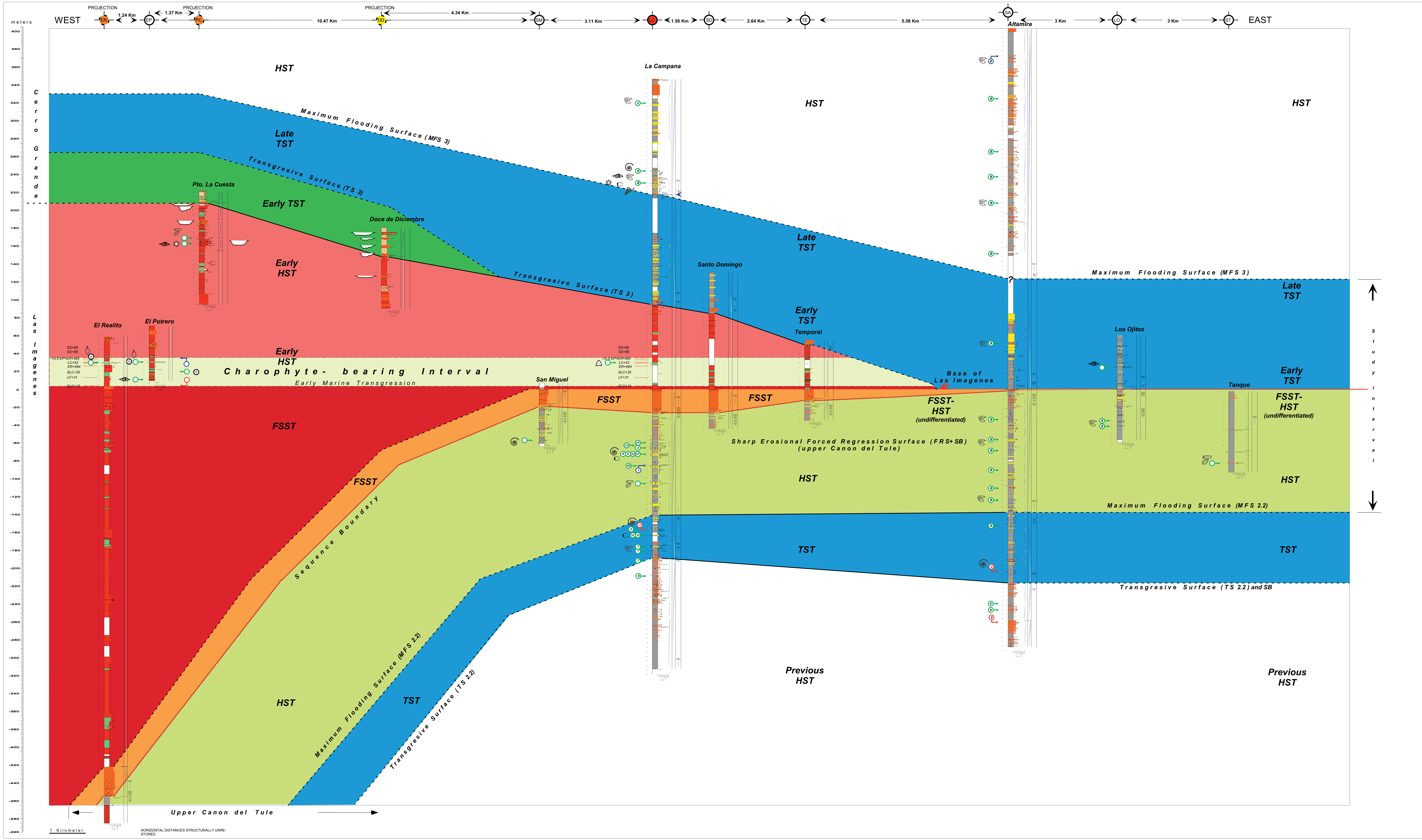

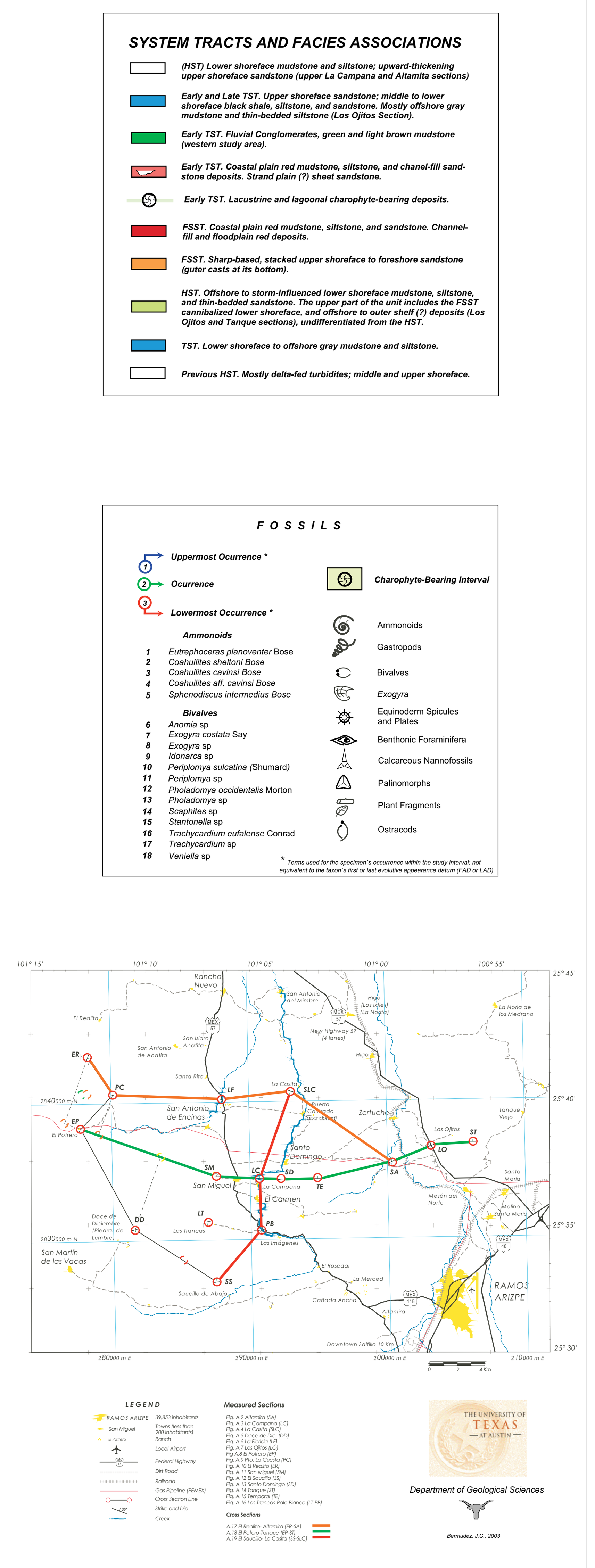

Figure A.18 El Potrero (EP) - Tanque (ST) Cross Section

West to east sequence stratigraphic cross section of the upper Cañon del Tule, Las Imagenes, and lower Cerro Grande formations, central Parras basin. The base of Las Imagenes coastal plain red beds (FSST) and the charophyte_bearing interval (Early TST) are used as the main correlation references. Coahuilites sheltoni is an index ammonite of the lower Upper Maastrichtian. The stacked upper shoreface to foreshore sandstone (FSST) is bounded at its bottom by the forced regression surface and sequence boundary (FRS+SB), interpreted to be produced during a forced regression in response to a relative sea level fall. The lower MFS 2.2 lies within a muddy fossiliferous interval on top of a transgressive systems tract (TST) characterized by a retrogradational stacking pattern; the upper maximum flooding surface MFS 3 within a muddy horizon that contains chert pebbles, small gastropods, bivalves, shell and diverse biogenic fragments (La Campana Section). The upper transgressive surface TS 3 roughly coincides with the contact between the red beds of Las Imagenes and the overlying shallow marine (TST) deposits of the Cerro Grande Formation. Pebble lags were observed at the transgressive surface TS 3 at Las Trancas-Palo Blanco and El Saucillo sections. See the stratigraphic sections in Appendix A for outcrop description and the text for additional explanations..

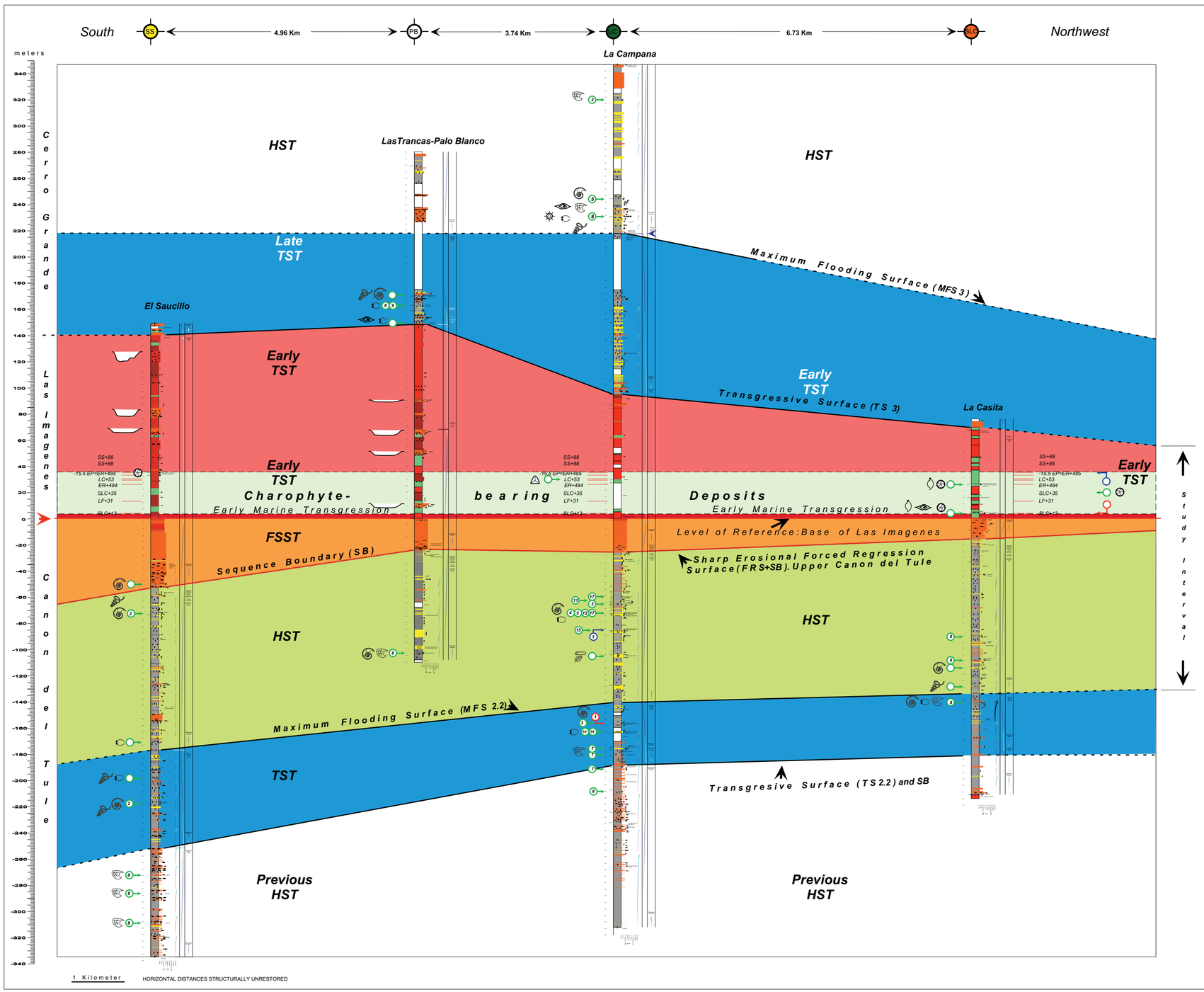

SYSTEM TRACTS AND FACIES ASSOCIATIONS

- *(HST) Lower shoreface mudstone and siltstone; upward-thickening upper shoreface sandstone (upper La Campana and Altamira sections)*
- *Early and Late TST. Upper shoreface sandstone; middle to lower shoreface black shale, siltstone, and sandstone. Mostly offshore gray mudstone and thin-bedded siltstone (Los Ojitos Section).*
- *Early TST. Fluvial Conglomerates, green and light brown mudstone (western study area).*
- *Early TST. Coastal plain red mudstone, siltstone, and chanel-fill sandstone deposits. Strand plain (?) sheet sandstone.*
- *Early TST. Lacustrine and lagoonal charophyte-bearing deposits.*
- *FSST. Coastal plain red mudstone, siltstone, and sandstone. Channel-fill and floodplain red deposits.*
- *FSST. Sharp-based, stacked upper shoreface to foreshore sandstone (guter casts at its bottom).*
- *HST. Offshore to storm-influenced lower shoreface mudstone, siltstone, and thin-bedded sandstone. The upper part of the unit includes the FSST cannibalized lower shoreface, and offshore to outer shelf (?) deposits (Los Ojitos and Tanque sections), undifferentiated from the HST.*
- *TST. Lower shoreface to offshore gray mudstone and siltstone.*
- *Previous HST. Mostly delta-fed turbidites; middle and upper shoreface.*

FOSSILS

- *Uppermost Ocurrence* *
- *Ocurrence*
- *Lowermost Occurrence* *
- *Charophyte-Bearing Interval*

Ammonoids

1. *Eutrephoceras planoventer* Bose
2. *Coahuilites sheltoni* Bose
3. *Coahuilites cavinsi* Bose
4. *Coahuilites aff. cavinsi* Bose
5. *Sphenodiscus intermedius* Bose

Bivalves

6. *Anomia* sp
7. *Exogyra costata* Say
8. *Exogyra* sp
9. *Idonarca* sp
10. *Periplomya sulcatina* (Shumard)
11. *Periplomya* sp
12. *Pholadomya occidentalis* Morton
13. *Pholadomya* sp
14. *Scaphites* sp
15. *Stantonella* sp
16. *Trachycardium eufalense* Conrad
17. *Trachycardium* sp
18. *Veniella* sp

Ammonoids
Gastropods
Bivalves
Exogyra
Equinoderm Spicules and Plates
Benthonic Foraminifera
Calcareous Nannofossils
Palinomorphs
Plant Fragments
Ostracods

* *Terms used for the specimen's occurrence within the study interval; not equivalent to the taxon's first or last evolutive appearance datum (FAD or LAD)*

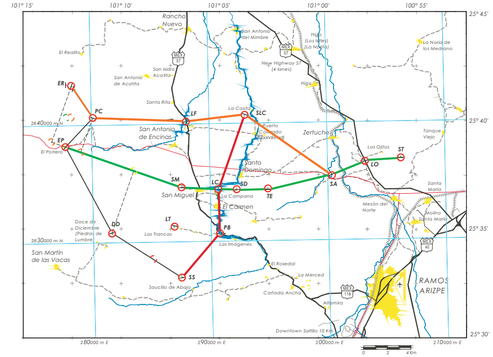

LEGEND

- RAMOS ARIZPE — 36,833 inhabitants
- San Miguel — Towns (less than 200 inhabitants)
- El Potrero — Ranch
- Local Airport
- Federal Highway
- DAY ROAD
- Railroad
- Gas Pipeline (PEMEX)
- Cross Section Line
- Strike and Dip
- Creek

Measured Sections

Fig. A.2 Altamira (SA)
Fig. A.3 La Campana (LC)
Fig. A.4 La Casita (SLC)
Fig. A.5 Doce de Dic. (DD)
Fig. A.6 La Punta (LF)
Fig. A.7 Los Ojitos (LO)
Fig. A.8 El Potrero (EP)
Fig. A.9 Pto. La Cuesta (PC)
Fig. A.10 El Realito (ER)
Fig. A.11 San Miguel (SM)
Fig. A.12 El Chorreon (CH)
Fig. A.13 Santo Domingo (SD)
Fig. A.14 Tanque (ST)
Fig. A.15 Temporal (TE)
Fig. A.16 Las Trancas-Palo Blanco (LT-PB)

Cross Sections

A.17 El Realito - Altamira (ER-SA)
A.18 El Potrero-Tanque (EP-ST)
A.19 El Saucillo- La Casita (SS-SLC)

THE UNIVERSITY OF TEXAS AT AUSTIN
Department of Geological Sciences
Bermudez J., 2003.

Fig. A.19 El Saucillo (SS)-La Casita (SLC) Cross Section

South to northwest sequence stratigraphic cross section of the upper Cañon del Tule, Las Imagenes, and lower Cerro Grande formations, central Parras basin. The base of Las Imagenes coastal plain red beds (FSST) and the charophyte_bearing interval (Early TST) are used as the main correlation references. Coahuilites sheltoni is an index ammonite of the lower Upper Maastrichtian. The stacked upper shoreface to foreshore sandstone (FSST) is bounded at its bottom by the forced regression surface and sequence boundary (FRS+SB), interpreted to be produced during a forced regression in response to a relative sea level fall. The lower MFS 2.2 lies within a muddy fossiliferous interval on top of a transgressive systems tract (TST) characterized by a retrogradational stacking pattern; the upper maximum flooding surface MFS 3 within a muddy horizon that contains chert pebbles, small gastropods, bivalves, shell and diverse biogenic fragments (La Campana Section). The upper transgressive surface TS 3 roughly coincides with the contact between the red beds of Las Imagenes and the overlying shallow marine (TST) deposits of the Cerro Grande Formation. Pebble lags were observed at the transgressive surface TS 3 at Las Trancas-Palo Blanco and El Saucillo sections. See the stratigraphic sections in Appendix A for outcrop description and the text for additional explanations.